The Anti-Microbial Effects of Carbon Monoxide and Carbon Monoxide-Releasing Molecule-3 (CORM-3)

A Thesis submitted by

Jayne Louise Wilson

In part fulfilment of the requirement for the degree of
Doctor of Philosophy

(September 2012)

Department of Molecular Biology & Biotechnology,
University of Sheffield,
Firth Court,
Western Bank,
Sheffield,
S10 2TN,
United Kingdom

The results, discussions and conclusions presented herein are identical to those in the printed version. The Appendix has been omitted in this electronic submission due to the size, format and number of documents. Referral to the University Library copy has been noted in the text where relevant. The final, awarded and examined version is available for consultation via the University Library.

"The best scientist is open to experience and begins with romance - the idea that anything is possible."

Ray Bradbury

Abstract

Intense research on carbon monoxide (CO) over recent years has demonstrated the increasing relevance of this gaseous signalling molecule in biology and medicine. A wide array of protective effects has been attributed to CO, including vasodilation, anti-inflammation and anti-apoptosis. The advent of carbon monoxide-releasing molecules (CO-RMs) has revolutionised this field, providing a means by which the interaction between transition metals and carbonyls can be exploited to allow more controlled endogenous delivery of this noxious gas. It is via such compounds that the bactericidal activity of CO against a number of bacterial species has been most effectively explored.

The best established CO-RM is the novel, water-soluble $Ru(CO)_3Cl$(glycinate) (CORM-3). In this thesis, CORM-3 is shown to inhibit respiration of diverse bacteria as well as *Candida albicans* and, interestingly, stimulates respiration of intact cells of *Escherichia coli* prior to inhibition. Proton translocation measurements (H^+/O quotients, i.e. proton extrusion on pulsing anaerobic cells with O_2, and the subsequent backflow of protons to the cytoplasm) show that respiratory stimulation cannot be attributed to dissipation of the protonmotive force, i.e. true uncoupling. Additionally, the bactericidal activity of CORM-3 is augmented in the absence of haem proteins and transcriptomic profiling of anaerobically-grown haem-deficient *E. coli* following exposure to CORM-3, and to a lesser extent inactivated CORM-3, reveals a multifaceted response. Of particular note is the up-regulation of iron-starvation response genes. Together, these data suggest that CORM-3 has targets additional to respiratory oxidases and that haem may act as a 'CO-sink', thereby providing protection against CO. Furthermore, CORM-3 is shown to be without effect on human macrophage functionality in a model of *Neisseria meningitidis* infection.

This is the most complete study to date on the anti-microbial effects of a CO-RM and it highlights the multifaceted and complex action of these compounds. Importantly, control molecules depleted of CO reveal that CORM-3 toxicity is due to CO release; however, its potent anti-bacterial activity is not mimicked by CO gas. It is therefore becoming increasingly evident that there are several unidentified mechanisms underlying the effectiveness of CO-RMs in tackling microbial sepsis and pathogenesis.

Acknowledgements

First and foremost, I would like to thank my supervisor Professor Robert Poole for his unwavering and continued support and guidance during firstly my Masters project and subsequently this PhD project. I would also like to extend my gratitude to Professor Robert Read as a co-supervisor on the immunological aspects of this work, and to the members of the Read laboratory for their kind technical assistance, in particular Mrs Margaret Lee, Dr. Luke Green, Dr. Jay Laver and Miss Sally Keats. I would also like to thank Professor Brian Mann and Dr. Roberto Motterlini for guidance on CO-RM chemistry and biological activity, but especially to Professor Brian Mann for his patience and assistance during the synthesis of CORM-3. Also, many thanks to Dr. Guido Sanguinetti and Dr. Ronald Begg for the mathematical modelling of the transcriptomic data presented in this thesis. Additional thanks must go to the following undergraduate students that contributed to this work: Miss Bethan Hughes and Miss Sarah Greaves.

I owe many thanks to the members of both the Poole and Green laboratories, past and present, not only for their invaluable assistance throughout my PhD, but for the many fantastic memories of social occasions over the years. I would particularly like to thank Dr. Kelly Davidge, Dr. Samantha McLean and Dr. Matt Rolfe for their guidance on countless aspects, and big thanks must go to the CO-RMies, what a wonderful team. I would also like to thank the many other friends I have made during my PhD for making my time in Sheffield so wonderful. Special thanks must go to Kate and Laura; I cannot even begin to list the reasons, thank you for being so supportive. Also, thank you to Lauren and Oly for housing me during the days before submission of this thesis, you have been the kindest hosts, I couldn't ask for lovelier friends.

Thank you also to Andris for giving me a place away from home to write, and for imparting computer-based knowledge during times of crisis! Your support has helped me more than I can say.

Most of all I would like to thank my family for their constant love and support during all of the years of my education; Mum and Dad, I could not have done this without you, thank you.

Publications

The work presented in this thesis has been, or will be, published in the following papers:

Davidge, K. S., Motterlini, R., Mann, B. E., **Wilson, J. L.** & Poole, R. K. (2009). Carbon monoxide in biology and microbiology: surprising roles for the "Detroit perfume". *Adv Microb Physiol* **56**: 85 - 167

Wilson, J. L., Jesse, H. E., Poole, R. K. & Davidge, K. S. (2012). Antibacterial effects of carbon monoxide. *Curr Pharm Biotechnol* **13**: 760 - 768

Wilson, J. L., Jesse, H. E., Hughes, B., Lund, V., Naylor, K., Davidge, K. S., Mann, B. E. & Poole, R. K. $Ru(CO)_3Cl$(glycinate) (CORM-3): a CO-releasing molecule with broad-spectrum antimicrobial and photosensitive activities against respiration and cation transport in *Escherichia coli*. *Submitted Antioxid Redox Signal* (July 2012).

Wilson J. L., McLean, S., Begg, R., Sanguinetti, G., Mann, B. E. & Poole, R. K. Non-haem targets of carbon monoxide in bacteria: transcriptomic analysis of $Ru(CO)_3Cl$(glycinate) (CORM-3) effects on a *hemA* mutant of *Escherichia coli*. *In preparation.*

Wilson J. L., Read, R. C. & Poole, R. K. Publication of the work presented in Chapter 6, title to be agreed. *In preparation*.

The following work is not presented herein, but it is linked to this thesis in terms of haem biochemistry and ligand interactions, including carbon monoxide:

Shepherd, M., Barynin, V., Lu, C., Bernhardt, P. V., Wu, G., Yeh, S. R., Egawa, T., Sedelnikova, S. E., Rice, D. W., **Wilson, J. L.** & Poole, R. K. (2010). The single-domain globin from the pathogenic bacterium *Campylobacter jejuni*: novel D-helix conformation, proximal hydrogen bonding that influences ligand binding, and peroxidise-like redox properties. *J Biol Chem* **285**: 12747 - 54

Arroyo Mañez, P., Lu, C., Boechi, L., Martí, M. A., Shepherd, M., **Wilson, J. L.**, Poole, R. K., Luque, F. J., Yeh, S. R. & Estrin, D. A. (2011). Role of the distal hydrogen-bonding network in regulating oxygen affinity in the truncated hemoglobin III from *Campylobacter jejuni*. *Biochemistry* **50**: 3946 - 56

Conferences Attended and Presentations Given

The work presented in this thesis has been presented in the form of a poster/oral presentation at the following conferences:

September 2009: **Poster presentation at Haem Oxygenases in Biology and Medicine 6th International Congress, Miami, USA.**
Title: Toxicity of Carbon Monoxide-Releasing Molecules to Gram-negative Bacteria
Grant awarded: Society for General Microbiology, Scientific Meetings Travel Grant

August 2010: **Poster presentation at the International Conference on Oxygen Binding and Sensing Proteins, Antwerp, Belgium.**
Title: Anti-Bacterial Effects of Carbon Monoxide-Releasing Molecule-3

May 2011: **Oral presentation at the 7th European Conference on Bacterial Respiratory Chains, Höör, Sweden.**
Title: Carbon Monoxide-Releasing Molecules (CO-RMs) as Inhibitors of Oxygen-Dependent Respiration in Bacteria
Grant awarded: Society for Experimental Biology, Company of Biologists Travel Grant

May 2012: **Poster presentation at Haem Oxygenases in Biology and Medicine 7th International Congress, Edinburgh, UK.**
Title: Carbon Monoxide-Releasing Molecule-3 (CORM-3): A Compound with Multifaceted Effects on Bacteria

Abbreviations

All abbreviations used are standard for microbiology, unless listed here:

ACS	Acetyl CoA synthase
δ-ALA	δ-aminolevulinic acid
BK_{Ca}	Big-conductance calcium-activated potassium channel
BSA	Bovine serum albumin
CBA	Columbia blood agar
CCCP	Carbonylcyanide *m*-chlorophenylhydrazone
cGMP	Cyclic guanosine monophosphate
CO	Carbon monoxide
CODH	Carbon monoxide dehydrogenase
COHb	Carboxyhaemoglobin
CO-RM	Carbon monoxide-releasing molecule
CPB	Cardiopulmonary bypass
DAPI	4',6-diamidino-2-phenylindole
DEPC	Diethylpyrocarbonate
dH_2O	Distilled water
DMEM	Dulbecco's Modified Eagle Medium
DMSO	Dimethyl sulfoxide
EcDos	*Escherichia coli* phosphodiesterase
EMEM	Eagle's Minimal Essential Medium
EPR	Electron paramagnetic resonance
ERK1/2	Extracellular signal-related kinases
ET-CORM	Enzyme-triggered carbon monoxide-releasing molecule
FCCP	Carbonylcyanide-p-trifluoromethoxyphenylhydrazone
Fe-S	Iron sulfur cluster
FITC	Fluorescein isothiocyanate
gdH_2O	Glass distilled water
HO	Haem oxygenase
iCORM	Inactive carbon monoxide-releasing molecule
ICP-AES	Inductively coupled plasma atomic emission spectroscopy
IL-X	Interleukin-X
JNK	c-Jun N-terminal kinase
K_{ca}	Calcium-signalled potassium channel
KPi	Inorganic potassium phosphate buffer
LB	Luria-Bertani broth
L-NAME	N^G-nitro-L-arginine methyl ester
LPS	Lipopolysaccharide

MAPK	Mitogen-activated protein kinase
MbCO	Carbonmonoxymyoglobin
MFI	Mean fluorescent intensity
MHB	Mueller-Hinton broth
miCORM	Myoglobin-inactivated carbon monoxide-releasing molecule
MOI	Multiplicity of infection
mQH_2O	MilliQ water
NA	Nutrient agar
NAC	*N*-acetylcysteine
NADP(H)	Reduced nicotinamide adenine dinucleotide phosphate
NF-κB	Nuclear factor kappa-light-chain-enhancer of activated B cells
NO	Nitric oxide
NOD2	Nucleotide-binding oligomerisation domain 2
(i)NOS	(Inducible) nitric oxide synthase
OxyHb	Oxyhaemoglobin
PBS	Phosphate-buffered saline
ROS	Reactive oxygen species
RPMI	Roswell Park Memorial Institute medium
sGC	Soluble guanyl cyclase
TB	Terrific broth
TBSA	Terrific broth soft agar
TCA	Tricarboxylic acid (cycle)
TLR-4	Toll-like receptor 4
TNF-α	Tumour necrosis factor-α
YEPD	Yeast Extract Peptone Dextrose

Contents

List of Figures

List of Tables

Chapter 1. Introduction

1.1 The importance of gasotransmitters

Although the focus of this thesis is carbon monoxide (CO), and the recently synthesised carbon monoxide-releasing molecules (CO-RMs, section 1.4.3), it is important to initially introduce additional gaseous molecules that are becoming increasingly relevant in pharmacology. A number of excellent reviews are now available regarding gas biology (e.g. (Fukuto *et al.* 2012; Kajimura *et al.* 2010)). The most widely known gaseous molecule is diatomic oxygen (O_2) (Table 1.1), which is best documented as the terminal electron acceptor in aerobic respiration. However, in recent years, CO, nitric oxide (NO) and the more modestly studied hydrogen sulfide (H_2S) have also been defined as important molecules (Table 1.1). The term 'gasotransmitters' was coined to collectively encompass the three gases (Wang 2002), which share a number of characteristics (Li *et al.* 2009; Li & Moore 2007; Wang 2002) that are described in brief herein. They are recognised as 'primordial gaseous molecules' as they have been present in the Earth's atmosphere from the beginning of time; however, modern day levels of CO, NO and H_2S in the environment are also affected by anthropogenic activity. All three gases are of small molecular weight (28, 30 and 34, respectively) and uncharged enabling their facile diffusion across membranes. Each is endogenously generated via finely regulated enzymatic actions and are key players in cell signalling, generally eliciting well-defined physiological effects as a result of interactions with important targets, such as metalloproteins. Major biochemical roles of the gases include regulation of vascular homeostasis, modulation of inflammation and central nervous system function, which are described in more detail for CO in section 1.4. Due to their natural synthesis within the body, often in the same cells as one another in the same organ, and their similar biological activity, it has been proposed that all three gases work in unison, hence their recent reference as the 'gaseous triumvirate' (Li *et al.* 2009). A degree of cross-talk is also considered to play an important role in their interactions; not only can they affect biological responses of the other, but they can also influence one another's biosynthesis. In a microbiological context, they have been associated with bacterial metabolism, particularly in hydrothermal vents where they are utilised as an alternate source of energy. However, CO, NO and H_2S are all poisonous at non-physiological concentrations owing, at least in part, to classical inhibition of

Table 1.1. Chemical and biological properties of reactive ligands.

Gas	Size (MW/pm*)	Chemistry	Biology
O_2	32/121	Requires biological activation, generally via metal centres. Reduced ultimately to water.	Biological oxidant and co-substrate.
NO	30/115	A radical that reacts with other radicals. Stable in water. Binds strongly to many transition metals.	Complex, versatile biological chemistry. May be reduced and oxidised.
CO	28/113	Relatively unreactive, but coordination to metals enhances reactivity.	Biological chemistry may be complex, but very few direct targets have been identified, including haems, iron and copper.
H_2S	34	Can be ionised in the physiological pH range. Reacts with oxidised thiol species. Soluble in water. Reacts with metals.	Limited literature is available regarding biological/physiological activity.

* Bond length in diatomic molecules is given in picomoles.

respiratory electron transfer to O_2, i.e. via inhibition of terminal oxidase function (Cooper & Brown 2008). The interaction of these gases with cytochrome oxidase of the respiratory chain is shown diagrammatically in Figure 1.1.

1.2 Historical perspectives of carbon monoxide

CO is a diatomic, chemically stable molecule due to its formal triple bond. At temperatures ≥ -191.5 °C it exists in the gaseous form and is relatively un-reactive, with a high activation energy (213 kJ/mol) to bind even O_2. CO is generated via the incomplete combustion of carbonaceous materials, both in nature and as a result of industrial processes. Examples of natural sources include the metabolism and production of CO by plants and oceans, as well as oxidation of hydrocarbons by hydroxyl radicals and ozone. The last is also a factor of anthropogenic activity, in addition to internal combustion engines, waste disposal and burning of carbon-containing fuels (Wu & Wang 2005). CO is a well-known noxious gas, having a notoriously bad reputation as a 'silent killer' (Krenzelok *et al.* 1996) due to its undetectable nature and subtle symptoms.

Although the existence of CO in the Earth's atmosphere extends to the beginning of time, it was only first identified by Cruikshank in 1800. Its toxicity was initially realised by Claude Bernard (c. 1846) via investigations into the effects of the gas on dogs (Bernard 1865). However, the experimental use of CO did not come into play until late in the 19th century when CO binding to haemoglobin and its reversibility by light was identified by Haldane and Smith (Keilin 1966). Thus, a long history of the use of CO as a probe for haems in biology was born, enabling the identification and quantification of haem proteins (e.g. in bacteria (Wood 1984)).

Initial studies on the inhibitory effect of CO on cellular respiration were carried out by Warburg in yeast (Keilin 1966). Inhibition by CO was seen to be reversible and required high partial pressures of the gas, with the inhibitory effect being diminished by increasing partial pressures of O_2. This work was therefore pivotal in demonstrating the importance of the CO/O_2 ratio, whereby different pressures of CO may give the same degree of inhibition so long as the ratio remains constant; thus CO competes with O_2 for binding to the same protein. The photosensitivity of the interaction between CO and

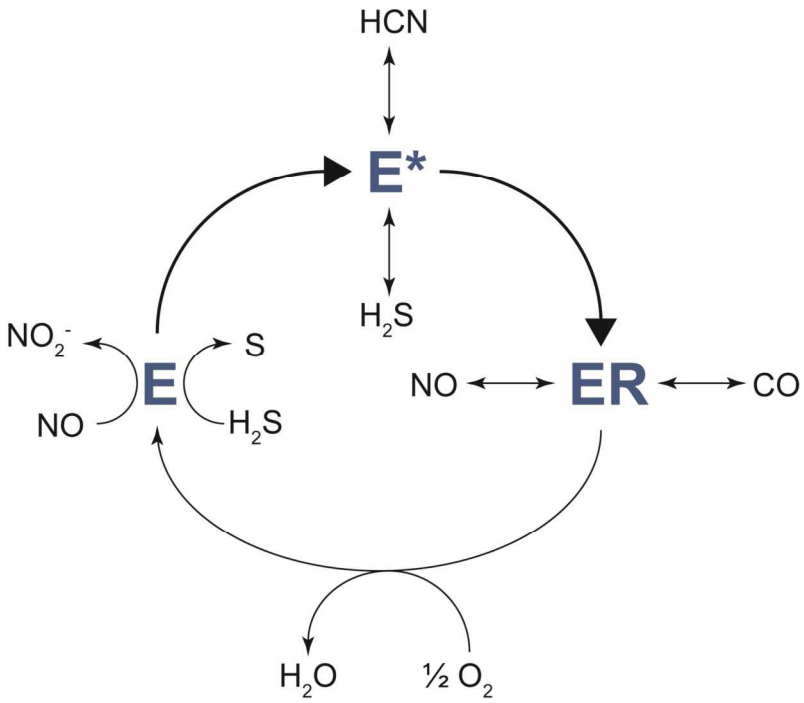

Figure 1.1. Interaction of respiratory inhibitors with cytochrome oxidase. E (oxidised enzyme), E* (turnover intermediate) and ER (reduced enzyme). Both NO and H_2S undergo oxidation by reaction with the oxidised enzyme, H_2S and hydrogen cyanide (HCN) reversibly inhibit a redox intermediate, and CO and NO reversibly inhibit the reduced form of the oxidase. The information enabling the generation of this figure was sourced from Cooper & Brown (2008).

haemoglobin led Warburg to study the effect of light on the inhibitory effects of this gas on the respiration of yeast. From this reaction, Warburg obtained the photochemical action spectrum of respiration, exhibiting absorbance maxima at wavelengths corresponding to the CO adducts of respiratory oxidases. The similarity in the reversibility of CO binding to haemoglobin and oxidases demonstrated a relationship between the two classes of proteins, i.e. binding of the gas to their haem moiety. Exploitation of the photolabile nature of the haem-CO adduct was utilised as a means for oxidase identification and also studies of ligand binding/exchange (e.g. (Gibson *et al.* 1965)). Higher resolution photochemical action spectra were obtained in the 1920s and the 1930s for many cell types. Such work led to a detailed study by Chance *et al.* showing the photodissociation of the cytochrome a_3-CO complex, consequently identifying a major oxidase in the bacterial respiratory chain (Chance *et al.* 1953). Later studies employed photochemical action spectra and measurements of CO-difference spectra at subzero temperatures for the identification of mitochondrial oxidases in microorganisms, e.g. in *Crithidia fasciculata* (Edwards & Lloyd 1973; Scott *et al.* 1983) and *Acanthamoeba castellanii* (Lloyd *et al.* 1981).

1.3 Carbon monoxide in mammals

1.3.1 Generation of carbon monoxide

Due to the poisonous nature of CO, the discovery of its endogenous generation in the human body (Sjostrand 1949) was surprising. Although subsequent work identified haem derived from haemoglobin as a source for the intracellular production of the gas (Coburn *et al.* 1964; Sjostrand 1952), it was not until later that the enzyme responsible for the degradation of haem was identified, namely haem oxygenase (HO) (Tenhunen *et al.* 1969). In addition to CO, the by-products of the reaction include iron(II), which can subsequently induce ferritin production, and the linear tetrapyrrole biliverdin. The latter is broken down by biliverdin reductase to yield bilirubin in amounts equimolar to CO (Figure 1.2). The complete system has an absolute requirement for reduced nicotinamide adenine dinucleotide phosphate (NADPH) and O_2 and is inhibited by CO (Tenhunen et al. 1969). In the human body over 500 μmol (12 ml) CO is produced per day (Coburn *et al.* 1964), with a production rate of 16.4 μmol/h (Wu & Wang 2005). Determining the concentration of CO in tissues is more complex; it cannot be estimated

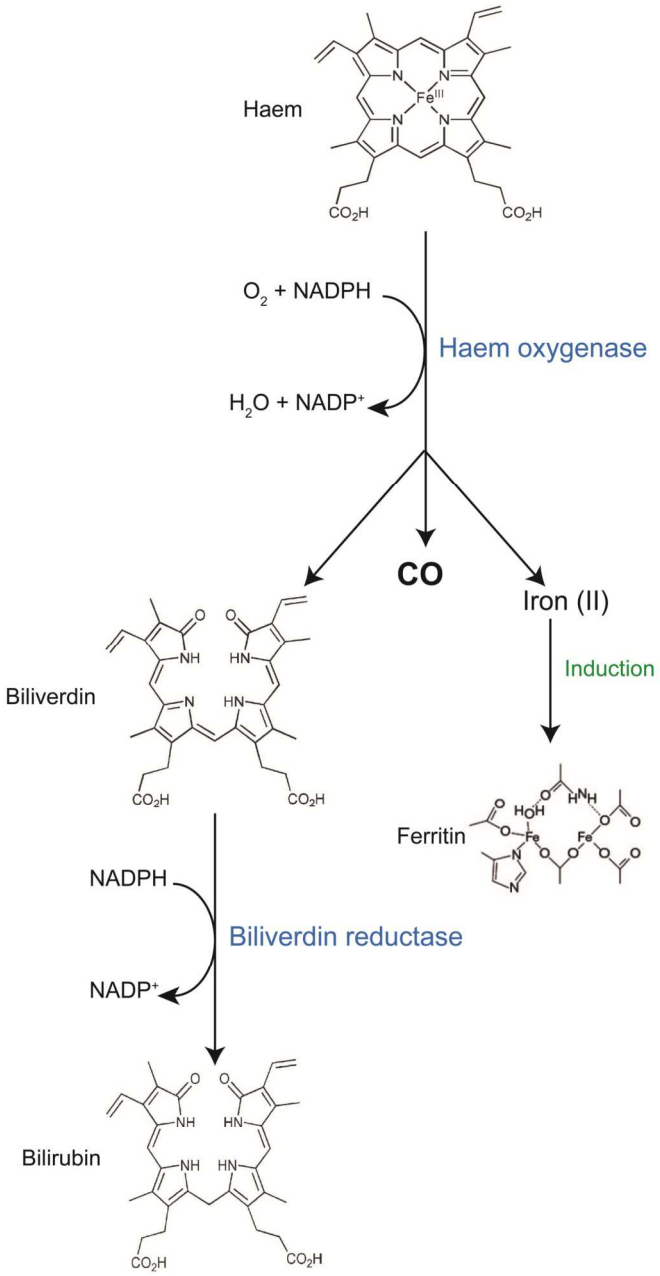

Figure 1.2. Degradation of haem by haem oxygenase. Reduced form of nicotinamide adenine dinucleotide phosphate (NADPH). The information enabling the generation of this figure was sourced from the following references (Mann & Motterlini 2007; Scott *et al.* 2007; Wu & Wang 2005).

from carboxyhaemoglobin (COHb) levels due to the intracellular scavenging of CO after its generation and prior to its diffusion into the bloodstream (Wu & Wang 2005).

The Maines laboratory was instrumental in the identification of the different isoforms of HO: inducible HO-1 and constitutively expressed HO-2 (Maines *et al.* 1986) and HO-3 (McCoubrey *et al.* 1997). HO-1 is induced in response to a number of cellular stresses, encompassing both endogenous and exogenous stimuli. Induction occurs in the majority of mammalian tissues, but the most abundant expression is in the spleen. Constitutively expressed HO-2 is predominantly synthesised in the nervous system and testes as well as other tissues, including the endothelium, liver and gut (Wu & Wang 2005). Expression of functional HO-3 protein is less well documented and it has been suggested (Hayashi *et al.* 2004) that HO-3 genes may be pseudogenes derived from those encoding HO-2 (Wu & Wang 2005).

The regulation of intracellular haem levels is an important function of HO (Wu & Wang 2005). However, intense research since the beginning of the 1990's suggests a wide array of beneficial effects elicited by the activity of this enzyme as a result of its anti-inflammatory, anti-apoptotic, anti-proliferative and cytoprotective capabilities. Moreover, the inducible nature of HO-1 shows great potential as a novel therapeutic mechanism due to the ability to induce the enzyme prior to a given insult, at levels above those generated physiologically (Scott *et al.* 2007). The by-products of the reaction have also become increasingly relevant with each eliciting their own protective effects, suggesting an involvement in the positive connotations associated with HO. For example, further to the activity of CO, which will be discussed in more detail in subsequent sections, bilirubin was defined as the most potent antioxidant molecule in serum (Stocker *et al.* 1987). Both bilirubin and biliverdin are powerful cytoprotective agents involved in the amelioration of a number of conditions similar to CO. Although perhaps a tenuous link, the generation of iron(II) may also elicit anti-oxidant effects via its ability to stimulate the synthesis of ferritin (Eisenstein *et al.* 1991), which sequesters free iron and thus prevents the generation of reactive oxygen species (ROS) via the Fenton reaction (Wu & Wang 2005).

1.3.2 Toxicity of carbon monoxide

At high, and therefore non-physiological concentrations, toxicity of CO occurs due to tissue hypoxia and direct targeting of intracellular components, primarily the respiratory electron transfer chain. Hypoxia is caused by preferential formation of COHb over oxyhaemoglobin (OxyHb) due to the higher affinity of haemoglobin for CO compared with O_2, typically 200 - 250 times greater (Rodkey *et al.* 1974). Thus binding of O_2 to haemoglobin is reduced resulting in the subsequent impairment of O_2 transport and delivery to tissues (Roughton & Darling 1944). Although binding of CO to other haem proteins such as myoglobin, hydroperoxidases, cytochrome *c* oxidase, and cytochrome P-450 may contribute to its toxic effects, collectively such interactions only account for 10 - 15 % of the total concentration of the gas in the human body (Stewart 1975).

The view that CO toxicity occurs as a result of hypoxia has been contested due to the persistence of symptoms associated with acute CO poisoning after COHb levels in the blood have been normalised (Coburn 1979). A study from 1975 showed that inhalation of CO by dogs elicited toxicity, as expected. However, dogs that were bled to an anaemic state and then transfused with COHb so that the concentration of COHb was in excess of 50 % of the total haemoglobin, showed no symptoms of toxicity. Additionally, a control group that were bled to the same anaemic state as the latter, but with no transfusion, survived (Goldbaum *et al.* 1975). The interaction of CO with other targets such as cytochromes was therefore considered more likely (Coburn 1979); the inhibitory effects of CO on haem a_3 of mitochondrial cytochrome oxidase had long before been demonstrated (e.g. (Chance *et al.* 1970)). This mechanism of toxicity was later confirmed in humans where exposure to CO resulted in inhibition of mitochondrial cytochrome *c* oxidase (Alonso *et al.* 2003; Miro *et al.* 1998). Progressive inhibition as a result of increased exposure to the gas led to a decrease in mitochondrial respiratory chain function (Alonso *et al.* 2003). This group proposed that the subsequent decay in mitochondrial energy production would result in cellular injury or dysfunction, or heightened generation of ROS, leading to injury. Furthermore, the inhibitory effect of exogenously and endogenously produced CO on respiration was reported in mammalian cells under hypoxic (1 % O_2) and ambient (21 % O_2) conditions. Respiratory inhibition was markedly increased during hypoxia, which is consistent with competitive binding of CO to cytochrome *c* oxidase in the presence of O_2 (D'Amico *et al.* 2006).

1.4 Carbon monoxide as a potential therapeutic agent

In spite of the negative connotations associated with CO, the growing field of research reporting the beneficial activity of this gas in various disease states is securing its place as a therapeutic agent. The literature on this subject has become increasingly intense over the past decade, so that justice cannot be demonstrated in the confines of this chapter. However, several recent reviews provide a comprehensive insight into the extensive positive biological roles of this multifaceted signalling molecule, including studies that have made use of the recently developed CO-RMs (section 1.4.3) as novel CO donors (e.g. (Davidge *et al.* 2009a; Gullotta *et al.* 2012; Motterlini & Otterbein 2010)).

1.4.1 Preclinical efficacy

The importance of CO was initially highlighted indirectly *in vitro* and *in vivo* using HO-1 deficient mice (*Hmox1* $^{-/-}$) (Poss & Tonegawa 1997), and in the first human case of HO-1 deficiency (Yachie *et al.* 1999). In the former study the intracellular formation of free radicals was increased, and cell survival was reduced, in *Hmox1* $^{-/-}$ murine embryonic fibroblasts exposed to oxidative stress. Additionally, *Hmox1* $^{-/-}$ mice exhibited increased sensitivity to endotoxemic stress. The latter was attributed to rapid iron-loading in the liver following lipopolysaccharide (LPS) administration, which correlated with the severity of hepatic injury and the incidence of mortality. Therefore, Hmox1 activity may play a role in the regulation of intracellular iron levels by attenuating iron accumulation (Poss & Tonegawa 1997), which could subsequently lead to the generation of ROS via the Fenton reaction. Human cells lacking HO-1 were also reported to exhibit extreme sensitivity to oxidant-induced injury and iron deposition was noted in renal and hepatic tissue (Yachie *et al.* 1999). Taken together, these data demonstrate an essential anti-oxidant role for HO-1 activity. The mechanism(s) behind such a role was poorly understood until Otterbein and co-workers showed the protective capabilities of CO (a by-product of HO-1) against oxidative stress caused by hyperoxia in the rat lung (Otterbein *et al.* 1999). Further to this, CO has been shown to modulate inflammation, apoptosis and cellular proliferation, in which it acts to best maintain homeostasis. For example, in endothelial cells, hepatocytes and cardiomyocytes, CO is anti-apoptotic and thus prevents tissue and cellular injury. However, in cells that pose a

threat such as aggressive T-cells that attack and destroy other cells and tissue, dysregulated hyperproliferative smooth muscle cells and cancer cells, CO elicits pro-apoptotic effects. The therapeutic potential of CO is particularly being realised in cardiovascular disease, inflammation and organ transplantation and preservation (Motterlini & Otterbein 2010).

A clear understanding of the molecular mechanism(s) responsible for the protective activity of CO remains to be elucidated. However, interactions of the molecule with soluble guanyl cyclase (sGC), NO synthase (NOS), cytochrome oxidase, NADPH oxidase, potassium channels and mitogen-activated protein kinase (MAPK) have all been implicated (Boczkowski *et al.* 2006). However, the CO-binding constants (*K*) of these potential targets are considerably smaller than for haemoglobin (583 μM^{-1} for type A sheep haemoglobin (Mims *et al.* 1983)). The interaction of CO with the haem-containing proteins NOS (White & Marletta 1992) and sGC (Kharitonov *et al.* 1995) were the first to be described, the latter having been identified as a preferential target of the gas (Furchgott & Jothianandan 1991). To emphasise the degree by which the affinity of these proteins differs from that of haemoglobin, the CO-binding constants are only c. 0.003 μM^{-1} for NOS (Abu-Soud *et al.* 1998) and c. 0.004 μM^{-1} for sGC (Martin *et al.* 2006). The interplay between the CO/HO and NO/NOS pathways is evident in the cardiovascular system, as well as in hepatic, pulmonary and renal circulation (Abraham & Kappas 2008). An effect that is specifically relevant to this thesis is the ability of HO/CO to suppress NO production, which is mentioned briefly in the context of microbial sepsis in section 1.5.3 and discussed in more detail in Chapter 6.

A number of the protective effects elicited by CO mirror those previously associated with NO. One of the best known mechanisms by which both gases achieve their therapeutic effects is via activation of sGC, subsequently leading to the generation of the secondary messenger cyclic guanosine monophosphate (cGMP). CO enhances sGC activity only 4-fold (Brune & Ullrich 1987) in comparison with up to a 400-fold increase elicited by NO (Stone & Marletta 1996). However, in combination with YC-1 (a benzyl indazole derivative) CO stimulates sGC to a similar extent as NO (Friebe *et al.* 1996). There has been much focus on the number of CO-elicited effects as a result of

its activation of sGC (Figure 1.3). However, as also shown in Figure 1.3, CO elicits protective effects independent of both NOS and cGMP.

An alternative, cGMP-independent means by which CO elicits vasorelaxation is via direct enhancement of big-conductance calcium-activated potassium channel (BK_{Ca}) activity in rat vascular smooth muscle cells (Wang & Wu 1997). The opening of BK_{Ca} channels leads to membrane hyperpolarisation, which closes voltage-dependent calcium channels and thus reduces the resting calcium concentration, subsequently leading to relaxation (Hou *et al.* 2009). There are numerous examples of the involvement of MAPK signalling pathways in the activity of CO, involving each of the three major groups: p38 kinase, c-Jun N-terminal kinase (JNK) and the extracellular signal-regulated kinase (ERK) (Kim *et al.* 2006; Wu & Wang 2005). For example, Otterbein and co-workers demonstrated that low concentrations of CO gas (250 ppm) applied to murine macrophages *in vitro* and rodents *in vivo* alleviated inflammation via a pathway involving p38 MAPK. The anti-inflammatory activity was attributed to reduced production of the LPS-induced pro-inflammatory cytokines, tumour necrosis factor-α (TNF-α), interleukin-1β (IL-1β) and macrophage inflammatory protein-1β, and increased accumulation of the anti-inflammatory cytokine IL-10 (Otterbein *et al.* 2000). Additionally, in murine RAW264.7 macrophages stimulated with LPS, inhibition of JNK phosphorylation by CO gas (250 ppm) prevented activation of the AP-1 transcription factor required for IL-6 gene expression, and the survival effect of CO was abrogated in mice deficient in the JNK pathway (Morse *et al.* 2003). Suppression of cytokine production has also been attributed to CO-elicited inhibition of ERK activation, thus leading to suppression of T cell proliferation (Pae *et al.* 2004). The p38 MAPK pathway was also reported to mediate the anti-apoptotic activity of extremely low levels of CO gas (15 ppm) during anoxia-reoxygenation in rat pulmonary artery endothelial cells, and in ischemia reperfusion injury in the mouse lung (Zhang *et al.* 2003). Furthermore, p38 MAPK has been implicated in the CO-elicited protection of endothelial cells from TNF-α-mediated apoptosis. This involved cooperation between HO-1/CO and nuclear factor-κB (NF-κB)-dependent apoptotic genes (Brouard *et al.* 2002).

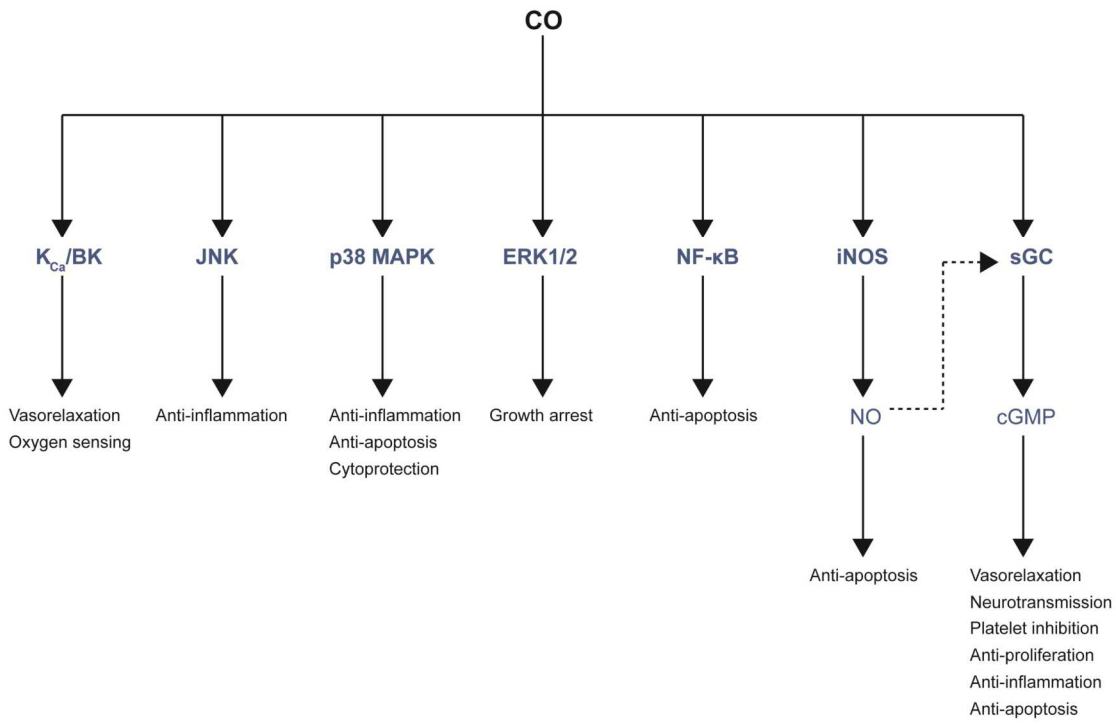

Figure 1.3. Pathways for CO-mediated protective effects. Carbon monoxide (CO); calcium signalled potassium channels (K_{Ca}); big-conductance calcium-activated potassium channel (BK); c-Jun N-terminal kinase (JNK); p38 mitogen activated protein kinase (p38 MAPK); extracellular signal-regulated kinases (ERK1/2); nuclear factor kappa-light-chain-enhancer of activated B cells (NF-κB); inducible nitric oxide synthase (iNOS); nitric oxide (NO); soluble guanyl cyclase (sGC); cyclic guanosine monophosphate (cGMP). The information enabling the generation of this figure was sourced from the following references (Lee & Otterbein 2004; Mann & Motterlini 2007).

Direct interactions between CO and proteins such as MAPK seem unlikely as such proteins lack a metal centre to which the molecule can coordinate. Therefore, although these pathways appear to be involved in the protective effects of CO, the exact mechanism by which the gas transduces its signal remains unclear. Perhaps to better understand CO action it is necessary to look more closely at its relationship with established targets, e.g. haem proteins.

Mitochondria may seem an unlikely candidate for mediating CO-elicited effects due to the well-known targeting of CO to the respiratory chain (sections 1.2 and 1.3.2), but investigations using physiological concentrations of the gas suggest otherwise, with a recent review highlighting the effects of interactions between CO and mitochondria (Queiroga *et al.* 2012). For example, CO-elicited inhibition of cytochrome *c* oxidase in murine macrophages, and consequent generation of low levels of ROS, was implicated in the anti-inflammatory activity of the gas (Zuckerbraun *et al.* 2007). ROS generated by mitochondria were also demonstrated to play a role in the CO-induced activation of mitochondrial biogenesis in the mouse heart. Here, transient elevations in cellular CO by 5 - 20-fold resulted in significant increase in the copy number of mitochondrial DNA, the content of respiratory complex I - V and mitochondrial density (Suliman *et al.* 2007). In a more recent study, low concentrations of CO (10 μM) were shown to elicit ROS-mediated inhibition of mitochondrial membrane permeabilisation in isolated liver mitochondria. This was demonstrated by the prevention of mitochondrial swelling, mitochondrial depolarisation and the opening of a non-specific pore in the inner membrane. In context, this may partly explain the anti-apoptotic activity of CO in hepatocytes, and/or the liver, by preventing the release of pro-apoptotic factors into the cytosol (Queiroga *et al.* 2011). Furthermore, in an experimental model of cardiopulmonary bypass and hypothermic cardiac arrest in pigs, pre-treatment with CO via inhalation resulted in higher levels of ATP and phosphocreatine, suggesting that CO leads to more effective ATP generation for cardiac function and thus improves the condition of the heart (Lavitrano *et al.* 2004). Interactions between CO and NADPH oxidase have also been suggested as a means of CO-elicited therapeutic activity. For example, CO generated via induction of HO-1, or administered as a gas (250 ppm), inhibited platelet-derived growth factor-induced migration of rat smooth muscle cells by inhibiting NADPH oxidase activity, and thus ROS generation. Such an effect may, in

part, explain the beneficial connotations associated with CO in terms of arterial inflammation and injury (Rodriguez *et al.* 2010).

As mentioned above, another key area in which CO has a clinical application, in addition to cardiovascular disease and inflammation, is in the preservation of organs and the alleviation of conditions associated with transplantation. Kidney grafts of rodent recipients exposed to CO (250 ppm) showed down-regulation of the pro-inflammatory cascade observed in control grafts, in addition to improved blood flow and reduced apoptosis of tubular epithelial cells, a hallmark of renal ischemia reperfusion injury (Neto *et al.* 2004). The same group reported similar protective effects of CO administered *ex vivo* to intestinal (Nakao *et al.* 2006) and kidney (Nakao *et al.* 2008) grafts, i.e transplantations were performed after preservation of the organs in solutions supplemented with CO gas. In the former study, the effects of CO were reversed by an inhibitor of sGC, suggesting an involvement of the sGC/cGMP pathway (Nakao *et al.* 2006). The effects of CO here have also been demonstrated in porcine models. Inhalation of CO at 2 - 3 mg/kg for 1 h at the time of renal allograft transplantation reduced ischemia reperfusion injury and restored kidney function more rapidly than in air-treated swine. Additionally, microarray analysis of biopsy samples revealed inhibition of pro-inflammatory and heat shock protein gene expression (Hanto *et al.* 2010). Successful *ex vivo* application of CO gas was also demonstrated in a porcine model of transplant-induced ischemia reperfusion injury (Yoshida *et al.* 2010). Studies using larger animal models have highlighted the pharmacological potential of CO elsewhere. For example, CO inhalation (250 ppm) prior to or after cardiopulmonary bypass (CPB) was shown to alleviate lung injury induced by CPB via anti-inflammatory, anti-apoptotic and cytoprotective effects, as well as induction of the heat shock response (Goebel *et al.* 2008; Goebel *et al.* 2011). Also, CO administered via inhalation at a concentration of 500 ppm for 6 h reduced LPS-induced lung inflammation in cynomolgus macaques (Mitchell *et al.* 2010).

1.4.2 Inhalation therapy

As can be seen by the examples introduced above, the pleiotropic beneficial effects of CO are applicable in a number of disease states. Such findings have fuelled investigations into a suitable mode of delivery of the gas, with initial efforts focusing on

inhalation therapy. Although this raises concerns due to the well established toxicity of CO, other noxious gases have already been approved for use in the clinic: inhaled NO is utilised as a treatment for infants suffering from pulmonary hypertension (Bloch *et al.* 2007), and H_2S is currently in clinical development as an intravenous pharmaceutical agent (Szabo 2007). The properties of CO that support its successful application include its relatively un-reactive nature, chemical stability and reversible interaction with targets, which by conventional thinking are limited to transition metal-containing proteins. Importantly, CO is not metabolised in mammals, rather it is eliminated from the lungs in its original state (Motterlini & Otterbein 2010). Concentrations of COHb between 15 - 20 % have been deemed the 'biological threshold' for CO tolerance in humans, with higher concentrations likely to elicit severe injury (Foresti *et al.* 2008).

Completion of the first Phase I trial in healthy humans showed that administration of CO at 3 mg/kg/h for a single 1 h dose, or as a course for 10 days (COHb levels increased by c. 12 %), did not elicit severe adverse effects (Motterlini & Otterbein 2010). Similarly, a pilot study revealed that 100 - 125 ppm CO elicited anti-inflammatory activity in patients suffering from chronic obstructive pulmonary disease and was well tolerated with a maximum resultant COHb level of 4.5 % (Bathoorn *et al.* 2007). Additional clinical trials testing the suitability and efficacy of inhaling CO mixed with air at a typical concentration of 250 ppm have been reported in different systems: lung inflammation (Phase I), kidney transplantation (Phase II) and the effect of HO-1 activity in male subjects after addition of haem arginate as a substrate for HO-1 (Phase I). The last was followed by a trial testing the effects of HO-1 induction in cardiac injury after myocardial infarction (Phase II/III) (Mann 2010). Furthermore, Phase I and Phase II clinical trials have been planned to determine whether very low doses of CO can shorten the duration of post-operative ileus and/or prevent the development of complications associated with this condition following colon surgery (Gullotta *et al.* 2012).

Although CO inhalation therapy may appear promising, challenges and concerns still cloud its potential use in the clinic. The high binding constant of CO to haemoglobin and its much lower binding constant to its possible targets (section 1.4.1) suggest that COHb is an unlikely candidate for the efficient transfer of the gas. However, the finding by Goldbaum *et al*. (1975) that CO is toxic when dissolved in plasma, whereas

haemoglobin-bound CO is not (section 1.3.2), may explain the paradoxical efficacy of inhaled CO. The temporal dissolution of the gas in plasma before it replaces O_2 bound to haemoglobin after a few minutes, may provide a window of time in which CO can be delivered to its targets throughout the body (Mann 2010). This subsequently leads to questions regarding the necessary duration of CO exposure and thus the COHb concentration that is required to achieve therapeutic effects. Furthermore, it is important to establish whether multiple exposures to low levels of CO will be as effective as one-time dosing at higher concentrations, and also whether a defined CO-dosing regimen will be applicable universally (Motterlini & Otterbein 2010). Directly relevant to such queries is the study previously mentioned by Mitchell and colleagues on cynomolgus macaques (section 1.4.1). To see the therapeutic effects of CO, prolonged (6 h) inhalation of the gas at relatively high concentrations (500 ppm) was required, which resulted in high levels of COHb (exceeding 30 %). The concentration of CO typically used in rodent and porcine models without deleterious effects (250 ppm) also resulted in relatively high COHb levels (c. 25 %) and was ineffective in this larger animal model (Mitchell *et al.* 2010). Such concerns were the catalyst for developing alternative methods of CO administration that constitute a safer and more efficient means of CO delivery to target tissues.

1.4.3 Development of carbon monoxide-releasing molecules (CO-RMs)

1.4.3.1 Initial discovery and principles of design

Metal carbonyls were discovered in the 1890's by Ludwig Mond and consist of a transition metal, e.g. manganese, cobalt or iron, surrounded by a certain number of carbonyl groups as coordinated ligands. Such compounds are renowned in the organometallic chemistry field for their versatile use in industrial catalysis and purification processes (Herrmann, 1990). Of particular significance is their susceptibility to modification as a result of the rich chemistry of the transition metals. Release of CO as well as toxicity and solubility in water can be adjusted by coordinating biological ligands onto the metal centre (Motterlini *et al.* 2003). The pioneers of the CO-RM field, Mann and Motterlini, exploited the natural interaction between CO and transition metals with the intention of providing a new means by which CO-delivery can be achieved. The advent of CO-RMs provides a number of advantages over CO inhalation. For example, CO is harnessed in a solid form therefore

preventing lethal leakage of the gas during storage, and dissolution of CO-RMs prior to use enables intravenous administration, which in turn would enable localised delivery of the CO donor to target sites.

There are a number of essential properties that are necessary for the development of a successful CO-RM. The compound must be pure and stable in solution after synthesis, non-toxic, preferably water-soluble for ease of use, and capable of relatively fast liberation of CO in biological environments after administration. The release of the carbonyl(s) from the metal backbone can be achieved by a number of mechanisms, typically including: 1) the presence of a suitable ligand, such as a haem protein like myoglobin that has a high affinity for CO, 2) coordination of a ligand to the transition metal thereby disrupting the interaction between CO and the metal, 3) the reduction or oxidation of the compound, 4) photolysis and 5) changes in pH (for a review see (Davidge *et al.* 2009a)).

Since the development of these compounds, which began over 10 years ago, numerous studies have described the use of CO-RMs, as well as the development of new CO-RMs. The literature now reports compounds based on vanadium, chromium, molybdenum, tungsten, manganese, rhenium, iron, ruthenium, cobalt and boron (Mann 2010). Their beneficial effects (a selection of which is introduced in the subsequent sections) were shown to correlate with those previously reported for CO gas (section 1.4.1). Importantly, confirmation that CO liberated from CO-RMs is responsible for the observed therapeutic activity is routinely demonstrated by the use of corresponding inactive compounds that are depleted of CO (Motterlini *et al.* 2005a; Motterlini *et al.* 2003).

1.4.3.2 The first carbon monoxide-releasing molecules

The first CO-RMs to be synthesised were the lipid-soluble dimanganesedecacarbonyl ($[Mn_2(CO)_{10}]$, CORM-1) and tricarbonyldichlororuthenium (II) dimer ($[(RuCl_2(CO)_3)_2]$, CORM-2) (Table 1.2). Both are exclusively soluble in organic solvents, typically dimethyl sulfoxide (DMSO) (Motterlini *et al.* 2002). Their ability to liberate CO was assessed spectrophotometrically by measuring the conversion of deoxy-myoglobin to carbonmonoxymyoglobin (MbCO), a method that has become universal for measuring kinetics of CO release from CO-RMs. Details of CO release from these compounds are

Landscape Table (Table 1.2), refer to page 1 of supplementary document.

shown in Table 1.2. Importantly, toxicity assays revealed that CORM-1 at concentrations up to 100 μM elicited no major toxicity to vascular smooth muscle cells after exposure for 24 h, and concentrations of CORM-2 up to 420 μM did not produce any detectable cytotoxicity during a 3 h exposure. However, > 50 % loss in cell viability was observed after a 24 h exposure to higher concentrations of the latter.

Both CORM-1 and CORM-2 have been reported to elicit a number of beneficial effects that mirror those previously described for the CO/HO pathway (section 1.4.1). CORM-1 (13 μM) significantly delayed vasoconstriction and maintained coronary perfusion pressure in isolated rat hearts treated with the NO synthase inhibitor N^G-nitro-L-arginine methyl ester (L-NAME). Intravenous administration of a single dose of CORM-2 (20 μmol/kg) into rodents, prior to L-NAME, suppressed the rapid increase in blood pressure caused by the latter compound. Importantly, OxyHb saturation remained unchanged throughout this study (Motterlini *et al.* 2002). Further, CORM-1 was seen to elicit cerebral vasodilation *in vitro* by activating large-conductance, calcium-dependent potassium channels in neonatal porcine cerebral arteriole smooth-muscle cells (Xi *et al.* 2004), and *in vivo* in piglets (Koneru & Leffler 2004). A permissive role for NO was implicated in the vasodilation elicited by CO in the latter study. Renal function was also improved by CORM-1 due to dilation of renal arteries and increased glomerular filtration, as well as urinary sodium and water excretion (Arregui *et al.* 2004). Additionally, this compound reduced neutrophil migration, leukocyte rolling and adhesion on endothelial cells in the inflammatory site during carrageenan-induced inflammation. However, this was seen to occur in parallel with an increase (> 74 %) in COHb formation (Freitas *et al.* 2006). All of these effects were suggested to be mediated by the sGC/cGMP pathway.

CORM-2 demonstrated cardioprotective effects by reversible, voltage-independent inhibition of human cardiac L-type calcium channels. Such activity was attributed to CO-elicited generation of ROS from complex III of mitochondria (Scragg *et al.* 2008), subsequently leading to redox modulation of critical cysteine residues in the channel. Inhibition by CORM-2 of NADPH oxidase cytochrome b_{558}, as well as increased mitochondrial ROS production, resulted in decreased phosphorylation of ERK1/2 and expression of cyclin D1, thus leading to inhibition of airway smooth muscle cell proliferation (Taille *et al.* 2005). These studies support the aforementioned idea that CO

elicits beneficial effects by generating low levels of ROS (Zuckerbraun *et al.* 2007) (section 1.4.1). A recent study supports the cardioprotective role of CORM-2 due to alleviation of doxorubicin-induced cardiotoxicity in mice, which was attributed to anti-oxidant and anti-apoptotic properties. However, the authors state that there was a fine line between CORM-2-elicited protection and toxicity, but this was not due to increases in COHb levels (Soni *et al.* 2011). Furthermore, CORM-2 (and CORM-3, section 1.4.3.3) protects against ischemia-induced acute renal failure (Vera *et al.* 2005) and, when administered to donor rats before kidney retrieval, protects renal transplants from ischemia reperfusion injury. This effect was attributed to CORM-2-induced modulation of inflammation (Caumartin et al. 2011). Additional anti-inflammatory activity has been reported. For example, in septic mice, CO liberated from CORM-2 attenuates LPS-induced production of ROS and NO, and via suppression of NF-κB activation, prevents the expression of adhesion molecules such as intercellular adhesion molecule-1 (Cepinskas et al. 2008).

Further reports support the beneficial effects of CORM-1 and CORM-2 in the cardiovascular, renal and neuronal systems that occur as a result of activation of sGC and potassium channels (Boissiere *et al.* 2006; Botros & Navar 2006; Matsuda *et al.* 2004). Other medically favourable effects include anal sphincter relaxation (Rattan *et al.* 2004), modulation of ion transport in human intestinal epithelial cells (Uc *et al.* 2005), immunophotoprotection against ultraviolet radiation in rat skin (Allanson & Reeve 2005) and reducing photocarcinogenesis in mice by modulating the inflammatory response and interfering with tumour development (Allanson & Reeve 2007).

1.4.3.3 The first water-soluble carbon monoxide-releasing molecule

Although the CO-RMs introduced above elicit a number of beneficial effects, they act more as a proof of concept for the use of metal carbonyls as CO carriers, as their pharmacological application is hindered by their lack of solubility in water. This led to the design and synthesis of a water-soluble, ruthenium-based compound, CORM-3 (tricarbonylchloro(glycinato) ruthenium(II), [$Ru(CO)_3Cl$(glycinate)]) (Clark *et al.* 2003) (Table 1.2), which is the compound used in the present work. Ruthenium boasts a versatile oxidation chemistry in aqueous solutions, which allows for the modulation of ligand affinities and substitutions onto the metal centre. Clark and co-workers exploited this feature and subsequently achieved the synthesis of a water-soluble compound using

CORM-2 as a precursor and co-ordinating glycine to the ruthenium centre. Dissolution of CORM-3 in distilled water produces an acidic solution (pH 2 - 3, depending on concentration) due to loss of H^+ and the attack of a carbonyl by hydroxide, i.e. the first step in the water-gas shift reaction (Johnson *et al.* 2007). The compound is relatively stable under these conditions, i.e. it does not lose its capacity for CO release even after incubation at room temperature for 24 h (Clark *et al.* 2003). Furthermore, use of a CO electrode demonstrated the lack of CO release from CORM-3 (100 μM) in an aqueous solution at 37 °C over a period of 83 min (Lo Iacono *et al.* 2011). However, upon addition of an aliquot of the solution to a buffer at physiological pH containing ferrous myoglobin, CO is lost rapidly to the formation of MbCO (Clark *et al.* 2003) (Table 1.2). Also, dissolving CORM-3 in PBS at pH 7 - 7.4 at room temperature enables the liberation of CO over a period of up to 48 h via a currently unknown mechanism. The resultant compound is inactive (measured as a lack of CO release to ferrous myoglobin) and can therefore be used as a negative control (Clark *et al.* 2003; Lo Iacono *et al.* 2011).

Although a promising compound, CORM-3 has a complex, pH-dependent solution chemistry (Johnson *et al.* 2007), which makes it difficult to obtain pure $[Ru(CO)_3Cl(glycinate)]$. Reaction of the compound with hydroxide from water gives rise to $[Ru(CO)_2(CO_2H)Cl(glycinate)]^-$, which exists as a mixture of two of three potential isomers, due to the three carbonyls of CORM-3. If the solution is acidified in an attempt to counteract the formation of this species and yield the desired product ($[Ru(CO)_3Cl(glycinate)]$), an additional species is formed, namely $[Ru(CO)_3Cl_2(NH_2CH_2CO_2H)]$. Further changes occur at physiological pH, but it is unknown whether the species generated are mainly isomers of $[Ru(CO)_2(CO_2)Cl(glycinate)]^{2-}$ or $[Ru(CO)_2(CO_2H)(OH)(glycinate)]^-$ (Mann 2010). Although this complex solution chemistry has impacted identification of the CO release mechanism of CORM-3, it is known that the chloride and glycinate ligands are labile; therefore loss of CO may occur in parallel with their substitution by higher affinity ligands (Clark *et al.* 2003). Candidates include sulfite species, as sodium dithionite enhances CO release from CORM-3, and to a lesser extent thiols, e.g. cysteine and glutathione (Hasegawa *et al.* 2010). A more recent and comprehensive study further supports the involvement of sulfite (McLean *et al.* 2012). Here the authors demonstrated that, contrary to popular belief, in the standard myoglobin assay used to determine rates of CO liberation from

CO-RMs (Motterlini *et al.* 2002), it is the reducing agent sodium dithionite that facilitates release of CO from ruthenium-based CORM-2 and CORM-3, not ferrous myoglobin. In the absence of dithionite, CO is not released to ferrous myoglobin within c. 1 h. Additionally, the effect of dithionite was also attributed to other sulfite-containing compounds, e.g. sodium sulfite and potassium metabisulfite (McLean *et al.* 2012).

As for CORM-1 and CORM-2, CORM-3 mimics the activity of the HO/CO pathway and exogenously applied CO gas. The compound exhibited cardioprotective effects *in vitro* in a model of hypoxia-reoxygenation in rat cardiomyocytes, *ex vivo* in ischemia-reperfusion injury in isolated rat hearts and *in vivo* in cardiac allograft rejection in mice. In each case, the activity of CORM-3 was attributed to the activation of mitochondrial ATP-dependent potassium channels, thus reducing intracellular calcium over-loading. Preliminary data also demonstrated CORM-3-induced increases in HO-1 activity in murine macrophages, which may contribute to the compound's cytoprotective effects *in vivo* (Clark *et al.* 2003). Additional examples of CORM-3 activity include limitation of myocardial ischemia-reperfusion injury *in vivo* (Guo *et al.* 2004), modulation of vessel tone and blood pressure by eliciting vasorelaxation (Foresti *et al.* 2004) and reduction of human platelet aggregation (Chlopicki *et al.* 2006). The anti-inflammatory properties of CORM-3 have also been exploited to mitigate microglia activity in strokes, as well as other neuroinflammatory diseases (Bani-Hani *et al.* 2006). In a recent rat model of haemorrhagic stroke, pre-treatment with CORM-3, or administration during the post-acute inflammatory phase following collagenase-induced intracerebral haemorrhage, promoted neuroprotection. However, administration of the compound 3 h after collagenase significantly increased brain injury and TNF-α production (Yabluchanskiy *et al.* 2012).

Studies utilising CORM-3 have also provided further support for the potential role of mitochondria in transducing the protective effects of CO. In a mouse model of peritonitis-induced sepsis, CORM-3-derived CO improved cardiac mitochondrial dysfunction by eliciting a mild oxidative response. CO-induced ROS generation stimulated mitochondrial biogenesis with increased mitochondrial DNA copy number and expression of peroxisome proliferator-activated receptor γ co-activator-1α, leading to improved survival of septic animals (Lancel *et al.* 2009). However, Sandouka and co-

workers revealed that CO liberated from CORM-3, as well as CORM-2 (section 1.4.3.2) and CORM-A1 (section 1.4.3.4), significantly decreased state 3 respiration (active respiration in the presence of ADP) in rat kidney mitochondria, suggesting an impairment of oxygen uptake and oxidative phosphorylation. Interestingly, they also observed a marked increase in state 4 respiration (ADP-independent O_2 consumption rate), i.e. more oxygen was consumed when it was not used for ATP synthesis. The authors proposed that CO released from the CO-RMs reduced the tightness of coupling between electron transfer and ATP synthesis, i.e. they act as uncoupling agents (Sandouka *et al.* 2005). Further investigations by the same group confirmed this activity using CORM-3. In addition they demonstrated CORM-3-induced decreases in mitochondrial membrane potential ($\Delta\psi$), as well as attenuation of CORM-3 activity by pharmacological agents known to inhibit mitochondrial uncoupling, e.g. guanosine 5'-diphosphate and carboxyatractyloside. However, they exclude a 'classical' uncoupling mechanism, i.e. protonophore activity, due to the ineffectiveness of a known inhibitor, 6-ketocholestanol, against CORM-3. The 'uncoupling' effect was attributed to CO released from the compound, since an inactive compound, or the presence of myoglobin as a CO scavenger, inhibited the effects of CORM-3. Overall, this finding may have highlighted a novel method for therapeutic application in conditions where targeting of mitochondrial uncoupling and metabolism are required (Lo Iacono *et al.* 2011).

1.4.3.4 Additional carbon monoxide-releasing molecules of note

The first non-metal CO-RM to be synthesised was the water-soluble sodium boranocarbonate, CORM-A1 ($Na_2[H_3BCO_2]$) (Motterlini *et al.* 2005b) (Table 1.2). Instead of a transition metal the compound has a carboxylic group that is converted into CO through hydrolysis. The release of CO from CORM-A1 under physiological conditions (as detailed in Table 1.2) is much slower than for CORM-2 and CORM-3. This was considered an advantage for the treatment of chronic diseases where the continuous effect of CO is better suited. Also, it more closely mimics the function of HO, which generates CO in a sustained manner. In keeping with its chemical properties, the compound was shown to elicit sGC-dependent vasodilation in isolated, precontracted aortic rings and reduce mean arterial pressure in rodents. An additional advantage of CORM-A1 is the more chemically inert nature and lesser toxicity of boron in comparison with the typically utilised transition metals (Motterlini *et al.* 2005b).

A newly synthesised, manganese-based, water-soluble compound has recently been reported, CORM-401 ([$Mn(CO)_4\{S_2CNMe(CH_2CO_2H)\}$]) (Crook *et al.* 2011) (Table 1.2). Unlike the CO-RMs described above, CORM-401 releases at least 3 moles CO per mole of compound. In theory, this should allow for the administration of lower concentrations of the CO-RM, which minimises exposure of the recipient to the backbone and any toxicity as a consequence. The compound is relatively stable in water or PBS buffer, but CO is rapidly lost in the presence of a suitable biological receptor (Table 1.2). As described for CORM-2 and CORM-3 (section 1.4.3.3) dithionite also enhanced the rate of CO release from CORM-401; however, CO liberation was not dependent on the presence of dithionite (McLean *et al.* 2012). Assays of RAW264.7 murine macrophage cell viability after exposure to 100 μM CORM-401 revealed minimal cytotoxicity, and its therapeutic potential was confirmed by a 70 % reduction in LPS-induced nitrite production (Crook *et al.* 2011). Furthermore, the compound has less complex solution chemistry and a manganese core, a metal that is found naturally within the body.

1.4.3.5 Advances in the field

Although successful in emulating the beneficial activity observed with CO gas, the existing CO-RMs have their limitations, in particular fast and unspecific CO release. This led to the evolution of compound design that further exploits the rich chemical flexibility of metal carbonyls, including exploring novel CO-release mechanisms that allow greater control over CO delivery. A prime example of this is the use of acyloxybutadiene-iron tricarbonyl complexes as enzyme-triggered CO-RMs (ET-CORMs), for which CO release is induced by enzymatic cleavage of the ester functionality (Romanski *et al.* 2011). Other groups have taken advantage of the potential of the CO release mechanisms that were initially tested, for example photodissociation (Schatzschneider 2011).

Additional advances include tailoring compounds for specific applications. Pitchumony and co-workers synthesised derivatives of CORM-A1 (section 1.4.3.4) in an attempt to yield compounds that maintain their CO-releasing properties for longer. This was achieved by converting the carboxylic group of the parent compound to an amide. CO cleavage from CORM-A1 is initiated by protonation of the carboxylate group and so by replacing this with an amide, for which protonation is more difficult, CO release was

slowed. In their concluding remarks, they suggest that a further improvement would be the use of molecules such as peptides, which would enable targeting of the CO-RMs to specific sites (Pitchumony *et al.* 2010). An example of creating a compound with a specific target was recently reported for cases of severe malaria (Pena *et al.* 2012). This study describes the design and synthesis of a new ruthenium (II) tricarbonyl (ALF 492, $Ru(CO)_3Cl_2$(Gal-S-Me)) that exhibits improved water solubility due to a galactose (Gal)-derived ligand coordinated to the ruthenium centre via a thioether linkage. The galactose ligand also confers a degree of specificity for the liver by targeting asialoglycoprotein receptors, which is desirable due to the role of the liver in the regulation of genes that contribute to the control of inflammation, e.g. HO-1. Accumulation of the compound in the liver, and subsequent induction of HO-1 expression by liberated CO, prevented an exacerbated host inflammatory response that is typical during *Plasmodium* infection (Pena *et al.* 2012). Interestingly, a couple of years earlier Hasegawa *et al*. (2010) described the synthesis of novel CO carriers for use in immunotherapy; ruthenium-based carbon monoxide-releasing micelles. Polymeric micelles were chosen to carry the complex ($Ru(CO)_3Cl$(amino acidate)) to enable targeted delivery of CO to lymph nodes. The CO-releasing micelles successfully attenuated the LPS-induced inflammatory response of human monocytes and were found to be non-toxic at concentrations below 1 mM (Hasegawa *et al.* 2010).

1.5 Carbon monoxide in microorganisms

Although the biological effects of CO are currently best described in mammalian systems, its pleiotropic activity is clearly complex and its precise modes of action are unclear. It may be possible to unravel more fully the mechanisms of CO action by exploiting the experimental advantages of microbes, namely their genetics, biochemistry and physiology. The literature regarding CO in this context is scant; however, it is well known that CO interacts with a number of proteins in bacteria, examples of which are shown in Figure 1.4. Additionally, the general consensus of recent studies demonstrating the anti-bacterial power of CO liberated from CO-RMs provides equal promise when considered in terms of positive clinical applications, in this case as a preventative therapy against bacterial infections (section 1.5.3). The paradox concerning CO in mammals is also mirrored in microbiology. Despite its

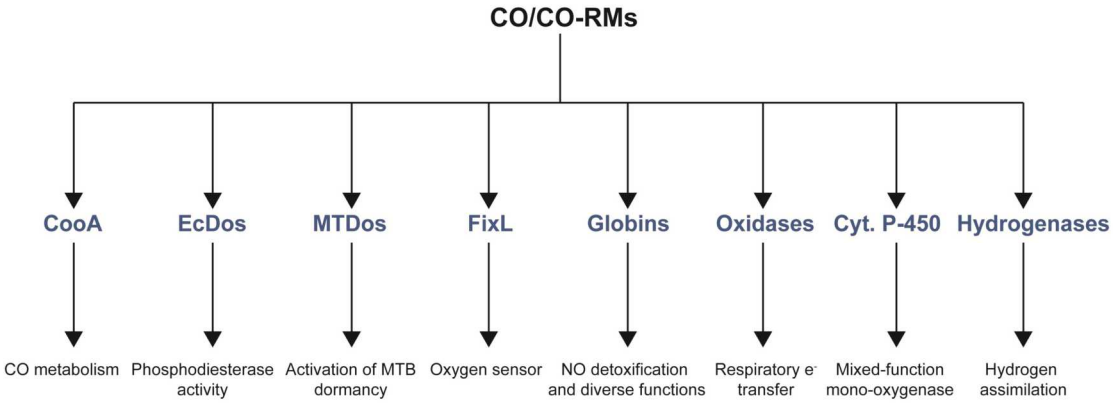

Figure 1.4. Bacterial proteins reported to interact with CO, and their physiological functions. *Escherichia coli* phosphodiesterase (EcDos), *Mycobacterium tuberculosis* dormancy system (MTDos), *M. tuberculosis* (MTB), Cytochrome P-450 (Cyt. P-450).

inherent toxicity, not only can some microbes utilise CO as a source of energy, but some species also generate CO endogenously as a result of microbial HO activity. It is therefore important to first introduce the natural interactions between CO and microbes.

1.5.1 Carbon monoxide metabolism and sensing

There are numerous examples of aerobic and anaerobic bacteria that are capable of using CO as a sole carbon and energy source (Ragsdale 2004). Energy transduction is achieved via CO oxidation, the physiology of which is based on the water-gas shift reaction:

$$CO + H_2O \rightarrow CO_2 + 2H^+ + 2e^-$$

The low redox potential of CO/CO_2 (-524 to 558 mV) allows anaerobic microorganisms to couple CO oxidation to a number of different terminal electron acceptors (Oelgeschlager & Rother 2008). The best established example of microbial CO utilisation is via the CO dehydrogenase (CODH) and hydrogenase system in the anaerobic, purple, non-sulfur, phototrophic bacterium *Rhodospirillum rubrum* (Bonam *et al.* 1989; Kerby *et al.* 1995). Genes encoding proteins required for CO metabolism in *R. rubrum* are located on the *coo* (CO oxidation) operon and include *cooS* (encoding a nickel-containing CODH), *cooF* (encoding a membrane-associated electron transfer Fe-S protein) and *cooH* (encoding a CO-tolerant hydrogenase) (Kerby *et al.* 1992). Induction of gene expression occurs in the presence of CO, which is sensed by a haem-containing protein, CooA (Shelver *et al.* 1995), a member of the CRP/FNR family of transcriptional activators (Aono 2003). The activity, i.e. DNA-binding capability, of CooA depends on the redox state of the haem moiety and the presence of CO. The protein exists either in an oxidised form where the haem is in the ferric (iron(III)) state (inactive), or in a reduced form where the haem is in the ferrous (iron(II)) state and is therefore capable of CO-binding, subsequently leading to its activation (Shelver *et al.* 1997). Binding of CO displaces an amino acid ligand of the ferrous haem, Pro2 (Yamamoto *et al.* 2001). This in turn triggers a conformational change in the protein whereby the haem moves upwards into an adjacent hydrophobic cavity, which causes a rearrangement of the hinge between the C- and D-helices, thus enabling the required orientation for DNA binding (Ibrahim *et al.* 2007).

A number of other groups of microorganisms also metabolise CO, including hydrogenogenic bacteria and archaea, methanogenic archaea (e.g. *Methanosarcina acetivorans*), aerobic carboxytrophic bacteria (e.g. *Oligotropha carboxidovorans*), aectogenic bacteria (e.g. *Moorella thermoacetica*) and sulfate-reducing bacteria (e.g. *Desulfovibrio vulgaris*) (Davidge *et al.* 2009a). Interestingly, the latter group includes an anaerobic bacterium, *Desulfotomaculum carboxydovorans*, which is capable of growth under an atmosphere of pure CO, suggesting the evolution of a currently unknown mechanism(s) that can detoxify or counteract CO toxicity (Parshina *et al.* 2005). The acetogen *M. thermoacetica* is a well established model of the activity of CODH in the acetyl CoA pathway for CO_2 fixation. Here, CODH catalyses the reverse of the aforementioned reaction, i.e.:

$$2e^- + 2H^+ + CO_2 \rightarrow CO + H_2O$$

Acetyl CoA synthase (ACS) then catalyses the condensation of CO with a methyl group and coenzyme A to form acetyl-CoA, which is used in ATP generation or cellular biosynthesis (Ragsdale 2004). *Carboxydothermus hydrogenoformans* is an anaerobic, thermophilic, hydrogenogenic carboxydotroph that provided the first genome sequence of a CO-utilising microbe and was found to encode five CODH (Wu *et al.* 2005). This bacterium was used as a model for a recent genomic and phylogentic survey of CODH operons and *cooA* genes in CooA-containing bacteria, which revealed the presence of two distinct groups of CooA homologues, CooA-1 and CooA-2 (Techtmann *et al.* 2011). Purification of the homologues from *C. hydrogenoformans* revealed that CooA-1 specifically regulates the CODH/hydrogenase system, whereas CooA-2 (found only in genomes encoding multiple CODH) was able to regulate both the CODH/hydrogenase and CODH/ACS systems. Dual CooA homologues therefore appear to allow the coordination between multiple pathways, thus ensuring efficient utilisation of CO (Techtmann *et al.* 2011).

In aerobic bacteria, CO oxidation occurs via a molybdenum-containing CODH that is encoded by the *cox* operon. Aerobic CODH consists of three subunits: an Fe-S protein, a flavin adenine dinucleotide-binding protein and a catalytic, molybdenum cytosine dinucleotide-binding protein, encoded by *coxS*, *M* and *L* genes, respectively. Electrons

derived from the oxidation of CO in aerobes are transferred to the respiratory chain for the reduction of O_2 (King & Weber 2007). The most notable species in this group include *Pseudomonas carboxydohydrogena*, which was one of the first aerobic carboxydotrophs to be identified (Kim & Hegeman 1981), and *Oligotropha carboxidovorans*, one of the most established examples of CO utilisation in aerobes. Interestingly, the CODH structural genes (*coxMSL*) in *O. carboxidovorans* make up only part of a large *cox* gene cluster that is specifically and co-ordinately transcribed in the presence of CO (Santiago *et al.* 1999). An interesting example of aerobic CO utilisation is seen in the chemolithotrophic H_2 bacterium *Streptomyces thermoautotrophicus*, whereby a novel linkage between CODH and a nitrogenase enables the oxidation of the gas during both energy metabolism and nitrogen fixation (Madigan *et al.* 2003). In addition, mycobacteria metabolise CO via CODH (Park *et al.* 2003), which exhibits NO dehydrogenase activity (Park *et al.* 2007). CO has also been implicated in the dormancy of *Mycobacterium tuberculosis* as the novel haem-based sensor histidine kinases involved in this system, DosS and DosT, are able to sense and bind CO (Kumar *et al.* 2007). Furthermore, physiological concentrations of CO can induce the Dos regulon (Kumar *et al.* 2008; Shiloh *et al.* 2008) (section 1.5.3.4).

Additional sensing mechanisms have been described for bacterial species that utilise CO. For example the anaerobic bacterium *Desulfovibrio* is able to sense the gas via its tetrahaem cytochrome c_3 (Takayama *et al.* 2006). In *Burkholderia xenovorans*, which can utilise CO under anaerobic conditions in the presence of nitrate (King 2006), a haem-containing protein RcoM acts as a CO sensor (Kerby *et al.* 2008). Potential haem-containing sensors have also been suggested, including FixLJ, EcDos, AxPDEA1, the HemATs and the globin-coupled sensors (Davidge *et al.* 2009a). It is therefore evident that, in an increasing number of microbial systems, haem-containing proteins are not only targets of CO, but also act as sensors that induce the transcription of CO-oxidising machinery upon detection of the gas.

1.5.2 Microbial haem oxygenases

The generation of CO from the breakdown of haem by bacteria was first identified by gas chromatography following aerobic incubation of *Staphylococcus* and *Bacillus* species with haem-containing compounds (Engel *et al.* 1972). However, only recently

was it discovered that a number of bacteria possess enzymes analogous to mammalian HO-1. As in mammals, bacterial HOs fall into two classes, the second of which contains completely novel enzymes. It is difficult to pinpoint the necessity for HO expression as the enzymes have been found in Gram negative and Gram positive organisms, as well as in both commensal and pathogenic species. Moreover, the identity between bacterial HOs is only maintained in important regions, making it difficult to identify these enzymes via similarity searches of published genomes. Three possible roles for bacterial HOs have been reported: acquisition of iron, production of chromophores, and, although documented to a lesser extent, the removal or consumption of O_2.

The Gram positive bacterium *Corynebacterium diphtheriae*, the causative agent of diphtheria, expresses HmuO, which was the first bacterial HO to be identified. It shares 33 % sequence identity and 70 % similarity with human HO-1 (Schmitt 1997b) and plays a role in iron acquisition, which was demonstrated by the optimal expression of the *hmuO* gene under iron-limiting conditions in the presence of haem or haemoglobin. Furthermore, *hmuO* was found to be regulated by the iron-dependent repressor DtrX (Schmitt 1997a) and by the haem-regulated two-component transcriptional systems ChrAS (Bibb *et al.* 2005) and HrrAS (Bibb *et al.* 2007). *Neisseria* species, both commensal and pathogenic, express HemO that breaks down haem as a source of iron (Zhu *et al.* 2000a; Zhu *et al.* 2000b). This was the first HO to be identified in a Gram negative bacterium and exhibited spectral properties similar to those of HmuO from *C. diphtheriae* and mammalian HO. However, their sequence identity revealed high similarity only in regions of importance (Zhu *et al.* 2000b). Other bacterial HOs involved in iron acquisition include the putative HO Cj1613c from the foodborne pathogen *Campylobacter jejuni*, which is regulated by iron and the ferric uptake regulator Fur (Ridley *et al.* 2006), and HugZ from *Helicobacter pylori*, which is regulated by iron levels and generates biliverdin and CO (Guo *et al.* 2008). Although non-pathogenic *E. coli* K12 is not known to possess a HO, the enterohemorrhagic strain *E. coli* O157:H7 expresses ChuS (Suits *et al.* 2005). Unlike other known bacterial HOs, ChuS is a dimer with N- and C-terminal halves that each act as a functional HO. However, HOs in *Enterobacter*, *Erwinia*, *Shigella*, and *Yersinia* showed significant sequence similarity to ChuS, suggesting the presence of this unusual enzyme in a number of pathogenic species (Suits *et al.* 2005).

The activity of bacterial HOs in the production of chromophores has been attributed to BhpO from *Pseudomonas aeruginosa*, the gene for which is located in the same operon as *bhpP*, encoding a bacterial phytochrome. The breakdown of haem by BhpO generates the typical form of biliverdin (i.e. biliverdin IX-α), which is a precursor for the synthesis of BhpP (Wegele *et al.* 2004). Furthermore, the cyanobacterium *Synechocystis* can synthesise phycobilin chromophores by the breakdown of haem using Syn HO-1 (Migita *et al.* 2003). In addition to BhpO, *P. aeruginosa* expresses PigA, which is under the control of Fur and is expressed only under iron-limiting conditions (Vasil & Ochsner 1999). PigA shows 37 % similarity to HemO from *Neisseria* species; however, the breakdown of haem by PigA yields unusual forms of biliverdin (IX-β and -γ instead of IX-α), suggesting that the enzyme has novel regiospecificity (Ratliff *et al.* 2001). HemT from *Clostridium tetani*, the causative agent of tetanus, is an example of a HO that has been proposed to act in the consumption of O_2. *C. tetani* is an anaerobic bacterium that has to colonise open, O_2-rich wounds in order to gain access to a host. The ability of the bacterium to express an enzyme that can consume O_2 is therefore pivotal for its survival. Interestingly, a CODH was discovered downstream of *hemT* and may be involved in utilisation of the generated CO (Bruggemann *et al.* 2004).

Staphylococcus aureus expresses two HOs involved in iron acquisition; however, they lack any identifiable sequence similarity and are structurally unrelated to those described above. They were therefore categorised as members of the novel class two enzymes. Genes encoding *S. aureus* HOs, IsdG and IsdI, are regulated by Fur but have different loci; *isdG* is part of an operon that contains iron-responsive genes, whereas *isdI*, a paralogue of *isdG*, is located outside of the *isd* operon (Skaar *et al.* 2004). HOs that have *isdG*-like sequences have been identified in other Gram-positive bacteria including *Bacillus* species and in *Listeria monocytogens* (Wu et al. 2005). In particular, *Bacillus anthracis* contains a HO called IsdG that shows 35 % identity with *S. aureus* HOs. Although it is required for growth when hemin is the only iron source, it has also been implicated in the bacterium's defence against haem-mediated toxicity as a result of hemin accumulation within the cell (Skaar *et al.* 2006). Weak homologues of *S. aureus* IsdG were found in the Gram-negative bacterium *Bradyrhizobium japonicum*, termed HmuQ and HmuD, and were shown to enable haem utilisation when expressed in a *Corynebacterium ulcerans* HO mutant. Furthermore, homologues of HmuQ and HmuD

were identified in many bacterial genera representing numerous taxonomic groups (Puri & O'Brian 2006).

Homologues of HO have also been identified in yeast, namely *Saccharomyces cerevisiae* and *Candida albicans*. Although structurally distinct, Hmx1 of *S. cerevisiae* shares 21 % sequence identity with human HO-1 and 19 % identity with HmuO from *C. diphtheria*. A role for Hmx1 in the degradation of haem under iron-limiting conditions was demonstrated by a lack of haem degradation in a strain deficient in the *hmx1* gene. However, membranes derived from the *hmx1*Δ strain were still able to degrade haem, albeit by less than half of the capacity of the wild type, suggesting the presence of an additional protein with similar function. Furthermore, growth of *hmx1*Δ was stimulated by hemin, although it was not capable of matching the cell density or growth rate of the wild type. The mutant also exhibited reduced iron accumulation and expansion of intracellular haem pools, which were restored by expression of HmuO as a substitute for Hmx1 (Protchenko & Philpott 2003). The putative HO of *C. albicans*, CaHMX1, has 25 % identity with human HO-1 and 35 % identity with Hmx1 from *S. cerevisiae*. It is also required for iron acquisition and expression of the *CaHMX1* gene is strongly induced by iron deprivation and hemin exposure. A double mutant was created by knocking out both copies of the *CaHMX1* gene and was shown to be unable to grow on hemin as the sole iron source, but growth was restored to normal levels after reconstitution with a wild type allele of *CaHMX1* (Santos *et al.* 2003). In an additional study, haemoglobin was shown to induce *CaHMX1* gene expression under conditions of iron sufficiency, a role also attributed to the cobalt analogue of haemoglobin, CoPPIX-globin. However, apoglobin was ineffective suggesting that it is the native conformation induced by porphyrin binding that is required for induction, not iron. Haem oxygenase activity was also confirmed in this study by the generation of α-biliverdin in cultures grown overnight in the presence of haemoglobin or hemin (Pendrak *et al.* 2004a).

Although some commensal species express HO, it appears that this feature is mainly one of pathogenic microbes, which may provide a survival advantage during colonisation of a host. In addition to the advantages in haem utilisation described above, the generation of CO as a result of HO activity may also be useful. For example, CO production could constitute a mechanism by which pathogens are able to kill competing, commensal microorgansims and better colonise a host (see section 1.5.3 for CO toxicity

against bacteria). It may also be hypothesised that bacteria expressing HO are exposed to endogenous CO, and thus may be adapted to resist CO when it is applied exogenously (in the gaseous form or via CO-RMs) due to inbuilt detoxification mechanisms. It is also interesting to note that bacterial HOs have been considered as potential anti-microbial targets (Furci *et al.* 2007). Computer-aided drug design was used to screen 800,000 compounds in order to identify chemical entities with a high probability of binding to HemO from *N. meningitidis*. Additionally, several of these compounds were able to bind PigA from *P. aeruginosa*. The efficacy of potential inhibitors was confirmed by the elicited inhibition of α-biliverdin production in *E. coli* cells expressing HemO, as well as inhibition of *P. aeruginosa* growth in the presence of haem or haemoglobin as the sole iron source.

1.5.3 Anti-bacterial activity of carbon monoxide

The first reports alluding to a possible anti-bacterial action of CO described the inhibition of *E. coli* DNA replication, which was attributed to the depletion of intracellular ATP (Cairns & Denhardt 1968) and deoxynuceloside triphosphates (Weigel & Englund 1975). Direct inhibition of enzymes involved in replication was ruled out due to the inhibition of DNA replication in aerobic but not anaerobic cells. Rather, depletion of ATP levels as a result of CO-elicited inhibition of cytochrome *c* oxidase, and thus the electron transport chain, was proposed (Weigel & Englund 1975). Additionally, a more recent study showed that exposure of the CODH-containing, sulfate-reducing bacterium *Desulfovibrio desulfuricans* to 5 - 6 % CO delayed growth and increased intracellular ROS levels as a consequence of inhibiting superoxide dismutase (Davydova & Tarasova 2005). Another recent report demonstrated that packaging meat in a CO atmosphere reduced bacterial growth (Brooks *et al.* 2006).

Furthermore, the beneficial activity of CO in models of sepsis has become apparent over the past decade (Chin & Otterbein 2009; Chung *et al.* 2009; Sun & Chen 2009), although the current literature gives quite conflicting stories. On the one hand, CO administered either via CO-RMs, or by induction of HO-1 expression, reduced NO production in LPS-stimulated murine macrophages (Sawle *et al.* 2005; Srisook & Cha 2005) and CORM-2 suppressed the oxidative burst, which acts as a first line of defence against invading pathogens (Srisook *et al.* 2006). This is consistent with previous

reports on the anti-inflammatory activity of CO, but suggests the innate immune response is less equipped to deal with a bacterial infection. On the other hand, CO was shown to augment phagocytosis (Chung *et al.* 2008; Otterbein *et al.* 2005), thus leading to enhanced bacterial clearance. This topic is discussed in detail in Chapter 6 where it has direct relevance to the work presented. The main focus of the following sections is the direct effect of CO on bacteria, typically assessed via use of CO-RMs. The literature on this subject has increased over the past few years, encompassing model laboratory organisms, pathogenic species and clinical isolates. For reference, a summary of these studies, which are described in more detail below, is given in Table 1.3.

1.5.3.1 *Escherichia coli* and *Staphylococcus aureus*

The first direct report on the anti-bacterial power of CO tested the effects of ruthenium-based CORM-2 (250 μM) and CORM-3 (400 or 500 μM) against *E. coli* and *S. aureus* grown under different O_2 tensions (Nobre *et al.* 2007). Both compounds strongly decreased bacterial viability, but CORM-2 was more potent than CORM-3, as demonstrated by the requirement for higher concentrations of the latter. Additionally, *S. aureus* also exhibited slightly greater resistance to CORM-3. In general, a rapid loss in cell viability was seen to extend over time after treatment with the compounds and their efficacy was reported to be greater in near-anaerobic environments. This was not unexpected as CO preferentially binds to the ferrous form of proteins and does not have to compete with O_2. However, such a finding suggests that CO activity is not restricted to the impairment of the respiratory chain. Micromolar concentrations of two less well-known CO-RMs, ALF 021 (bromo(pentacarbonyl)manganese) (200 or 500 μM) and ALF 062 (tetraethylammonium molybdenum pentacarbonyl bromide) (50 μM) also significantly reduced bacterial viability. Additionally, treatment of *E. coli* with ALF 062 resulted in intracellular accumulation of the compound as determined by measuring levels of molybdenum using inductively coupled plasma mass spectrometry analysis. Confirmation that the bactericidal activity is due to CO liberated from the compounds was demonstrated by the ability of haemoglobin to abolish CO-RM toxicity (Nobre *et al.* 2007). However, CO binds only to ferrous haemoglobin and the details of how this experiment was performed were not given.

Nobre and co-workers built on this study by employing transcriptomic profiling in an attempt to further elucidate the intricate details of CORM-2 activity (Nobre *et al.* 2009).

Landscape Table (Table 1.3), refer to page 2 of supplementary document.

Table 1.3 continued, refer to page 3 of supplementary document.

In support of their previous work (Nobre *et al.* 2007), the transcriptome was more perturbed in anaerobically grown *E. coli* exposed to CORM-2. This was demonstrated by the repression of genes belonging to eight functional classes that were not seen in the aerobic response: 1) cell cycle, 2) cell wall biogenesis, 3) central intermediary metabolism, 4) intracellular trafficking, 5) phage-related functions and prophages, 6) post-translational modification and chaperones, 7) secondary metabolites biosynthesis and transport, and 8) translation, ribosomal structure and biogenesis. Regardless of this, a large number of genes were commonly affected under both aerobiosis and anaerobiosis and fold-changes in expression level did not greatly vary between the conditions. Biological assays revealed heightened sensitivity of *E. coli* mutants deficient in genes encoding proteins involved in general and oxidative stress response, as well as biofilm formation and methionine biosynthesis (Nobre *et al.* 2009). A recent study by this group demonstrated that both CORM-2 and ALF 062 stimulate the production of ROS in *E. coli*, an activity that was shown to be CO-dependent due to the ineffectiveness of control compounds depleted of CO. Interestingly, CORM-2 promoted ROS generation even in the absence of cells, which was attributed to an attack of water on a carbonyl, i.e. the first stage of the water-gas shift reaction. CORM-2 induced oxidative stress subsequently resulted in DNA damage and increased levels of intracellular free iron due to the destruction of Fe-S clusters. Alleviation of CO-RM effects was achieved by supplementing bacterial cultures with the anti-oxidants glutathione and cysteine, or methionine (Tavares *et al.* 2011), but the mechanism(s) behind this finding has not been described in the literature.

In contrast, another study, which utilised much lower CORM-3 concentrations (30 - 250 μM) showed that cultures of *E. coli* were more sensitive to the compound during growth under aerobiosis (Davidge *et al.* 2009b). In support of this, transcriptomic profiling of the *E. coli* genome following CORM-3 exposure revealed the down-regulation of genes encoding key aerobic respiratory complexes. This was confirmed by reductions in β-galactosidase activity in a Φ(*cyo-lacZ*) strain. Furthermore, probabilistic modelling revealed an involvement of FNR and ArcA, both of which have direct roles in the regulation of respiration. Additional casualties of CORM-3 stress under both aerobic and anaerobic conditions were metal homeostasis and general stress response induced by cell envelope perturbations; the latter contained some of the most highly up-regulated genes in the study. Interestingly, several genes involved in acetate and acetyl

group metabolism were among those most dramatically down-regulated, including *acs*, which encodes acetyl-CoA synthase (Davidge *et al.* 2009b).

Davidge and co-workers extended the finding that CO-RMs are taken up by bacterial cells, again determined by measuring intracellular ruthenium levels using inductively coupled plasma atomic emission spectroscopy (ICP-AES) after treatment of *E. coli* with CORM-3. Although anaerobic cultures were exposed to a higher (c. 3-fold) concentration of the compound, accumulation of ruthenium was greater in aerobic cells. The estimated intracellular ruthenium concentration in the latter exceeded the concentration in culture by 7-fold, in comparison to 2.1-fold for bacteria grown anaerobically. Further support for the uptake of CORM-3 was obtained from spectroscopic analysis of MbCO formation in the presence of *E. coli* cells, termed a myoglobin 'competition assay'. When compared with control, a 28 % reduction in the availability of CO was observed within 10 min after addition of CORM-3, with a further 15 % reduction after 20 min. Additional spectra revealed the formation of carbonmonoxy adducts of respiratory oxidases in intact *E. coli* cells treated with CORM-3. Furthermore, inhibition of respiration was observed in aerobically grown cultures stressed with the compound. Taken together, these data strengthen the evidence that CO-RMs enter bacterial cells and, under aerobic conditions, CO liberated from CORM-3 targets terminal oxidases (Davidge *et al.* 2009b).

1.5.3.2 *Pseudomonas aeruginosa*

Bactericidal activity of CORM-3 was confirmed using a laboratory strain (PAO1) and three clinical isolates (from hospitalised patients in intensive care units) of *P. aeruginosa* (Desmard *et al.* 2009). However, the concentrations of compound required to produce a significant effect were markedly lower (only 0.1 - 10 μM) than for *E. coli* (Davidge *et al.* 2009b; Nobre *et al.* 2007) and *S. aureus* (Nobre *et al.* 2007). The effect of CORM-3 on PAO1 was comparable to that of the antibiotic amikacine and greater than that of ticarciline; antibiotics to which this strain is sensitive. Consistent with a very early report showing that CO gas binds to cytochrome *c* oxidase in *P. aeruginosa* (Parr *et al.* 1975), and in support of the data presented by Davidge *et al.* (2009b), absorption spectra obtained following exposure of PAO1 cells to CORM-3 revealed the formation of carbonmonoxy adducts of terminal oxidases. Furthermore the compound also resulted in inhibition of oxygen consumption by respiring suspensions of the

bacterium, which was seen to occur in the absence of ROS overproduction and preceded the anti-bacterial action of the compound. CORM-3 mediated effects were again alleviated by thiol compounds: cysteine, glutathione and the thiol donor *N*-acetylcysteine (NAC) (Desmard *et al.* 2009).

In vivo analysis of CORM-3 activity demonstrated reduced mortality of mice with PAO1-induced bacteraemia and decreased bacterial counts in the spleen of both immunocompetent and immunosuppressed animals, suggesting a direct bactericidal effect of the compound. Assessment of CORM-3-induced cytotoxicity in murine RAW264.7 macrophages revealed that CO-RM concentrations 50-fold higher than those eliciting anti-bacterial effects were required to elicit significant reductions in cell viability. Moreover, treatment of healthy mice with CORM-3 did not induce any sign of mortality or illness during a two week observation period (Desmard *et al.* 2009). In a more recent study by the same group, CO-RM-induced bactericidal effects and inhibition of *P. aeruginosa* respiration were shown to be, at least in part, due to the specific metal carbonyl used. Although bacterial O_2 consumption was similarly affected, ruthenium-based CORM-2 and CORM-3 were more bactericidal than a novel, slow CO releaser, manganese-based CORM-371 ($t½$ c. 20 min). CORM-A1, which does not contain a metal centre, but releases CO at a similar rate (Table 1.2) to CORM-371, was found to elicit only a bacteriostatic effect and mild perturbations in the respiratory capacity of *P. aeruginosa*. The abolishment of CO-RM function by NAC was also compound-dependent with the activity of ruthenium-based CO-RMs being the most affected (Desmard *et al.* 2012). However, the mode of action of the thiol compound was not resolved.

An additional aspect of *P. aeruginosa* infection is the formation of biofilms that enable the pathogen to evade the host immune response and provide protection against anti-microbials (Flemming & Wingender 2010). Murray and co-workers showed that CORM-2 rapidly killed planktonic PAO1, with a minimal growth inhibitory concentration of 10 μM and no recovery of viable bacteria 30 min post-stress. CORM-2 (25 - 200 μM) decreased biofilm formation as early as 60 min after addition and 100 μM reduced the number of viable bacteria recovered from the biofilm after only 30 min, persisting for a further 6 h. CORM-2 prevented biofilm maturation to a similar extent as tobramycin, an antibiotic to which *P. aeruginosa* is sensitive, and had an additive effect

when used in combination with the drug. Additionally, CORM-2 prevented *P. aeruginosa* colonisation of human bronchial epithelial cells without eliciting a cytotoxic effect on the latter. As seen in other work (Desmard *et al.* 2009; Desmard *et al.* 2012; Tavares *et al.* 2011), the inhibitory activity of the compound was abolished by NAC and cysteine. CORM-2 treatment was also associated with an increase in ROS, as observed in other studies using this particular CO-RM (Nobre *et al.* 2009; Tavares *et al.* 2011). However, Murray and colleagues concluded this was not the mechanism of toxicity, as although cysteine inhibited CO-RM activity, ROS production was still observed. The inhibitory effect of the compound on biofilm formation and planktonic growth of *P. aeruginosa* strains isolated from patients either with or without cystic fibrosis was also demonstrated (Murray *et al.* 2012). However, several clinical isolates exhibited resistance to CORM-2 activity, as did another laboratory strain PA14. Furthermore, the inhibitory effect of CORM-2 was abolished when added to bacteria grown in rich media. Taken together, these findings suggest that the efficacy of CORM-2 against *P. aeruginosa* depends heavily on the strain, as well as the nutrients available and the energy pathways utilised by the bacterium. It is also important to note that the inhibitory activity of CORM-2 was attributed to the liberated CO, as a corresponding inactive compound was ineffective (Murray *et al.* 2012).

1.5.3.3 *Campylobacter jejuni*

Growth of the microaerophilic foodborne pathogen *Campylobacter jejuni* was unaffected by concentrations of CORM-3 that were previously efficacious in *E. coli* (30 and 100 μM), even though the dissolved O_2 concentration was up to 25-fold lower than the concentration of CO liberated from the compound (Smith *et al.* 2011). Furthermore, CORM-3 (i.e. CO) at a concentration c. 100-fold higher than the dissolved O_2 concentrations was still ineffective. Access of CORM-3 into the cell was not impeded as demonstrated using the myoglobin 'competition assay' as reported for *E. coli* (Davidge *et al.* 2009b). Surprisingly, although bacterial growth was unaffected, respiration of *C. jejuni* cell suspensions was inhibited by 100 μM CORM-3. Such activity of the CO donor was not influenced by the enhanced expression of both globins of *C. jejuni* (Cgb and Ctb) following addition of the nitrosative agent *S*-nitrosoglutathione. An interaction between CO liberated from CORM-3 and the respiratory chain of *C. jejuni* was confirmed by spectra showing characteristic signals of CO-bound terminal oxidases. However, the respiration rates of growing cultures

previously treated with CORM-3 were unaffected. Furthermore, respiratory inhibition was accompanied by increased generation of ROS, namely hydrogen peroxide, as determined by addition of bovine liver catalase to CORM-3-treated respiring cell suspensions (Smith *et al.* 2011).

1.5.3.4 *Mycobacterium tuberculosis*

Contrary to the anti-bacterial activity of CO described above, CO induces the dormancy regulon of *M. tuberculosis*, thereby aiding infection. Transcriptome profiling of *M. tuberculosis* exposed to 50 µM CO revealed rapid DosR-mediated induction of the complete Dos regulon (DosRST two-component system). An investigation employing *dos* knockout mutants identified DosS as the preferred, but not sole, sensor of CO. The physiological relevance of these findings was determined by *in vivo* studies using bone marrow-derived macrophages isolated from HO-$1^{+/+}$ and HO-$1^{-/-}$ mice. Macrophages infected with *M. tuberculosis* specifically up-regulated HO-1, subsequently leading to an increase in CO. In addition, *M. tuberculosis*-infected RAW264.7 macrophages displayed c. 8-fold higher HO-1 activity when compared with uninfected control cells. Importantly, the up-regulation and increased activity of HO-1 were confirmed to be independent of the NO pathway (Kumar *et al.* 2008). Induction of HO-1 expression by *M. tuberculosis* and induction of the dormancy regulon by CO was also reported by another group, who additionally showed that 800 nM and 80 µM CO were tolerated by the bacterium (Shiloh *et al.* 2008). However, as mentioned below, CO gas is generally ineffective against bacteria unless used at high concentrations (c. 1 mM).

1.5.3.5 Efficacy of CO-RMs relative to CO gas

Interestingly, CO gas (applied as a saturated solution) at equimolar concentrations to CORM-3 was ineffective against aerobically and anaerobically grown cultures of *E. coli* (Davidge *et al*. 2009b), and concentrations almost 100-fold higher than that of the highest CORM-3 concentration did not result in as intense or as long-lasting an effect on *P. aeruginosa* growth and viability (Desmard *et al*., 2009). CO gas fluxed for 15 min into microaerobic cultures of *E. coli* and *S. aureus* (final concentration of c. 1 mM), significantly impaired growth, but not to the same extent as seen after addition of much lower (micromolar) concentrations of CORM-3 (Nobre *et al.* 2007). Automatically, one might think that the effect of CO-RMs is therefore due to the scaffold rather than the liberated CO; however, control compounds depleted of CO were without effect in each

of the studies described above. An alternative explanation is that the uptake of CO-RMs by cells enables the intracellular accumulation of CO at levels significantly higher than can be achieved by diffusion of CO gas through membranes. The preferential release of CO inside cells is consistent with recent data showing that CO release rates from CORM-3 are greatly enhanced by species such as sulfite, but not by reaction of CORM-3 with globins in the absence of such a ligand (McLean *et al.* 2012).

1.6 Conclusions and scope of this thesis

It is evident from the wealth of studies that have been published since the 1990's that CO is a valuable therapeutic signalling molecule with multifaceted effects, which acts to best maintain cellular homeostasis. However, the mechanism of CO activity cannot yet be fully understood at a fundamental, biochemical level. Nevertheless, it is becoming increasingly accepted that, in mammalian systems, CO may relay its protective affects via consequence of its interaction with haem proteins. For example, CO-binding to respiratory components in mitochondria alters the redox status of the cell, which may subsequently trigger the activation of additional pathways that play a role in the amelioration of several disease states. This seems perfectly logical given the wide distribution of haem proteins within cells. Such an interchangeable role between 'CO sensing' versus 'CO targeting' of haem proteins has been suggested in bacteria that possess CODH (section 1.5.1).

The advent of CO-RMs, as an alternative delivery mechanism for CO, has provided a means by which this gas can be better applied, and therefore studied, in biology. Although investigations into the effects of CO in a microbiological context are in their infancy, this field poses an attractive means by which the effect of CO can be studied in a less complex system. Although the aim of CO-RM utilisation in microbiology is to determine the anti-bacterial activity of CO, the targets with which CO-RMs or CO interact are also relevant to mammalian studies aimed at using CO as a protective agent. For example, the relationship between CO and mitochondria can be beneficial so long as non-toxic concentrations of the gas are utilised. However, at present, even in bacteria we do not understand the biochemical basis of CO-RM action. Nevertheless, respiratory components have been highlighted as targets (Davidge *et al.* 2009b; Desmard *et al.* 2009; Desmard *et al.* 2012) and CO-induced production of ROS has been implicated

(Nobre *et al.* 2009; Tavares *et al.* 2011). It is in question, however, whether such interactions constitute the sole or major toxic mechanisms of CO-RM action. Both Desmard *et al*. (2012) and Smith *et al*. (2011) demonstrate that the effects of CO on respiration are a separate event from bactericidal activity. Also, alleviation of CORM-2 toxicity was observed in the absence of reduced ROS production (Murray *et al.* 2012). Furthermore, the inhibitory action of CO liberated from CO-RMs under anaerobic conditions (albeit to different extents in two separate studies (Davidge *et al.* 2009b; Nobre *et al.* 2007)), as well as the transcriptomic data reported by these two groups, further supports the possibility of additional targets. To recap on the current activity of CO-RMs against bacteria, as determined from the literature, a model is shown in Figure 1.5. Thus the potent anti-bacterial behaviour of CO-RMs against Gram negative and Gram positive, as well as aerobic and anaerobic species, in addition to clinical isolates (section 1.5.3), provides great potential for their pharmacological application in the future. Nevertheless, more work is required to determine the fundamental biochemical basis of CO/CO-RM activity in bacteria.

The scope of this thesis encompasses three important aspects highlighted in the current literature. Firstly, further investigations were carried out in an attempt to improve understanding of the interaction between CO liberated from CORM-3 on microbial respiration. Respiratory studies to date have focused on *E. coli* (Davidge *et al.* 2009b) and *P. aeruginosa* (Desmard *et al.* 2009; Desmard *et al.* 2012). To provide a broader view of CO activity, the work presented herein tested the effect of CORM-3 on these species in addition to the enteric pathogens *E. coli* O157 and *Salmonella enterica* serovar Typhimurium, as well as a clinical isolate of the opportunistic fungal pathogen, *C. albicans*. Secondly, due to the likelihood that CO has targets additional to those in the respiratory chain, and perhaps haem proteins in general, the anti-bacterial effect of CORM-3 was tested on a haem-deficient mutant of *E. coli* and naturally haem-deficient *Lactococcus lactis*. Additionally, to provide a more in-depth analysis of the interaction between CORM-3 and the haem-deficient mutant of *E. coli*, transcriptomic profiling and mathematical modelling of transcriptomic data were performed. This is a common method used within the Poole laboratory for the identification of bacterial responses to external stimuli (e.g. (Davidge *et al.* 2009b; Graham *et al.* 2012; McLean *et al.* 2010)). Lastly, as mentioned previously (section 1.5.3), the current literature on the effect of CO

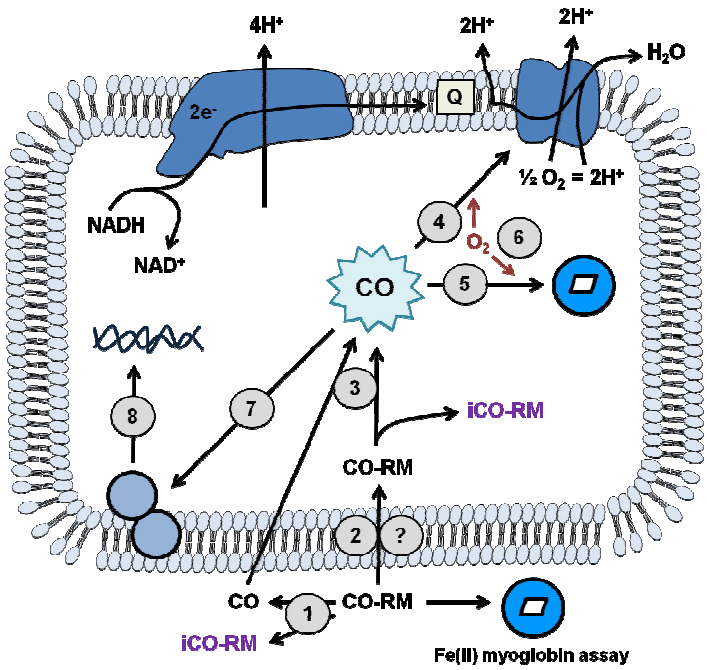

Figure 1.5. Model for the interactions of CO/CO-RM in bacteria. CO-RM liberates CO in solution (1) or is transported into the cell by a currently unknown mechanism (2) where CO is then released (3). Depending on the location where liberation of CO occurs, the remaining scaffold, i.e. inactive (i)CO-RM, may either remain in the external medium or accumulate intracellularly (purple). CO that is released extracellularly is detectable via reaction with ferrous myoglobin or haemoglobin. Inside the cell, CO targets oxidases (4) or other haem proteins (5); an activity that is inhibited competitively by O_2 (6). CO is sensed by transcription factors (7), either by direct interaction of CO with metal-containing transcription factors, or via a secondary response to another target (e.g. Arc (Davidge *et al.* 2009b)). The effects elicited by transcription factors in response to CO are reflected in the transcriptome (8). This model is derived from (Wilson *et al.* 2012).

in cases of microbial sepsis provides conflicting data; CO may either enhance or hinder the innate immune response. If CO-RMs are to be considered as anti-microbial agents in the clinic, it is imperative to understand their effect on host functionality. In an attempt to clarify these findings, *in vitro* assays were employed to determine the effect of CORM-3 in a model of meningococcal infection of human macrophages isolated from donated whole blood.

Chapter 2. Materials and Methods

2.1 Bacteriological techniques

2.1.1 Strains

Strains used in this study are shown in Table 2.1.

2.1.2 Media

Solid and liquid media were sterilised by autoclaving at 121 °C for 15 min at a pressure of 15 p.s.i., unless otherwise stated. Chemicals were purchased from Sigma, Fisher Scientific or BDH, unless otherwise stated. Nutrient agar, Columbia blood agar, Mueller-Hinton broth, tryptone and yeast extract were obtained from Oxoid. Casamino acids and Luria-Bertani-Broth Miller were purchased from Scientific Laboratory Supplies and ForMedium, respectively. Filter sterilisation of chemicals was carried out using Millipore filters, pore size of 0.22 μm.

2.1.2.1 Luria-Bertani (LB)-Broth Miller

LB was dissolved in distilled water (dH_2O) at 25 g/L and the pH adjusted to 7. The broth contains tryptone (10 g/L), yeast extract (5 g/L) and sodium chloride (10 g/L).

2.1.2.2 Mueller-Hinton broth (MHB)

MHB was dissolved in dH_2O at 21 g/L. The broth contains beef, dehydrated infusion (300 g/L), casein hydrolysate (17.5 g/L) and starch (1.5 g/L). The divalent cation content of the broth includes calcium (3.36 mg/L) and magnesium (6.53 mg/L).

2.1.2.3 Haem-deficient bacteria rich broth/agar

K_2HPO_4 (4 g), KH_2PO_4 (1 g), tryptone (10 g) and yeast extract (5 g) were added to 1 L dH_2O and the pH adjusted to 7. To prepare solid medium, agar (15 g/L) was added. After autoclaving, the medium was supplemented with 25 ml/L 20 % w/v D-glucose anhydrous (filter-sterilised) as a sole carbon source, and 1 ml of the following sterile stock solutions: 1 M $MgCl_2.6H_2O$ and, for haem-deficient mutant strains of *E. coli* only, 50 mg/ml kanamycin. Only when stated in the text, 2 ml/L of 0.05 M δ-aminolevulinic

Table 2.1. Strains and bacteriophage used in this study

Escherichia coli	Genotype	Source/Reference
RKP3101	Wild type MG1655	Laboratory stock
RKP5416	Wild type MG1655	Laboratory stock made from RKP3101
RKP5418	0157:H7 *stx*	Stock made from JRG5107 *[1] Veterinary Laboratories Agency
RKP5461	Wild type W3110	Chris Rensing *[2] Grass & Rensing (2001)
RKP3905	W3110 *hemA*::Km^R	National BioResource, Japan
RKP5421	MG1655 *hemA*::Km^R	Laboratory stock made by P1-mediated transduction from RKP3905
RKP5422	MG1655 *hemA*::Km^R	As for RKP5421
RKP5423	MG1655 *hemA*::Km^R	As for RKP5421
Lactococcus lactis		
RKP5900	Wild type	Marc Solioz *[3]
***Salmonella enterica* serovar Typhimurium**		
RKP4901	Wild type 14028s	ATCC
Pseudomonas aeruginosa		
RKP5417	Wild type PAO1	Jorge Boczkowski *[4]
Neisseria meningitidis		
MC58	Wild type	McGuinness *et al.* (1991)
Candida albicans		
CA3153	Wild type (clinical isolate)	Strain 3002 Pete Sudbery laboratory *[5]
Bacteriophage		
P1	-	Laboratory stock

*[1] Kind gift from Professor Jeff Green, The University of Sheffield
*[2] Kind gift from Dr. Chris Rensing, The University of Arizona
*[3] Kind gift from Dr. Marc Solioz, University of Berne, Switzerland
*[4] Kind gift from Dr. Jorge Boczkowski, University Paris 12
*[5] Kind gift from Professor Pete Sudbery, The University of Sheffield

acid (δ-ALA) (filter-sterilised) was added immediately prior to pouring plates or inoculating liquid medium.

2.1.2.4 TY broth

Tryptone (16 g), yeast extract (10 g) and NaCl (10 g) were dissolved in 1 L dH_2O (Sambrook and Maniatis, 2001).

2.1.2.5 Terrific broth (TB)

Tryptone (8 g) and NaCl (5 g) were dissolved in 1 L dH_2O and adjusted to pH 7. To make terrific broth soft agar (TBSA), 7 g agar were added to TB prior to autoclaving.

2.1.2.6 Defined minimal medium/agar

K_2HPO_4 (4 g), KH_2PO_4 (1 g), NH_4Cl (1 g), $CaCl_2.2H_2O$ (0.01 g), K_2SO_4 (2.6 g) and glycerol (5 g) were dissolved in 1 L dH_2O. Trace elements solution was added at 10 ml/L. After autoclaving, sterile 1 M $MgCl_2.6H_2O$ was added to the medium at 1 ml/L. For growth work involving haem-deficient bacteria (RKP5421 and RKP5900, see Table 2.1), glycerol was omitted from the above medium and further modifications include addition of 0.1 % casamino acids (1 g/L) and 5 % LB. After autoclaving, the medium was supplemented with 25 ml/L 20 % D-glucose anhydrous (filter-sterilised) to act as the sole carbon source, and for RKP5421 only, 1 ml/L 50 mg/ml kanamycin. To prepare plates for validation of the haem-deficient mutant of *E. coli*, 5 % LB was omitted from this medium and succinate or glycerol (5 g/L) were used in place of glucose. Agar was added at 15 g/L. Parallel control plates were prepared for which the medium was supplemented with 2 ml/L 0.05 M δ-ALA (filter-sterilised) after autoclaving, immediately prior to pouring.

2.1.2.7 Trace elements

Na_2EDTA (5 g) was dissolved in 700 ml dH_2O and adjusted to pH 7.4 before the addition of: $FeCl_3.6H_2O$ (0.8 g), ZnO (0.05 g), $CuCl_2.2H_2O$ (0.01 g), $CoNO_3.6H_2O$ (0.01 g), H_3BO_3 (0.01 g), ammonium molybdate (0.12 mg) and sodium selenite (0.017 g). The solution was made up to 1 L with dH_2O, filter-sterilised and stored at 4 °C (Flatley *et al.* 2005).

2.1.2.8 M9 medium

The published recipe (Miller 1992) was modified as follows: Na_2HPO_4 (6 g), KH_2PO_4 (3 g), NaCl (0.5 g), NH_4Cl (1 g) and 10 ml trace elements solution were added to 990 ml dH_2O. After autoclaving, sterile 1 M $MgSO_4.7H_2O$ was added at 1 ml/L and 20 % glucose (filter-sterilised) at 10 ml/L.

2.1.2.9 *Neisseria meningitidis* defined medium

NH_4Cl (1.26 g), NaCl (5.96 g), K_2HPO_4 (2.18 g), KH_2PO_4 (0.62 g/L), $Na_2S_2O_3.5H_2O$ (0.094 g), D-glucose anhydrous (5.6 g) were dissolved in 1 L milliQ water (mQH_2O). The medium was filter-sterilised after addition of trace elements solution at 2 ml/L. Just before use, the medium was supplemented with 10 ml/L 30 mM $FeCl_3.6H_2O$ made up in 0.6 M HCl and 2.43 ml/L 1 M $MgSO_4.7H_2O$ (all sterile) (Baart *et al.* 2007).

2.1.2.10 *Neisseria meningitidis* defined medium trace elements

$CaCl_2H_2O$ (10 g), $ZnSO_4.7H_2O$ (0.049 g), $Na_2MoO_4.2H_2O$ (0.019 g), $MnCl_2.4H_2O$ (0.079 g), $CoCl_2.6H_2O$ (0.0095 g), and $CuSO_4.5H_2O$ (0.01 g) were added to 1 L mQH_2O and filter-sterilised (Baart *et al.* 2007).

2.1.2.11 *Candida albicans* defined medium

D-glucose anhydrous (20 g) and Difco^{TM} yeast nitrogen base (free of amino acids) (6.8 g) were dissolved in 1 L dH_2O.

2.1.2.12 Dulbecco's Modified Eagle Medium (DMEM) (without sodium pyruvate)

DMEM containing L-glutamine and 4.5 g/L glucose was purchased from Lonza and supplied by the University of Sheffield Medical School, Department of Infection and Immunity.

2.1.2.13 Eagle's Minimal Essential Medium (EMEM)

EMEM containing Earle's balanced salt solution and L-glutamine was purchased from Lonza and supplied by the University of Sheffield Medical School, Department of Infection and Immunity.

2.1.2.14 Roswell Park Memorial Institute medium (RPMI-1640)

RPMI-1640 containing L-glutamine was purchased from Lonza and supplied by the University of Sheffield Medical School, Department of Infection and Immunity. The medium was supplemented with 10% heat inactivated foetal bovine serum (FBS), purchased from BioSera, prior to use.

2.1.2.15 Nutrient agar (NA)

NA was dissolved in dH_2O at 28 g/L. The medium contains 'Lab-Lemco' powder (1 g/L), yeast extract (2 g/L), peptone (5 g/L), NaCl (5 g/L) and agar (15 g/L).

2.1.2.16 Columbia blood agar (CBA)

Plates were provided by The University of Sheffield Infection and Immunity department, Medical School. CBA was dissolved in dH_2O at 39 g/L. The medium contains special peptone (23 g/L), starch (1 g/L), NaCl (5 g/L) and agar (10 g/L).

2.1.2.17 Yeast Extract Peptone Dextrose (YEPD) agar

Yeast extract (10 g), Bacto™ peptone (20 g), D-glucose anhydrous (20 g) and agar (20 g) were dissolved in 1 L dH_2O.

2.1.2.18 Phage lysate agar

Tryptone (4 g), yeast extract (2.5 g), NaCl (2.5 g), glucose (1 g) and agar (6 g) were dissolved in 500 ml mQH_2O. After autoclaving, 5 ml 0.5 M $CaCl_2$, 5 ml 1 M $MgCl_2.6H_2O$ and 0.5 ml 10 mM $FeCl_3$ (all filter-sterilised) were added (Miller 1972). Plates were stored at 4 ºC immediately after pouring.

2.1.2.19 P1 plates

Tryptone (5 g), yeast extract (0.5 g), glucose (1 g) and agar (6 g) were dissolved in 500 ml mQH_2O. After autoclaving, 5 ml 0.5 M $CaCl_2$ was added. Plates were stored at 4 °C immediately after pouring.

2.1.2.20 Antibiotic selection

Kanamycin was added as a stock solution to liquid agar (c. 50 °C) and liquid media at 1/1000 dilution. Stock solutions were prepared at 50 mg/ml in dH_2O, filter-sterilised and stored at -20 °C. A cocktail of 100 µg/ml gentamicin (Cidomycin®, Sanofi Aventis)

and 10 μg/ml penicillin were added to wells containing human macrophages infected with *N. meningitidis*. Stock solutions were prepared at 40 mg/ml and 60 mg/ml, respectively, in glass dH_2O (GDW) and stored at 4 °C for 2 - 3 weeks.

2.1.3 Buffers and solutions

2.1.3.1 Inorganic potassium phosphate buffer (KPi)

KPi was prepared using 1 M stock solutions of K_2HPO_4 and KH_2PO_4 (filter-sterilised). For a 0.1 M solution of pH 7, 61.5 ml K_2HPO_4 and 38.5 ml KH_2PO_4 were combined and diluted with 900 ml dH_2O. The final solution was sterilised by filtration. For preparation of 40 mM KPi pH 6.8, aliquots of 40 mM stock solutions of K_2HPO_4 and KH_2PO_4 were combined, during continuous pH monitoring, until a pH of 6.8 was achieved.

2.1.3.2 Tris

A 50 mM solution was prepared, altered to pH 7.5 and filter-sterilised.

2.1.3.3 Phosphate-buffered saline (PBS)

A 1 x stock was produced by dissolving NaCl (8 g), KCl (0.2 g), Na_2HPO_4 (1.44 g), and KH_2PO_4 (0.24 g) in 1 L dH_2O, adjusted to pH 7.4 and autoclaved. For the preparation of iCORM-3 (section 2.1.3.9) PBS was made up using tablets (Sigma); one tablet dissolved in 200 ml of dH_2O yields 0.01 M phosphate buffer, 0.0027 M KCl and 0.137 M NaCl, pH 7.4, at 25 °C. The solution was sterilised by filtration.

2.1.3.4 Phage dilution buffer

Tris base (0.61 g), $MgSO_4.7H_2O$ (1.23 g), $CaCl_2.2H_2O$ (0.37 g), NaCl (1.46 g) were dissolved in 500 ml mQH_2O, adjusted to pH to 7.5 and autoclaved (Miller 1972).

2.1.3.5 TBE buffer

A 5 x stock solution was prepared by dissolving Tris base (54 g) and H_3BO_3 (27.5 g) in 1 L diethylpyrocarbonate (DEPC) mQH_2O. Sodium EDTA was added as a solution to a final concentration of 0.01 M from a 0.5 M stock. A 1 x stock of TBE was prepared by diluting 200 ml 5 x TBE in 800 ml DEPC mQH_2O.

2.1.3.6 TE buffer

Tris HCl (0.316 g) was dissolved in 200 ml DEPC mQH_2O. Sodium EDTA was added as a solution to a final concentration of 1 mM from a 0.5 M stock. The solution was adjusted to pH 8 and filter-sterilised.

2.1.3.7 Myoglobin

A fresh 100 μM stock solution was prepared in buffer or media on the day of use, unless otherwise stated.

2.1.3.8 CO saturated solution

A CO saturated solution was prepared fresh each day by bubbling CO gas (CP grade) from a cylinder (BOC, Guildford, GU2 5XY) through 5 ml 50 mM Tris base buffer (pH 7.5) in a 7 ml bijou bottle, fitted with a Suba-Seal and vent, for 10 - 20 min. This creates a c. 1.15 mM (section 6.2.5) stock solution.

2.1.3.9 Sodium dithionite solution

A fresh 200 mM stock solution of sodium dithionite was made up before each use in 5 ml degassed (nitrogen, 10 min) 0.1 M KPi buffer (pH 7) in a sealed 7 ml bijou bottle fitted with a Suba-Seal and vent. The solution was degassed with nitrogen for a further 10 min after addition of sodium dithionite grains, to ensure complete removal of oxygen.

2.1.4 Maintenance of bacteria and phage

2.1.4.1 Strain storage

Long term storage of strains was at -70 °C in glycerol. Production of glycerol stocks was by addition of 0.75 ml of an overnight culture grown in rich medium to 0.75 ml 50 % glycerol in a cryovial (Nalgene). Glycerol stocks for the haem-deficient strains of *E. coli* (RKP5421, RKP5422, RKP5423, see Table 2.1) were prepared by pipetting 2 ml of rich broth (section 2.1.2.3) without supplementation and containing 25 % glycerol as opposed to glucose, onto the mutant growing on rich broth agar (section 2.1.2.3). The colonies were resuspended using a sterile spreader and transferred to a cryovial. In the short-term, wild type microbial strains and the haem-deficient strain of *E. coli* were

stored on solid media for up to two weeks. *N. meningitidis* MC58 (serogroup B) was stored on solid media for up to two days.

2.1.4.2 Bacteriophage

Phage P1 lysates were stored at 4 °C in air-tight vials containing a few drops of chloroform.

2.1.5 Culture conditions

2.1.5.1 Aerobic batch culture

E. coli K-12 MG1655, *E. coli* O157, *Pseudomonas aeruginosa* PAO1, *Salmonella enterica* serovar Typhimurium were streaked onto NA and incubated overnight at 37 °C. Starter cultures were grown overnight in 5 - 10 ml LB from a single colony. *C. albicans* was streaked out onto YEPD plates and incubated for 24 h at 30 °C. Starter cultures of *C. albicans* were grown in 5 ml defined medium (section 2.1.2.11) for 24 h at 37 °C, whilst shaking at 200 rpm. Cells were harvested and re-suspended in the respective defined medium before inoculation. Microbial cultures were grown at 37 °C in 20 - 30 ml defined medium to mid-log phase in 250 ml flasks fitted with side arms, or 250 ml sterile conical flasks (*C. albicans*), during shaking at 200 rpm. Optical density measurements were made using a Klett-Summerson photoelectric colourimeter (Klett Manufacturing Co., New York, N.Y.) with a no. 66 (red) filter, or a Jenway 7315 spectrophotometer, against a medium blank.

2.1.5.2 Batch culture of wild type *Escherichia coli* and haem-deficient bacteria

RKP5416 (wild type *E. coli* K-12 MG1655) was streaked onto NA, RKP5421 (*E. coli* K-12 MG1655 *hemA*) and *Lactococcus lactis* were streaked onto rich broth agar plates (section 2.1.2.3) and incubated overnight at 37 °C. Where large volumes of cells were required, aerobic cultures were grown in 200 ml rich broth (2.1.2.3) in 500 ml conical flasks during shaking at 200 rpm. Anaerobic cultures were grown in 100 ml Duran bottles filled to the brim with defined medium modified for the growth of haem-deficient bacteria (section 2.1.2.6), and rotated gently on a roller mixer SRT2 (Stuart). Aerobic and anaerobic cultures were inoculated with 5 % v/v and 1 % v/v of overnight cultures grown in rich broth, respectively. For microarray analysis, anaerobic cultures were grown in 250 ml defined medium in mini-fermenter vessels (Lee *et al.* 2005)

continually sparged with nitrogen, during stirring at 200 rpm. A constant temperature of 37 °C was maintained in the growth vessel using a water jacket from a water bath set to 49 °C. Cultures were inoculated with 5 % v/v of overnight cultures grown in rich broth. Optical density measurements were made using a Jenway 7315 spectrophotometer. For anaerobic growth, starters grown in rich broth were harvested and re-suspended in defined medium prior inoculation.

2.1.5.3 Anaerobic growth curves

To determine the sensitivity of the haem-deficient mutant of *E. coli* and *L. lactis* to 100 - 300 μM, or 100 and 200 μM CORM-3 (section 2.3.1.1), respectively, anaerobic liquid cultures were grown in defined medium modified for the growth of haem-deficient bacteria (2.1.2.6) at 37 °C in 8 ml screw-cap tubes containing a glass bead to aid re-suspension. Cultures were inoculated with 1 % v/v of an overnight culture grown in rich broth (2.1.2.3) that was harvested and re-suspended in defined medium prior to inoculation. Optical density measurements were made using a Jenway 7315 spectrophotometer. Sensitivity to CORM-3 control compounds: $RuCl_2(DMSO)_4$ (section 2.3.1.2) and inactive (i)CORM-3 (section 2.3.1.3) (100 and 200 μM) was also tested. Due to poor growth of the mutant, cultures were stressed at an OD_{600} of c. 0.15 or 0.25. Cultures of *L. lactis* were stressed at an OD_{600} of c. 0.4.

2.1.5.4 *Neisseria meningitidis* growth curves

N. meningitidis was streaked onto CBA and grown overnight at 37 °C in a humidified atmosphere containing 95 % air and 5 % CO_2. Colonies (8 - 12) were picked to inoculate 20 ml defined medium (section 2.1.2.9) in 25 ml loosely fastened universals. Optical density measurements were made using a Jenway 6310 (Jencons) spectrophotometer. Cultures were stressed with CORM-3, CO saturated solution or a control compound, $RuCl_2(DMSO)_4$, at an OD_{600} of c. 0.3. Due to a high volume of myoglobin-inactivated (mi)CORM-3 (section 2.3.1.4) being required, the solution was added to *N. meningitidis* defined medium before inoculation. For these experiments exclusively, a CORM-3 stock was made up at the same concentration as miCORM-3 so that equal volumes of the two compounds were added at the same time.

2.1.5.5 Viability studies

Serial dilutions of culture samples were made in PBS ranging between 10^{-1} to 10^{-8}. From each dilution, 10 µl drops were plated onto the respective agar. Drops were allowed to dry and plates were incubated overnight at 37 °C (in a humidified atmosphere in the case of *N. meningitidis*). Following incubation, the average number of colonies was calculated for the dilution giving the highest number of colonies without confluence. The average was used to determine the number of colony forming units per ml (CFU/ml).

2.1.5.6 Gram stain

Growth of *N. meningitidis* was confirmed by carrying out a Gram stain test. Bacterial culture at a volume of 10 µl was pipetted onto a slide, allowed to dry and heat-fixed. The slide was covered in methyl violet for 1 min, rinsed then covered in Gram's iodine for 1 min and rinsed. Acetone was poured onto the slide and immediately rinsed off. The slide was covered in dilute fuchsin for 20 s, rinsed and dried. All rinses were carried out using dH_2O. Cells were visualised under a light microscope. A pink colouration is indicative of Gram-negative bacteria and a purple colouration shows the presence of Gram-positive bacteria.

2.1.6 Bacteriophage transduction

2.1.6.1 Preparation of P1 lysates

Due to poor growth of the haem-deficient strain of *E. coli*, the published protocol by Miller (1972) was adjusted to enable transduction of the *hemA* mutation. Lysates were produced by growing the donor strain (W3110 *hemA*) overnight at 37 °C, during shaking at 200 rpm, in 5 ml rich broth (section 2.1.2.3) supplemented with 25 µM δ-ALA and 5 mM $CaCl_2$. The culture was concentrated to 1 ml in supplemented rich broth and 0.05 ml added to 0.1 ml of the wild type MG1655 P1 lysate (2×10^9 plaque forming units / ml) diluted as follows: 10^{-5}, 10^{-4}, 10^{-3} and 10^{-2}. The mix was incubated at 37 °C for 20 min. Pre-warmed TB (1 ml) (supplemented with 0.5 % glucose), 25 µM δ-ALA and 1.5 ml molten TBSA were added to the bacteria/phage cultures, mixed and poured on top of pre-warmed (37 °C) phage lysate plates. Once solidified, the plates were incubated correct side up at 37 °C in a moist atmosphere until plaques began to form. Upon reaching the point at which the plaques had become nearly confluent (usually c. 8

h) plates were chilled at 4 °C for 30 min then overlaid with 5 ml of phage dilution buffer and left overnight at 4 °C. The overlaying liquid was removed using a Pasteur pipette and filtered through a sterile 45 μM nitrocellulose filter into a cryovial (Nalgene) and stored at 4 °C under a few drops of chloroform.

2.1.6.2 P1 transduction of the recipient strain

An overnight culture of the recipient strain (MG1655) was grown in 5 ml of TY supplemented with 5 mM $CaCl_2$. Aliquots (0.1 ml) of the recipient culture were mixed with 0.1 ml of the W3110 *hemA* lysate at the following dilutions: 10^0, 10^{-1} and 10^{-2}. The mix was incubated for 20 min at 37 °C. The entire mixture was plated on rich broth agar (section 2.1.2.3) supplemented with 0.125 mM $Na_4P_2O_7$ (an efficient Ca^{2+} chelator). Before plating the bacteria/phage cultures, 25 μM δ-ALA was spread onto the above plates. After overnight incubation at 37 °C, any putative transductant colonies were re-streaked and verified by: 1) streaking a colony onto mutant validation defined medium agar plates containing succinate instead of glucose (section 2.1.2.6), with and without δ-ALA, and; 2) by cytochrome analysis to confirm cytochrome deficiency.

2.2 Tissue culture

2.2.1 Human macrophages

Macrophages were harvested from donated whole blood by Ian Geary (Department of Infection and Immunity, The University of Sheffield Medical School) and cultured for 10 - 12 days in 24-well flat-bottom plates (2 x 10^6 cells/ml) in RPMI (section 2.1.2.14) at 37 °C in a humidified atmosphere containing 95 % air and 5 % CO_2. One plate was used for each time-point to avoid disrupting the experiment by sequential removal of a tray from the incubator at separate time-points. Each plate for internalisation assays contained six active wells to allow for two technical repeats of each condition: control (PBS), 50 μM CORM-3 and 100 μM CORM-3. Plates for gentamicin exclusion assays contained two additional control wells in which macrophages were fixed. For fluorescence microscopy, macrophages were cultured on sterile glass coverslips (BDH, UK) in the wells. Blood from a different donor was used for each biological repeat. All incubations detailed below, and growth of *N. meningitidis*, were carried out at 37 °C under a humidified atmosphere.

2.2.1.1 Internalisation assays

A starter culture of *N. meningitidis* MC58 was grown in MHB to an OD_{600} of c. 0.2 (c. 2 x 10^8 CFU/ml). Cultures were harvested and resuspended in RPMI. Before infection, macrophages were incubated with 3 ml 5 % v/v bovine serum albumin (BSA), prepared by diluting a sterile 30 % w/v stock solution (First Link (UK) Ltd.) in RPMI, for 30 min. This treatment prevents non-specific binding. Macrophages were infected with *N. meningitidis* at a multiplicity of infection (MOI) of c. 10. Immediately after infection, control (PBS), 50 μM CORM-3 or 100 μM CORM-3 was added to the wells. After incubation for 90 min, wells were washed twice with PBS to remove un-associated bacteria. Six drops of 2 % v/v paraformaldehyde were added to each well to fix the cells, followed by four drops of PBS to prevent the samples drying out. Trays were wrapped in foil and left at room temperature for 30 min before staining, or before storage at 4 °C for up to 1 month. To ensure that CORM-3 did not kill the bacteria during the 90 min incubation period, a control plate was set up in which the suspension of *N. meningitidis* in RPMI was added to wells that did not contain macrophages. Samples (10 μl) were removed from each well every 30 min for 90 min to assay bacterial viability using standard dilution techniques. Diluted samples (10^{-1} - 10^{-6}) were prepared and plated on CBA and incubated overnight. Bacterial viability was determined the following day.

2.2.1.2 Fluorescence microscopy

Previously fixed cells were washed twice with GDW to remove the paraformaldehyde. To stain the cells, they were treated for 12 min in the dark with three separate preparations and washed twice with GDW between each treatment. The first addition was 200 μl of a 1:200 dilution (in PBS) of anti-*Neisseria* serogroup B polysaccharide IgG antibody (Difco™). To visualise the anti-*Neisseria* antibody, a second addition of a 1:80 dilution of fluorescein isothiocyanate (FITC)-conjugated goat anti-mouse antibody (Sigma-Aldrich) prepared in PBS containing a 1:20 dilution of goat serum (First Link (UK) Ltd.) were added to the wells. FITC has a maximum excitation wavelength of 495 nm and a maximum emission wavelength of 520 nm. It has green fluorescence when viewed down the fluorescence microscope. The final addition was 400 μl of 4',6-diamidino-2-phenylindole (DAPI) (Molecular Probes, Eugene, Oregon) diluted 1:2250 in PBS containing 0.1 % Triton X-100 and 0.02 % SDS. DAPI is a nucleic acid stain, which when bound to DNA has a maximum excitation wavelength of 368 nm and a

maximum emission wavelength of 461 nm. It has blue fluorescence when viewed down the fluorescence microscope. Coverslips were allowed to dry then removed from the wells, mounted in Vectashield (Molecular Probes) and viewed at a magnification of x 100 using a DMRB 1000 fluorescence microscope (Leica, Wetzlar, Germany). Internalisation of bacteria was determined by subtracting the number of extracellular bacteria, identified by their co-localisation with the FITC antibody, from the total number of bacteria exhibiting the DAPI stain, as previously described (Stevanin *et al.* 2002).

2.2.1.3 Gentamicin exclusion assays

Cultures and resuspensions of *N. meningitidis* were prepared as described in section 2.2.1.1. Before each new addition described in this protocol, the wells were washed twice with PBS. 'Fixed' control macrophages were prepared by addition of 6 drops of 2 % v/v paraformaldehyde and 2 drops of PBS to the respective wells followed by 30 min incubation. All macrophages were then incubated with 3 ml 5 % v/v BSA for 30 min followed by infection with *N. meningitidis* at an MOI of c. 25. Internalisation was allowed for 90 min. To kill extracellular bacteria, 3 ml of a cocktail of 100 µg/ml gentamycin and 10 µg/ml penicillin made up in RPMI was added to each well followed by 30 min incubation. RPMI (1 ml) was added to each well followed by immediate addition of 50 or 100 µM CORM-3. After 30 min, 60 min and 90 min incubations post-treatment, a 30 µl sample was taken from each well for serial dilution to determine the efficiency of the cocktail. Cells were then lysed with 250 µl 2 % saponin for 10 min at 37 °C under a humidified atmosphere. PBS (750 µl) was added to the lysates and mixed to achieve maximum recovery of bacteria. Samples (30 µl) were removed from each well to assay bacterial viability using standard dilution techniques. For samples taken before, and samples taken after lysis, the following dilutions were prepared and plated on CBA: 10^{-1}, 10^{-2} and 10^{-3}. Plates were incubated overnight and bacterial viability determined the following day.

2.2.1.4 Statistical analysis

To analyse data, normal distribution was confirmed using the Shapiro-Wilks test. Differences between comparators and control were assessed using a two-tailed Students *t*-test, with a correction for multiple comparators (Bonferroni). Statistical calculations

were performed using SigmaPlot (Systat Software Inc.). Significant difference, after application of the Bonferroni correction, was accepted at $P < 0.025$.

2.3 Biochemical techniques

2.3.1 Carbon monoxide-releasing molecules (CO-RMs)

2.3.1.1 CORM-3 (tricarbonylchloro(glycinato)ruthenium(II))

CORM-3 was provided by Dr. Roberto Motterlini and Professor Brain Mann (Hemocorm), or synthesised in-house following the published method (Johnson *et al.* 2007). Purity of the in-house preparation was tested by infrared Anvel cell spectrophotometry and ^{1}H NMR in D4 methanol, carried out by Dr. Robert Hanson and Dr. Brian Taylor, respectively (Chemistry Department, The University of Sheffield). Extent of CO release was determined using a myoglobin assay (Johnson *et al.* 2007). Stock solutions were made up at 10 or 100 mM in dH_2O and stored on ice. For use the following day, solutions were stored at 4 °C overnight.

2.3.1.2 $RuCl_2(DMSO)_4$

$RuCl_2(DMSO)_4$ was supplied by Professor Brian Mann or Dr. Tony Johnson (Chemistry Department, The University of Sheffield). Stock solutions were made up in dH_2O at 10 or 100 mM fresh each day.

2.3.1.3 Inactivated (i)CORM-3

A 10 mM stock solution of iCORM-3 was prepared by dissolving CORM-3 in PBS (tablets) and allowing liberation of CO for 48 h at room temperature, with the solution open to the atmosphere during working hours. The solution was bubbled with nitrogen gas from an oxygen-free cylinder (BOC, Guildford, GU2 5XY) for 5 min every 2 h on the second day and the day of use, until immediately prior to addition, to ensure dissociation of the CO groups. Inactivation was tested by assaying CO release to ferrous myoglobin spectrophotometrically.

2.3.1.4 Myoglobin-inactivated (mi)CORM-3

A stock solution of 455 μM miCORM-3 was prepared by treating CORM-3 twice with a 2-fold excess of 1 mM ferrous Mb; 2.2 mM of sodium dithionite solution (0.1M KPi

pH 7) was used to reduce myoglobin to prevent an excess of sodium dithionite. Following each treatment, MbCO was separated from the CORM-3 skeleton by centrifugation in a vivaspin 20 concentrator (Sartorius Stedim Biotech) with a molecular mass cut-off of 5 kDa. Inactivation was determined by assaying CO release to ferrous myoglobin spectrophotometrically.

2.3.2 Spectroscopic assays

2.3.2.1 Myoglobin assay to determine CO release from CORM-3

Difference spectra (CO plus reduced *minus* reduced) of myoglobin were measured in a custom-built SDB-4 dual-wavelength scanning spectrophotometer (University of Pennsylvania Biomedical Instrumentation Group and Current Designs Inc., Philadelphia, PA, USA) (Kalnenieks *et al.* 1998). Optical components were arranged in a classical dual-wavelength configuration. Spectra were scanned in 0.5 mm step sizes from 400 to 700 nm and data were analysed using *Soft*SDB (Current Designs Inc.) and plotted using SigmaPlot (Systat Software Inc.). Myoglobin was added to 0.1 M KPi buffer (pH 7) or media at a final concentration of 5 or 10 μM and reduced with grains of sodium dithionite. Spectra were recorded in triplicate, using a baseline of reduced myoglobin, after treatment with 2 - 20 μM CORM-3. Additional CORM-3 (5 μM aliquots) was added if a plateau in MbCO formation was not reached after the addition of 20 μM CORM-3. The resulting data were averaged in Excel and plotted as CO reduced *minus* reduced spectra. The ΔA in the Soret region was used to determine rates of CO release.

2.3.2.2 Cytochrome assays

Large cultures were grown as described in section 2.1.5.2 for 7 - 8 h, unless otherwise stated. Cultures were harvested, washed in 0.1 M KPi (pH 7) and resuspended to give a thick cell suspension. The presence of cytochromes in whole cells of haem-deficient bacteria, compared with wild type, was determined using the dual-wavelength scanning spectrophotometer in cuvettes of 10 mm path length. Dithionite-reduced *minus* persulphate-oxidised difference spectra were computed. To record CO plus reduced *minus* reduced difference spectra, the dithionite-reduced samples were bubbled with CO for c. 2 min. Samples were scanned in triplicate and analysed as described in section 2.3.2.1. Protein concentrations were measured using the Markwell assay (Markwell *et*

al. 1978) (section 2.3.5.1). Concentrations of cytochromes *b* and *d* were calculated in nmol mg protein^{-1} from reduced *minus* oxidised spectra using extinction coefficients found in the literature: $b_{560\text{-}575}$ (ε 17.5 nM cm^{-1}) and $d_{630\text{-}655}$ (ε 19 nM cm^{-1}) (Jones 1985).

2.3.3 Oxygen electrode for the measurement of respiration rates

Cells were grown as described in section 2.1.5.1. Cultures were harvested at mid-exponential phase, washed and resuspended in 50 mM Tris (pH 7.5), or the respective defined medium, at a quarter of the volume of the original culture to achieve a high cell concentration. The O_2 electrode was calibrated using either air-equilibrated 50 mM Tris (pH 7.5), or air-equilibrated defined medium, and the addition of sodium dithionite (a few grains) to achieve anoxia (Gilberthorpe & Poole 2008). Cells were suspended in 50 mM Tris (pH 7.5), or the respective defined medium (final volume of 2 ml) in a sealed, stirred chamber to achieve a protein concentration of c. 1 mg ml^{-1}. The chamber was fitted with a Clark-type polarographic oxygen electrode (Rank Brothers) operating at 37 °C and a polarising voltage of -0.6 V (Gilberthorpe & Poole 2008). Data were recorded using a chart reader (Amersham Pharmacia Biotech) or DataTrax2 software (World Precision Instruments Inc.). Respiration was stimulated by the addition of 5 mM glycerol. At 0 % O_2 in the sealed chamber, the lid was removed to allow utilisation of an 'open' system, in which a stirred sample is open to the atmosphere allowing continuous oxygen diffusion from the vortex surface into the sample (Degn *et al.* 1973; Hendgen-Cotta *et al.* 2008). To make a parallel between oxygen consumption and bacterial viability, cell suspension samples were taken directly from the chamber at specified time-points for serial dilution in PBS followed by plating 10^{-1} - 10^{-8} drops on NA. Protein concentrations were measured using the Markwell assay (Markwell *et al.* 1978) (section 2.3.5.1).

2.3.4 Proton translocation measurements

The apparatus used is based closely on that described previously (Lawford & Garland 1972; Lawford & Haddock 1973). Cells were suspended in a sealed, stirred Perspex chamber fitted with a Clark-type polarographic O_2 electrode (OXY040A, Rank Brothers Ltd) and held at 30 °C. The lid of the chamber was custom-modified to support a semi-

micro calomel combined pH electrode (pHC4000-8, MeterLab) from Radiometer Analytical for measuring pH changes. The signal from the pH electrode was taken to a pH/ion meter (PHM240, MeterLab, Radiometer Analytical) and then to a chart recorder (Amersham Biosciences) fitted with a 0.47 µF capacitor to dampen noise and a 10 Ω resistor to allow for a low sensitivity setting (2 mV) to detect small changes in pH (Figure 2.1). Wild type *E. coli* MG1655 (RKP5416, Table 2.1) was grown aerobically in 2 L baffled flasks at 37 °C and 200 rpm in 500 ml defined medium (section 2.1.2.6) supplemented with 0.1 % casamino acids to mid-exponential phase, followed by starvation in 1 L conical flasks at 37 °C and 200 rpm in 200 ml defined medium lacking a carbon source and casamino acids. Cells were harvested by centrifugation at 4 °C, washed twice and resuspended in 100 µl cold 150 mM KCl. An aliquot of the suspension was added to 2.5 ml lightly buffered medium (150 mM KCl, 50 mM KSCN, 1.5 mM glycylglycine, pH 7, 30 °C) in the chamber to achieve a final bacterial protein concentration of 5 - 10 mg. Valinomycin (22 µM final concentration, added as a methanolic stock solution) was added immediately after cells, followed by 1 mM glycerol to stimulation respiration. The experiment commenced after complete consumption of O_2. Additions of an anoxic solution of 5 mM HCl were used to calibrate the apparatus (25 - 75 ng-ion H^+). Addition of 25 µl air-saturated 150 mM KCl (30 °C; 11 ng-atom O) was added to promote respiration-driven proton translocation and medium acidification. Carbonylcyanide *m*-chlorophenylhydrazone (CCCP) solubilised in dimethyl sulfoxide (DMSO) was used as a proven uncoupler at a final concentration of 1.6 µM. H^+/O ratios were calculated from deflections caused by acid and O_2 pulses. Protein concentrations were measured using the Markwell assay (Markwell *et al.* 1978) (section 2.3.5.1).

2.3.5 Protein analysis

2.3.5.1 Markwell protein assay

The protein content of whole cells was determined using the protocol of Markwell *et al*. (1978). Reagent A (100 parts), consisting of Na_2CO_3 (20 g/l), NaOH (4 g/l), sodium tartrate (1.6 g/) and sodium dodecyl sulphate (10 g/l), were mixed with 1 part of reagent B (4 % copper sulphate); 3 ml of this was incubated with varying volumes of sample for 60 min at room temperature. Subsequently, 0.3 ml of a 1:1 dilution of (Lowry) Folin-Ciocalteau reagent with dH_2O was added to the samples, followed by incubation for 45

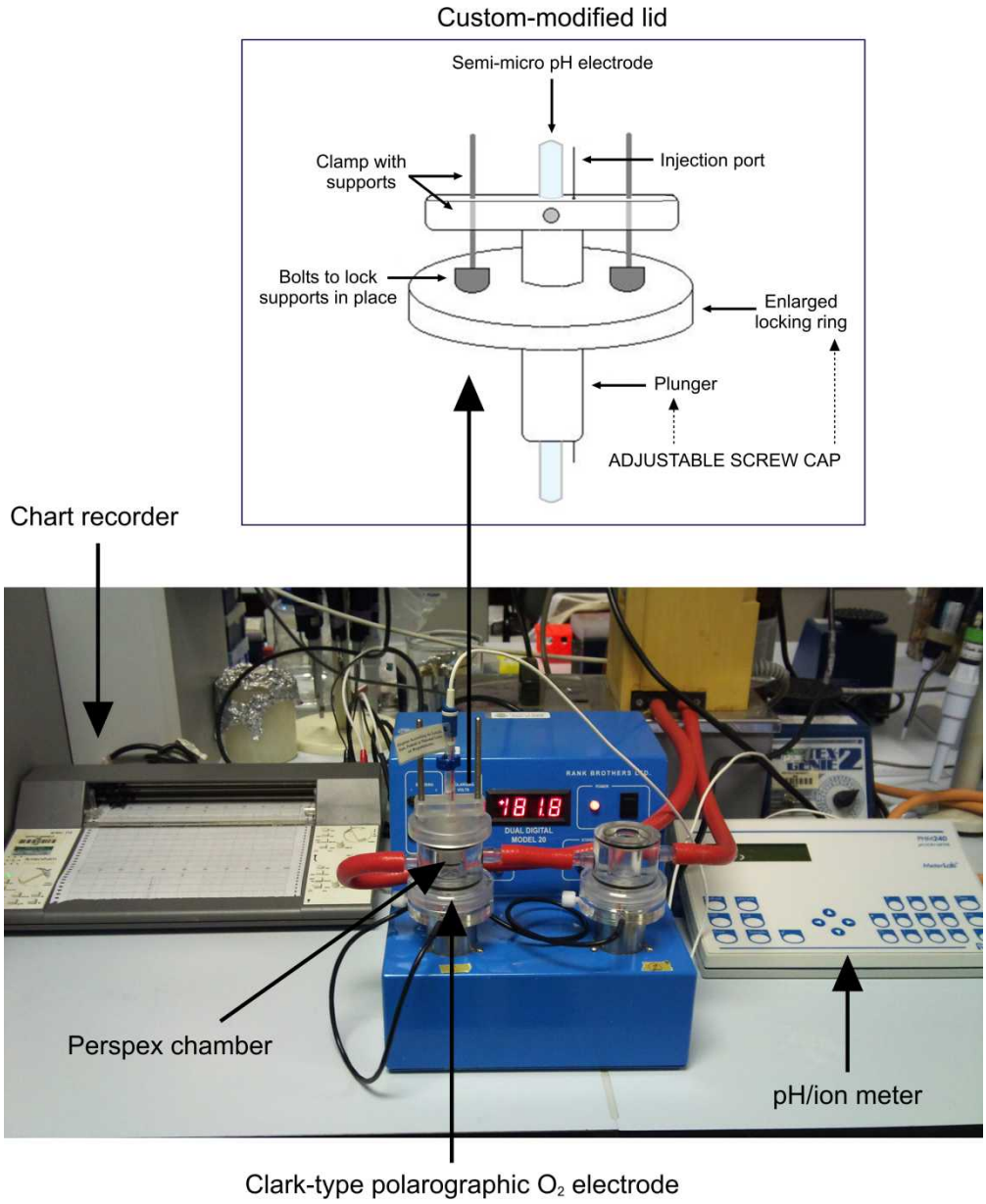

Figure 2.1. Apparatus for measuring proton translocation in bacterial cells.

min. Absorbance was read at 660 nm using a Beckman DU® 650 absorbance spectrophotometer, against a dH_2O blank. Protein concentrations (mg/ml) were determined using a protein standard curve generated from a set of BSA dilutions ranging from 20 - 200 µg/ml.

2.4 Molecular methods

2.4.1 Microarray analysis

All reagents were prepared using mQH_2O treated with 0.2 % DEPC overnight at 37 °C to remove RNases that may degrade RNA. After overnight treatment, DEPC mQH2O was autoclaved to eliminate toxicity. The microarrays detailed in this work were carried out using a 'Two-Color Microarray-Based Prokaryote Analysis (FairPlay III Labeling)' by Agilent Technologies, Inc. 2009. All solutions described in sections 2.4.1.4 and 2.4.1.5 were obtained from Agilent Technologies, unless otherwise stated.

2.4.1.1 Sampling and RNA stabilisation

At each time-point, culture samples of 20 ml were removed from minifermenter vessels (anaerobic), added to a chilled mix of 125 µl phenol and 2.375 ml ethanol and after vortexing immediately for 5 s, incubated on ice for 5 min followed by centrifugation for 5 min at 5500 rpm, 4 °C. Excess supernatant was removed by gentle tapping of inverted tubes. Pellets were stored at -70 °C. At an OD_{600} of c. 0.2, a control sample was taken, immediately followed by addition of 100 µM CORM-3, or equimolar iCORM-3. Five further samples were taken at 10, 20, 40, 60 and 120 min post addition of compound.

2.4.1.2 RNA isolation

RNA was isolated from pellets using a Qiagen 'RNeasy Mini Kit (50)' according to the manufacturer's instructions. Sample pellets were thawed on ice then resuspended in 200 µl of TE buffer containing lysozyme (15 mg/ml) and vortexed for 10 s followed by incubation at room temperature for 5 min. Samples were vortexed every minute during the 5 min incubation. RLT buffer (700 µl) containing β-mercaptoethanol (10 µl/ml) was added followed by vigorous vortexing and the addition of 500 µl 96 % ethanol. The samples were mixed by gentle swirling and the resultant lysates applied to an RNeasy Mini column placed in a 2 ml collection tube, centrifuged for 30 s at 10,000 rpm and the

flow through discarded. Buffer RW1 (350 µl) was added to the column followed by centrifugation for 30 s at 10,000 rpm. After removal of the flow-through, a mixture of 10 µl DNase I with 70 µl buffer RDD was transferred directly onto the RNeasy silica-gel membrane and incubated at room temperature for 15 min to allow for DNase digestion. Buffer RW1 (350 µl) was then added to the column followed by a further 5 min incubation at room temperature and centrifugation for 30 s at 10,000 rpm. The column was transferred into a fresh 2 ml collection tube and washed twice with 500 µl buffer RPE. To elute any remaining ethanol, the column was transferred into a clean, RNase-free 1.5 ml eppendorf tube and centrifuged for 30s at 10,000 rpm. For elution of the RNA, the column was transferred into a fresh, RNase free 1.5ml eppendorf, 30 µl RNase-free water pipetted onto the RNeasy silica-gel membrane followed by centrifugation for 1 min at 10,000 rpm. To increase the yield of RNA, the eluted 30 µl was put back through the column. RNA was stored at -70 °C or used immediately.

2.4.1.3 RNA determination

The concentration of RNA was determined specrophotometrically using a Beckman DU 650 UV/Vis spectrophotometer. After blanking the machine with 99 µl DEPC-treated mQH_2O in UVettes (Eppendorf), 1 µl of RNA was added and its quantity measured. One A_{260} unit is equal to 40 µg RNA per ml. The quality of the RNA was determined by running the samples on a 0.8 % agarose gel in 1 x TBE (made using DEPC-treated mQH_2O). Samples producing clear bands corresponding to 16S and 23S were used for microarray analysis.

2.4.1.4 cDNA synthesis

RNA (16 µg) for each sample was incubated with random primers (5 µg) at 72 °C in a PCR block for 10 min then chilled on ice for 10 min. cDNA synthesis was initiated by the addition of a reaction mix consisting of 6 µl 5 x First Strand (FS) buffer (Invitrogen), 3 µl 0.1 M DTT (Invitrogen), 0.6 µl 50 x dNTP master mix (0.1 mM dATP, dGTP, dTTP and 0.05 mM dCTP) (Roche) and 2.9 µl nuclease-free water (Qiagen). Samples were treated with either 2 µl Cy3 or 2 µl Cy5 (with a technical repeat for each, where the dyes were swapped). SuperScript III (1.5 µl 200 U μl^{-1}) was added to each sample followed by 5 min incubation at 25 °C then an overnight incubation at 50 °C. Samples were hydrolysed by addition of 15 µl 0.1M NaOH and incubation at 72 °C for 10 min. To neutralise, 15 µl 0.1M HCl were added. The samples were cleaned up

using a QIAquick PCR purification kit (Qiagen) according to the manufacturer's instructions. Buffer PB was added to the samples at a ratio of 5:1 volumes and mixed by inverting. The mix was transferred into a spin column in a 2 ml collection tube and centrifuged for 1 min at 10,000 rpm. The flow-through was discarded and the column was washed twice with 750 µl buffer PE. To ensure removal of all liquid, the column was put back into the same tube and centrifuged for 1 min at 10,000 rpm. For elution of the cDNA, the column was transferred to a fresh 1.5 ml eppendorf, 50 µl nucelase-free water applied to the centre of the membrane and centrifuged for 1 min at 10,000 rpm. To measure the concentration of single-stranded cDNA, 2 µl of the labelled cDNA was denatured by heating to 95 °C for 5 min. cDNA was quantified using a Nanodrop ND-1000 UV-VIS spectrophotometer version 3.2.1 against a nuclease-free water blank. The following equations were used to calculate the yield of cDNA and its specific activity, respectively:

cDNA (ng) = A_{260} x 330 ng/µl x 50 µl sample volume

pmol Cy3 or Cy5 per µg cDNA = ([Cy3] or [Cy5])/([cDNA]) x 1000

The samples were suitable for hybridisation if the yield was > 825 ng and the specific activity was > 8 pmol Cy3 or Cy5 per µg DNA.

2.4.1.5 Hybridisation

For each reaction, an appropriate volume of Cy3-labelled cDNA and Cy5-labelled cDNA were added to a 0.5 ml nuclease-free tube to each give a final concentration of 400 ng. The mix was made up to a final volume of 20 µl with nuclease-free water, boiled at 100 °C for 2 min in a PCR block, then chilled on ice for 2 min followed by a 2 min incubation at room temperature. Blocking agent (5 µl of 10x stock) and 25 µl of 2 x GEx hybridisation buffer HI-RPM were added to each reaction tube. The contents were mixed by careful pipetting, centrifuged for 1 min at 13,000 rpm and the samples loaded onto the array immediately. The Agilent microarray hybridization assembly consists of an Aglient SureHyb chamber, a gasket slide, an array slide and a clamp to hold the assembly in place. To assemble the chamber, a clean gasket slide was inserted into the Agilent SureHyb chamber base and 40 µl of sample was slowly dispensed onto a gasket well in a 'drag and dispense' manner, avoiding contact between the pipette tip or

hybridisation solution and the gasket walls. An array slide was placed 'active side' down onto the SureHyb gasket slide and the two slides held in place by the SurehHyb chamber cover and the clamp. The assembled chamber was then vertically rotated to wet the gasket and assess the mobility of the bubbles. If stationary bubbles are present, the assembly can be tapped on a hard surface to aid movement. The chamber was placed in a rotisserie in an oven and the samples allowed to hybridise for 17 h at 65 °C during gentle rotation.

2.4.1.6 Washing of slides

The microarray wash procedure for Agilent's two-colour platform was carried out according to the manufacturer's instructions. Three glass staining dishes, a metal slide rack and two magnetic stirrer bars were dedicated to the two-colour array experiments to avoid contamination. Dishes were thoroughly rinsed with mQH_2O at least 5 times prior to use. Two gene expression (GE) wash buffers (Agilent), supplemented with 0.005 % Triton X-102 (Agilent) prior to first use, were used in this protocol. GE wash buffer #2 (400 ml) was preheated to 37 °C overnight in a sterile Duran. After hybridisation, dish one (separation of array-gasket sandwich) and dish two (first wash) were filled with GE wash buffer #1 at room temperature. Hybridisation chambers were removed from the oven one at a time and disassembled. The array-gasket sandwich was removed from the chamber base by grabbing the slides from their ends and submerging the slides in GE wash buffer #1 in dish one. Whilst completely submerged, the sandwich was pried open. The array slide was then placed into the slide rack in dish two, containing GE wash buffer #1 at room temperature, with minimum exposure of the slide to air. These steps were repeated for any subsequent slides to allow for uniform washing. After all slides were placed into the slide rack in dish two, the stirrer bar was set to a medium speed and the slides washed for 1 min. During the first wash, GE wash buffer #2 was removed from the 37 °C incubator and poured into dish three. After the first wash was complete, the slide rack was transferred to dish three, the stirrer bar was set to medium speed and the slides washed for 1 min. The slide rack was then removed slowly (taking c. 10 s) to minimise droplets on the slides. Slides were scanned immediately to minimise the impact of environmental oxidants on signal intensities. If necessary, the slides could be stored in slide boxes, in a nitrogen purge box, in the dark.

2.4.1.7 Scanning of slides

Slides were scanned using an Agilent DNA microarray scanner (Agilent Technologies, G2505) controlled by Agilent Scan Control software (v8.5). Output two-colour .tiff image files were produced according to the scanning instructions in the Fairplay III microarray protocol (Agilent Technologies, 252009).

2.4.1.8 Analysis of data

Data acquisition was carried out using Agilent Feature Extraction software (v6.5), which allows measurement of the Cy3 and Cy5 fluorescence of each feature in the scanned microarray image. Data were normalised and interpreted using GeneSpring 7.3.1 (Agilent Technologies), by dividing the experimental channel by the control channel and applying a global LOWESS normalisation. The LOWESS normalisation removes dye intensity-dependent artefacts caused by the fact that Cy5 and Cy3 fluorescence are not linear at low fluorescence levels. Identification of statistically significant gene expression changes was achieved by applying a t-test with a 2-fold cut-off and $p < 0.05$. Each condition tested using microarrays had four replicates consisting of two biological repeats, CORM-3- or iCORM-treated samples hybridised against a non-treated control, each with two technical (dye-swap) repeats.

2.4.1.9 Inferring transcription factor activity using TFInfer

Transcription factor modelling was performed in collaboration with Dr Ronald Begg and Dr Guido Sanguinetti at the School of Informatics, University of Edinburgh. Gene expression time-series, generated from microarray analysis, were used to infer transcription factor activities using a probabilistic model (Sanguinetti *et al.* 2006). The model essentially adopts a log-linear approximation for the regulation of genes by the activity of transcription factors. Changes in gene expression are modelled as a weighted linear combination of changes in transcription factor activity using the following equation:

$$y_n(t) = \sum_m X_{nm} b_{nm} c_m(t) + \mu_n + \varepsilon_{nt}$$

Here, $y_n(t)$ is the log-fold change for the n-th gene at time t, X_{nm} is a binary matrix encoding the structure of the regulatory network (obtained typically from the literature),

b_{nm} are the unknown rate constants for activation/repression, $c_m(t)$ is the (log) change in transcription factor activity, μ_n is the perturbed baseline expression level of gene *n* and ε_{nt} is an error term. Standard statistical inference techniques can then be employed using TFInfer (Asif *et al.* 2010), which is an implementation of the probabilistic model (Sanguinetti *et al.* 2006). This enables estimates of the changes in the activity of regulators from an analysis of the behaviour of their targets. The inference procedure gives probability distributions for the transcription factor profiles, rate constants and mean gene-expression levels based on the model and the observed gene-expression data. The means of the distributions provide point estimates for the terms listed above. Although the model is a simplified representation of transcriptional regulation, it is this simplicity that makes it possible to perform large-scale statistical inference, so that one may obtain data-driven estimates of transcription factor activities (Graham *et al.* 2012).

2.4.1.10 Analysis of TFInfer data

Absolute Pearson correlation coefficients were used to compare conditions. Calculations were performed by Dr Ronald Begg at the School of Informatics, University of Edinburgh. The output from two different TFInfer runs was loaded, e.g. the *hemA* mutant exposed to CORM-3 versus iCORM-3. For each condition, transcription factor profiles were discarded if a constant time-series could fit within the error bars given by TFInfer. This is due to the likelihood that their profiles were constant and the coefficient is undefined if one profile is constant. Profiles that were discarded from one condition, but not from the other were given a 'place-holder' value of two. The absolute value of the Pearson correlation coefficient was calculated for the remaining pairs of transcription factor profiles. A value between zero and one is given, where a value close to zero represents a low correlation between transcription factor profiles and a value close to one represents transcription factor profiles that are highly correlated. Taking the absolute value means that positive correlations are scored as highly as negative correlations. This is done because TFInfer does not know *a priori* the sign of TF-gene interactions, which means that transcription factor profiles generated from TFInfer could be inverted. Only after the data have been received from the modellers can this be corrected by comparing inferred signs with information from databases on transcription factor activity and flipping a transcription factor profile, as well as the signs of its interactions, where necessary. Flipping a transcription factor profile will not affect the absolute value of the correlation coefficient.

Chapter 3. CORM-3 Results in Species- and Concentration-Dependent Inhibition of Microbial Respiration

3.1 Introduction

Although the bactericidal activity of CO-RMs has been reported (Davidge *et al.* 2009b; Desmard *et al.* 2009; Nobre *et al.* 2007), the mode(s) of action of these CO donors remains unclear. The effect of CO on cellular respiration as a result of interaction with haem-containing terminal oxidases is well known. Of particular relevance is the effect of CO on the respiratory oxidases of bacteria (Keilin 1966). Nevertheless, there is limited information on whether the potent lethality induced by CO liberated from these compounds can be attributed to inhibition of the bacterial respiratory chain.

As introduced in section 1.5.3, recent reports identified bacterial respiratory targets of CO released from CORM-3 (reviewed in (Wilson *et al.* 2012)). It has previously been established that high partial pressures of CO in relation to O_2 (typically 19:1) are required for significant inhibition (Keilin 1966). An unexpected finding was therefore the rapid inhibition of the respiration of vigorously aerated cultures of *Escherichia coli* at CORM-3 concentrations equimolar with dissolved O_2 (c. 200 μM). Furthermore, 125 μM CORM-3 resulted in 50 % inhibition within 10 min. Neither CO gas (applied as a saturated solution) nor $RuCl_2(DMSO)_4$ were effective under these conditions (Davidge *et al.* 2009b). However, in a conventional closed oxygen electrode experiment whereby bacterial cells are suspended in buffer within the electrode chamber, as opposed to measuring respiration in a culture sample, inhibition of respiration was not observed unless the respiring cell suspension was exposed to CORM-3 concentrations exceeding 600 μM (Davidge & Poole, unpublished). Inhibition of respiration was also reported for suspensions of *Pseudomonas aeruginosa*. Concentrations as low as 10 and 50 μM CORM-3 elicited a dose-dependent decrease in respiration within 10 min, which continued to decrease for a further 30 min. Moreover, the decrease in oxygen consumption was seen to precede the bactericidal effect; a concentration of 50 μM inhibited respiration immediately, whereas a decrease in viability was not observed until 30 min after addition of the compound (Desmard *et al.* 2009). In a more recent study, pre-incubation of non-respiring suspensions of *C. jejuni* at 100 % air saturation (c. 195 μM O_2 at 42 °C) for 5 min with 100 μM CORM-3, followed by stimulation of

respiration using formate, revealed inhibition of the initial respiration rate in a closed oxygen electrode system when compared with non-treated suspensions, and resulted in a non-linear rate of respiration over the measurement period. However, CORM-3 did not have an effect on the growth of *C. jejuni* in this study (Smith *et al.* 2011).

In support of an interaction of CO liberated from CORM-3 with respiratory oxidases, CO difference spectra of intact *E. coli* cells revealed that respiratory inhibition was accompanied by rapid formation of carbonmonoxy adducts of cytochrome *d* and cytochrome *bo'* (Davidge *et al.* 2009b). In particular the rapid reaction with cytochrome *d* was noteworthy, and is consistent with the high affinity of this oxidase for CO binding (Borisov 2008). In a *cyo* mutant containing only cytochrome *bd*, reduced *minus* oxidised spectra revealed increased levels of the oxidase in CORM-3-treated cells. Furthermore, cytochrome *d* was not detectable in CO difference spectra of cultures exposed to the compound, which was attributed to the interaction of CO from CORM-3 with the oxidase during growth; hence the baseline spectrum would not be perturbed by further exposure to the gas (Davidge *et al.* 2009b). Similar spectra were also recorded for *P. aeruginosa* (Desmard *et al.* 2009) and *C. jejuni* (Smith *et al.* 2011) whole cells treated with 100 μM CORM-3. Desmard and colleagues demonstrated the formation of CO-bound cytochrome *o* in *P. aeruginosa* following CORM-3 treatment, and Smith and co-workers obtained spectra characteristic of CO-bound cytochrome *c* and/or *b* 1 min after addition of CORM-3 to *C. jejuni* cells. Moreover, the spectra observed in both of these studies mirrored that seen following exposure of the bacterial suspensions to CO gas (Desmard *et al.* 2009; Smith *et al.* 2011).

Evidence for the targeting of bacterial respiration was additionally demonstrated by transcriptome profiling of the response of *E. coli* to CORM-3. Genes encoding key components of the aerobic respiratory chain were down-regulated. The most prominent changes were 10 - 22-fold reductions in expression levels of the *cyo* operon (*cyoABCDE*) encoding cytochrome *bo'* and the *sdh* operon (*sdhABCD*) encoding the membrane succinate dehydrogenase. Additionally, down-regulation of genes was observed in the *nuo* operon encoding NADH dehydrogenase, *fdo* genes encoding subunits of the membrane-bound formate dehydrogenase and *glp* genes encoding aerobic and anaerobic glycerol 3-phosphate dehydrogenases and glycerol/glycerol 3-phosphate transporters. However, the *cydAB* operon encoding the alternative oxidase

cytochrome *bd* was up-regulated, which is consistent with the spectral data mentioned above. Anaerobic energy conservation was also affected, albeit to a lesser extent, with differential regulation of genes in the *cyo* and *cyd* operons, as well as genes encoding formate dehydrogenase, glycerol 3-phosphate dehydrogenase and succinate dehydrogenase. Mathematical modelling of the transcriptomic data identified the involvement of two transcription factors, ArcA and FNR, which have direct roles in the regulation of respiration. The activity of ArcA was explained in terms of CO-elicited inhibition of respiration. This would result in ubiquinone reduction consequently preventing its ability to inhibit autophosphorylation of ArcB and subsequent formation of ArcA-P. Increased levels of ArcA-P result in repression of respiratory gene expression, thereby explaining down-regulation of respiratory genes (Davidge *et al.* 2009b). However, the modularity and redundancy of bacterial respiration (Poole & Cook 2000) suggests that a functioning respiratory system could persist under such conditions (Davidge *et al.* 2009b). In another transcriptomic study employing CORM-2 as the CO donor, respiratory genes were not major targets (Nobre *et al.* 2009), but respiration was not measured. The impact of CO on respiration and the relation to anti-bacterial activity therefore remains uncertain.

Assays of CO release from CORM-3 with dithionite-reduced myoglobin showed that liberation of CO was complete in c. 10 min, half-time of 2 - 3 min (Clark *et al.* 2003; McLean *et al.* 2012). On the other hand, recent measurements with myoglobin in the absence of dithionite (which greatly enhances CO release), or OxyHb, as traps for the released CO show that CORM-3 liberated no detectable CO in 1 h (McLean *et al.* 2012). However, the study by Davidge *et al*. (2009b) revealed that high CORM-3 concentrations (125 - 250 μM) dramatically inhibited *E. coli* respiration within 30 min, whereas the major changes in transcript levels were seen within 15 min after exposure to 30 μM CORM-3 (Davidge *et al.* 2009b). The aim of the work presented herein was therefore to determine directly, for the first time, whether CO/CORM-3 acts as a 'classical' inhibitor of respiration, in particular within a time-frame consistent with the rapid loss of CO in certain biological environments.

To accomplish the above and due to the ineffectiveness of using a closed system to determine the effect of CORM-3 on respiring suspensions of *E. coli* (Davidge & Poole, unpublished), an open system was utilised in the experiments described below. *E. coli*

cells were incubated in an O_2 electrode chamber and the O_2 tension allowed to fall to zero. After complete anoxia (maximum CO:O_2 ratio) was achieved, the chamber was opened to the atmosphere after a given period of time to allow inward diffusion of air. Under these 'open' conditions, the respiration rate is given by (Degn *et al.* 1973; Degn *et al.* 1980):

$$v_r = K(T_G - T_L) - dT_L/dt \quad (1)$$

where v_r is the respiration rate, K is a constant dependent on reaction volume, surface area, temperature etc., T_G is the molar concentration of O_2 in the buffer when equilibrated with the gas phase, and T_L is the concentration of O_2 in the liquid sample at time t. That is, at a constant rate of O_2 entry from the atmosphere, which is governed by the stirrer and liquid/air interface, inhibition or stimulation of respiration is indicated by an increase or decrease, respectively, in the measured O_2 tension.

3.2 Results

3.2.1 CORM-3 both stimulates and inhibits bacterial respiration

Initial experiments tested the effect of adding a range of concentrations of CORM-3 to respiring suspensions of *E. coli* at c. 100 µM O_2 (50 % air-saturation in the closed chamber). The chamber was opened c. 1 min after complete anoxia. Addition of 30 µM CORM-3 did not inhibit respiration in either the closed system (Figure 3.1 A, shaded portion), or once the chamber was opened to the atmosphere (Figure 3.1 A, un-shaded portion, solid line), i.e. within a period of c. 50 min. Unexpectedly, respiration was stimulated marginally in the closed chamber (25 %, mean value of 17.1 %, SEM 3.97 %, 3 determinations in 2 biological replicates) and again in the open chamber (13.8 %, mean value of 16.2 %, SEM 5.25 %, 3 determinations in 3 biological replicates), seen here as a depression of the electrode trace when compared with the no-CORM-control (dashed line). Furthermore, 100 µM CORM-3 did not inhibit respiration in the closed phase of the measurement either (Figure 3.1 B, shaded portion), but again stimulated respiration (36.8 %, mean value of 34.7 %, SEM 6.46 %, 4 determinations in 2 biological replicates). After the chamber was opened, stimulation was still observed (Figure 3.1 B, un-shaded portion, solid line) when compared with the control (dashed

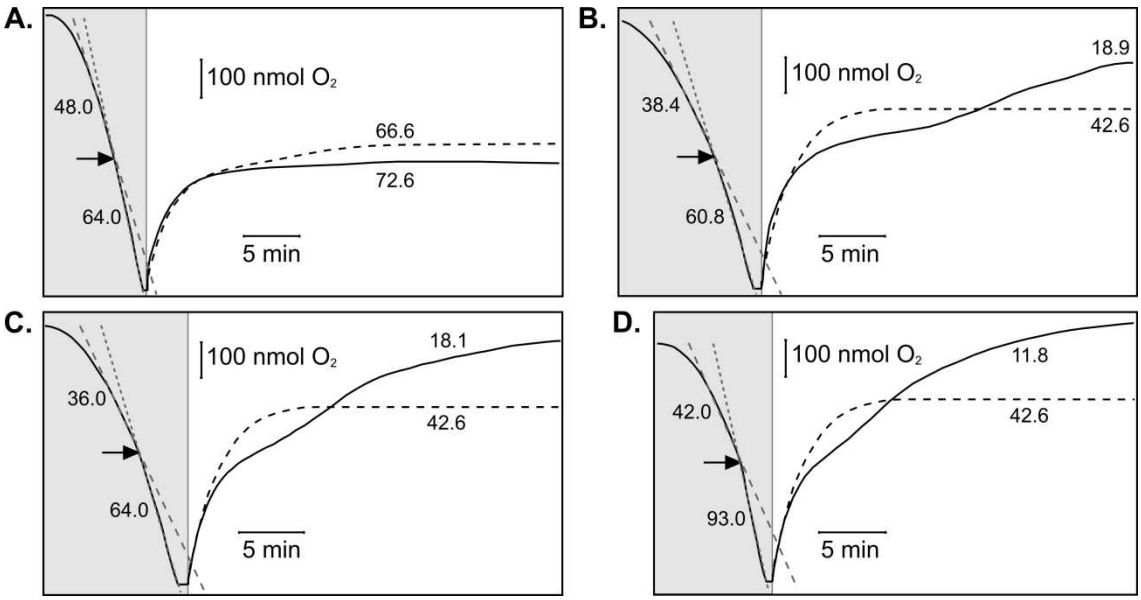

Figure 3.1. CORM-3 both stimulates and inhibits bacterial respiration in a concentration-dependent manner. O_2 utilisation in a suspension of *E. coli* K-12 is represented as O_2 tension versus time. Bacteria were suspended in 50 mM Tris buffer (pH 7.5) and respiration was stimulated by addition of 5 mM glycerol. Shaded and un-shaded sections indicate respiration traces recorded from the closed and open chamber, respectively. CORM-3 was added to the respiring suspension of *E. coli* at 50 % air-saturation (arrow) in the closed chamber. Dashed (before CORM-3 addition) and dotted (after CORM-3 addition) lines show extrapolated traces that highlight the change in gradient after addition of compound. Rates of respiration (v_r: nmol min^{-1}) are shown for each trace. The effects of 30 μM (1.03 mg protein) (**A**) 100 μM (**B**), 250 μM (**C**) and 500 μM (**D**) CORM-3 on bacterial respiration are shown (1.16 mg protein). The control (nothing added) is shown as a dashed line. Traces are representative of ≥ 2 biological replicates with a maximum of 3 technical repeats per experiment.

line). However, c. 20 min after addition of CORM-3 inhibition of respiration was seen as the electrode trace increased above the steady-state level of the control; at 30 min the percentage inhibition was 55.7 % (mean value of 48.5 %, SEM 4.11 %, 4 determinations in 2 biological replicates). As the CORM-3 concentration was increased to 250 μM (Figure 3.1 C) and then to 500 μM (Figure 3.1 D), the initial stimulation in the closed system increased (up to 49.8 % stimulation, SEM 3.53 %, ≥ 4 determinations in ≥ 2 biological replicates) and inhibition occurred progressively earlier upon opening the chamber. Consistent with the observation by Davidge & Poole (unpublished), respiratory inhibition is not measurable in conventional short-term O_2 measurements. However, by making prolonged measurements in the open electrode system, it is clear that an initial phase of respiratory stimulation is followed by inhibition.

3.2.2 CORM-3 inhibition of bacterial respiration is enhanced by prior anoxia

Maximal inhibition of respiration is expected when the CO:O_2 ratio is increased, since CO is a competitive inhibitor of O_2 binding (Keilin 1966). The method in section 3.2.1 was therefore modified to allow increased anoxic contact between CORM-3 and cells. On opening the chamber after a short period of anoxia respiration resulted in a steady-state O_2 tension (Figure 3.2 A, dashed line); constant respiratory O_2 consumption being balanced by *K*, the inward O_2 diffusion rate. However, when 100 μM CORM-3 was added at anoxia and the chamber opened immediately (Figure 3.2 A, solid line), bacterial respiration was initially stimulated (O_2 trace below the control level) and then inhibited (O_2 trace above the control level). As anoxia was lengthened (Figure 3.2 B and C), respiratory stimulation decreased and inhibition occurred progressively earlier. Incubation of cells with CORM-3 for 10 min (Figure 3.2 B) and 20 min (Figure 3.2 C) before re-admitting O_2 resulted in increasing final degrees of respiratory inhibition (0 min anoxia, 41.4 % ± 3.58; 10 min, 53.7 % ± 1.46; 20 min, 61.2 % ± 2.63, means of 3 biological replicates, all measured 35 min after opening the chamber). A lower CORM-3 concentration (50 μM) elicited a similar response, but the stimulatory phase was not further pronounced (Figure 3.3). An additional period of anoxia (5 min) is shown for reference (Figure 3.3 B).

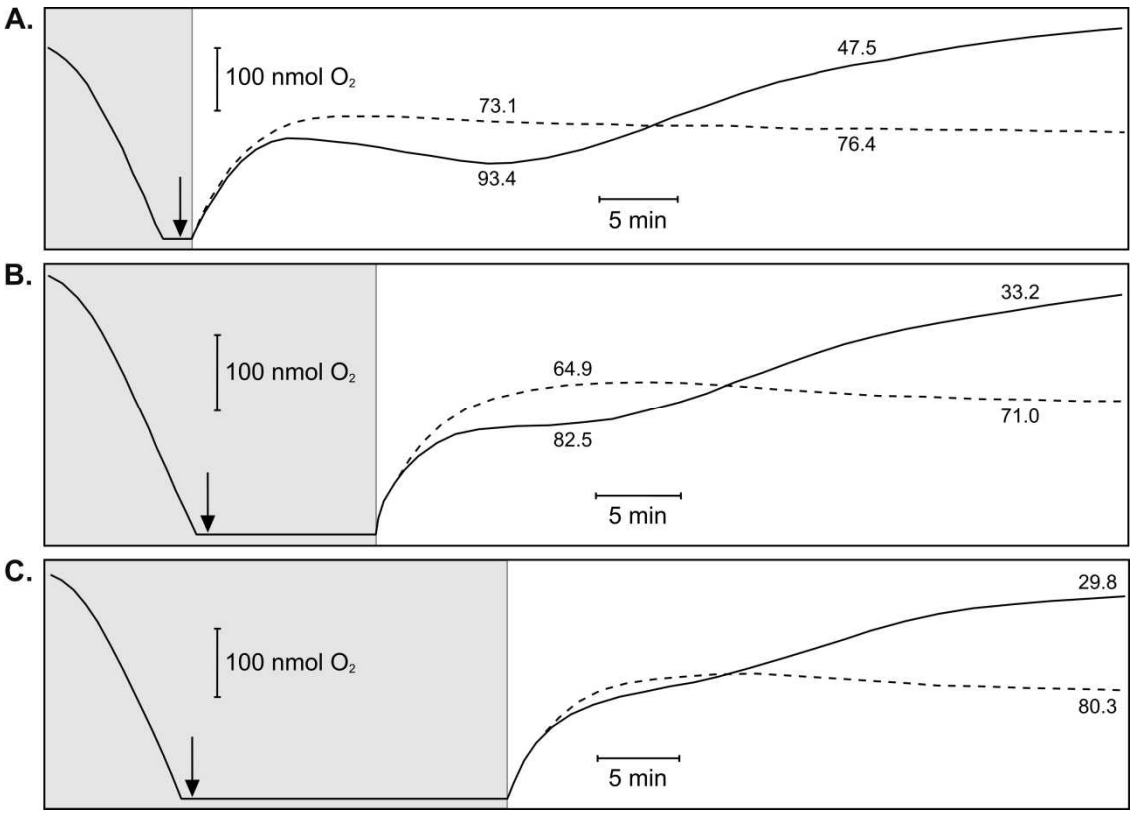

Figure 3.2. Inhibition of bacterial respiration is more potent after anoxic cell incubation with CORM-3. O_2 utilisation in a suspension of *E. coli* K-12 is represented as O_2 tension versus time. The experimental design is as for Figure 3.1, except that, after complete consumption of O_2, nothing (control, dashed line) or 100 μM CORM-3 (arrow, solid line) were added to the chamber and the lid removed **A.** immediately (1.17 mg protein), **B.** after 10 min or, **C.** after 20 min (0.8 mg protein). Rates of respiration (v_r: nmol min^{-1}) are shown for each trace. Traces are representative of 3 biological replicates.

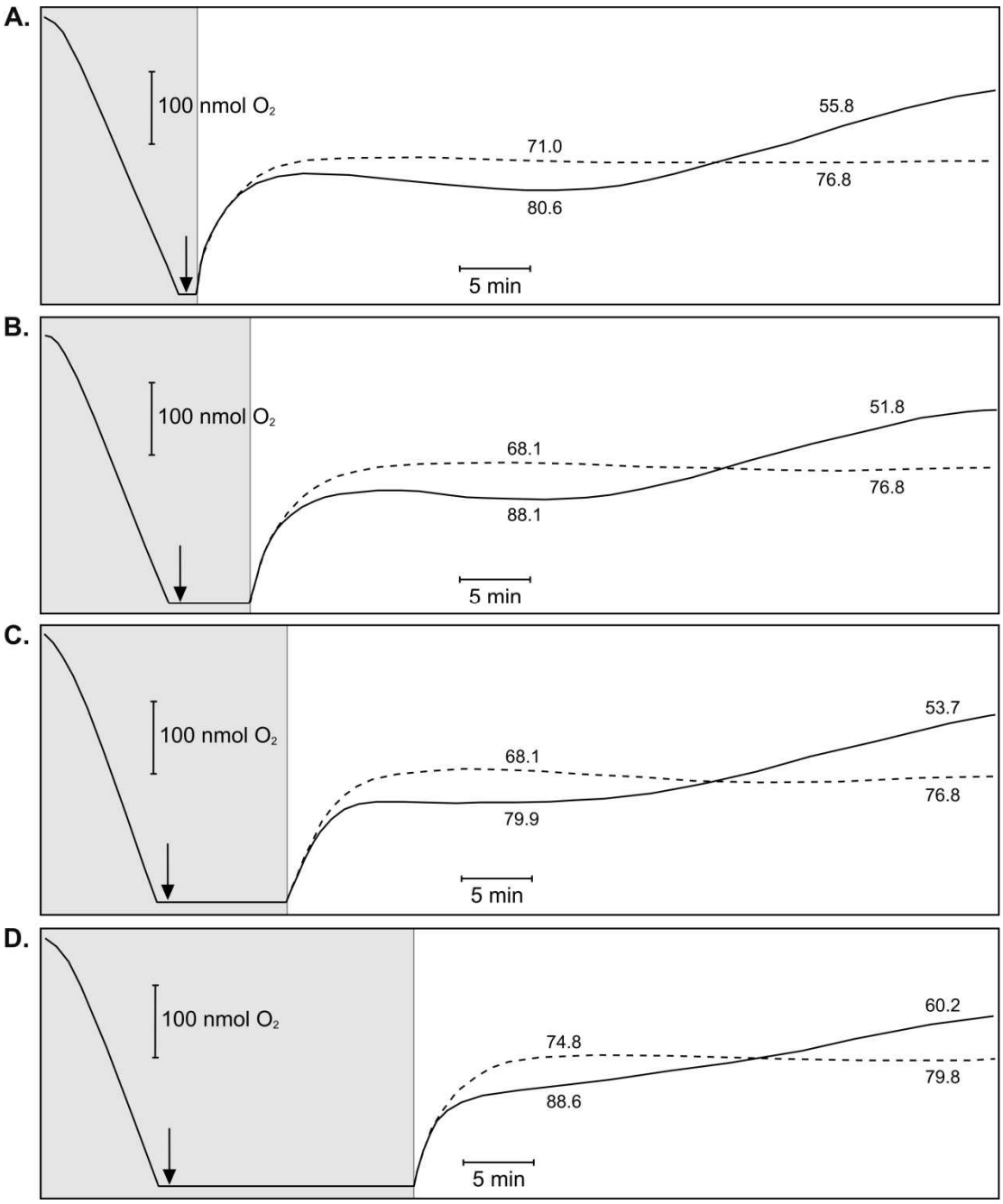

Figure 3.3. A lower CORM-3 concentration elicited a longer period of stimulation and lesser inhibition. O_2 utilisation in a suspension of *E. coli* K-12 is represented as O_2 tension versus time. The experimental design is as for Figure 3.2, except that, after complete consumption of O_2, nothing (control, dashed line) or 50 μM CORM-3 (arrow, solid line) were added to the chamber and the lid removed **A.** immediately, **B.** after 5 min, **C.** after 10 min or, **D.** after 20 min (0.79 mg protein). Rates of respiration (v_r: nmol min^{-1}) are shown for each trace. Traces are representative of 3 biological replicates.

3.2.3 CORM-3 and a classical uncoupler elicit similar respiratory stimulation in an open electrode system

Initial transient stimulation of respiration elicited by CORM-3 was an unexpected finding that warranted further investigation. To determine whether this initial phase followed a similar pattern to the effect of a classical uncoupler, a range of concentrations of carbonylcyanide *m*-chlorophenylhydrazone (CCCP, solubilised in DMSO) were added to respiring suspensions of *E. coli* in an open electrode system, employing the same method as used in Figure 3.2 A. As expected the stimulatory effect of CCCP was concentration-dependent (Figure 3.4). Furthermore, addition of 5 and 10 μM CCCP elicited the same downward deflection of the aerobic steady-state of the no-compound control (i.e. stimulation of respiration; Figure 3.4 A and B) as seen with 100 μM CORM-3 (refer to Figure 3.2 A). Additions of 25 μM (Figure 3.4 C) and 50 μM (Figure 3.4 D) CCCP resulted in a biphasic reaction. Initially respiratory stimulation was more pronounced than observed after addition of lower concentrations of the compound, to an extent where the O_2 level in the chamber was undetectable due to the cells utilising all of the O_2 in solution. After c. 20 min post-addition of 25 μM CCCP the O_2 level in the chamber started to rise and the same was observed slightly earlier (c. 15 min) after addition of 50 μM CCCP. An initial consideration was that the compound may be toxic at higher concentrations. However, *E. coli* viability was unaffected over 60 min after addition of 10 μM CCCP, which was the highest relevant concentration tested here (Figure 3.4 B, inset). Viable counts were measured from suspension samples taken directly from the chamber every 20 min for 60 min post addition of the uncoupler. An initial sample was taken immediately prior to addition. These results are consistent with a report showing that the optimal CCCP concentration for stimulation of respiration in intact cells of yeast is 15 - 20 μM (Poole *et al.* 1973).

3.2.4 CORM-3-mediated uncoupling of respiration?

Although CCCP and CORM-3 elicited similar patterns of activity in the open system (compare Figure 3.2 A with Figure 3.4 A and B) and thus suggesting the latter may act as an uncoupler, the effect is only mild in comparison to CCCP, which caused the same extent of respiratory stimulation at concentrations 10- and 20-fold lower. A ‘mild’

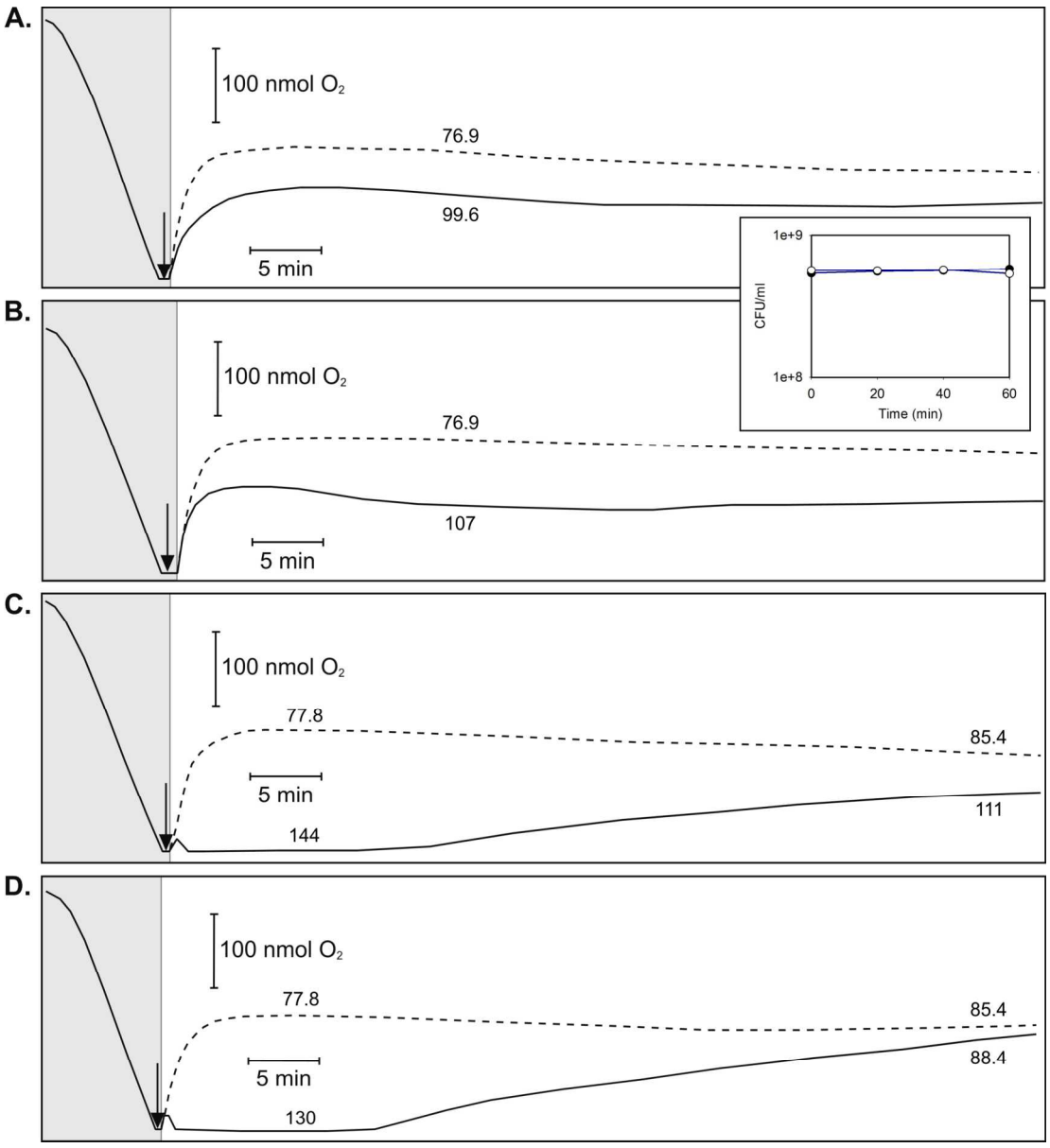

Figure 3.4. CCCP stimulates bacterial respiration in a concentration-dependent manner. O_2 utilisation in a suspension of *E. coli* K-12 is represented as O_2 tension versus time. Bacteria were suspended in 50 mM Tris buffer (pH 7.5) and respiration was stimulated by addition of 5 mM glycerol. The chamber was opened immediately after addition of CCCP (arrow, solid line). The control (an equivalent volume of DMSO) is shown as a dashed line. Rates of respiration (v_r: nmol min^{-1}) are shown for each trace. The effect of 5 µM (**A**), 10 µM (**B**), 25 µM (**C**) and 50 µM (**D**) CCCP is shown (0.91 mg protein). Traces are representative of ≥ 3 biological replicates. Inset of panel B shows viable counts recorded from chamber samples of control (closed circles) or 10 µM CCCP-treated (open circles) suspensions. Data are representative of 2 biological replicates; viability data are plotted as means ± SEM from 6 individual spots.

uncoupling activity of CORM-3 has been suggested in mitochondria. However, bacterial membranes are not known to possess the uncoupling proteins or adenine nucleotide transporters implicated in this work (Lo Iacono *et al.* 2011). More direct evidence was therefore sought by measuring effects on proton translocation *per se* using the well-established oxidant pulse technique (Mitchell & Moyle 1967). Here a bacterial (or mitochondrial) suspension is allowed to become anoxic by substrate oxidation in a lightly buffered solution. Respiration is re-initiated by injection of a known amount of O_2 (air-saturated 150 mM KCl, 30 °C) and subsequent H^+ efflux driven by H^+ pumps, or vectorial chemistry, is recorded using a micro-pH electrode (refer to section 2.3.4). Uncouplers act as protonophores and collapse the H^+ gradient. Initial experiments utilised a final bacterial protein concentration of between 2 - 4 mg, as previously described in (Lawford & Haddock 1973). However, due to the weakly buffered medium and a weak internal buffering capacity of the cells at this concentration, the system was unstable as determined by the extent of pH drift. As a result H^+/O ratios were inconsistent, increasing with each successive addition of O_2. To correct for this the concentration of bacterial protein in the chamber was increased to 5 - 10 mg to improve intracellular buffering capacity and consequently produce consistent H^+/O ratios.

Figure 3.5 A shows H^+ pulses from *E. coli* cells in a medium containing K^+ and SCN^- as counter-ions and valinomycin to promote K^+/H^+ exchange, collapse the transmembrane electrochemical potential ($\Delta\psi$), and minimise back-pressure on H^+ translocation. Successive additions of air-saturated 150 mM KCl (11 ng-atom O) elicited acidification of the bulk medium due to respiration-driven proton translocation. H^+/O ratios calculated after calibration of the apparatus with anoxic HCl were c. 3 (mean 2.65 ± 0.11, 9 determinations in 3 biological replicates), i.e. within the range of values reported previously for *E. coli* (Lawford & Haddock 1973). Treatment of cells with CCCP before O_2 additions dramatically reduced the magnitude and length of the H^+ pulses due to rapid H^+ exchange across the bacterial membrane, i.e. true uncoupling (Figure 3.5 B). Thus CCCP demonstrates classical protonophore activity in *E. coli* cells, namely stimulation of respiration rates and collapse of respiration-driven H^+ translocation.

In contrast, prior treatment of cells with CORM-3, followed by pH readjustment to compensate for loss of a proton from the CO-RM on addition to biological buffers, had

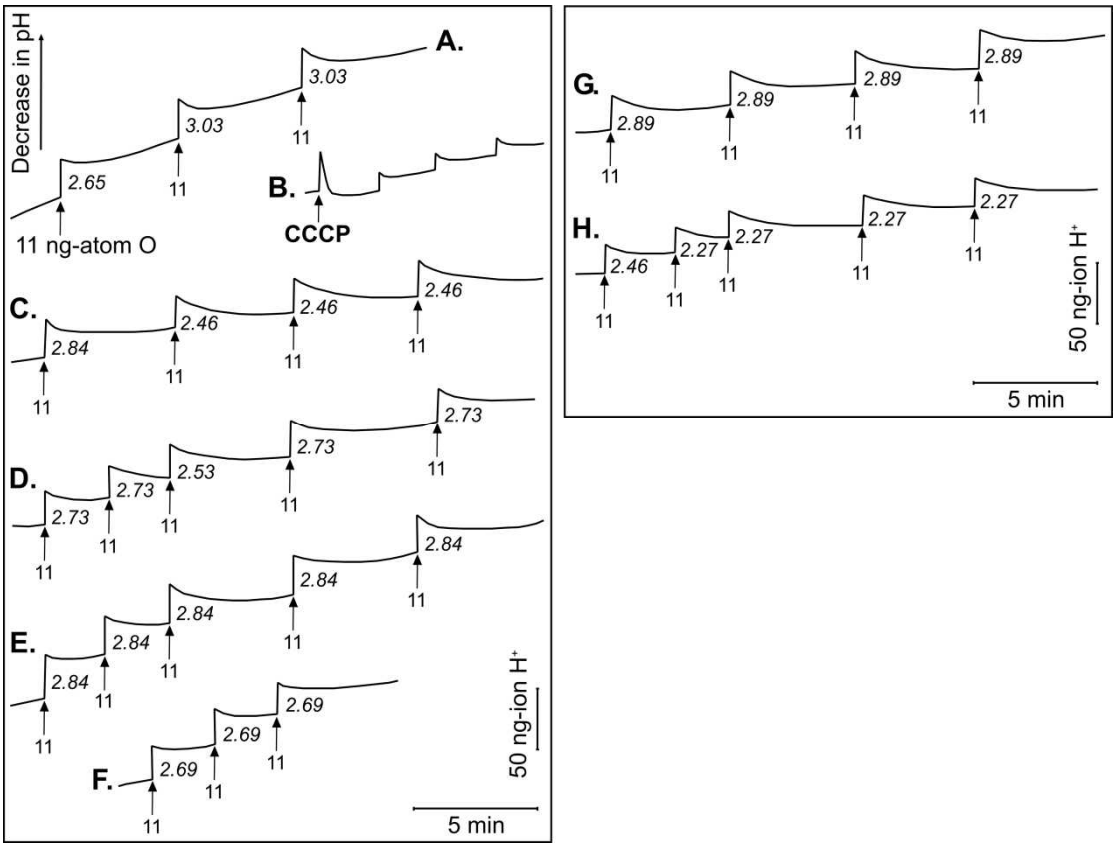

Figure 3.5. CORM-3 is not a true uncoupler. Bacteria were added to a lightly buffered solution in a closed O_2 electrode chamber, followed by immediate addition of valinomycin (22 μM) and stimulation of respiration (1 mM glycerol). The experiment commenced after complete consumption of O_2. Arrows show additions of air-saturated 150 mM KCl (30 °C, 11 ng-atom O), which is immediately followed by proton efflux (acidification, upward deflection). The H^+/O ratio for each pulse is shown. **A.** Representative control pulses (nothing added, 5.43 mg protein), mean H^+/O = 2.65 ± 0.11, 9 determinations, **B.** pulses after addition of 4 nmol (1.6 μM) CCCP (5.43 mg protein), **C.** 20 μM CORM-3 (5.64 mg protein), mean H^+/O = 2.51 ± 0.06, 13 determinations (1.2 % lower than control), **D.** 50 μM CORM-3 (4.90 mg protein), H^+/O = 2.67 ± 0.04, 18 determinations (5.6 % higher than control), **E.** 100 μM CORM-3 (5.43 mg protein), H^+/O = 2.56 ± 0.07, 15 determinations (3.4 % lower than control), and **F.** 150 μM CORM-3 (7.35 mg protein), H^+/O = 2.43 ± 0.07, 9 determinations (4.7 % lower than control). The right-hand panel shows pulses after addition of **G.** 20 μM iCORM-3 (5.64 mg protein), H^+/O = 2.35 ± 0.17, 13 determinations (5.2 % lower than control), and **H.** 100 μM iCORM-3 (8.85 mg protein), H^+/O = 2.39 ± 0.05, 14 determinations (9.1 % lower than control). Data are representative of the given number of determinations from 3 biological replicates.

a minimal effect on the H^+/O ratio. CORM-3 at 20 - 150 μM (Figure 3.5 C - F) attenuated only marginally the H^+/O ratios in intact bacteria (refer to the legend of Figure 3.5). Inactive CORM-3 (iCORM-3) at 20 μM (Figure 3.5 G) and 100 μM (Figure 3.5 H) produced similar results. Note that control H^+ pulses were recorded in triplicate prior to each addition of compound. The pulses presented in Figure 3.5 A are representative of the pattern obtained before treatment of the cell suspensions with CORM-3/iCORM-3 and correspond to the 100 μM CORM-3 data shown in Figure 3.5 E. To enable a better comparison between the pulses before and after addition of compound in each experiment, the percentage difference between the average H^+/O ratios is provided in the Figure legend.

In addition to measuring H^+/O ratios, the rate of H^+ backflow after the O_2 pulse was measured in the absence and presence of 20 μM CORM-3 and iCORM-3. In both cases the $t_{½}$, measured from semi-log plots of pH changes, were not significantly lowered by CORM-3 (Figure 3.6 A; 1.45 min and 1.66 min for corresponding control pulses), or iCORM-3 (Figure 3.6 B; 1.47 min and 1.57 min for corresponding control pulses). CORM-3-induced respiratory stimulation therefore does not appear to be a consequence of true uncoupling (i.e. protonophore activity).

3.2.5 CO-depleted ruthenium compounds have minimal effects on respiration

Commonly used CO-RMs have properties other than CO release that may interfere with biological processes. In particular, CORM-3 is a ruthenium-based carbonyl and ruthenium is a metal ion with redox chemistry that does not occur naturally in biology. Furthermore, CO release may also be accompanied by loss of glycinate, chloride and other unknown processes and interactions. To demonstrate that the perturbing effects of CORM-3 on bacterial respiration are due specifically to CO release, the effects of three ruthenium-containing control molecules were tested. $RuCl_2(DMSO)_4$ (section 2.3.1.2) is typically a control for CORM-2, a precursor in CORM-3 synthesis (Clark *et al.* 2003), in which the CO groups are replaced by DMSO (Sawle *et al.* 2005). When used at 50 μM (Figure 3.7 A, solid line) or 100 μM (Figure 3.7 B, solid line), neither stimulation nor inhibition of respiration was observed. The same result was obtained with 50 μM (Figure 3.7 C, solid line) and 100 μM (Figure 3.7 C, long-dash line) iCORM-3, i.e. CORM-3 that was allowed to lose CO and then flushed with N_2 to displace CO from

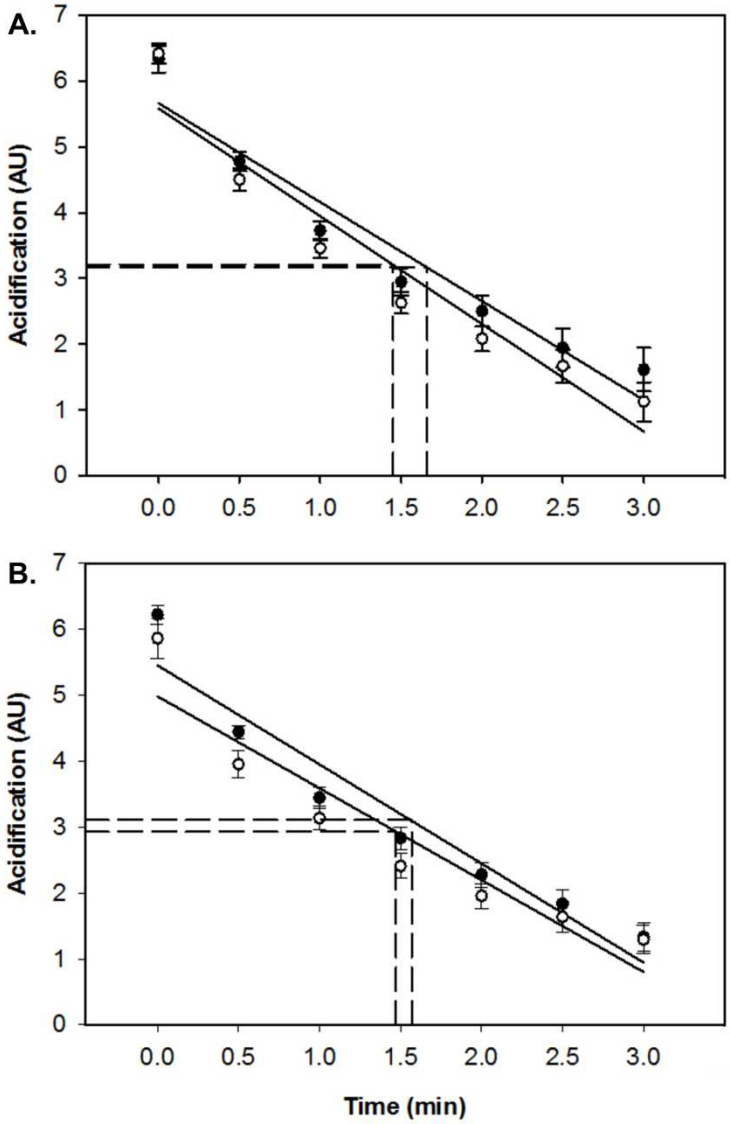

Figure 3.6. CORM-3 does not increase the rate of proton backflow after respiration-driven proton translocation across the membrane. Bacteria were added to a lightly buffered solution in a closed chamber, followed by immediate addition of valinomycin (22 µM) and stimulation of respiration (1 mM glycerol). The experiment commenced after complete consumption of O_2. Rates of decay were calculated from pulses as shown in Figure 3.5. **A.** Control (nothing added, closed circles), $t½$ = 1.66 min compared with 20 µM CORM-3 (open circles), $t½$ = 1.45 min (6.08 ± 0.23 mg protein) and **B.** control (nothing added, closed circles), $t½$ = 1.57 min compared with 20 µM iCORM-3 (open circles), $t½$ = 1.47 min (6.08 ± 0.23 mg protein). Data are plotted as means ± SEM from 3 biological replicates, with ≥ 3 technical repeats per experiment. Protein concentrations are shown as means ± SEM from 3 biological replicates, with a range from 5.64 - 6.39 mg.

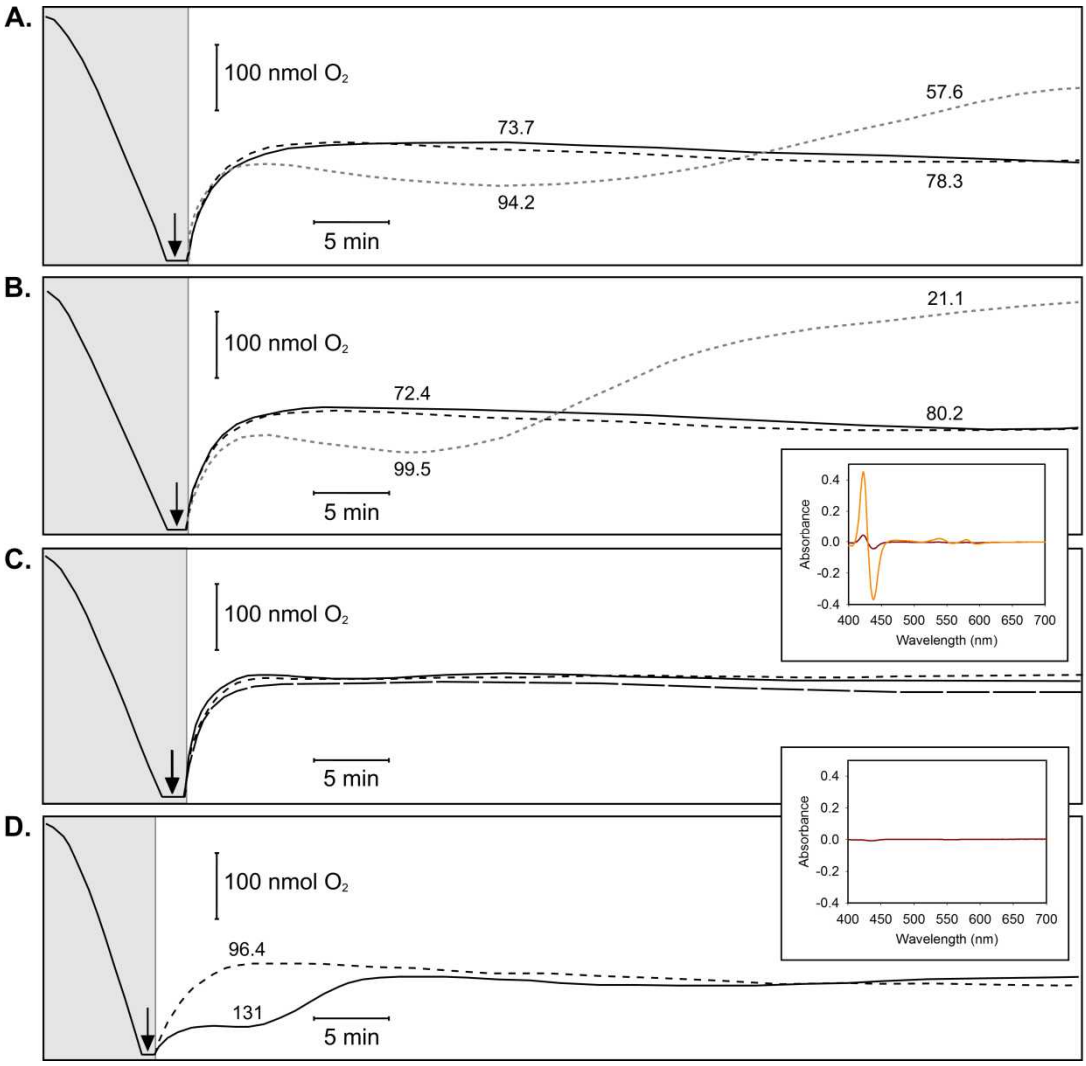

Figure 3.7. CO-deficient compounds have minimal effects on bacterial respiration. O_2 utilisation in a suspension of *E. coli* K-12 is represented as O_2 tension versus time. Bacteria were suspended in 50 mM Tris buffer (pH 7.5) and respiration was stimulated by addition of 5 mM glycerol. Control compounds (black solid lines) were added after complete O_2 consumption (arrows) and the chamber was opened immediately. Rates of respiration (v_r: nmol min^{-1}) are shown where relevant. **A.** 50 µM $RuCl_2(DMSO)_4$, 50 µM CORM-3 (grey dotted line) is shown for reference (0.53 mg protein), **B.** 100 µM $RuCl_2(DMSO)_4$, 100 µM CORM-3 (grey dotted line) is shown for reference (0.53 mg protein), **C.** 50 µM (black solid line) and 100 µM (black long-dash line) iCORM-3 (0.67 mg protein), CO release from iCORM-3 (red) in comparison with CORM-3 (orange) is shown inset and **D.** 50 µM miCORM-3 (0.85 mg protein), inactivity of miCORM-3 is shown by the lack of CO release to ferrous myoglobin (inset). The control (nothing added, or in the case of miCORM-3 an equivalent volume of KPi) is shown as a black dashed line. Traces are representative of ≥ 2 biological replicates.

solution (Clark *et al.* 2003; Lo Iacono *et al.* 2011) (section 2.3.1.3). The compound generated via such a method releases residual CO to ferrous myoglobin (Figure 3.7 C, inset, red line), but CO release never exceeds 10 % of the quantity liberated by intact CORM-3 (Figure 3.7 C, inset, orange line).

Both of these compounds are imperfect controls: $RuCl_2(DMSO)_4$ lacks the glycinate group of CORM-3 and, in addition to residual CO release, iCORM-3 has not been exposed to biological molecules, or intracellular species, that may induce further release of CO. Thus a new CORM-3 control, namely myoglobin-inactivated (mi)CORM-3, was devised. Removal of CO was achieved by two treatments with ferrous myoglobin (section 2.3.1.4) due to its high affinity for CO (K_{on}/K_{off} 2.7 x 10^7 (Smerdon *et al.* 1995)). Such a preparation, when tested with fresh ferrous myoglobin, gave no detectable CO release (Figure 3.7 D, inset) and at a final concentration of 50 μM did not elicit the same respiratory response as the active CO donor (Figure 3.7 D, solid line, compare with grey dotted line in panel A). However, a slight biphasic reoxygenation was noted in some experiments, an observation that cannot be explained at present. Due to the generation of a low stock concentration of miCORM-3, this inactive compound can be used only as a control for CORM-3 concentrations of ≤ 50 μM. In conclusion, the data suggest CO release is necessary for the complete perturbing effects of the CO-RM on bacterial respiration.

3.2.6 CO gas is ineffective against respiring whole-cell suspensions of *E. coli*

As mentioned in section 1.5.3.5, CO gas does not elicit the same effect as CO-RMs in bacterial systems. In line with this observation, Figure 3.8 shows that, irrespective of the period (up to 20 min) during which 100 μM CO (applied as a CO-saturated solution) and cells were incubated anoxically to maximise the $CO:O_2$ ratio, CO did not inhibit subsequent respiration. Furthermore, no initial stimulation of respiration was observed.

3.2.7 CORM-3 is an inhibitor of respiration in pathogenic bacteria and yeast

To establish a wider knowledge-base for the effects of CORM-3 on microbial respiration, the compound was added to respiring cultures of three pathogenic species of bacteria and a pathogenic yeast (Figure 3.9). CORM-3 at 25, 50 and 100 μM inhibited

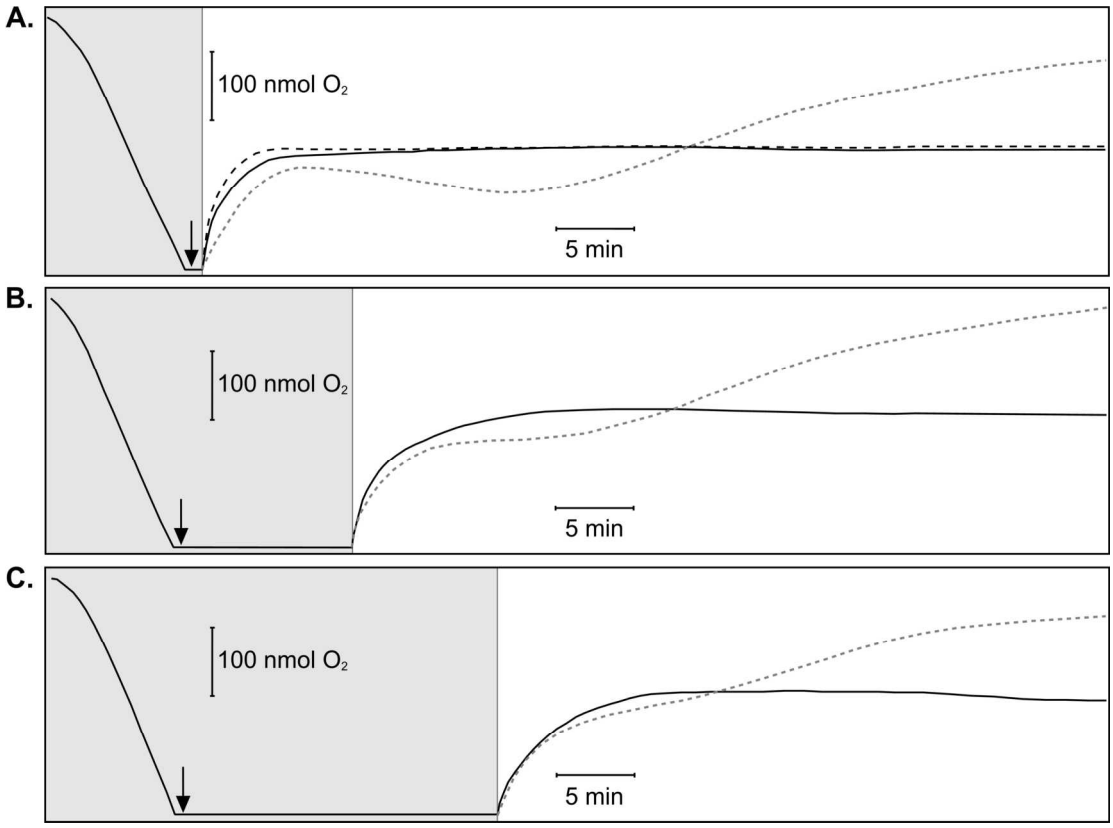

Figure 3.8. CO gas does not affect bacterial respiration, even after anoxic incubation with cells. O_2 utilisation in a suspension of *E. coli* K-12 is represented as O_2 tension versus time. Bacteria were suspended in 50 mM Tris buffer (pH 7.5) and respiration was stimulated by addition of 5 mM glycerol. CO saturated solution (50 mM Tris buffer, pH 7.5) at 100 μM (solid lines) was added after complete O_2 consumption (arrows) and the chamber opened **A.** immediately (0.73 mg protein), **B.** after 10 min (0.73 mg protein) or, **C.** after 20 min (0.72 mg protein). The control (an equal volume of buffer) is shown as a black dashed line in panel A. Control traces overlapped those recorded after exposure to CO in panels B and C. Data presented for 100 μM CORM-3 in Figure 3.2 have been superimposed for reference (grey dotted lines). Traces are representative of ≥ 2 biological replicates.

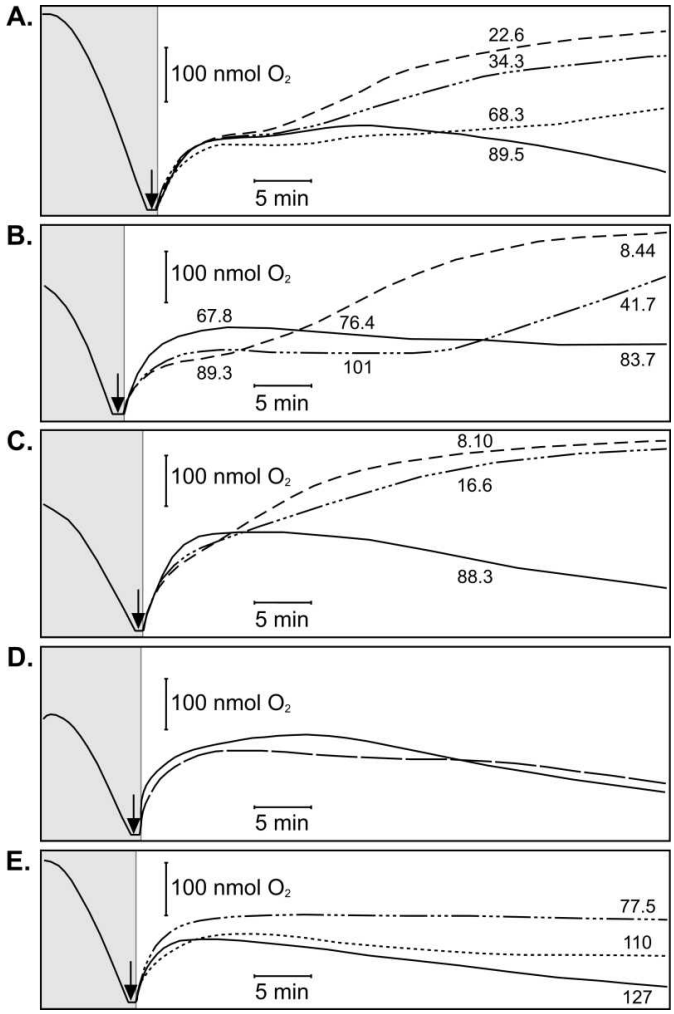

Figure 3.9. CORM-3 activity is species- and concentration-dependent. O_2 utilisation is represented as O_2 tension versus time. Bacteria were suspended in their respective defined medium containing respiratory substrate. CORM-3 was added after complete O_2 consumption in the closed chamber (arrows) and the chamber opened immediately. Rates of respiration (v_r: nmol min^{-1}) are shown. Effect of **A.** 25 μM (dotted line), 50 μM (dashed-dotted line) and 100 μM (dashed line) CORM-3 on *P. aeruginosa* (1.22 mg protein), **B.** 50 μM (dashed-dotted line) and 100 μM (dashed line) CORM-3 on *E. coli* O157 (0.62 mg protein), **C.** 50 μM (dashed-dotted line) and 100 μM (dashed line) CORM-3 on *S.* Typhimurium (0.65 mg protein), **D.** 50 μM miCORM-3 (dashed line) on *S.* Typhimurium (0.50 mg protein), and **E.** 250 μM (dotted line) and 500 μM (dashed-dotted line) CORM-3 on *C. albicans* (0.47 mg protein). In each panel, the control (nothing added, solid line) is shown for reference. Traces of *C. albicans* respiration after addition of 50 and 100 μM CORM-3, and 250 and 500 μM iCORM-3, overlaid the control trace in panel E. Traces are representative of ≥ 2 biological replicates. This work was carried out, in part, by Bethan Hughes (undergraduate project student).

the respiration of the opportunistic, nosocomial pathogen *P. aeruginosa* by typically 23.7, 61.7, and 74.7 %, respectively, after 30 min (Figure 3.9 A). Respiration of *E. coli* O157, an enterohemorrhagic strain that is a major cause of food-borne illness (Karch *et al.* 2005), elicited a biphasic response after exposure to the CO donor (Figure 3.9 B), which was similar to that of non-pathogenic *E. coli* (Figure 3.2 A and Figure 3.3 A). Respiratory stimulation was seen to a similar extent after addition of both 50 and 100 μM CORM-3, typically 24.4 and 24.1 % (measured after 21 min and 6 min, respectively, due to the markedly shorter period of stimulation following addition of 100 μM CO-RM). The degree of inhibition, however, differed considerably between the two concentrations (50.2 % for 50 μM and 89.9 % for 100 μM, after 50 min). Additionally, at equimolar concentrations the compound inhibited respiration of the food-borne pathogen *S.* Typhimurium by typically 81.3 % and 90.8 %, respectively, after 30 min (Figure 3.9 C).

Control experiments employing one or more inactive CORM-3 compounds (iCORM-3, miCORM-3 and $RuCl_2(DMSO)_4$) showed that only CO-releasing molecules were effective. An example is shown for *S.* Typhimurium and demonstrates that 50 μM miCORM-3 was not a respiratory inhibitor (Figure 3.9 D). Neither the ruthenium of CORM-3, nor other properties of the molecule, can therefore explain the effects elicited by the CO donor. Although CORM-3 also inhibited respiration of the opportunistic fungal pathogen, *Candida albicans*, concentrations as high as 250 and 500 μM were required (Figure 3.9 E) and only inhibited respiration by typically 13.4 and 39.0 %, respectively. Lower concentrations (50 and 100 μM) were ineffective and resulted in a continuous decline in dissolved O_2, which mirrored the trace of the control (nothing added). Again, equimolar concentrations of an inactive control compound, in this case iCORM-3, were ineffective and overlaid the control trace. CORM-3-elicited respiratory stimulation was not observed in *P. aeruginosa, S.* Typhimurium or *C. albicans*. However, the increased uptake of O_2 observed over time in the control (nothing added) traces, shown as a decline in dissolved O_2, may be due to growth of the microbes during incubation in the oxygen electrode chamber.

3.3 Discussion

The data presented herein demonstrate unequivocally that CORM-3 is a potent inhibitor of bacterial respiration in three species as well as in a pathogenic yeast. This effect can be attributed to CO liberated from the CO-RM as inactive control compounds were ineffective (Figure 3.7 and Figure 3.9 D). Prolonged observation in the open electrode revealed that respiratory inhibition is accelerated by pre-incubation of *E. coli* with CO-RM under anoxic conditions (Figures 3.2 and 3.3), which maximises the CO:O_2 ratio and favours binding of CO to haem targets, as reported previously for hypoxic mitochondria (D'Amico *et al.* 2006). The inhibitory effects on bacterial respiration were to be expected due to the well-known reaction of CO with haem-containing oxidases. In further support of the studies detailed in section 3.1 (Davidge *et al.* 2009b; Desmard *et al.* 2009; Smith *et al.* 2011), the direct reaction of CO liberated from CO-RM and the terminal oxidases of bacteria has been demonstrated by exploiting the classic observation that the haem-CO bond is photosensitive (Keilin 1966). The data revealed that moderate intensities of visible light reversed the inhibition of *E. coli* respiration by CORM-3 at ambient temperatures, with subsequent alleviation of reductions in cell viability (Wilson *et al.* submitted). However, this demonstration does not exclude the possibility that CO/CO-RMs interact with additional targets.

A complexity observed in this study is the transient stimulation of respiration that preceded respiratory inhibition in *E. coli* (Figures 3.1 - 3.3). Again this is an effect that can be attributed to CO, as inactive control compounds did not elicit the same response (Figure 3.7). CORM-3 (100 μM) was also seen to elicit a modest, transient stimulation of respiration in *C. jejuni* cells deficient in the cyanide insensitive oxidase (*cioAB*) (Smith *et al.* 2011). The mechanism(s) behind this finding was not investigated, but it was proposed that CORM-3 may stimulate electron flux to the sole remaining oxidase, cytochrome *cbb'*. This may occur as a result of CO-RM-mediated increases in membrane permeability or disscociation of electron flux through the oxidase from proton translocation. In turn this would prevent electron leakage that leads to generation of hydrogen peroxide, which if subjected to the activity of endogenous catalase would result in the regeneration of O_2 (Smith *et al.* 2011).

Respiratory stimulation similar to that seen in the present study was also observed in mitochondria exposed to low concentrations of CORM-3 (Lo Iacono *et al.* 2011). As in the present study, Lo Iacono et al. showed that the effect of CORM-3 was unlike that of a classical uncoupler, FCCP. First, far higher CO-RM concentrations (around 2 - 50 μM) were needed than for FCCP (0.02 - 1 μM) to observe State 2 (substrate-dependent basal respiration that occurs in the absence of exogenous ADP) stimulation, which was more marked and instantaneous with the latter compound (2.4-fold stimulation with 20 μM CORM-3 versus 6.3-fold with 1 μM FCCP). Second, mitochondrial membrane potential ($\Delta\psi$) was minimally affected by CORM-3 compared with FCCP. The effect of 0.02 μM FCCP was similar to that of 20 μM CORM-3, whereas 1 μM FCCP collapsed the potential instantaneously. No direct measurements of H^+ fluxes accompanying respiratory stimulation were reported, although the 'recoupler' 6-ketocholestanol did not affect mitochondrial stimulation by the CO donor (Lo Iacono *et al.* 2011). Furthermore, in models of renal function and sepsis, low CORM-3 concentrations increased the respiratory control index, a measure of the tightness of coupling (Lancel *et al.* 2009; Sandouka *et al.* 2006). The data presented herein reveal that CORM-3 does not collapse the protonmotive force, determined by measuring: 1) H^+/O ratios after addition of the CO donor (Figure 3.5 C - F), or its inactive counterpart (Figure 3.5 G and H), and 2) rates of O_2 pulse decay elicited by CORM-3 (Figure 3.6 A) or the inactive compound (Figure 3.6 B). Although the mode by which CO/CORM-3 elicits respiratory stimulation cannot be readily explained at present, it is clear that the action is not that of a classical uncoupler, i.e. a protonophore (Nicholls & Ferguson 2002) that causes dissociation between electron transfer and ATP synthesis.

Lo Iacono *et al*. (2011) showed that 5-hydroxydecanoate, an inhibitor of mitochondrial ATP-dependent K^+ channels, did not reduce CO-RM-elicited respiratory stimulation. However, recent experiments carried out by an undergraduate student (Victoria Lund) revealed that CORM-3 effectively promotes the transport of K^+ and Na^+ across the membrane in an ionophore-like manner (Wilson *et al*. submitted). This is consistent with previous reports demonstrating that CO gas and CORM-2 effect the movement of small molecules through ion channels (Wilkinson *et al.* 2009; Wilkinson & Kemp 2011). Nevertheless, the basis of the effect on K^+ transport is unclear. *E. coli* possesses several systems for the transport of K^+, the major intracellular cation present at concentrations of 0.1 - 0.5 M in the cell. An example of such a transporter is Kch (Kuo

et al. 2003), which was the first prokaryotic K^+ channel to be identified with clear homology to eukaryotic voltage-activated K^+ channels shown to be modulated by CORM-2 (Jara-Oseguera *et al.* 2011). However, a recent report suggests CO prevents, not promotes, mitochondrial permeabilisation and thus prevents swelling (Queiroga *et al.* 2011), but the effect appears unlinked to K^+ permeability. The impact of CORM-3 activity on ion movement may therefore explain the mild respiratory stimulation elicited by the compound.

Interestingly, CO gas at an equimolar concentration to CORM-3 (100 μM) did not elicit respiratory stimulation or inhibition of intact *E. coli* cells, even after periods of extended anoxia (Figure 3.8). As detailed in section 3.2.6, this is in line with previous reports showing the ineffectiveness of CO gas in comparison with CO-RMs. However, in mitochondria a modest increase in State 2 respiration can be demonstrated, but only at non-physiological (960 μM) CO concentrations (Lo Iacono *et al.* 2011). On the other hand, another group showed that concentrations as low as 10 μM CO slightly enhanced terminal oxidase activity (Almeida *et al.* 2012; Queiroga *et al.* 2011). The ineffectiveness of CO gas in comparison with CORM-3 in the current study may be explained by the ability of the compound to enter bacterial cells (Davidge *et al.* 2009b; Nobre *et al.* 2007) and enable intracellular delivery/accumulation of CO, which cannot be achieved to the same extent by diffusion of the gas across the membrane.

Consistent with previous reports (Davidge *et al.* 2009b; Desmard *et al.* 2012; Nobre *et al.* 2009; Smith *et al.* 2011), the data presented in the present work suggest the anti-bacterial activity of CORM-3 cannot be explained by inhibition of respiration alone. For instance in the current study, unlike the action of other classical inhibitors of bacterial oxidases e.g. cyanide (Jackson *et al.* 2007; Zlosnik *et al.* 2006), inhibition by CORM-3 in whole cells is slow and not readily observed in a conventional closed O_2 electrode (shaded regions of Figures). This may be due to the need for the CO-RM to penetrate the cell and interact with cellular species (perhaps including sulfites (McLean *et al.* 2012)) that displace CO. However, 125 μM CORM-3 reduced the viable count of aerobically grown cultures of *E. coli* by 4-log within 30 min (Davidge *et al.* 2009b). Furthermore, recent data obtained by an undergraduate project student (Kate Naylor) has shown that rapid loss of bacterial viability correlates with the interference of respiratory metabolism (Wilson *et al.* submitted). Within 10 min of adding 100 μM

CORM-3 to a respiring culture of low cell density, cell viability was reduced to 10 % of the initial count and within 20 min, the number of viable cells was below the limits of detection (< 9 x 10^6 cells). Parallel measurements of O_2 tension showed that loss of viability in the CO-RM-treated culture began, and was largely complete, during the phase of stimulation and therefore prior to respiratory inhibition. This is inconsistent with the data obtained by Desmard *et al*. (2009) showing that inhibition of respiration preceded loss of *P. aeruginosa* viability. However, this group did not observe respiratory stimulation, an observation also noted in the current study (Figure 3.9 A). Additionally, their recent data revealed that, although different CO-RMs elicited similar inhibitory effects on bacterial respiration, they exhibited differential bactericidal capacity (Desmard *et al.* 2012).

The variable effect of CORM-3 on different bacterial species cannot be explained at present. In particular, the biphasic response was only observed in *E. coli*. Although data have not been reported for *S.* Typhimurium or *E. coli* O157, the results presented herein for *P. aeruginosa* are consistent with those presented by Desmard *et al*. (2009). Perhaps the response depends on the potency of the compound against each species; concentrations of 50 and 100 µM may be too inhibitory and a more complete survey of concentrations may be required. For example, CORM-3 is effective at inhibiting growth of *P. aeruginosa* at concentrations between 0.1 - 10 µM, with 10 µM eliciting a 4-log reduction in bacterial counts 180 min after addition (Desmard *et al.* 2009). In non-pathogenic *E. coli* concentrations of between 30 - 100 µM were required to inhibit growth and 30 µM CORM-3 only reduced viability by 1-log after 120 min (Davidge *et al.* 2009b). However, as just mentioned, viability of *P. aeruginosa* was lost after the onset of respiratory inhibition (Desmard *et al.* 2009). The effect of the CO donor on respiration may therefore be more complex and may depend on how it interacts with the species in question. The situation with *C. albicans* could be more readily explained by cell structure. Higher concentrations of CORM-3 might be necessary as the respiratory chain of eukaryotes is situated in the membrane of intracellular mitochondria and is therefore not as easily accessible as it is in bacteria. Such an explanation has been given previously with regard to the sensitivity of *P. aeruginosa* to CORM-3 in comparison with murine macrophages (Desmard *et al.* 2009).

In conclusion, the effect of CO liberated from CORM-3 on microbial respiration is evident; however, there are some outstanding questions. Although CORM-3 acts as a K^+ and Na^+ ionophore (Wilson *et al*. submitted), which may explain the mild 'uncoupling' activity of the compound, it cannot be ruled out that other mechanisms are at play. For example, could CORM-3 stimulate ATP synthase activity? Also, in light of suggestions that inhibition of respiration might not explain entirely the potent bactericidal nature of CO-RMs, and the growing evidence for a multifaceted activity of the compounds, it is important to try to identify additional interactions of CO. The following two chapters aim to explore this area by investigating the effect of CORM-3 on haem-deficient bacteria, in an attempt to determine the effectiveness of the compound in the absence of the most widely recognised target of CO.

Chapter 4. Bactericidal Activity of CORM-3 against Haem-Deficient Bacteria

4.1 Introduction

Haem proteins are essential components of energy-conserving electron transport chains, as well as co-factors for several proteins in almost all organisms. They are well-known sensors of diatomic gases and, as a result, enzymes such as cytochromes, and therefore respiration in general, are considered main targets for the deleterious effects of exposure to high concentrations of poisonous gasotransmitters. However, as mentioned in section 1.6, work published to date on the anti-bacterial effects of CO-RMs raises the possibility that CO may have additional targets and perhaps achieve toxicity via a diverse range of effects. There are reports of non-haem targets in the literature, including many examples of non-haem iron(II) carbonyls, as well as the interaction of CO with ligands from amino acids such as S from cysteine and N from histidine. These ligands may constitute targets in mammalian voltage-gated Slo1 BK channels, which are important in vasodilation (Hou *et al.* 2008), or in bacterial ion channels (Wilson *et al*. submitted) leading to subsequent respiratory stimulation (Figures 3.1 - 3.3), as suggested in Chapter 3. Other examples of non-haem interactions include the binding of CO to iron in [Fe]-, [Fe-Fe]- and [Fe-Ni]-hydrogenases (Armstrong 2004), for example the [Fe-Fe]-hydrogenase of *Chlamydomonas* (Stripp *et al.* 2009). CO also binds to binuclear copper sites, for example in tyrosinase (Kuiper *et al.* 1980) and hemocyanins (Finazzi-Agro *et al.* 1982; van der Deen & Hoving 1979). The focus of the current chapter was therefore to test the efficacy of CORM-3 on bacteria deficient in the synthesis of haem, with an aim to determine the presence of additional intracellular targets and their contribution to bacterial survival during CORM-3 insult.

Haem is one of the main representatives of modified cyclic tetrapyrroles. Generally, tetrapyrroles are made up of four pyrrole rings attached via methine bridges. The biosynthesis process is reviewed in Heinemann *et al*. (2008) and involves the coordination of up to 10 different enzymes. The production of protohaem begins with the formation of δ-ALA, which acts as the sole source of carbon and nitrogen in the pathway. Two pathways exist in nature for the formation of this precursor: the 'Shemin pathway' that is used by animals, fungi and α-proteobacteria and the C_5-pathway, which

is found in most bacteria, all archaea and plants. The latter is used by *E. coli* and consists of an ATP-dependent two-step process starting with glutamyl-tRNA as the initial substrate. Glutamyl-tRNA is generated by glutamyl-tRNA synthetase in a reaction of the C_5-skeleton of glutamate with $tRNA^{Glu}$. Glutamyl-tRNA reductase, encoded by *hemA*, catalyses the subsequent NADPH-dependent reduction of the product to form unstable glutamate-1-semialdehyde. δ-ALA is then yielded from glutamate-1-semialdehyde via a PLP-dependent transamination reaction catalysed by *hemL*-encoded glutamate-1-semialdehyde-2,1-aminomutase (Figure 4.1). δ-ALA acts as the initial substrate for the haem biosynthesis pathway, consisting of 7 consecutive steps. The process involves two stages: formation of uroporphyrinogen III via a central pathway that is common to the biosynthesis of all tetrapyrroles, and finally the subsequent formation of haem using a conserved pathway employed by eukaryotes and most bacteria (Figure 4.2) (Heinemann *et al.* 2008).

Initial work utilising *E. coli* deficient in haem biosynthesis was carried out by Haddock & Schairer (1973) who isolated and characterised a strain carrying a *hemA* mutant allele. Synthesis of δ-ALA in strains carrying this mutation is halted at the second step in the C_5-pathway (Avissar & Beale 1989). Phenotypic analysis of the mutant revealed an inability to grow on oxidisable substrates such as glycerol, succinate and malate when δ-ALA was not present. This was attributed to the absence of functional cytochromes, as confirmed by spectral analysis. The strain survives via an alternative, fermentative lifestyle. Experiments involving growth of the mutant in the presence of δ-ALA showed that reconstitution of respiration is achieved in the absence of protein synthesis. This suggests that the apoproteins of cytochromes are synthesised and incorporated into the membrane in the absence of haem synthesis (Haddock & Schairer 1973). Furthermore, reconstitution of oxidase activity was associated with the formation of a functional proton-translocating respiratory chain (Haddock & Downie 1974). For the present work, a haem-deficient strain of *E. coli* was obtained from the Keio Collection (RKP3905, Table 2.1). The inability of the bacterium to produce haem was achieved by disruption of the *hemA* gene according to a published method (Datsenko & Wanner 2000).

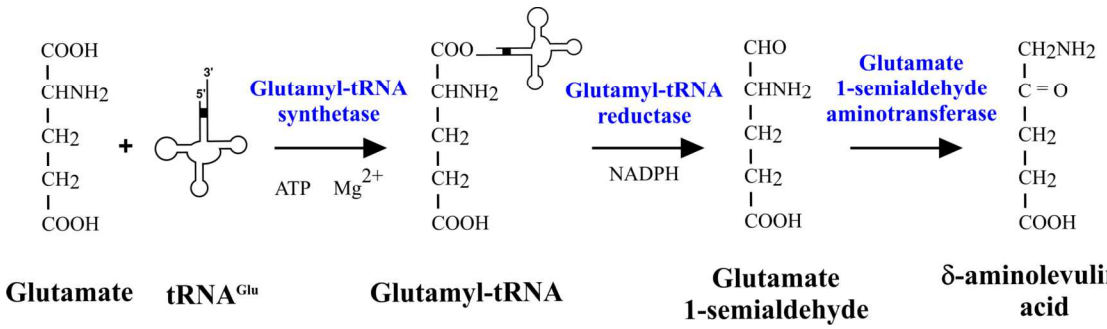

Figure 4.1. C_5-pathway for δ-aminolevulinic acid synthesis in *Escherichia coli*. The enzymes catalysing each step are shown in blue. The information enabling the generation of this figure was sourced from the following references (Heinemann *et al.* 2008; O'Brian & Thony-Meyer 2002).

Landscape Figure (Figure 4.2), refer to page 4 of supplementary document.

Although a useful tool for this investigation, the mutant is a laboratory model and growth of the strain is very poor. Therefore a set of parallel experiments employing *Lactococcus lactis* was used to complement the present study. *L. lactis* is a Gram-positive, homofermentative bacterium that is naturally devoid of haem biosynthesis. Lactic acid bacteria such as *Lactococcus* species are therefore unable to produce cytochromes and subsequently cannot carry out electron transport phosphorylation. As an obligate fermentative bacterium, *L. lactis* metabolises hexoses through the Embden-Meyerhof pathway to generate ATP, with lactic acid being a major end-product (Kim 2008). Under anaerobic conditions the bacterium grows well and serves as a good representation of the effect of CORM-3 against a healthy, haem-deficient microorganism. The work in this chapter uses the *hemA* mutant and *L. lactis* to explore the hypothesis that the toxicity of CO extends beyond disruption of haem proteins. The effect of CORM-3 and its control compounds on the growth and viability of these strains was determined, with a comparison of the response of the *E. coli hemA* mutant with that of the corresponding wild type.

4.2 Results

4.2.1 Growth of haem-deficient *Escherichia coli* and validation of the *hemA* mutation

To ensure sufficient growth of the haem-deficient mutant, RKP5461 (*E. coli* W3310 wild type) and RKP3905 (*E. coli* W3310 *hemA*::Km^R) (Table 2.1) were plated onto rich agar plates +/- δ-ALA (section 2.1.2.3). Plates were incubated at 37 °C overnight in aerobic and anaerobic environments. Plates for anaerobic growth were incubated in a sealed anaerobic jar (Oxoid) containing an Anaero*Gen*™ Compact (Oxoid) sachet for the generation of anaerobic conditions. As expected, the wild type grew well under all conditions. The mutant grew well in the presence of the selective antibiotic, kanamycin, with better growth observed in the presence of δ-ALA in both aerobic and anaerobic environments. *L. lactis* was also able to grow effectively on this medium (in the absence of δ-ALA). Growth under these conditions partly validates the *hemA* mutation. For further confirmation of the mutant phenotype, the mutant and, for comparison, the wild type, were streaked onto defined medium plates +/- δ-ALA and containing either glycerol or succinate (0.5 %) in place of glucose (section 2.1.2.6). Plates were incubated

aerobically overnight at 37 °C. Succinate and glycerol do not permit fermentative growth, so the strain lacking the *hemA* gene should not produce colonies unless δ-ALA is present. As expected, growth of the mutant was noted only on plates containing δ-ALA whereas the wild type was able to grow on all plates.

4.2.2 Transduction of the *hemA* mutation into *Escherichia coli* K-12 MG1655

To complement previous work, the *hemA* mutation was transduced into *E. coli* K-12 MG1655 (section 2.1.6). Successful transduction of the mutation was confirmed by selection on kanamycin, growth on a non-fermentable substrate (succinate) only in the presence of δ-ALA, and via spectroscopy demonstrating a lack of reduced and CO-reduced forms of cytochromes (section 2.3.2.2). Cytochrome assays were carried out on three successful transductants, RKP5421, RKP5422 and RKP5423 (Table 2.1), grown aerobically in the absence of δ-ALA. The *hemA* transductants did not appear to be producing haem as the pellets were white in comparison with wild type pellets that had a reddish-brown colour. This was confirmed by the characteristic haem protein signals observed in the wild type reduced *minus* oxidised and CO reduced *minus* reduced spectra, whereas the signals were not seen in the transductant spectra (Figure 4.3). The trough at c. 450 nm in the transductant spectra may be due to oxidation of flavins. The domination of wild type spectra by cytochrome *bd* is not unexpected as the concentration of this oxidase increases as cells age. The cultures were grown for 7 - 8 h and therefore harvested after entry into stationary phase. Concentrations of cytochromes *b* (0.68 nmol mg protein^{-1}) and *d* (0.63 nmol mg protein^{-1}) were calculated from the wild type reduced *minus* oxidised spectrum as described in section 2.3.2.2.

4.2.3 Transductant growth trials and final growth conditions

Initial growth trials involved testing the ability of a *hemA* transductant (RKP5421) to grow in defined medium under aerobic conditions and testing the ability of CORM-3 to function effectively in the medium. The usual defined medium for wild type *E. coli* (section 2.1.2.6) was too minimal to support growth of the mutant. Additionally, whilst sequential reduction of tryptone and yeast extract concentrations in the rich medium (section 2.1.2.3) yielded a composition that enabled sufficient growth, CORM-3 at concentrations of up to 200 μM was not effective against the wild type, presumably due

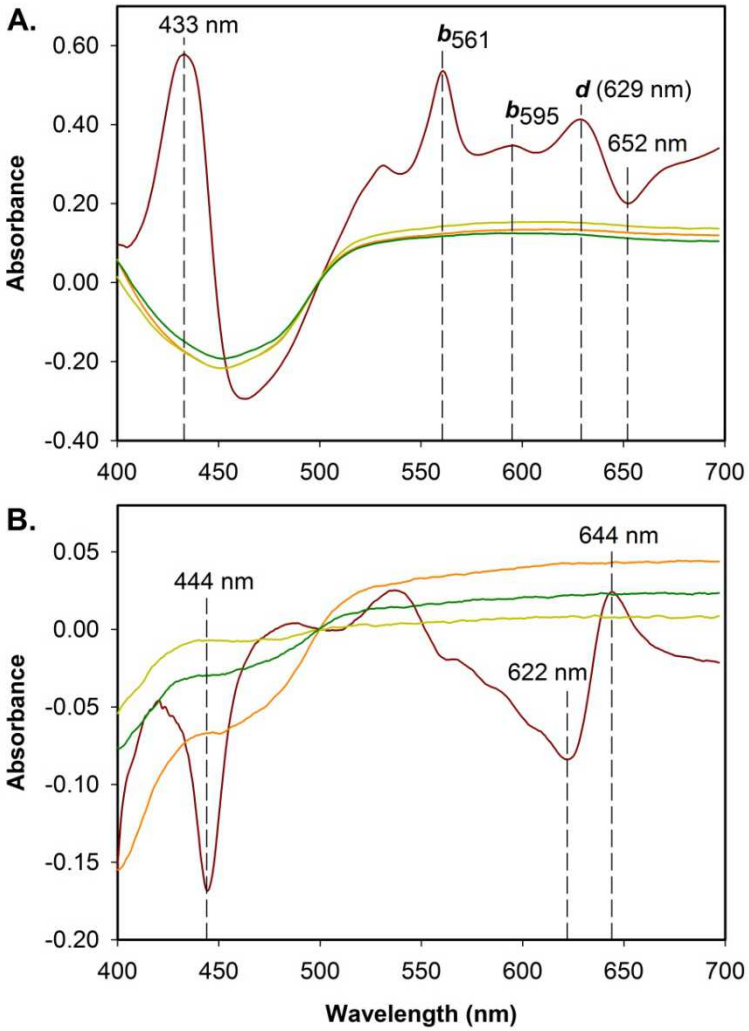

Figure 4.3. *Escherichia coli* K-12 MG1655 *hemA* constructed by transduction does not synthesise cytochromes. Cultures were grown aerobically in rich broth (2.1.2.3) for 7 - 8 h then harvested, washed thoroughly and resuspended in 0.1 M KPi (pH 7) for dual wavelength spectroscopic analysis of cytochrome content. Samples were scanned between 400 - 700 nm and resultant data were smoothed in SigmaPlot (Systat Software Inc.). Recorded wavelength positions are shown. **A.** Reduced *minus* oxidised spectra. The wild type spectrum (red) contains signals from reduced cytochrome *bd*: b_{558}, b_{595} and *d* (17.8 mg ml protein^{-1}). The trough at c. 650 nm is due to the loss of the oxidised form of *d*. No signals were seen in the spectra for the 3 successful transductants (orange, 15.9 mg ml protein^{-1}; light green, 17.5 mg ml protein^{-1}, and; dark green, 18.6 mg ml protein^{-1}). **B.** CO-reduced *minus* reduced spectra. The trough at 444 nm and the complex trough region (550 - 630 nm) in the wild type spectrum (red) are due to disappearance of the reduced form of *d* and b_{595}. The presence of CO-reduced *d* is characterised by the peak at 644 nm. No signals were seen in the transductant spectra.

to the richness of the medium. However, supplementation of the usual defined medium (section 2.1.2.6) with 0.1 % casamino acids and 5 % LB as described in Davidge *et al.* (2009b) resulted in improved growth of the mutant. For further optimisation, anaerobic conditions were used to support fermentative growth and to act as an additional barrier for CORM-3/CO against traditional targets. CORM-3 at 100, 200 and 300 μM effectively inhibited wild type growth in this medium and under these conditions. It was considered that such high concentrations of the compound were necessary due to the diminution of CO-RM activity in rich media. The rich medium (section 2.1.2.3) and the defined medium modified for growth of haem-deficient bacteria (section 2.1.2.6) were also able to support the growth of *L. lactis* allowing conditions to be standardised. To ensure haem proteins were not produced in the haem-deficient mutant of *E. coli* and *L. lactis* under such conditions, cytochrome assays were carried out (section 2.3.2.2). Characteristic signals were seen in the wild type spectra, but no signals were seen in the mutant, or *L. lactis* spectra, even after the last was treated with CORM-3 (Figure 4.4). Concentrations of cytochromes *b* (0.68 nmol mg protein^{-1}) and *d* (0.53 nmol mg protein^{-1}) were calculated from the wild type reduced *minus* oxidised spectrum.

4.2.4 CORM-3 is bactericidal against haem-deficient *Escherichia coli* and naturally haem-deficient *Lactococcus lactis*

RKP5421, its corresponding wild type RKP5416 and *L. lactis* were grown anaerobically in defined medium modified for the growth of haem-deficient bacteria (section 2.1.2.6) in the absence of δ-ALA. Cultures of RKP5421 and RKP5416 were stressed at low cell densities due to poor growth of the haem-deficient mutant. Unless otherwise stated, mutant cultures were incubated overnight following inoculation to allow for sufficient growth before CORM-3 stress in the morning. Micromolar concentrations of the compound caused a concentration-dependent inhibition of wild type and mutant growth with no recovery over 24 h (Figure 4.5). In both cases, growth was suspended within 2 h and 1 h after addition of 200 and 300 μM, respectively. Cultures treated with 100 μM followed the same growth pattern as the control. The mutant control culture grows to a maximum OD_{600} of c. 0.4; therefore to see the effects of CORM-3 over a longer period of growth, cultures were stressed at an OD_{600} of c. 0.1 (Figure 4.6). Again, the compound elicited a concentration-dependent effect with significantly slowed growth of both strains observed after treatment with CORM-3 at all concentrations. Wild type

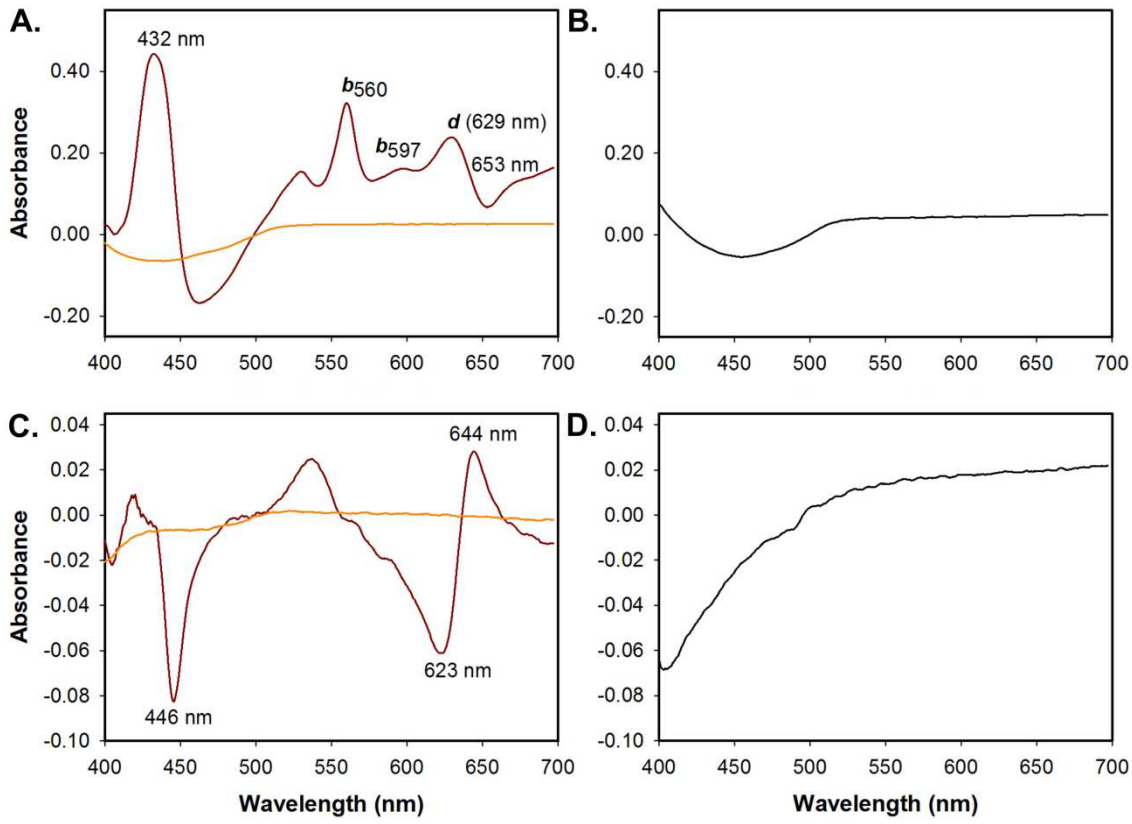

Figure 4.4. The haem-deficient mutant of *Escherichia coli* and naturally haem-deficient *Lactococcus lactis* do not produce cytochromes under anaerobic growth conditions. Cultures were grown anaerobically in defined medium modified for the growth of haem-deficient bacteria (2.1.2.6). Due to the slow growth of the mutant, mutant and wild type cultures were grown for 24 h. *L. lactis* was grown for 7 - 8 h and treated with 200 µM CORM-3 at an OD_{600} of c. 0.4. Cultures were harvested, washed thoroughly and resuspended in 0.1 M KPi (pH 7). The figure shows reduced *minus* oxidised spectra for the haem-deficient mutant (orange, 17.3 mg ml protein^{-1}) in comparison with the corresponding wild type (red, 17.5 mg ml protein^{-1}) (**A**) and *L. lactis* (12.8 mg ml protein^{-1}) (**B**), and CO-reduced *minus* reduced spectra for the mutant compared with wild type (**C**) and *L. lactis* (**D**). Data were smoothed in SigmaPlot (Systat Software Inc.). Wavelength positions of labelled signals are those recorded by the spectrophotometer. Spectral analysis of *L. lactis* suspensions was carried out by Sarah Greaves (vacation student).

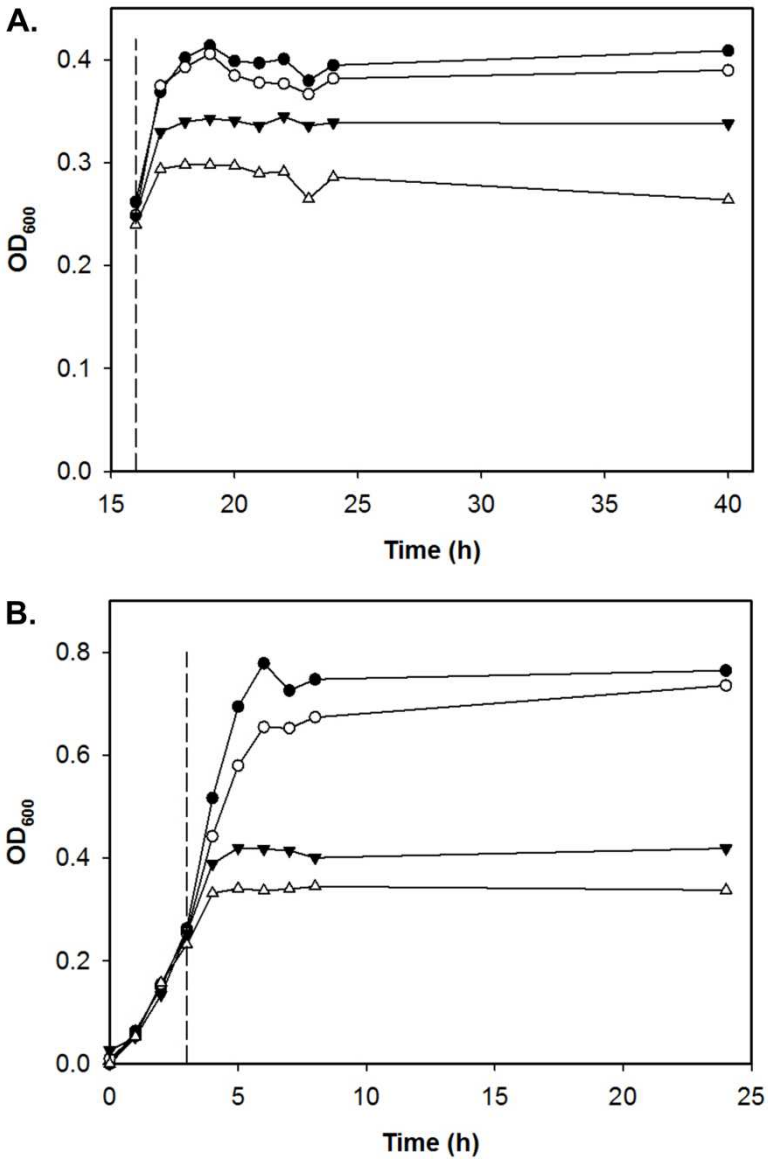

Figure 4.5. Micromolar concentrations of CORM-3 inhibit the growth of the haem-deficient mutant of *Escherichia coli*. Cultures were grown anaerobically in defined medium modified for the growth of haem-deficient bacteria (section 2.1.2.6) and stressed with 100 µM (open circles), 200 µM (closed triangles) and 300 µM (open triangles) CORM-3 at an OD_{600} of c. 0.25 (dashed line). Growth of CORM-3-treated cultures was compared with that of control cultures (nothing added, closed circles). Hourly OD_{600} readings were taken for 8 h followed by a 24 h reading to complete the experiment. **A.** Haem-deficient mutant and **B.** corresponding wild type. Data represent the pattern seen in ≥ 3 biological replicates.

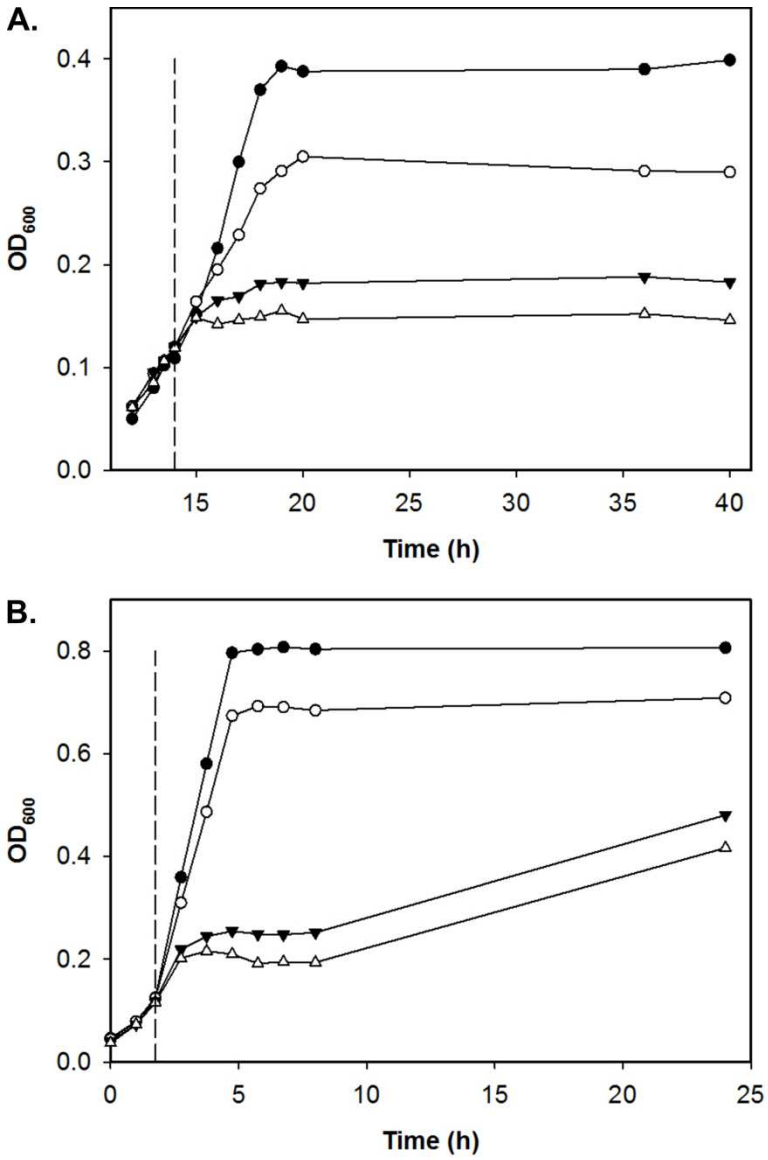

Figure 4.6. The response of haem-deficient *Escherichia coli* and the corresponding wild type to CORM-3 stress at a lower cell density. Cultures were grown as described previously and stressed with 100 µM (open circles), 200 µM (closed triangles) and 300 µM (open triangles) CORM-3 at an OD_{600} of c. 0.1 (dashed line). Growth of CORM-3-treated cultures was compared with that of control cultures (nothing added, closed circles). Hourly OD_{600} readings were taken for 6 h post-addition of the compound, followed by a 24 h reading to complete the experiment. **A.** Haem-deficient mutant and **B.** wild type. Data represent the pattern seen in ≥ 3 biological replicates.

cultures stressed with 200 and 300 μM showed some recovery between 8 - 24 h, but cell densities did not reach the level of control or 100 μM-treated cultures. Mutant cultures did not recover within 24 h (36 h time-point in Figure 4.6 B), or after an extra 4 h of growth (40 h). Viability assays revealed a 3-log drop in mutant cell counts within 1 h after addition of 200 μM CORM-3 (Figure 4.7 A), whereas wild type viability dropped gradually by 0.5-log over 3 - 4 h, with a 2- to 3-log drop within 24 h (Figure 4.7 B). Levels of viable mutant cells were maintained for 4 h after treatment with 100 μM, but dropped by 2-log to a similar level as the recovered 200 μM-treated cultures within 24 h (Figure 4.7 A). CORM-3 (100 μM) had less of an effect on the wild type for which cell counts were similar to that of the control culture for 4 h, with a 0.5-log drop within 24 h (Figure 4.7 B).

Micromolar concentrations of CORM-3 also elicited a concentration-dependent effect on the growth and viability of *L. lactis* (Figure 4.8). At a concentration of 200 μM the compound suspended growth within 1 h after addition and caused a gradual decrease in viability over 4 h, with a 2.5- to 3-log drop 24 h following treatment. At 100 μM the CO donor slowed growth and reduced viable cells by 0.5- to 1-log over 24 h. Cell counts were lowered 1 h after addition of the compound and remained lowered during the period of observation.

4.2.5 The effect of CORM-3 control compounds on haem-deficient bacteria in comparison with wild type *Escherichia coli*

The synthetic control compound $RuCl_2(DMSO)_4$ had no effect on the growth of wild type *E. coli* or the haem-deficient mutant (Figure 4.9 A and B). To more aptly determine whether the skeleton of the compound has an effect on bacterial growth and viability, iCORM-3 was tested (section 2.3.1.3) (Figure 4.9 C - F). At 100 μM the inactive compound had no effect on the wild type, with growth following the same pattern as that of the control (nothing added). At 200 μM, iCORM-3 slowed growth, but the effect was insignificant when compared with that previously seen for CORM-3 (Figure 4.6). This may be explained by residual CO release from the inactive compound, which is ≤ 10 % of the CO liberated from CORM-3 (Chapter 3, section 3.2.5, Figure 3.7 C inset). Again, iCORM-3 had a concentration-dependent effect on the mutant (Figure 4.9 D), but not to the same extent as seen after CORM-3-treatment

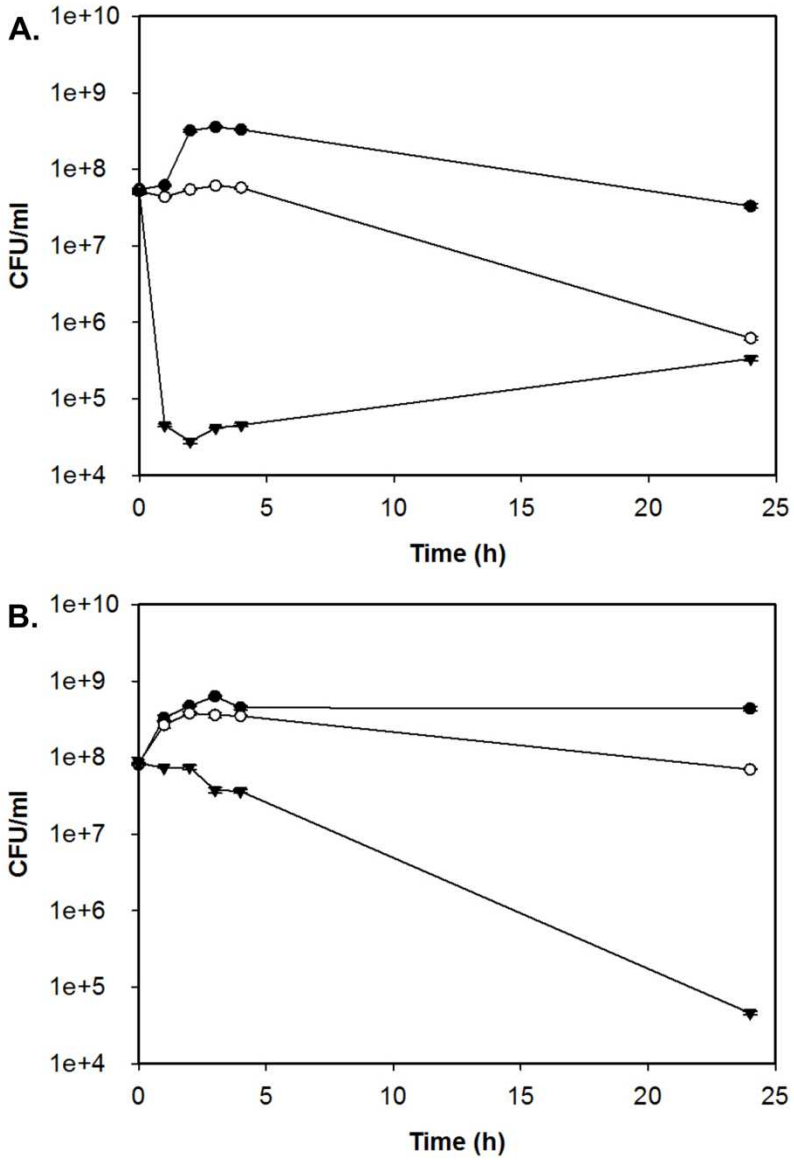

Figure 4.7. CORM-3 is more bactericidal against the haem-deficient mutant than wild type. Cultures were grown as described previously and stressed with 100 μM (open circles) and 200 μM (closed triangles) CORM-3 at an OD_{600} of c. 0.1. Viability of CORM-3-treated cultures was compared with that of control cultures (nothing added, closed circles). A culture sample was taken immediately prior to addition of the compound, followed by sampling every hour for 4 h post-stress and at 24 h to complete the experiment. OD_{600} readings were taken in parallel (data not shown). **A.** Haem-deficient mutant and **B.** wild type. Data represent the pattern seen in 3 biological replicates. Viability data are plotted as means ± SEM from ≥ 3 individual spots. In each case, error bars are within the size of the experimental points.

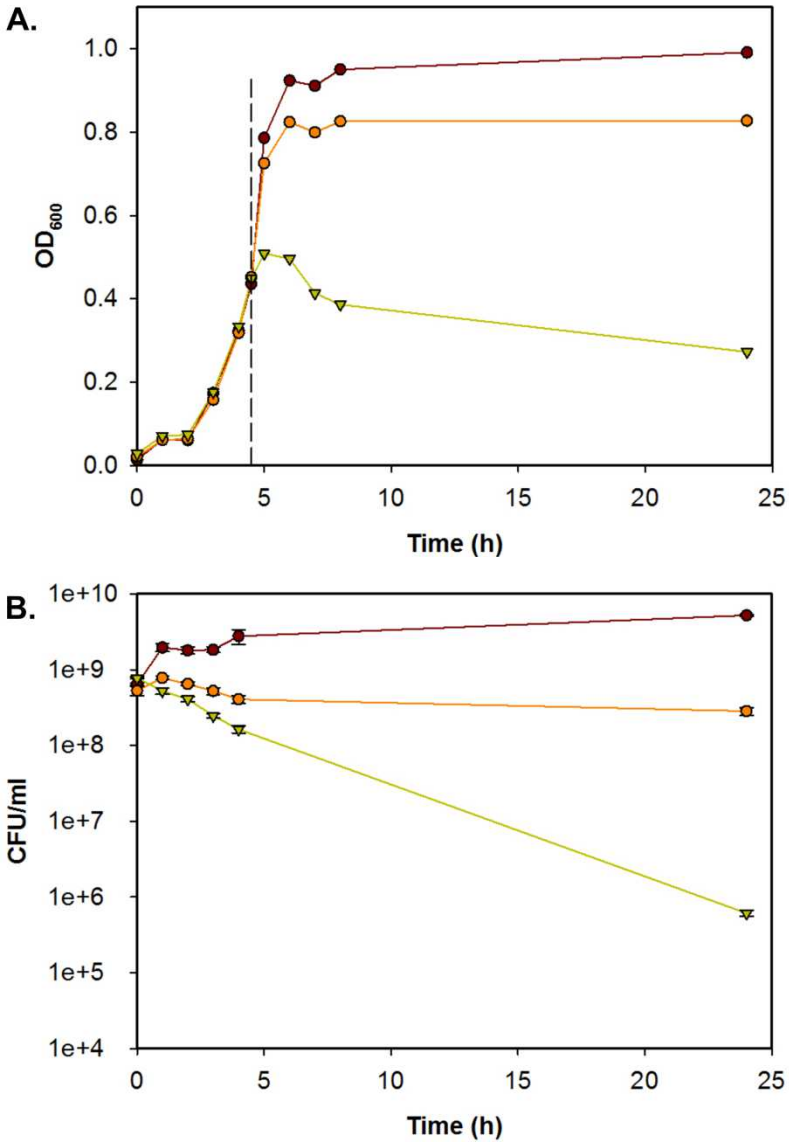

Figure 4.8. CORM-3 is bactericidal against naturally haem-deficient *Lactococcus lactis*. Cultures were grown anaerobically in defined medium modified for the growth of haem-deficient bacteria (section 2.1.2.6) and stressed with 100 µM (orange) and 200 µM (green) CORM-3 at an OD_{600} of c. 0.4. **A.** Growth and **B.** viability of treated cultures were compared with that of control cultures (nothing added, red). The point of CORM-3 addition is shown as a dashed line in panel A. A culture sample was taken immediately prior to CORM-3 addition to assay for cell viability (t = 0 in panel B). Hourly OD_{600} readings and culture samples were taken for 4 h post-addition of the compound, followed by a 24 h reading to complete the experiment. Data represent the pattern seen in ≥ 3 biological replicates. Viability data are plotted as means ± SEM from 3 individual spots. In most cases, the error bars are within the size of the experimental points. This work was carried out by Sarah Greaves (vacation student).

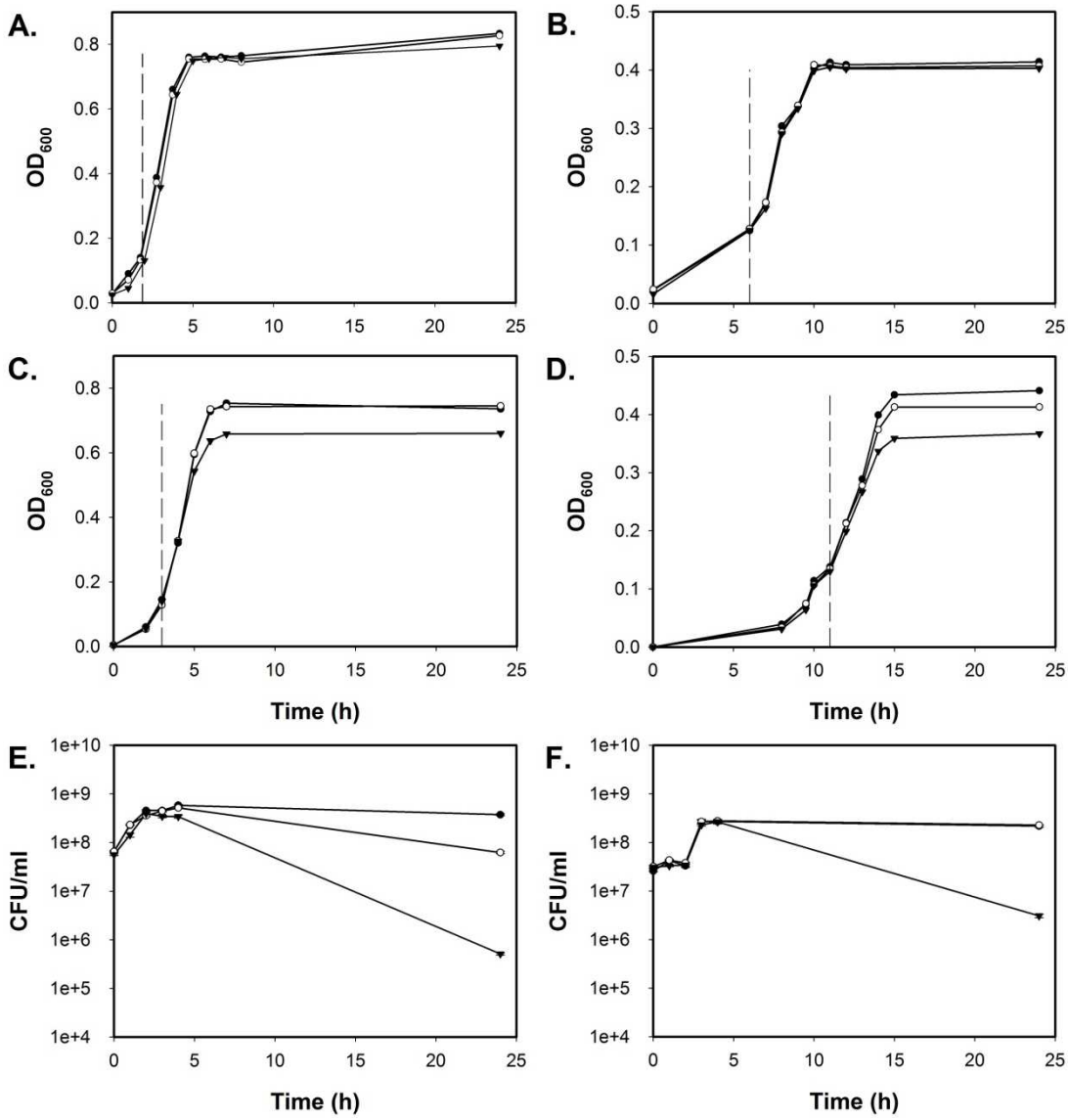

Figure 4.9. The effect of control compounds on wild type and haem-deficient *Escherichia coli*. Cultures were grown as described previously and treated with 100 μM (open circles) and 200 μM (closed triangles) $RuCl_2(DMSO)_4$, or iCORM-3, at an OD_{600} of c. 0.1. Control cultures are shown in parallel (closed circles). The figure shows the effect of $RuCl_2(DMSO)_4$ on the growth of wild type (**A**) and mutant (**B**), and the effect of iCORM-3 on the growth of wild type (**C**) and mutant (**D**). The point of CORM-3 addition is shown as a dashed line in panels A - D. Viability of wild type (**E**) and mutant (**F**) in response to iCORM-3 is also shown. A culture sample was taken immediately prior to addition of the inactive compound (t = 0 in panels E and F) followed by hourly samples for 4 h, and at 24 h to complete the experiment. Data represent the pattern seen in ≥ 3 biological replicates. Viability data are plotted as means ± SEM from ≥ 3 individual spots. In each case, error bars are within the size of the experimental points.

(Figure 4.6). Viability of wild type and mutant cells was unaffected by iCORM-3 for 4 h post-addition. However, after 24 h the viability of wild type cultures treated with 100 and 200 μM was reduced by 1- and 3-log, respectively. At the same time-point, 200 μM iCORM-3 decreased the mutant cell count by 2-log, whilst 100 μM was ineffective (Figure 4.9 E and F). Neither $RuCl_2(DMSO)_4$, nor iCORM-3, at 100 and 200 μM had an effect on the growth or viability of *L. lactis* (Figure 4.10 A - D).

4.2.6 Reconstitution of the *hemA* mutant reduces CORM-3 toxicity

The haem-deficient mutant of *E. coli* was grown as described in section 4.2.4, but in the presence of δ-ALA. As expected, the maximum OD reached by the reconstituted mutant control culture (i.e. no CO-RM) was comparable with that seen for the wild type, and cultures were treated with CORM-3 at the same time-point (c. 2 h). Growth was slowed within 1 h following exposure to the compound, with further inhibition observed over the remaining 3 h of the experiment (Figure 4.11 A). Cell viability dropped by a maximum of 2-log over 4 h after addition of the CO donor, with a c. l-log drop within 1 h (Figure 4.11 B). Both growth and viability recovered after 24 h, but a greater effect was seen in cell counts, which increased to above control levels. Successful reconstitution of the mutant phenotype was confirmed by assaying cytochrome content of intact cells grown under anaerobic growth curve conditions (as described in section 4.2.3), which revealed characteristic haem protein signals (Figure 4.11 C and D). Concentrations of cytochromes *b* (0.46 nmol mg protein^{-1}) and *d* (0.36 nmol mg protein^{-1}) were calculated from the reduced *minus* oxidised spectrum.

4.3 Discussion

The work detailed in this chapter demonstrates the potent toxicity of CORM-3 against haem-deficient bacteria, including a *hemA* mutant of *E. coli* and naturally haem-deficient *L. lactis*. Stressing the mutant and its corresponding wild type with CORM-3 at an OD_{600} of c. 0.2 suggested the wild type may be more sensitive (Figure 4.5). Growth rates of CO-RM-treated wild type cultures were much slower than the control when compared with mutant growth rates. The haem-deficient mutant might exhibit a lesser degree of inhibition after stress at this OD as cell growth is reaching its maximum (c. 0.4) and so slowing down even in the absence of CORM-3. This makes it difficult to

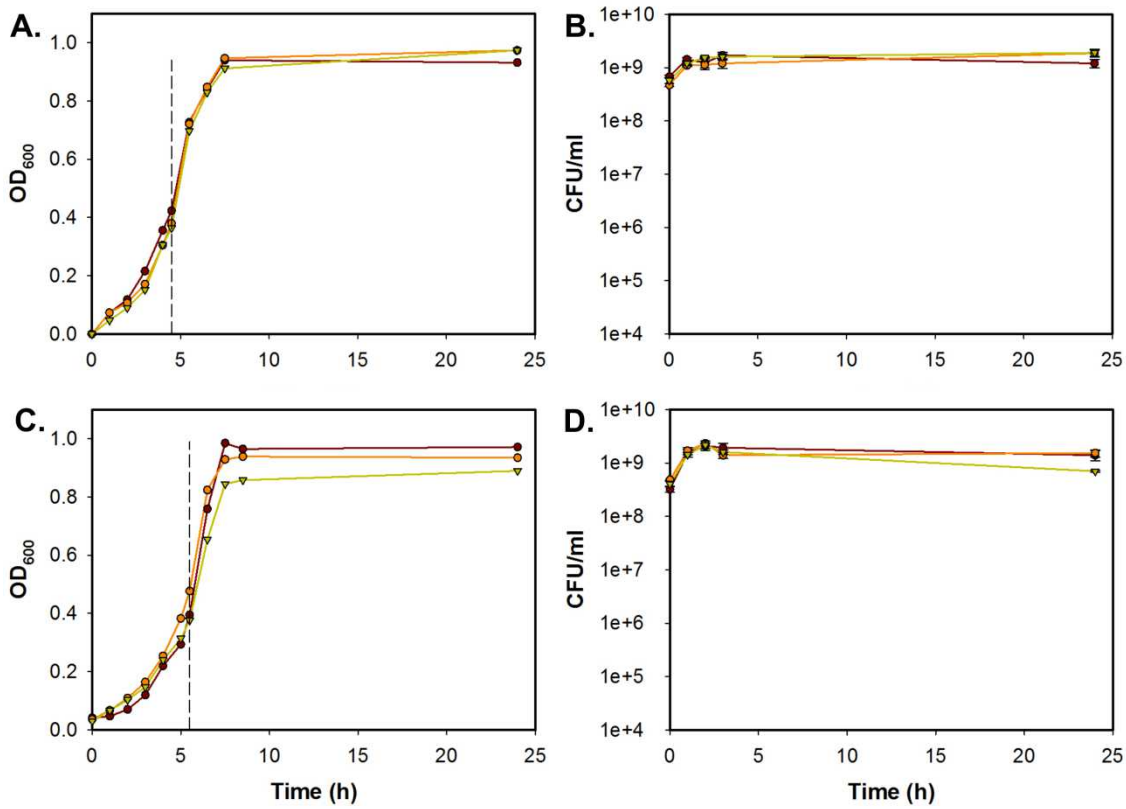

Figure 4.10. Control compounds are ineffective against *Lactococcus lactis*. Cultures were grown as described previously and treated with 100 µM (orange) and 200 µM (green) $RuCl_2(DMSO)_4$, or iCORM-3, at an OD_{600} of c. 0.4. Growth and viability of treated cells were compared with that of untreated cells (red). The effect of $RuCl_2(DMSO)_4$ on growth (**A**) and viability (**B**), and the effect of iCORM-3 on growth (**C**) and viability (**D**) are shown. The addition of CORM-3 is shown as a dashed line in panels A and C. A culture sample was taken immediately prior to CORM-3 addition to assay for cell viability (t = 0 in panels B and D). Hourly OD_{600} readings and culture samples were taken for 3 h post-addition of the compound and at 24 h to complete the experiment. Data represent the pattern seen in ≥ 3 biological replicates. Viability data are plotted as means ± SEM from 3 individual spots. In most cases, the error bars are within the size of the experimental points. This work was carried out by Sarah Greaves (vacation student).

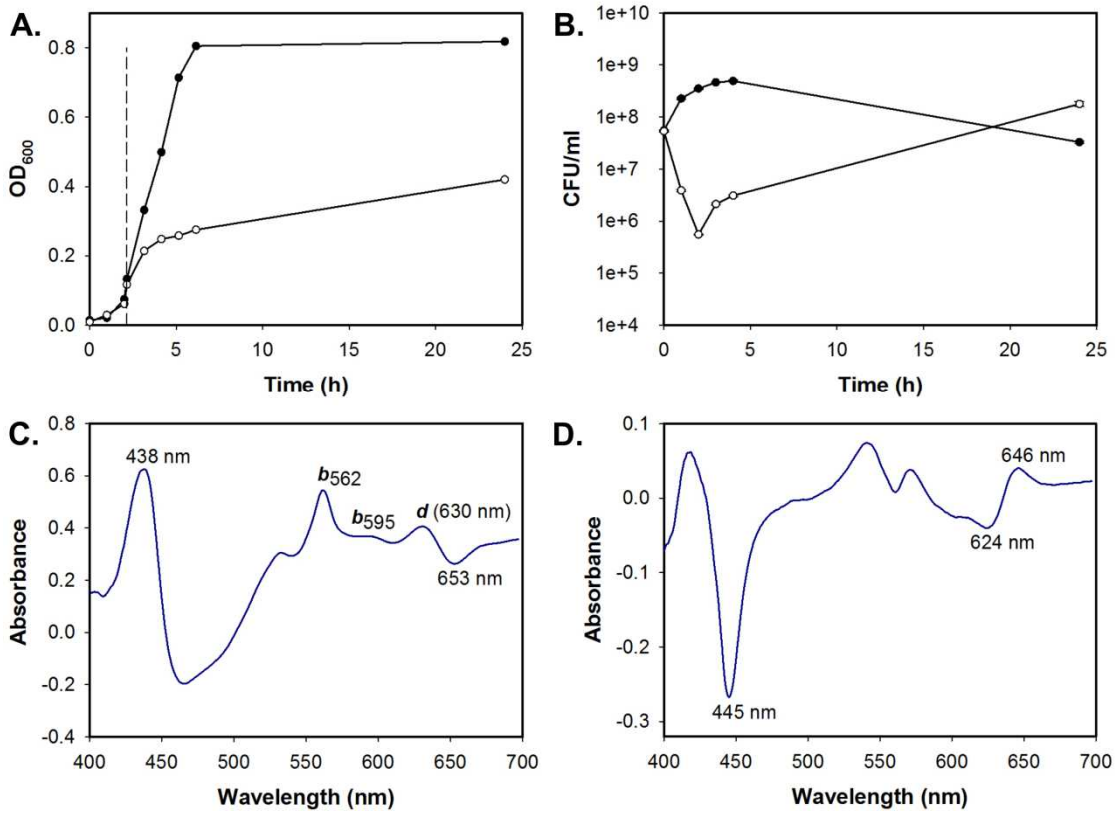

Figure 4.11. Reconstitution of the *hemA* mutant provides some protection against CORM-3 toxicity. Cultures were grown anaerobically in defined medium modified for the growth of haem-deficient bacteria (section 2.1.2.6) supplemented with 2ml/L 50 mM δ-ALA. Growth (**A**) and viability (**B**) of cultures treated with 200 µM CORM-3 (open circles) were compared with that of control cultures (nothing added, closed circles). CORM-3 was added at an OD_{600} of c. 0.1 (dashed line in panel A) and a culture sample was taken immediately prior to addition of the compound to assay for cell viability (t = 0 in panel B). Hourly OD_{600} readings and culture samples were taken for 4 h post-addition of CO-RM and at 24 h to complete the experiment. Growth data represent the pattern seen in 3 biological replicates. Viability data are plotted as means ± SEM from 6 individual spots and represent the pattern seen in 2 biological replicates. For dual wavelength spectroscopic analysis of cytochrome content, cultures were grown as described above (but without CORM-3 treatment) for 7 - 8 h then harvested, washed thoroughly and resuspended in 0.1 M KPi (pH 7) (21.8 mg ml protein^{-1}). Typical reduced *minus* oxidised (**C**) and CO-reduced *minus* reduced (**D**) spectra were observed. Data were smoothed in SigmaPlot (Systat Software Inc.). Wavelength positions of labelled signals are those recorded by the spectrophotometer.

see the difference in growth between the control and treated cultures. The compound was more potent against the mutant after addition at an OD_{600} of c. 0.1 and so its activity may be dependent, in part, on cell density. Additionally, wild type growth recovered by c. OD_{600} of 0.1 24 h after stress at the lower OD, whereas the mutant did not. This may be due to the number of healthy bacteria that are able to keep on multiplying while CO/CORM-3 is taking effect, which will be higher in the wild type. It would appear that treating cultures at a lower cell density, and therefore allowing the response of the mutant to be observed over a longer period of growth, shows the effect of the CO donor more clearly. Under these conditions the compound elicits a similar degree of toxicity against both strains (Figure 4.6). However, the difference in cell viability is much more apparent, suggesting that CORM-3 is more bactericidal against the mutant (Figure 4.7). In support of the bactericidal activity of the compound in the absence of haem targets, CORM-3 was also effective against *L. lactis* in a concentration-dependent manner (Figure 4.8). However, the response was more similar to that of wild type *E. coli* rather than the mutant. This could be due to the higher cell density at the point of stress (OD_{600} of c. 0.4), or it could be due to healthier cultures as a result of the natural haem-deficiency of *L. lactis*. Nevertheless, the compound was still toxic against another bacterium that does not produce haem.

Although this outcome was proposed in the initial hypothesis, it is still surprising that CORM-3 is such a potent inhibitor of bacterial growth and viability in the absence of haem targets. The results cannot be attributed to the presence of small quantities of haem in the mutant or *L. lactis* as cytochrome assays revealed none of the characteristic signals in these strains (Figure 4.3 and 4.4). Additionally, the application of CO via CO-RMs will always raise the question as to whether it is the CO liberated from the compound that causes the observed effects, or whether the backbone also plays a part. In support of CO activity, neither $RuCl_2(DMSO)_4$, nor iCORM-3, resulted in as profound an effect as the active compound against any of the strains tested herein (Figure 4.9 and 4.10). However, iCORM-3 did result in a significant drop in wild type *E. coli* and mutant cell counts after 24 h. Again, this may be due to residual CO release from the compound (see section 3.2.5 and Figure 3.7 C inset), and/or the low OD at which the cultures were stressed, as the inactive compound did not affect the viability of *L. lactis* after addition at mid-log phase of growth. Interestingly, in support of the results presented in the current study, recent data in the Poole laboratory has demonstrated that

CORM-3-liberated CO binds to membrane particles of the bioluminescent marine bacterium *Vibrio fischeri* expressing only a non-haem 'alternative' oxidase (AOX) (Jesse & Poole, unpublished), which contains a di-iron centre (Berthold *et al.* 2002). However, these membranes were insensitive to respiratory inhibition by CO when applied as a saturated solution (Jesse & Poole, unpublished), which is consistent with previous observations for NO (Dunn *et al.* 2010).

The finding that CO is not only lethal to bacteria that do not contain haem, but that it may also be more toxic in the absence of this moiety, suggested another hypothesis: perhaps haem proteins are protecting the wild type from the full potential of CO toxicity by acting as a 'CO-sink'. To investigate this further, the *hemA* mutant was reconstituted by addition of δ-ALA to the growth medium, which enabled synthesis of haem proteins. As shown in Figure 4.11, the reconstituted mutant was less sensitive to the CO donor. However, although the growth of the strain was returned to wild type levels, it was still more sensitive than the wild type. This may be explained by incomplete reconstitution, i.e. the degree of haem synthesis not being fully restored to wild type levels. Samples of wild type cells prepared under anaerobic growth curve conditions contained 0.68 nmoles mg^{-1} of cytochrome *b* and 0.53 nmoles mg^{-1} cytochrome *d* (section 4.2.3), in comparison with 0.46 and 0.36 nmoles mg^{-1} of cytochromes *b* and *d* in the reconstituted mutant, respectively (section 4.2.6). Again, the improved resistance of the mutant after reconstitution may be due to the health of the cells and consequently a higher multiplication rate after CORM-3 addition. This would result in less CO-RM per cell and in turn a dilution of the deleterious effects. However, even though growth rates and cell counts are similar to the wild type and so the degree of sensitivity to CORM-3 should be the same, it is not. This seems to lend support to the previously stated hypothesis, as even though reconstitution results in cell concentrations comparable with that of the wild type, less haem proteins are available to sequester CO and thus the reconstituted mutant still shows heightened sensitivity to CORM-3.

The work in this chapter has unequivocally demonstrated that CO administered via CORM-3 is an efficient bactericidal agent against haem-deficient bacteria. It is now important to investigate the mechanism behind this finding. What are the other targets of CO? How is it still, and perhaps even more toxic, when haem proteins are not

present? To try to shed light on the possible additional targets of this poisonous molecule, microarray analyses were carried out (see Chapter 5).

Chapter 5. CORM-3 Exerts Global Transcriptomic Effects Against a Haem-Deficient Mutant of *Escherichia coli*

5.1 Introduction

The finding that CORM-3 is bactericidal against bacteria in the absence of haem targets invited an in-depth analysis of the effects of the compound on haem-deficient bacteria. The effect of CO-RMs on the transciptome of wild type *E. coli* has been reported (Davidge *et al.* 2009b; Nobre *et al.* 2009) and produced interesting results with regard to the mechanisms behind CO/CO-RM activity. Although such studies elucidate only the response pathways and cannot reveal direct targets, they provide a useful means by which one can look at global effects. Understanding the molecular and biochemical mechanisms underpinning CO-RM activity is paramount for these compounds to be considered for pharmacological use. To date, transcriptomic profiling of cells exposed to CO-RMs has been performed solely at the microbial level, with the analyses being carried out by only these two independent groups. Different CO donors, namely CORM-2 and CORM-3, respectively, were employed and several functional groups of genes were reported to be differentially regulated in response to both. The compounds altered transcription under aerobic and anaerobic conditions, but the condition under which most genes were affected differed between the studies.

Under aerobiosis Davidge *et al*. (2009b) observed a 2-fold ($p < 0.05$) up-regulation of 63 genes and down-regulation of 183 genes in response to a 15 min treatment with 30 μM CORM-3. Under anaerobiosis 29 genes were up-regulated by more than 2-fold ($p < 0.05$) and 41 genes were down-regulated after exposure to 100 μM CORM-3 for 15 min. Bacterial respiration was identified as a main target due to the dramatic down-regulation of many genes encoding components of the aerobic respiratory chain. However, CORM-3 was also seen to perturb metal biochemistry. The most dramatically affected gene in the study was *spy*, which was up-regulated by 26-fold under aerobic conditions and >100-fold under anaerobic conditions. It encodes a periplasmic protein that is induced by zinc and copper ions (Yamamoto *et al.* 2008) and envelope stress (Raffa & Raivio 2002). Genes that have been implicated in zinc homeostasis and regulation were up-regulated under both conditions: *yodA* that encodes a periplasmic zinc- and cadmium-binding protein (David *et al.* 2003; Kershaw *et al.* 2007; Puskarova

et al. 2002) and *znuA*, which encodes a zinc-binding protein (Li & Jogl 2007; Yatsunyk *et al.* 2008) associated with the high affinity ATP-binding cassette ZnuABC transporter (Patzer & Hantke 1998). Up-regulation of *zraP*, encoding another periplasmic zinc-binding protein, was seen exclusively under anaerobic conditions. Additionally, genes encoding ferritin-like proteins were differentially regulated: down-regulation of *bfr* and up-regulation of *ftnB* under aerobiosis and down-regulation of *ftnA* under anaerobiosis were reported. Under aerobic conditions, genes involved in diverse membrane transport processes were differentially regulated, including the *mdtABC* and *cus* operons that are up-regulated in response to high zinc levels (Lee *et al.* 2005). A separate functional class, acetate and acetyl group metabolism, contained some of the most dramatically down-regulated genes (Davidge *et al.* 2009b).

Modelling of microarray data revealed the involvement of 8 regulators in the aerobic response to CORM-3: ArcA, CRP, Fis, FNR, Fur, BaeR, CpxR and IHF (Davidge *et al*. 2009b). However, no significant change in activity was predicted for CRP, Fis and FNR under anaerobic conditions. In each case, the predicted activities for regulators other than Fur and IHF were increased. As described in section 3.1, the activity of ArcA was explained in terms of CO-elicited inhibition of respiration. Involvement of the remaining transcription factors was not so readily explained. However, they suggested that interaction of CO with intracellular metal targets other than ferrous haem may be the reason for the observed activity of FNR and Fur, which both contain iron centres. Furthermore, the Cpx stress response is activated by misfolded envelope proteins. The role of CpxR and BaeR was therefore attributed to the maintenance of envelope protein integrity and general response to envelope stress, as *spy*, which is regulated by both BaeR and CpxR (Raffa & Raivio 2002; Yamamoto *et al.* 2008) and *cpxP* (encodes the periplasmic inhibitor of the Cpx response) were highly up-regulated under both growth conditions (Davidge *et al*. 2009b).

The response of *E. coli* to CORM-2 (Nobre *et al*. 2009) was reported to be more multifaceted than observed with CORM-3 (Davidge *et al*. 2009b). Genes in almost all functional categories were differentially affected. In response to 15 min exposure to 250 μM CORM-2, the regulation of 175 and 396 genes was altered in aerobic and anaerobic cultures, respectively. Under anaerobic conditions 228 of the genes were repressed, with 84 % of the genes being involved in cellular metabolic processes including catabolic

processes, nucleotide metabolism and energy production by oxidation of organic compounds. The 168 genes with increased expression levels were divided into three categories: inorganic ion transport, post-translational modification and transcription. Of particular note was the strong induction of *ibpA* (19-fold) and *ibpB* (40-fold), which encode two heat-shock proteins that are associated with protein stability. Consistent with Davidge *et al*. (2009b), iron metabolism was also affected with down-regulation of *bfr* and *ftnA* and up-regulation of *ftnB*. However, only *ftnA* was implicated in the anaerobic response reported by Davidge *et al*. (2009b). Genes involved in biofilm formation were also induced (*tqsA*, *bhsA*, *bssS* and *bssR*). Under aerobic conditions, 46 genes were down-regulated and 129 genes were up-regulated. Repressed genes were split into three main categories: amino acid and carbohydrate transport and metabolism and energy production, in which genes involved in coenzyme catabolic processes, the tricarboxylic acid (TCA) cycle and aerobic respiration were altered. Up-regulated genes included those encoding proteins with a role in inorganic ion transport, sulfur metabolism e.g. *tauABC*, *ssuAD*, *cysWA* and *sbp*, and methionine metabolism e.g. *metNI* and *metBLF*. As seen by Davidge *et al*. (2009b), *cpxP* was up-regulated under both growth conditions but in parallel with a number of other genes involved in cell wall biogenesis and protein folding. Such genes encode heat-shock proteins (*hslJ*, *htpX*), chaperones (*dnaJ*, *htpG*, *clpB*) and proteases (*ftsH*) and were mainly up-regulated under anaerobiosis (Nobre *et al*. 2009). Furthermore, biological assays revealed heightened sensitivity of *E. coli* deficient in genes encoding SoxS and OxyR to CORM-2. However, whereas the *soxS* mutant was sensitive under both aerobic and anaerobic conditions, the *oxyR* mutant was unaffected when treated with CORM-2 anaerobically. The compound was also more potent against anaerobically grown *E. coli* deficient in the heat-shock proteins IbpA and IbpB and the extracytoplasmic stress regulator CpxP, as well as aerobically grown cells deficient in methionine metabolism. Interestingly, deletion of genes involved in biofilm formation increased the resistance of *E. coli* to CORM-2 (Nobre *et al.* 2009).

In each of these studies, confirmation that altered transcription levels were a response to liberated CO, and no other part of the CO-RM skeleton, was achieved for genes of interest during validation of microarray data. Quantitative RT-PCR showed no effect of 500 μM $RuCl_2(DMSO)_4$ on the expression levels of ten genes chosen from different classes including transcriptional regulators, heat shock proteins, oxidative stress

response, biofilm formation, energy metabolism, methionine biosynthesis and hypothetical proteins (Nobre *et al*. 2009). Additionally, β-galactosidase activity was unaffected in an aerobically grown Φ(*cyo-lacZ*) strain and an anaerobically grown Φ(*spy-lacZ*) strain treated with $RuCl_2(DMSO)_4$ (Davidge *et al.* 2009b).

In an attempt to understand the mechanisms of CORM-3 activity in haem-deficient *E. coli* in the present study, transcriptomic analyses were carried out as described in section 2.4.1 and also in brief below. Although the above reports provide a safe comparison for the new data, microarray experiments were also performed using the corresponding wild type treated under the same conditions as the mutant. The aim of this work is to determine whether there are any differences between the response of the mutant and the wild type, which may explain the potent toxicity of CORM-3 in the absence of haem. Additionally, and for the first time, microarrays employing inactive CORM-3 will be described in parallel to determine whether the observed effects are CO-specific.

5.2 Results

In the following experiments, the haem-deficient mutant of *E. coli* (RKP5421) and the corresponding wild type (RKP5416) (Table 2.1) were grown under anaerobiosis in defined medium modified for the growth of haem-deficient bacteria (section 2.1.2.6), as described in Chapter 4. However, bacteria were cultured on a larger scale in minifermentor vessels (2.1.5.2) to enable the removal of adequate volumes for RNA isolation over a time-series consisting of 5 time-points: 0 min (i.e. immediately prior to stress) and then 10, 20, 40, 60 and 120 min following stress. Cultures were exposed to 100 μM CORM-3/iCORM-3, as the active compound did not considerably decrease bacterial viability within the time-frame of the experiment (120 min) when administered at this concentration (Figure 4.7). A diagram showing the experimental process used in the present study is shown in Figure 5.1. In brief, control (prior to stress) and experimental (post-stress) RNA was isolated from culture samples and cDNA was synthesised from the purified RNA. The cDNA was labelled with two fluorescent dyes, Cy3 (green) and Cy5 (red), and transferred to a microarray slide so that control cDNA was labelled with one dye and the experimental DNA was labelled with the other. A technical repeat was performed for each sample by exchanging the dyes, i.e. a 'dye-

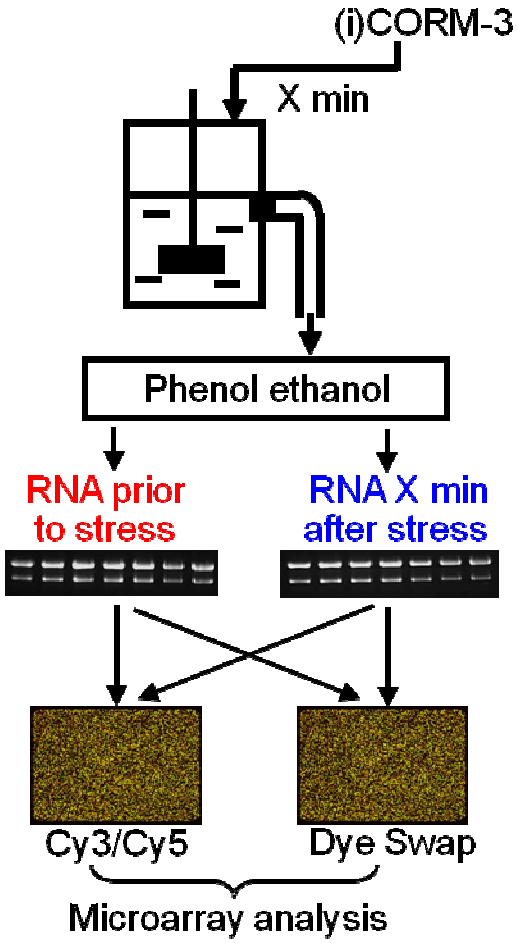

Figure 5.1. Diagram of the microarray process.

swap', which minimises variation caused by differential binding or fluorescence of the two individual dyes. The cDNA was hybridised to the oligos on the array slide overnight and the slides were then scanned. The resultant data were analysed using software that compares the levels of fluorescence emitted by spots (corresponding to the cDNA concentration for a given gene) in the control versus experimental samples, which determined the effect of CORM-3/iCORM-3 administration on gene transcript levels. To further interpret the results obtained from the transcriptomic profiling, the gene expression patterns were analysed by mathematical modelling as described in section 5.2.7. In the microarray data presented herein, an arbitrary cut-off value of ≥ 2-fold up- or down-regulated has been chosen to represent genes that are differentially affected by CORM-3/iCORM-3. Information about gene products and their function was provided in the gene-lists generated by GeneSpring 7.3.1 (Agilent Technologies) (section 2.4.1.8). References are therefore not provided in the text unless further details were sought from the literature. The relevant regulatory proteins for each gene were identified (where available) using regulonDB and EcoCyc (both are available on the World Wide Web).

5.2.1 CORM-3 elicits multifaceted transcriptomic effects, even in the absence of haem proteins

To provide an overall representation and comparison of the effect of CORM-3 on the transcriptome of the haem-deficient mutant and corresponding wild type, a comparative bar chart was compiled in which the percentages of up- and down-regulated genes in a number of functional categories in the two strains are shown for each time-point (Figure 5.2). A comparison of the data obtained for the mutant treated with CORM-3 and iCORM-3 is also presented in this way (Figure 5.3). For reference, the differences in gene expression between the mutant and wild type under control conditions, i.e. immediately prior to CORM-3 addition, are presented (Figure 5.4 A). Panel B of this figure illustrates the frequency of genes with altered transcription in the mutant compared with wild type. Across all of the functional categories presented, only 2 % of the genome, which contains a total of 4,598 genes, was up-regulated (≥ 2-fold, red) and 3.91 % was down-regulated (≥ -2-fold, blue) in comparison with the wild type (Figure 5.4 A). The groups with the most changes were those containing genes involved in Fe-S protein assembly and metabolism, energy metabolism, glycolysis, the TCA cycle and

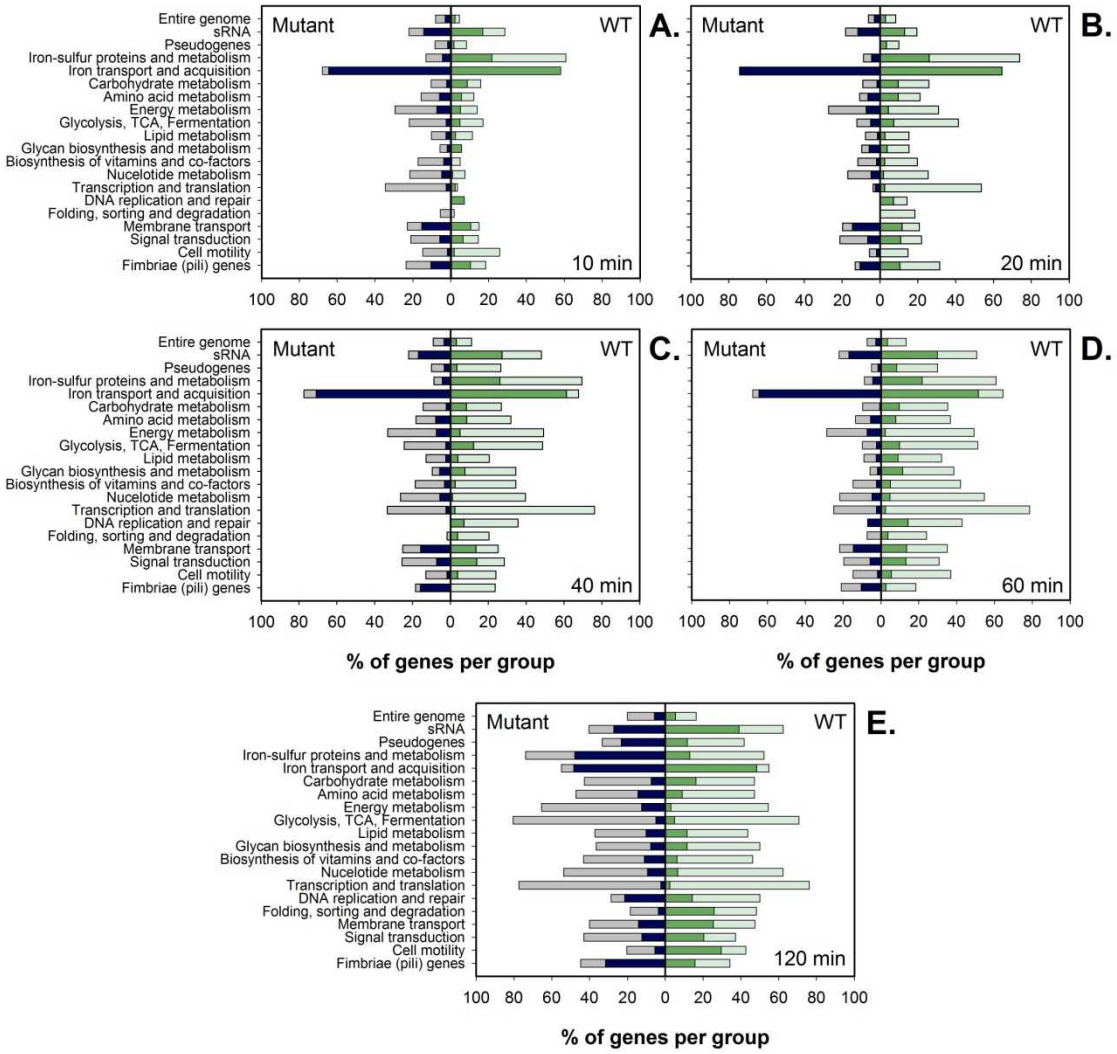

Figure 5.2. Functional categories of genes affected by CORM-3 in the haem-deficient mutant of *Escherichia coli* versus the corresponding wild type. Cultures were grown anaerobically in defined medium modified for the growth of haem-deficient bacteria. The bars show the percentage of genes in each group that exhibit altered expression after treatment with 100 μM CORM-3. Data are shown for the mutant on the left (dark blue and grey) and the wild type (WT) on the right (dark green and light green). Data are shown for each of the following time-points after addition of the compound: **A.** 10 min, **B.** 20 min, **C.** 40 min, **D.** 60 min and **E.** 120 min. In each category, dark blue (mutant) and dark green (wild type) bars indicate the proportion of up-regulated genes and grey (mutant) or light green (wild type) bars indicate the proportion of down-regulated genes. Microarray data-sets were analysed using GeneSpring 7.3.1. Functional category gene-lists were created using KEGG (Kyoto Encyclopedia of Genes and Genomes) (Kanehisa & Goto 2000; Kanehisa *et al.* 2012).

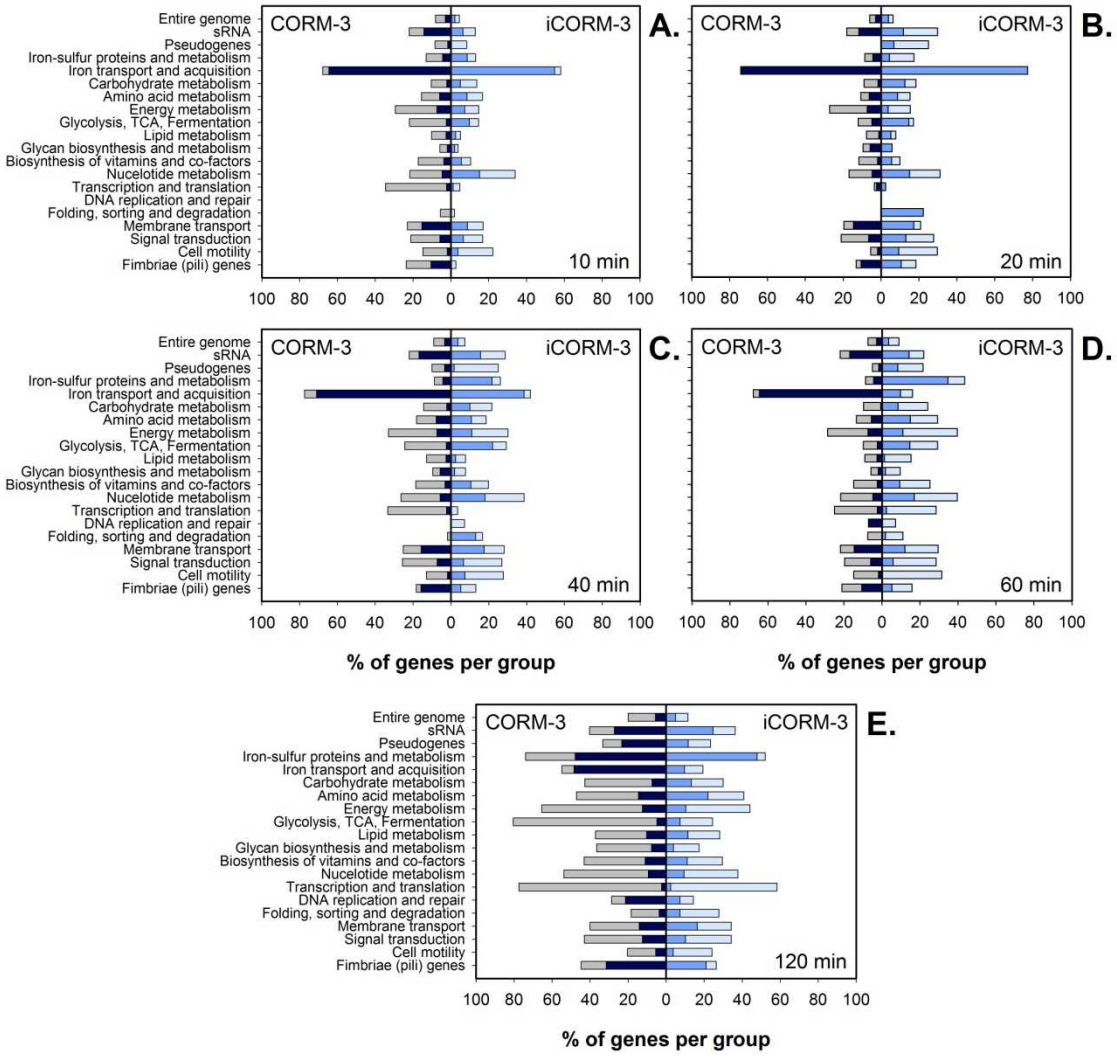

Figure 5.3. Functional categories of genes affected by CORM-3 versus iCORM-3 in the haem-deficient mutant of *Escherichia coli*. Cultures were grown anaerobically in defined medium modified for the growth of haem-deficient bacteria. The bars show the percentage of genes in each group that exhibit altered expression after treatment with 100 μM CORM-3 (left, dark blue and grey) and iCORM-3 (right, blue and light blue). Data are shown for each of the following time-points after addition of the compound: **A.** 10 min, **B.** 20 min, **C.** 40 min, **D.** 60 min and **E.** 120 min. In each category, dark blue (CORM-3) and blue (iCORM-3) bars indicate the proportion of up-regulated genes and grey (CORM-3) and light blue (iCORM-3) bars indicate the proportion of down-regulated genes. Microarray data-sets were analysed using GeneSpring 7.3.1. Functional category gene-lists were created using KEGG (Kyoto Encyclopedia of Genes and Genomes) (Kanehisa & Goto 2000; Kanehisa *et al.* 2012).

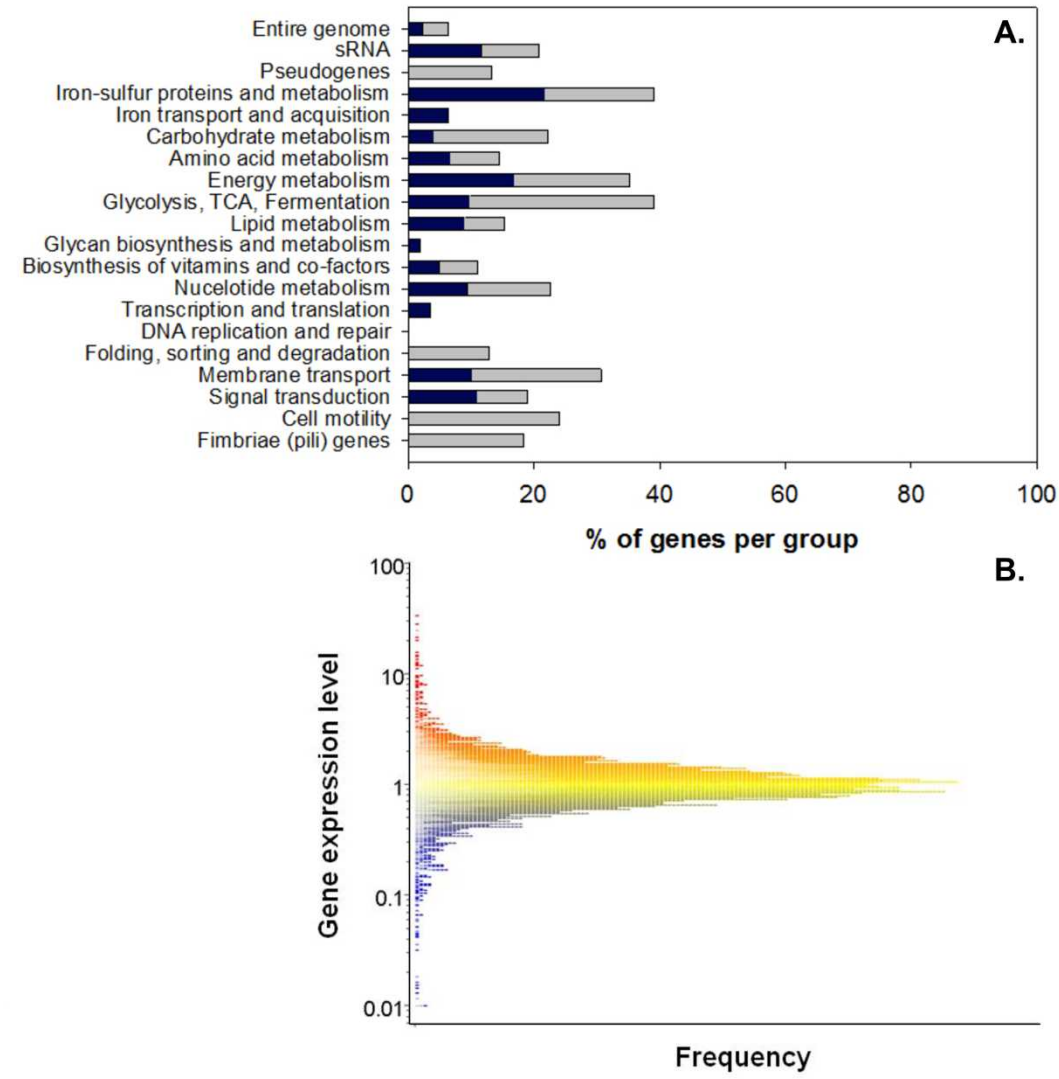

Figure 5.4. Functional categories of genes affected in the haem-deficient mutant of *Escherichia coli* in comparison with the wild type. Cultures were grown anaerobically in defined medium modified for the growth of haem-deficient bacteria. **A.** The bars show the percentage of genes in each group with altered expression in the haem-deficient mutant when compared with the wild type immediately prior to CORM-3 addition ($t = 0$). The dark blue and grey bars indicate the proportion of up- and down-regulated genes, respectively. **B.** Expression profile showing the frequency of genes with altered transcription in the haem-deficient mutant compared with the wild type. Red indicates up-regulated genes (≥ 2-fold), blue indicates down-regulated genes (≥ -2-fold) and yellow represents genes with unaltered expression. Microarray data-sets were analysed using GeneSpring 7.3.1 and functional category gene-lists were created using KEGG (Kyoto Encyclopedia of Genes and Genomes) (Kanehisa & Goto 2000; Kanehisa *et al.* 2012).

fermentation, as well as membrane transport. Pseudogenes (non-functional DNA sequences that resemble functional genes) and genes encoding proteins required for DNA folding, sorting and degradation, cell motility and formation of fimbriae (pili) were solely down-regulated in the mutant when compared with the wild type.

The charts shown in Figure 5.2 suggest that the wild type responds to CORM-3 more so than the mutant. However, the percentage of the genome that was affected with respect to the selected functional groups over 120 min was similar: 53.7 % and 50.8 %, respectively, consisting of 17.1 % of genes being up-regulated (≥ 2-fold) and 36.6 % down-regulated (≥ -2-fold) in the wild type, and 17.8 % up-regulated and 32.9 % down-regulated in the mutant. Furthermore, the magnitude of the effect, i.e. the fold-changes in gene expression levels at each time-point, is also similar (compare panels A and B of Figure 5.5). The difference between the two strains lies in the functional categories that contain the most affected genes. The CORM-3-elicited response in the wild type is generally more diverse. This may be expected in the presence of haem-containing targets as they have roles in a number of cellular processes. On the other hand, for the first 60 min post addition the effect of the compound on iron transport and acquisition in the mutant is striking. Interestingly, at 120 min, the percentage of the genome with altered transcription in the mutant is considerably increased.

In contrast, the diversity of the effect of CORM-3 and iCORM-3 on the mutant is similar (Figure 5.3). Over 120 min, 17.8 % of the genome was up-regulated in both CORM-3- and iCORM-3-treated cells. However, 32.9 % was down-regulated after exposure to CORM-3, compared with 20.7 % for iCORM-3. The CO donor altered the expression of 50.8 % of the genome over the time-series, whereas 38.5 % was altered in response to the inactive compound. Additionally, the fold-changes in gene expression for the majority of genes in the haem-deficient mutant treated with iCORM-3 are approx. 10-fold lower than seen in response to CORM-3. For example, the maximum fold-change in the mutant treated with CORM-3 is c. 1,000-fold, however in the mutant treated with iCORM-3, the maximum fold-change is c. 100-fold (compare panels A and C of Figure 5.5). This is in agreement with the percentage of CO release from iCORM-3 to ferrous myoglobin (< 10 %), when compared with the active compound (see Chapter 3, section 3.2.5 and Figure 3.7 C inset). The residual release of CO from iCORM-3 may explain the transcriptomic response of the mutant.

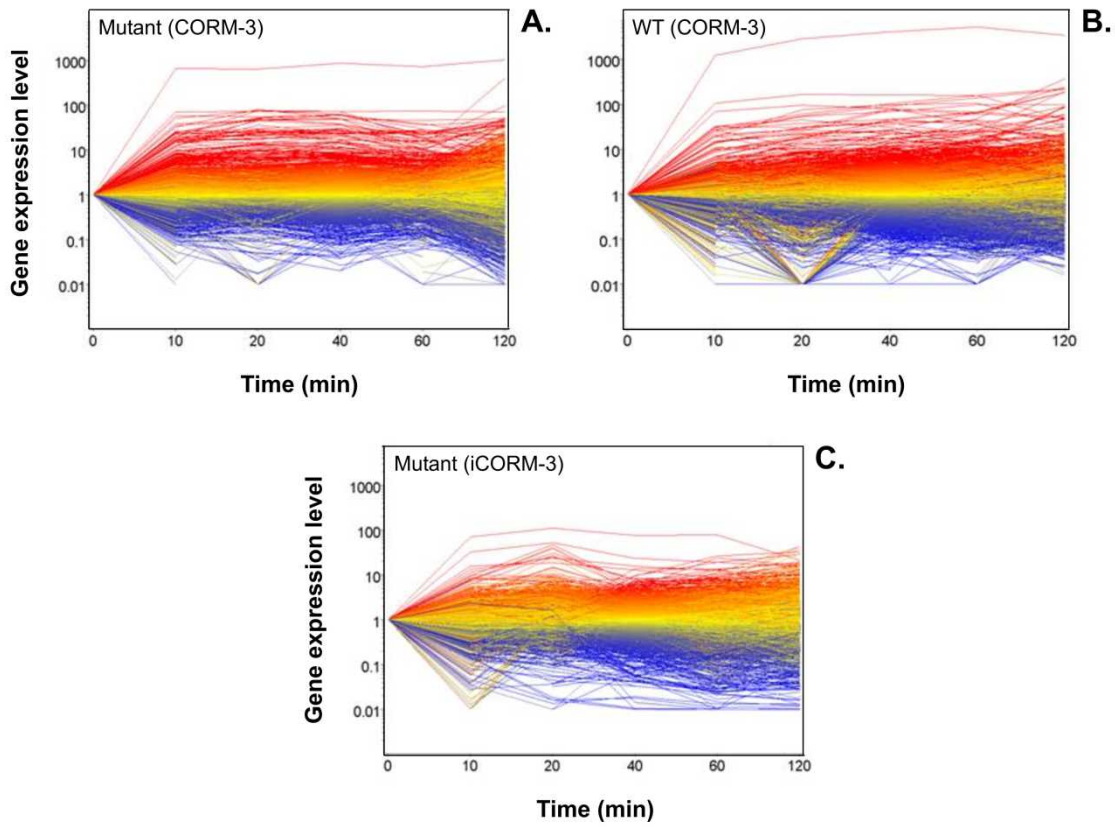

Figure 5.5. Expression profiles showing the magnitude of the effect of CORM-3/iCORM-3 on all genes. Cultures were grown anaerobically in defined medium modified for the growth of haem-deficient bacteria. Graphs were generated by GeneSpring 7.3.1 during the analysis of data-sets. Red indicates up-regulated genes (≥ 2-fold), blue indicates down-regulated genes (≥ -2-fold) and yellow represents genes with unaltered expression in: **A.** the haem-deficient mutant treated with 100 μM CORM-3, **B.** the wild type (WT) treated with 100 μM CORM-3 and **C**. the haem-deficient mutant treated with 100 μM iCORM-3.

Although the graphs described above provide a means by which one can view the microarray data in a broader sense, it can be deceptive. The fold-changes in gene expression within the functional categories are not shown; therefore the magnitude of the effect in each condition is not properly presented. Due to this, and the large amount of data obtained in this study, it was decided to choose functional categories of particular interest, and indeed those that contain some of the most differentially regulated genes. For this purpose, heat tables were used and in each case they incorporate data for the mutant and the wild type treated with CORM-3 and the mutant treated with iCORM-3. Such tables enable a better representation of the magnitude of the effect and allow visual comparisons to be made between different conditions. However, complete gene-lists are provided in Tables 1 - 3 of the Appendix (available from the University Library) should there be an interest in any genes that are not discussed in this chapter. Please note that fold-changes of ≤ 0.5 are indicative of ≥ 2-fold down-regulation and genes with values between 0 - 2 and 0 - 0.5 are considered to be unaffected.

5.2.2 Genes involved in iron homeostasis are highly up-regulated in response to CORM-3, particularly in the haem-deficient mutant

As mentioned in section 5.2.1, the effect of CORM-3 on the expression of genes involved in iron transport and acquisition in the mutant is striking, with between 48.4 - 74.2 % of the genes being up-regulated and only between 0 - 6.45 % being down-regulated over 120 min (Figure 5.2). This response was made even more prominent by the majority of genes with altered transcription, across all of the functional classes over the course of the time-series, being down-regulated. As can be seen in Figure 5.6, the genes are more affected in the mutant than in the wild type (see below for examples). Additionally, iCORM-3 has much less of an effect between 20 - 60 min, suggesting that CO released from CORM-3 is the effector. The genes exhibiting the most highly altered levels of expression in the mutant treated with the active compound are those involved in biosynthesis of the catecholate siderophore enterobactin (*ent*), reaching a maximum of 79.7-fold (*entE*, 20 min post CORM-3 addition). In the wild type, the change in gene expression of the majority of *ent* genes did not exceed 10-fold.

Landscape Figure (Figure 5.6), refer to page 5 of supplementary document.

Enterobactin utilisation in *E. coli* has been reviewed (e.g. (Crosa & Walsh 2002)) and is described briefly below. The genes included in this group, i.e. those involved in the transport of ferric enterobactin, and genes involved in intracellular release of iron from enterobactin, were up-regulated in the current study. The only exceptions were *exbB* and *exbD* in the mutant treated with iCORM-3, which were down-regulated -2.94-fold and -3.23-fold at 120 min, respectively. Enterobactin is synthesised under iron-limiting conditions and secreted into the extracellular environment to scavenge iron(III). Transport of ferric enterobactin into the cell is achieved in two stages. The ferric enterobactin receptor, FepA, is an outer membrane protein that actively transports ferric enterobactin into the periplasm using energy provided by the TonB energy transducing system (TonB-ExbB-ExbD) (Sansom 1999). The iron(III)-bound siderophore is then transported through the cytoplasmic membrane via an ABC transporter encoded by *fepBCDG*. Once in the cell, the siderophore is broken down by an enterobactin/ferric enterobactin esterase (Fes), the gene for which is highly up-regulated in the mutant (25.2- to 35.4-fold from 10 - 40 min and 19.1- and 22.3-fold at 60 and 120 min, respectively) compared with the wild type (minimum of 2.27-fold and maximum of 6.44-fold over 120 min).

In addition, genes encoding the hydroxamate siderophore uptake system (*fhu*) that enables utilisation of ferrichrome, ferric coprogen and ferrioxamine B as sources of iron under low iron conditions were also up-regulated. Again, two modes of transport are employed: active transport across the outer membrane via the receptors FhuA and FhuE, which utilise energy provided by the TonB energy transducing system (Hantke 1983; Sansom 1999), followed by transport across the cytoplasmic membrane by the ABC transporter FhuCDB. Once inside the cell, FhuF acts as a ferric siderophore reductase enabling the release of iron (Matzanke *et al.* 2004). As for *fes* in the enterobactin utilisation system, *fhuF* is also more highly up-regulated than the other genes involved in hydroxamate siderophore usage (minimum of 15.2-fold and maximum of 32.0-fold in the mutant, and minimum of 7.93-fold and maximum of 21.9-fold in the wild type, over 120 min). Additional iron acquisition methods were also highlighted by up-regulation of the ferric citrate system (*fec*) and ferrous iron-uptake (*feoA*).

The gene encoding the iron storage protein, ferritin (*ftnA*), is down-regulated in both the mutant and the wild type (minimum of -2.08-fold and maximum of -3.70-fold in the

mutant, and minimum of -4.55-fold and maximum of -8.33-fold in the wild type, over 120 min). In contrast, *bfd* (encoding bacterioferritin-associated ferredoxin) is up-regulated (minimum of 7.60-fold and maximum of 19.8-fold in the mutant, and minimum of 3.39-fold and maximum of 5.73-fold in the wild type, over 120 min). It has been suggested that Bfd is involved in the release/delivery of iron to/from bacterioferritin, or other iron complexes e.g. siderophores or Fe-S clusters (Andrews 1998). Interestingly a sRNA gene, *ryhB*, was highly up-regulated in both the mutant (minimum of 21.0-fold and maximum of 62.3-fold over 120 min) and the wild type (minimum of 6.88-fold and maximum of 181-fold). RyhB reduces iron consumption under low-iron conditions by down-regulating iron-containing proteins including ferritins, superoxide dismutase and some genes of the TCA cycle (Masse & Gottesman 2002), as well as promoting enterobactin synthesis (Salvail *et al.* 2010). Overall, the transcript level changes observed for genes in this category suggest the mutant senses a shortage of biologically available iron after CORM-3 stress.

5.2.3 CORM-3 differentially alters transcription of genes involved in Fe-S cluster assembly and repair in the mutant and the wild type

Although significant changes in the expression of genes involved in iron acquisition were observed, genes implicated in processes involving Fe-S proteins (Figure 5.2 and Figure 5.7) were not altered to a similar degree in the mutant treated with CORM-3. Furthermore, there were a number of differences in the response of Fe-S cluster genes in the mutant and the wild type treated with CORM-3 (Figure 5.7). Genes encoding the house-keeping Fe-S cluster assembly system (*isc*) were generally down-regulated in the wild type, whereas the *suf* system, which is adapted to build Fe-S clusters during iron starvation and oxidative stress (Outten *et al.* 2004), was up-regulated. However, in the mutant, both systems were affected only at 120 min, whereas hardly any of the genes were affected in the wild type at this later time-point. In the mutant, fold-changes for *iscR*, encoding the repressor of *isc* expression, and *sufA*, encoding an A-type carrier protein (Vinella *et al.* 2009), reached 17.7 and 13.7-fold, respectively. The latter is thought to act as an Fe-S cluster shuttle that receives its cluster from SufBCD before insertion into target apoenzymes (Chahal *et al.* 2009). Moreover, *sufA* was the only Fe-S cluster assembly gene in the mutant that showed altered transcription over the entire 120 min (minimum of 2.38-fold). Although *iscR* was up-regulated 2.71-fold in the wild

Landscape Figure (Figure 5.7), refer to page 6 of supplementary document.

type at this later time-point, the *p*-value (0.16) is too high to be reliable. Furthermore, *ytfE* is up-regulated in the mutant (up to a maximum of 17.6-fold at 120 min) and unaffected in the wild type. The product of this gene has been implicated in the repair of damaged Fe-S clusters (Justino *et al.* 2007) and its expression is stimulated by iron starvation (Justino *et al.* 2006).

Unexpectedly, genes in the category of Fe-S proteins and their metabolism were slightly more affected in the mutant treated with iCORM-3 than CORM-3 (Figure 5.3). The majority (between 8.70 - 47.8 %) of genes were up-regulated in comparison with 4.35 - 8.70 % being down-regulated over 120 min, with an exception at 20 min (4.35 % up and 13.0 % down). A larger portion of these genes were up-regulated at later time-points (also refer to Figure 5.7). However, the expression of *ytfE* was not perturbed to the same degree, with a maximum fold-change of 5.27 (Figure 5.7).

5.2.4 CORM-3 perturbs the expression of genes involved in general stress response, zinc homeostasis and signal transduction

Although one cannot tell from looking at the signal transduction category in Figures 5.2 and 5.3, some of the most highly altered genes in this study are within this class and that of general stress response. Further to the pronounced effect of CORM-3 on iron homeostasis, zinc homeostasis was also affected. The genes presented in Figure 5.8 were the most altered and the majority have previously been reported to change in response to CO-RM stress (Davidge *et al.* 2009b; Nobre *et al.* 2009) (see section 5.1). Exceptions include up-regulation of *hns*, the product of which is a global transcriptional regulator that responds to environmental changes and adaptation to stress, and marked up-regulation of *hmp*, encoding a flavohaemoglobin (Vasudevan *et al.* 1991) with NO dioxygenase activity (Gardner *et al.* 1998). Strikingly, gene expression alterations for the latter were seen in the mutant treated with CORM-3 (minimum of 6.68-fold and maximum of 94.2-fold over 120 min), but not in the wild type. Expression of *hmp* was also altered in the mutant post-addition of the inactive compound, albeit to a lesser degree and only between 40 - 120 min (minimum of 5.20-fold and maximum of 23.9-fold). This is consistent with a proposed role for the residual CO that is released from iCORM-3.

Landscape Figure (Figure 5.8), refer to page 7 of supplementary document.

In agreement with Davidge *et al*. (2009b), the most up-regulated gene in this study was *spy*, with a minimum fold-change of 630 and a maximum of 1,021 in the mutant in comparison with 1,218 and 5,131 in the wild type. Up-regulation was also noted in the mutant treated with iCORM-3, but again by c. 10 % less than seen after stressing with CORM-3 (minimum of 20.9-fold and maximum of 109-fold). Other genes within the same regulatory network as *spy* (i.e. regulated by BaeR and/or CpxR) were also greatly altered, including *mdtABC* encoding the multidrug efflux system, as well as *baeR* and *cpxP*. In addition, consistent with both Davidge *et al*. (2009b) and Nobre *et al*. (2009), genes encoding proteins that respond to intracellular stresses and biofilm formation were also up-regulated to varying extents: *bhsA*, *bssR*, *bssS*, *clpB*, *htpX*, *yodA*, *ibpA* and *ibpB*. Interestingly, altered expression was observed for the sRNA gene *oxyS*, the product of which responds to oxidative stress. At later time-points this gene was highly up-regulated in the mutant (maximum of 41.7-fold at 120 min), and particularly the wild type (maximum of 87.6-fold at 120 min), after exposure to CORM-3. The inactive compound resulted in only a 2.51-fold up-regulation of *oxyS* at 120 min and the *p*-value was too high to be reliable ($p = 0.15$). These patterns point to a profound stress at the cell membrane following exposure of the mutant and the wild type to CORM-3, which, importantly, appears to be significantly less pronounced after treatment with iCORM-3.

Some of the genes mentioned above also have roles in zinc homeostasis, namely *spy* and *yodA*, as well as the *mdtABC* operon that is up-regulated in response to zinc (Lee *et al.* 2005). Furthermore, genes encoding the zinc(II)-transporter protein (*znuABC*) were up-regulated, particularly in the mutant treated with CORM-3. However, expression levels of the majority of the genes highlighted in this section were much higher in the wild type than in the mutant, and the general effect of iCORM-3 was minimal.

5.2.5 CORM-3 treatment results in differential regulation of genes required for the use of cysteine and sulfate in the mutant versus the wild type

Davidge *et al*. (2009b) and Nobre *et al*. (2009) reported the up-regulation of genes involved in cysteine biosynthesis and sulfate assimilation (*cys*) in *E. coli* treated with CO-RMs. However, the latter group only observed changes in *cys* gene expression under aerobic conditions. In the current study, differential regulation of these genes was noted across all conditions tested (Figure 5.9). A striking finding was that CORM-3 and

Landscape Figure (Figure 5.9), refer to page 8 of supplementary document.

iCORM-3 elicited similar gene expression changes in the mutant. However, the response in the wild type was quite distinct; all of the selected genes were down-regulated, as opposed to the modest up-regulation generally observed in the mutant. In particular, *cysH* encoding PAPS reductase and *cysJI* encoding sulfite reductase were the most down-regulated in the wild type (maximum of 33.3-fold for *cysJ* at 120 min). These results seem to indicate that the CO-RM skeleton has an effect on cysteine metabolism, and that this effect is independent of the presence of haem proteins. Nobre *et al*. (2009) also reported up-regulation of *tauABC* and *ssuAD* (albeit again under aerobic conditions), which encode ABC-type transport systems that enable uptake of aliphatic sulfonates as a source of sulfur during sulfate-starvation (van der Ploeg *et al.* 2001). However, these genes were not greatly affected under any of the conditions tested in the current study (data not shown); therefore the observed up-regulation of *cys* genes in the mutant does not appear to be a result of reduced levels of sulfate.

Cysteine, glutathione and the thiol-containing compound NAC have been reported to abolish the anti-bacterial activity of CO-RMs (Desmard *et al.* 2009; Desmard *et al.* 2012; Murray *et al.* 2012; Tavares *et al.* 2011). It was therefore of interest to see how CORM-3 affected genes involved in thiol chemistry. In the study described here, the expression of genes encoding the ABC-type glutathione transporter (*gsiABCD*) (Suzuki *et al.* 2005) was altered (data not shown). Modest up-regulation was observed in the mutant treated with both the active and inactive compound, with the gene encoding the ATP-binding component of the transporter (*gsiA*) being the most affected (maximum of 2.96-fold and 3.80-fold following exposure to CORM-3 and iCORM-3, respectively). In the wild type on the other hand, genes encoding glutathione synthesis and transport were generally down-regulated, but only at one or two time-points and by a maximum of -3.85-fold. Glutathione synthesis was unaffected in the mutant bar a -2.13-fold down-regulation of *gor*, encoding glutathione oxidoreductase, at 120 min after CORM-3-treatment.

5.2.6 Other functional categories of note

In addition to the categories mentioned in the above sections, a number of others were also affected and agree with the findings of Nobre *et al*. (2009) and Davidge *et al*. (2009b). There is therefore no need to recapitulate other than to highlight the relevant

classes of targets. Under all of the conditions tested, the expression of genes involved in carbohydrate, energy, amino acid and nucleotide metabolism, biosynthesis of vitamins and co-factors, as well as genes encoding membrane transport, signal transduction, translation and transcription were altered. However, as previously demonstrated, the fold-changes of gene expression observed after exposure to iCORM-3 were, for the most part, lower than seen after CORM-3 treatment. Another observation worth noting is the large number of genes encoding sRNAs that were also altered in the wild type, particularly at later time-points.

5.2.7 Modelling of transcriptomic data

Mathematical modelling of the microarray data was carried out in collaboration with Dr. Ronald Begg and Dr. Guido Sanguinetti at the School of Informatics, University of Edinburgh, as described in section 2.4.1.9 using TFInfer (Asif *et al.* 2010; Sanguinetti *et al.* 2006). The programme enables the activity of transcription factors to be inferred from gene expression data obtained from the time-series microarray experiments. The complete raw transcriptomic data-sets obtained from GeneSpring 7.3.1 were used for the analysis; therefore no limitations with regard to significance or gene expression level were enforced prior to the application of TFInfer. In an attempt to focus the results, transcription factors with ≤ 6 targets, as determined from RegulonDB, were discarded from the runs.

Key transcription factors of interest were chosen from the TFInfer data and their inferred activity over 120 min is presented in this chapter alongside relevant gene expression levels. For the complete list of transcription factors with predicted activity under each condition, refer to Tables 4 - 6 of the Appendix (available from the Library). Information on transcription factor function was obtained from regulonDB and EcoCyc and is provided on the second spreadsheet of each Excel Workbook. For the complete set of graphs presenting the regulatory profiles over 120 min, refer to the labelled folders in the Appendix, which show the theoretical activity of the regulators 1) in the mutant treated with CORM-3 versus iCORM-3 (mutant CORM-3 *vs* iCORM-3) and 2) the mutant versus wild type treated with CORM-3 (mutant *vs* WT CORM-3). However, as stated in section 2.4.1.10, TFInfer does not know *a priori* the sign of TF-gene interactions, which means that transcription factor profiles generated in this way may be

inverted. This can be corrected manually by comparing inferred signs with information from RegulonDB and/or EcoCyc on transcription factor activity and flipping a transcription factor profile, as well as the signs of its interactions, depending on the activity of the genes it regulates. Therefore the profiles presented in the Appendix are not absolute and can be flipped if the regulation does not match the direction of fold-changes in gene expression. For example, if a known repressor was predicted to have increased activity, but the genes it controls are up-regulated, then the profile of this transcription factor can be flipped as its activity should be decreased in this case.

5.2.7.1 Regulation of iron homeostasis

The regulation of genes involved in the response to iron-starvation (*ent* and *ryhB*) by Fur is evident under all conditions (Figures 5.10 and 5.11). The pattern of Fur activity in each case follows closely the pattern of gene expression, whereas the same is not true for the transcriptional activator of the *ent* operon, CRP. The regulatory network for the genes encoding the alternative Fe-S cluster assembly system (*suf*) is more complex (Figure 5.12), involving the activity of three transcription activators, IHF, IscR and OxyR, and the inhibitor Fur. In the case of the mutant treated with both CORM-3 (Figure 5.12 A) and iCORM-3 (Figure 5.12 B), IHF appears to follow a similar pattern to gene expression in comparison with the other regulators. Also, the predicted activity of IscR fits well with the gene expression. In its 'mature' Fe-S cluster-bound form, IscR represses the expression of the *isc* operon, but under conditions in which Fe-S cluster assembly becomes rate-limiting, or the Fe-S cluster is damaged, the apo form of the protein alleviates repression of the operon in addition to activating the *suf* operon (Yeo *et al.* 2006). As may be expected due to the greater effects of CORM-3 on the *isc* and *suf* systems, the regulation of the *suf* genes in the wild type is more complex (Figure 5.12 C), with a mix of transcription factors being involved in the regulation. This may also include a contribution from the inhibitor of transcription, Fur, which more closely resembles the pattern of gene expression in the wild type than in the mutant. Regulation of *isc* genes on the other hand is simply controlled by the activity of the transcription repressor IscR, the activity of which is again in line with that of gene expression levels (Figure 5.13). However, the activity of IscR is more modest in the mutant treated with the active compound (Figure 5.13 A). This may be explained by the lesser affect of CORM-3 on *isc* genes in this context, as demonstrated in Figure 5.7. Activity of the positive regulators NarP and NarL and the negative regulators FNR and NsrR in relation

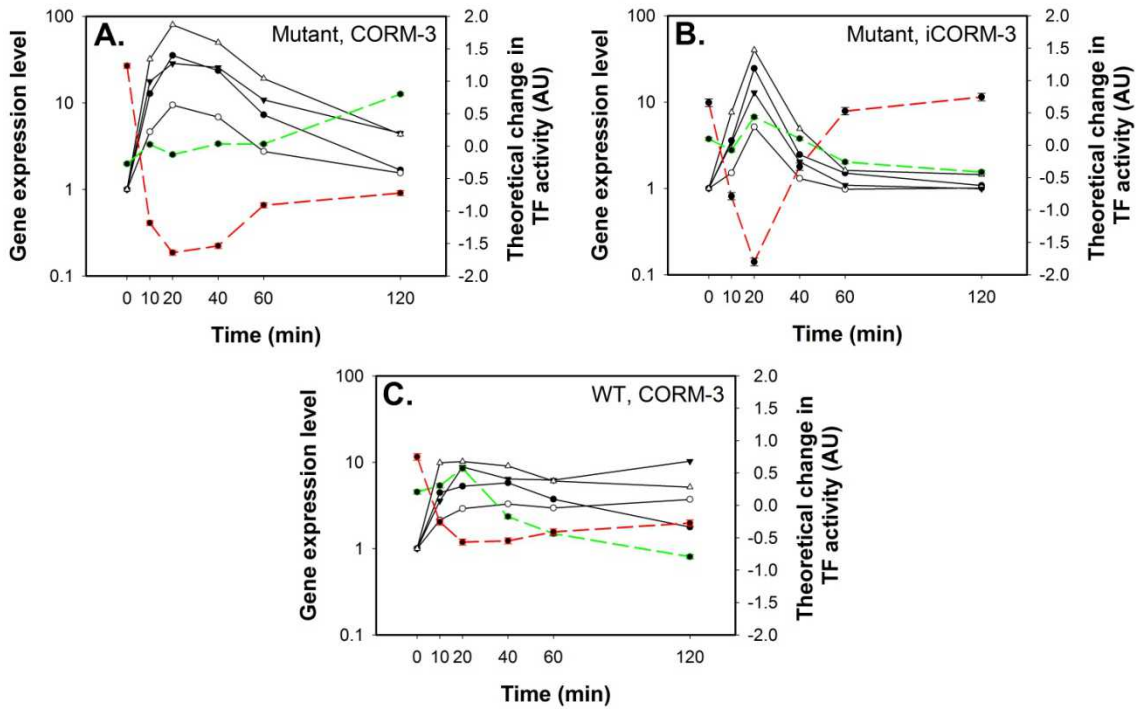

Figure 5.10. Regulation of genes involved in enterobactin synthesis by CRP and Fur. Theoretical transcription factor activity is presented as dashed green lines (positive regulator) or dashed red lines (negative regulator). Expression of *ent* genes (black lines) is shown over a period of 2 h: *entA* (closed circles), *entB* (open circles), *entC* (closed triangles) and *entE* (open triangles). Profiles for CRP (green, closed circles) and Fur (red, closed circles) are shown in parallel. **A.** The haem-deficient mutant of *E. coli* treated with 100 µM CORM-3, **B.** the haem-deficient mutant treated with 100 µM iCORM-3 and **C.** the wild type (WT) treated with 100 µM CORM-3. Analysis of microarray data-sets using TFInfer was performed by Dr. Ronald Begg at The University of Edinburgh.

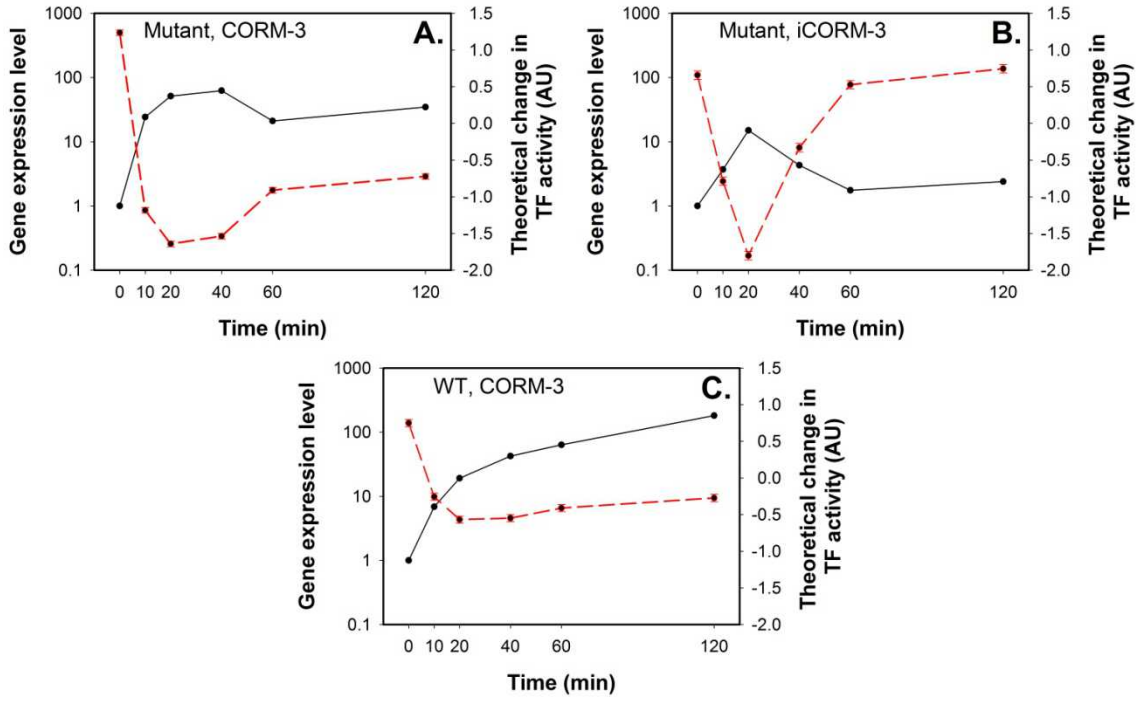

Figure 5.11. Regulation of the highly induced *ryhB* gene, encoding a sRNA that reduces iron consumption, by Fur. Theoretical transcription factor activity is presented as a dashed red line (negative regulator). Expression of *ryhB* (black, closed circles) is shown over a period of 2 h. Activity of Fur (red, closed circles) is shown in parallel. **A.** The haem-deficient mutant of *E. coli* treated with 100 µM CORM-3, **B.** the haem-deficient mutant treated with 100 µM iCORM-3 and **C.** the wild type (WT) treated with 100 µM CORM-3. Analysis of microarray data-sets using TFInfer was performed by Dr. Ronald Begg at The University of Edinburgh.

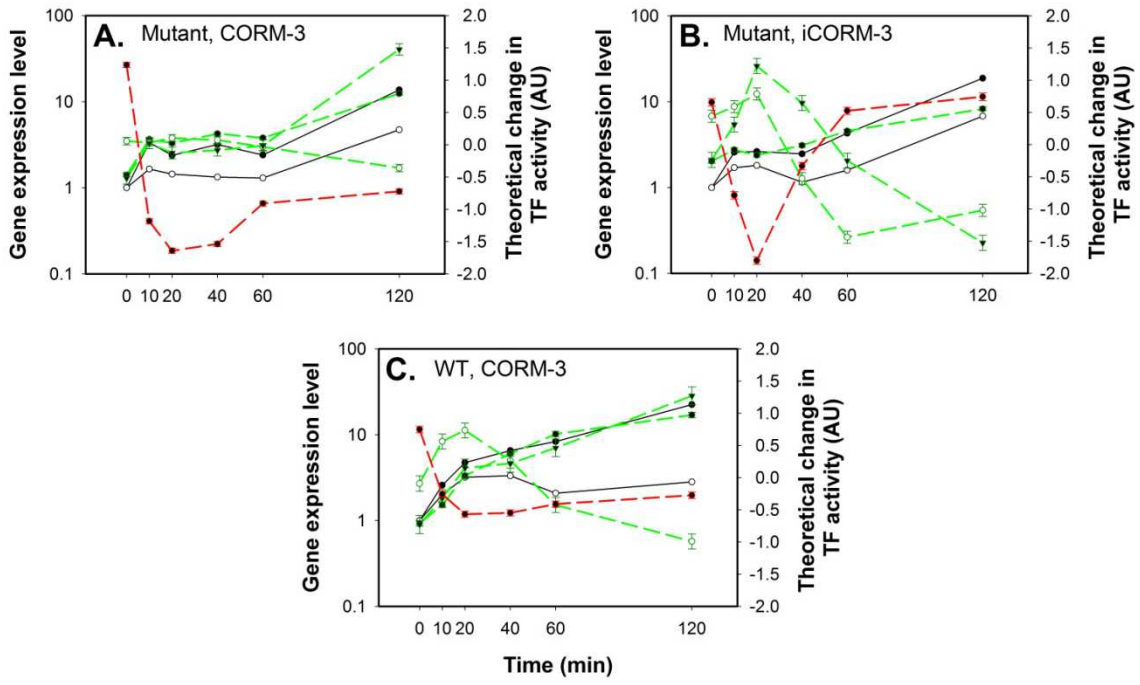

Figure 5.12. Regulation of *suf* genes, which encode an alternative Fe-S cluster assembly system during stress conditions. Theoretical transcription factor activity is presented as dashed green lines (positive regulator) or dashed red lines (negative regulator). Expression of *suf* genes (black lines) is shown over a period of 2 h and *sufB* (open circles) acts as a representative of the gene expression pattern generally observed for the members of this operon. However, in all conditions, the pattern of gene expression for *sufA* (closed circles) differed from that seen for the other genes and is therefore presented for reference. Profiles for IHF (green, closed circles), IscR (green, open circles), OxyR (green, closed triangles) and Fur (red, closed circles) are shown in parallel. **A.** The haem-deficient mutant of *E. coli* treated with 100 µM CORM-3, **B.** the haem-deficient mutant treated with 100 µM iCORM-3 and **C.** the wild type (WT) treated with 100 µM CORM-3. Analysis of microarray data-sets using TFInfer was performed by Dr. Ronald Begg at The University of Edinburgh.

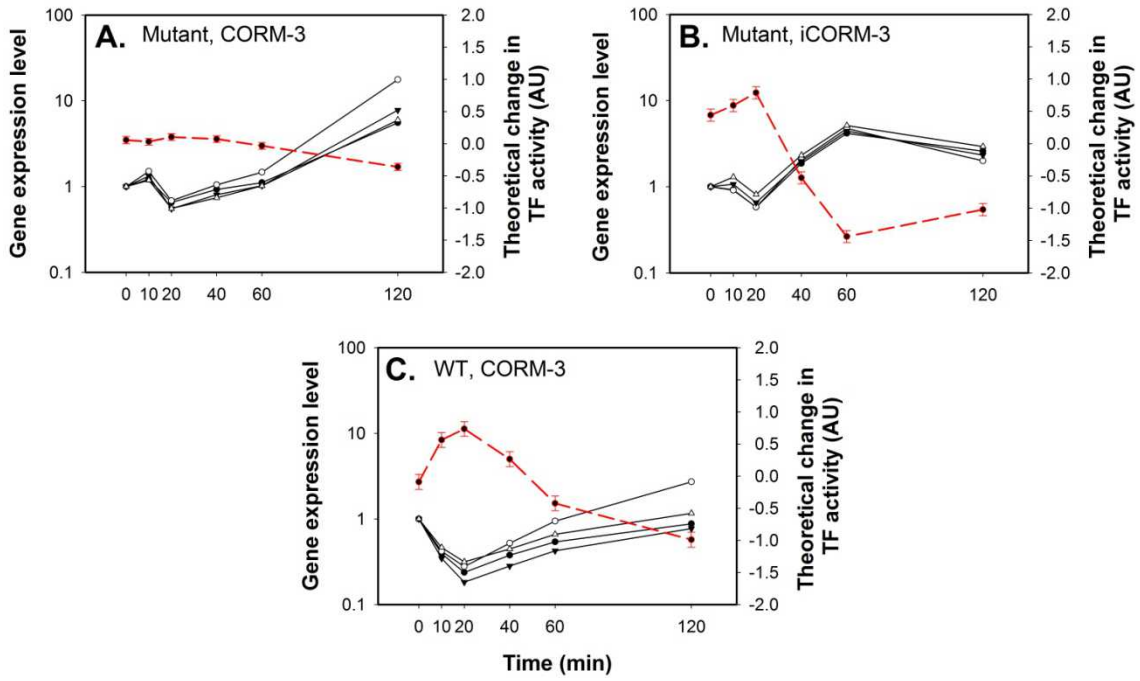

Figure 5.13. Regulation of *isc* genes, which encode the house-keeping Fe-S cluster assembly system. Theoretical transcription factor activity is presented as a dashed red line (negative regulator). Expression of *isc* genes (black lines) is shown over a period of 2 h: *iscA* (closed circles), *iscR* (open circles), *iscS* (closed triangles) and *iscU* (open triangles). Activity of IscR (red, closed circles) is shown in parallel. **A.** The haem-deficient mutant treated with 100 µM CORM-3, **B.** the haem-deficient mutant treated with 100 µM iCORM-3 and **C.** the wild type (WT) treated with 100 µM CORM-3. Analysis of microarray data-sets using TFInfer was performed by Dr. Ronald Begg at The University of Edinburgh.

to the expression of *ytfE*, which encodes an Fe-S cluster repair protein, is also shown for reference in Figure 5.14.

5.2.7.2 Additional regulators of note

BaeR and CpxR control the regulation of some of the most highly up-regulated genes in this study: *spy*, *mdtABC* and *baeS* (Figure 5.15). Under all of the conditions, BaeR and CpxR exhibit similar activity profiles, suggesting they both may be involved in the regulation of each gene (except *cpxP*, which is not regulated by BaeR). However, the extent of change in BaeR is generally greater, which is particularly noticeable in the mutant treated with CORM-3 (Figure 5.15 A). However, it is interesting to note that in the wild type (Figure 5.15 C) the activity of CpxR most resembles the expression of *spy*. CysB controls expression of genes involved in cysteine biosynthesis and sulfate assimilation. Theoretical activity of CysB is presented alongside the expression of a selection of these genes in Figure 5.16. The figure also includes the activity of IHF, which is implicated in the regulation of *cysJIH*. In the mutant, CysB activity appears to follow the gene expression profile more closely, whereas in the wild type the regulation appears to be more complex once again, with both transcription factors having similar profiles.

5.2.8 Analysis of modelling data

In order to better compare the data generated by TFInfer, absolute Pearson correlation coefficients were calculated by Dr Ronald Begg at the School of Informatics, University of Edinburgh (as described in section 2.4.1.10). This enables the similarity between the profiles of transcription factors under each condition to be determined, i.e. 1) the mutant treated with CORM-3 versus iCORM-3 and 2) the wild type versus the mutant after exposure to CORM-3. The correlation between the profiles of transcription factors of interest in this study, i.e. those that are involved in the regulation of genes highlighted in Figures 5.6 - 5.9, are presented in Table 5.1. The only exception is Zur, which regulates the expression of the ZnuABC zinc transporter (Figure 5.8). This regulatory protein was not included in the modelling data.

The concept of correlation is explained graphically in Figure 5.17. For example, BaeR exhibits similar profiles in the mutant treated with CORM-3 versus iCORM-3 (Figure

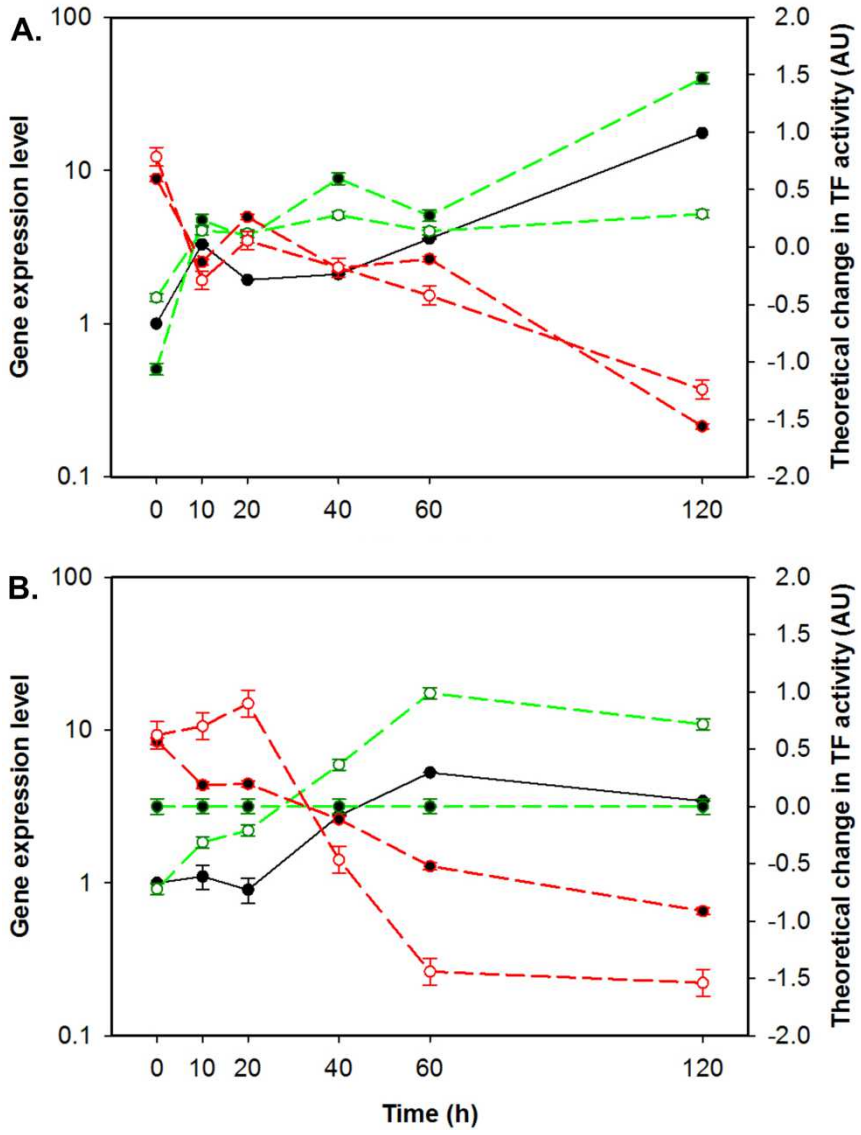

Figure 5.14. Regulation of *ytfE*, involved in Fe-S cluster repair, correlates with the predicted activity of its regulators. Theoretical transcription factor activity is presented as dashed green lines (positive regulator) or dashed red lines (negative regulator). Expression of *ytfE* (black, closed circles) is shown over a period of 2 h. Profiles for NarP (green, closed circles), NarL (green, open circles), FNR (red, closed circles) and NsrR (red, open circles) are shown in parallel. **A.** The haem-deficient mutant of *E. coli* treated with 100 µM CORM-3 and **B.** the haem-deficient mutant treated with 100 µM iCORM-3. Analysis of microarray data-sets using TFInfer was performed by Dr. Ronald Begg at The University of Edinburgh.

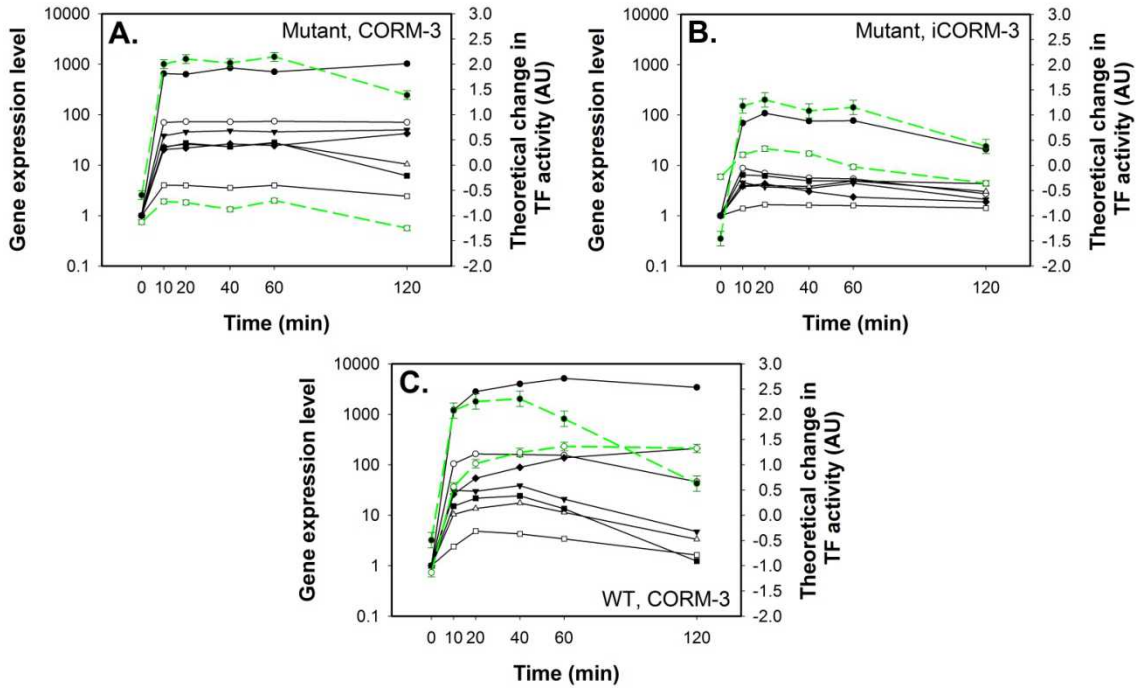

Figure 5.15. Regulation of genes involved in signal transduction by BaeR and CpxR. Theoretical transcription factor activity is presented as dashed green lines (positive regulator). Gene expression levels (black lines) are shown over a period of 2 h: *spy* (closed circles), *mdtA* (open circles), *mdtB* (closed triangles), *mdtC* (open triangles), *baeS* (closed squares), *baeR* (open squares) and *cpxP* (closed diamonds). Profiles for BaeR (green, closed circles) and CpxR (green, open circles) are shown in parallel. BaeR is not involved in the regulation of *cpxP*. **A.** The haem-deficient mutant of *E. coli* treated with 100 µM CORM-3 **B.** the haem-deficient mutant treated with 100 µM iCORM-3 and **C.** the wild type (WT) treated with 100 µM CORM-3. Analysis of microarray data-sets using TFInfer was performed by Dr. Ronald Begg at The University of Edinburgh.

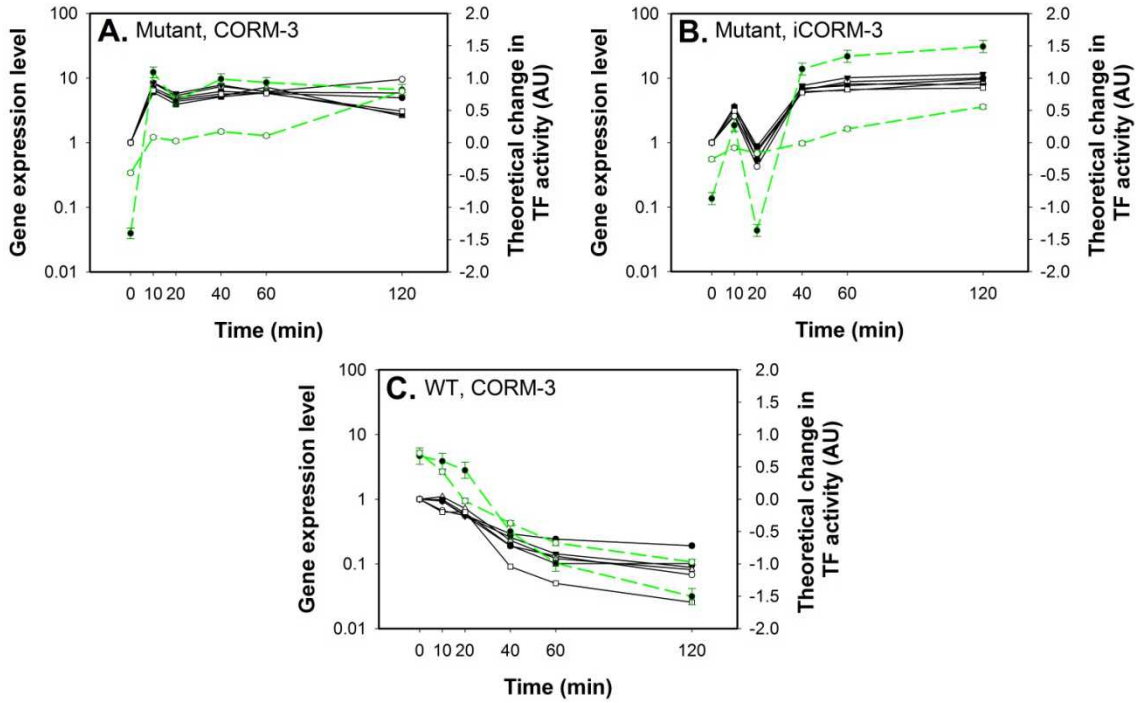

Figure 5.16. Regulation of sulfate assimilation genes by CysB and IHF. Theoretical transcription factor activity is presented as dashed green lines (positive regulator). Gene expression levels (black lines) are shown over a period of 2 h: *cysC* (closed circles), *cysD* (open circles), *cysN* (closed triangles), *cysH* (open triangles), *cysI* (closed squares) and *cysJ* (open squares). Profiles for CysB (green, closed circles) and IHF (green, open circles) are shown in parallel. IHF is not involved in the regulation of *cysC*, *D* and *N*. **A.** The haem-deficient mutant of *E. coli* treated with 100 µM CORM-3, **B.** the haem-deficient mutant treated with 100 µM iCORM-3 and **C.** the wild type (WT) treated with 100 µM CORM-3. Analysis of microarray data-sets using TFInfer was performed by Dr. Ronald Begg at The University of Edinburgh.

Transcription factor	Function	Correlation of transcription factor activity	
		hemA CORM-3 *vs* iCORM-3	Wild type *vs hemA* (CORM-3)
BaeR	Drug resistance, flagellum biosynthesis, chemotaxis, and maltose transport	0.997	0.942
CpxR	Adaptation to stress e.g. envelope and oxidative stress, heat shock, high pH	0.265	0.956
CRP	Catabolite gene activator protein, regulates over 180 genes	0.736	0.793
CysB	Dual regulator of *cys* genes	0.555	0.458
Fis	DNA inversion stimulation factor	0.759	0.842
FNR	Mediates the transition from aerobic to anaerobic growth	0.883	0.777
Fur	Ferric uptake regulator	0.641	0.979
GadX	Controls pH-inducible genes, including the principal acid resistance system	0.871	0.811
H-NS	Response to environmental changes and adaptation to stress	0.771	0.634
IHF	Maintenance of DNA architecture	0.902	0.841
IscR	Fe-S cluster regulator	0.595	0.861
NarL	Nitrate/nitrite response regulator	0.700	2.000
NarP	Nitrate/nitrite response regulator	2.000	2.000
NsrR	Nitrosative stress response	0.734	0.789
OxyR	Oxidative stress regulator	0.723	0.875
SoxS	Superoxide/nitric oxide removal, protection from organic solvents and antibiotics	0.607	0.892

Table 5.1. Correlation of predicted activity of transcription factors of interest under different conditions. Pearson correlation coefficient values are given for transcription factor activity profiles in the haem-deficient mutant of *E. coli* (*hemA*) treated with CORM-3 versus iCORM-3 and the haem-deficient mutant versus wild type after exposure to CORM-3. Values close to 1 indicate transcription factors that exhibit a similar pattern of activity over 2 h post-treatment of haem-deficient or wild type *E. coli* with the compound. A 'place-holder' value of 2 indicates transcription factor activity in only one of the two conditions. Analysis of microarray data-sets using TFInfer was performed by Dr. Ronald Begg at The University of Edinburgh.

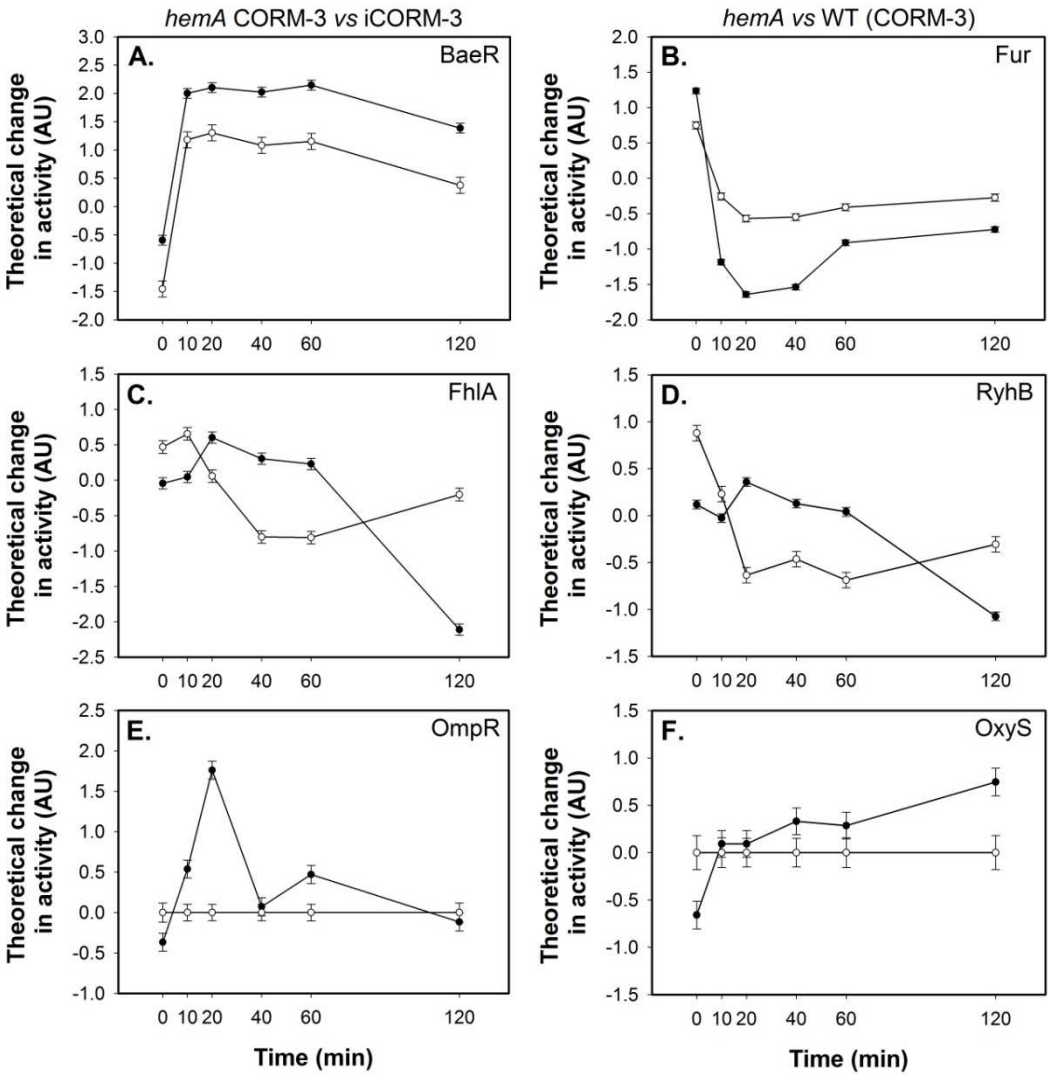

Figure 5.17. Correlation of transcription factor activity represented graphically. Theoretical activity is shown over a period of 2 h post-treatment of the haem-deficient mutant of *E. coli* (*hemA*) with 100 μM CORM-3/iCORM-3 and the wild type (WT) with 100 μM CORM-3. BaeR exhibits similar profiles in the haem-deficient mutant exposed to CORM-3 (closed circles) and iCORM-3 (open circles) (**A**), and the same for Fur in the haem-deficient mutant (closed circles) compared with the wild type (open circles) (**B**). Dissimilar profiles were observed for FhlA in the haem-deficient mutant in response to CORM-3 (closed circles) and iCORM-3 (open circles) (**C**), and RyhB in the haem-deficient mutant (closed circles) compared with the wild type (open circles) (**D**). OmpR has predicted activity in the haem-deficient mutant treated with CORM-3 (closed circles), but not iCORM-3 (open circles) (**E**), and the same for OxyS in the haem-deficient mutant (closed circles) compared with the wild type (open circles) (**F**). Analysis of microarray data-sets using TFInfer was performed by Dr. Ronald Begg at The University of Edinburgh.

5.17 A). The same is true for Fur in the wild type versus the mutant after addition of CORM-3 (Figure 5.17 B). Both transcription factors therefore have Table values close to 1 in these conditions (refer to Table 5.1). Examples of transcription factors that have different patterns of activity are shown in Figure 5.17 C and D. Such regulators will have Table values closer to zero. Finally, activity of some transcription factors was predicted in one condition but not the other. In this case, a place-holder value of 2 is given to highlight under which condition the regulator is active. Examples of such a situation are presented in Figure 5.17 E and F.

Table 5.1 suggests that a greater number of transcription factors of interest have a higher correlation in the wild type versus the mutant as opposed to the mutant treated with CORM-3 versus iCORM-3. These include BaeR, CpxR, GadX, OxyR and SoxS, which are involved in response to stress. Fur and IscR that are involved in iron metabolism and Fe-S cluster assembly also showed a high correlation, in addition to Fis and IHF which are involved in DNA maintenance. In the case of CORM-3 versus iCORM-3, BaeR, GadX and IHF exhibit similar patterns of activity, along with FNR, which mediates the switch from aerobic to anaerobic metabolism (Spiro & Guest 1991). FNR activity is also similar in the mutant and the wild type, but the correlation is not as high as for the previously mentioned regulators. Interestingly, the profiles of CpxR have very low correlation, suggesting its activity may differ between the two conditions.

To further compare the data, the transcription factors that are active in one condition but not the other were compiled (Table 5.2). A number of regulators involved in carbohydrate metabolism and carbon utilisation were active in the mutant treated with iCORM-3. Likewise, Cbl (aliphatic sulfonate utilisation), CytR (ribonucleoside and deoxy- ribonucleoside transport and utilisation), DpiA (catabolism of citrate) and GadW (acid resistance) were active. PaaX, which controls the regulation of genes involved in the catabolism of phenylacetic acid and may also be involved in DNA replication, recombination and repair (Yang *et al.* 2004), was also involved in the response to the inactive compound. Treating the mutant with CORM-3, however, elicited activity of transcription factors involved in amino acid biosynthesis as well as CueR (copper homeostasis), NarP (response to nitrate/nitrite), OmpR (regulation of outer membrane proteins) and PspF (response to extracytoplasmic stress). Activity of HyfR was also seen exclusively after the mutant was exposed to CORM-3. This regulator controls

Landscape Table (Table 5.2), refer to page 9 of supplementary document.

genes involved in formate transport and proton translocation via formate dehydrogenase. The only transcription factor that was involved in carbon utilisation that was not affected after iCORM-3 treatment was IdnR, which regulates L-idonate metabolism.

Interestingly, a number of transcription factors that were active in the wild type, but not the mutant following CORM-3 stress, were the same as those that were exclusively implicated in the mutant's response to iCORM-3 (as described above). Such regulators include AgaR, DgsA and MalT that are involved in carbohydrate metabolism and carbon utilisation, as well as CytR and DpiA. Additional regulators that were active in the wild type were CaiF (carnitine metabolism), DnaA (DNA replication) and EvgA (acid and multidrug resistance). Likewise, a number of transcription factors that were active in the mutant after treatment with CORM-3, but not iCORM-3, were also only identified for the mutant when compared with the wild type after CORM-3 treatment. These include ArgP and TrpR (amino acid biosynthesis), CueR, HyfR, IdnR, NarP and PspF. Other regulators that were active in the mutant but not the wild type have roles in carbohydrate metabolism/carbon utilisation (CdaR, GalR, GlpR), energy metabolism (TorR), pH homeostasis (GadE and NhaR), regulation of the response to oxidative stress (OxyS) and nitrate/nitrite (NarL), as well as utilisation of alternative nitrogen sources (AllR) and the transition metal, molybdenum (ModE).

5.3 Discussion

The transcriptomic analysis presented in this chapter substantiates the activity of CORM-3 against a haem-deficient mutant of *E. coli*. Direct evidence that CO targets moieties other than haem has not been reported, although the idea has been proposed in light of the multifaceted CO-RM-induced alterations in the transcriptome of bacterial cells (Nobre *et al.* 2009). As far as we know, this chapter and the previous provide the first growth, viability and transcriptomic data that confirm CO liberated from CO-RM interacts with non-haem proteins in bacteria. As mentioned previously, transcriptomic analyses are useful for determining global cellular responses and the pathways involved, but they cannot directly identify targets. However, based on the information at hand, hypotheses can be made. It is evident from Figures 5.2 and 5.3 that CORM-3 also exerts multifaceted effects on the mutant, albeit to a lesser extent than seen in the wild type,

with a number of the observed changes being reported previously (see section 5.1). Each of the following sections will incorporate relevant comparisons with these reports and draw parallels, or propose explanations for any conflicting results, where possible.

5.3.1 CORM-3 alters metal biochemistry, in particular iron homeostasis

Among the perturbed genes involved in metal biochemistry was the most dramatically up-regulated gene in this study, *spy*, in addition to the divalent metal binding protein, *yodA* and the zinc(II) ABC transporter, *znuABC* (Figure 5.8). The former was the most highly up-regulated gene in the analysis carried out by Davidge *et al*. (2009b) and was also altered in response to CORM-2 treatment (Nobre *et al.* 2009). Davidge *et al*. (2009b) also reported the up-regulation of *yodA* and *znuA* in addition to other zinc-binding proteins and demonstrated by means of a Φ(*zntA-lacZ*) fusion that CORM-3 elicits intracellular zinc release; thus they concluded that metal homeostasis, in particular intracellular zinc levels, were casualties of CORM-3 addition. However, the genes that were highly represented in this class in the current study were those involved in iron homeostasis (Figure 5.6). Altered transcription levels of some of these genes have been reported previously, namely down-regulation of *ftnA* (Davidge *et al.* 2009b; Nobre *et al.* 2009) and *bfr* and up-regulation of *ftnB* (Nobre *et al.* 2009) under anaerobiosis. Furthermore, a number of transcription factors involved in the regulation of metal genes/response to intracellular metal levels were identified in the current study: Fur, CueR, ModE and of course, CpxR and BaeR, which regulate *spy* in response to zinc and copper (Yamamoto *et al.* 2008) (Tables 5.1 and 5.2). Theoretical activity of CueR and ModE, however, was exclusively implicated in the response of the mutant (Table 5.2).

Some of the transcription factors highlighted in the analysis of the data presented in this chapter, which may be involved in the observed effect of CORM-3 on iron homeostasis, were among those selected for mathematical modelling by Davidge *et al*. (2009b), including CRP, FNR, Fur and IHF (Table 5.1). A hypothesis was proposed by Davidge and co-workers whereby an interaction of CO with the iron centres of FNR and Fur may explain their involvement. In particular the [4Fe-4S] cluster of FNR was considered, which is known to react with NO (Cruz-Ramos *et al.* 2002). Furthermore, NO also interacts with the active form of Fur (FeFur) and inhibits its activity (D'Autreaux *et al.*

2002). As mentioned in Chapter 1 (sections 1.1 and 1.4.1) CO and NO behave similarly in some respects, therefore CO may also target iron centres including Fe-S clusters. Such an interaction has recently been reported in the literature; CORM-2 was shown to lower the activity of the Fe-S-containing enzymes aconitase and glutamate synthase in bacterial cells by approx. 75 and 82 %, respectively (Tavares *et al.* 2011). As discussed in Chapter 4 (section 4.1) and Chapter 1 (section 1.5 and Figure 1.4), CO also interacts with other non-haem iron-containing enzymes, for example CODH and O_2-sensitive hydrogenases, in addition to numerous examples of non-haem iron(II) carbonyls. However, Fur is the chief regulator of intracellular iron levels and acts by repressing genes involved in iron-uptake. In its active form it contains a non-haem ferrous iron site, but when the levels of iron in the cell become too low iron(II) is lost from the protein resulting in de-repression of genes involved in siderophore biosynthesis and iron transport (Lee & Helmann 2007). Additionally, Fur is capable of sensing different divalent metal ions including zinc(II) (Althaus *et al.* 1999). This metalloprotein function may also be a reason for the involvement of Fur in the transcriptomic response to CORM-3.

In light of such examples of CO interactions, it is perhaps not surprising that the expression of genes involved in iron transport and acquisition are affected by CORM-3 (Figure 5.6). However, the situation regarding Fe-S clusters is not so clear (Figure 5.7). Although a gene implicated in the repair of damaged Fe-S clusters (*ytfE*) (Justino *et al.* 2007), and perhaps iron centres in general (Overton *et al.* 2008), is up-regulated in the mutant treated with CORM-3, the Fe-S cluster assembly systems are unaffected for 60 min after CORM-3 exposure (Figure 5.7). The reverse is true for the wild type, with a further observation being the down-regulation of *isc* genes and the up-regulation of *suf* genes. An unexpected finding is the greater effect of iCORM-3 on the transcription of these genes when compared with CORM-3.

One hypothesis is that CORM-3 may induce iron-starvation, particularly in the mutant. In such a situation the assembly of Fe-S clusters would be restricted, or such clusters may be degraded in an attempt to provide free intracellular iron. In this case, repair mechanisms, such as that elicited by YtfE, may be up-regulated to substitute for the inability of the cells to generate new clusters. However, like AOX (Chapter 4, section 4.3) YtfE contains a di-iron centre (Justino *et al.* 2006) and therefore may be targeted by

the compound. If this alternative option to reconstitute the clusters is also blocked by CORM-3 as part of the compound's multifaceted effects, then no repair would take place, thus resulting in the observed continual up-regulation of *ytfE* over, and reaching a maximum at, 120 min (Figure 5.7). The up-regulation of both the *isc* and *suf* systems at this later time-point may serve to jump-start the synthesis of Fe-S clusters. Up-regulation of *isc* and *suf* genes at 120 min coincides with a lesser up-regulation of the majority of genes involved in the response to iron-starvation (compare Figure 5.6 and 5.7). Perhaps up-regulation of these systems may be due to an increase in intracellular iron levels between 60 - 120 min as a result of the acquisition of extracellular iron by siderophores. In the wild type, however, the iron-starvation response is not as pronounced (Figure 5.6). As a result, Fe-S cluster synthesis may still occur, but via the *suf* system, which is the route used during iron-limiting conditions and oxidative stress (Outten *et al.* 2004). The hypothesis fits well with the theoretical activity of IscR (Figure 5.12, section 5.2.7.1) and the more complex regulatory situation in the wild type (Figure 5.12 C). A possible involvement of Fur could further explain up-regulation of the *suf* system as opposed to *isc*.

The only Fe-S cluster assembly gene that was up-regulated in the mutant for the entire 120 min was *sufA* (Figure 5.7). This was unexpected as *sufA* is the first gene in the *sufBCDES* operon and the remaining genes were unaltered for the first 60 min. An explanation for this could be attenuation, as observed for the *trp* operon (Russel 2010), which enables premature termination of transcription allowing for only certain genes to be expressed. However, such regulation of the *suf* operon has not been reported. Furthermore, it could be argued that the up-regulation (maximum of 3.35-fold over the first 60 min) is inconsequential as the cut-off limit for what is considered up- or down-regulated, in this case 2-fold, is arbitrary. If this is a case of attenuation, then expression of the SufA protein may be increased as a means by which iron can be transported to where it is needed in the cell. IscA, the A-type carrier protein of the *isc* system, has been implicated as an iron donor due to its identification as a ferric iron-binding protein with an apparent iron association constant of 3×10^{19} M^{-1} (Ding *et al.* 2005; Ding & Clark 2004).

An additional perplexity was the up-regulation of genes encoding cysteine and sulfate assimilation in the mutant, but their down-regulation in the wild type (Figure 5.9). L-

cysteine is the source of sulfur for the synthesis of Fe-S clusters (Mihara & Esaki 2002); thus sulfur limitation may also explain why the assembly is not up-regulated in the mutant treated with CORM-3. In contrast, the *suf* system is up-regulated in the wild type, so levels of iron and sulfur in the cell may not be as limited as in the mutant. Interestingly, the sulfite reductase (encoded by *cysJI*) has been shown to act as a ferrisiderophore reductase thereby enabling the release of iron from siderophores (Coves *et al.* 1993). Although *cysI* encodes the haemoprotein component, which is not functional in the mutant, the aforementioned role was attributed to the flavin reductase activity of the subunit encoded by *cysJ* (Coves *et al.* 1993).

A possible hypothesis for the above interpretations incorporates the proposal made in section 4.3 that haem may act as a 'CO-sink' in the wild type. In this case, iron-starvation may not be induced to the same degree as in the mutant and thus Fe-S clusters may not damaged to the same extent in an attempt to accumulate free intracellular iron. The cell may therefore be able to down-regulate *cys* genes, thereby forfeiting sulfur availability required for Fe-S cluster assembly in an attempt to prevent the formation of sulfite, an intermediate during cysteine biosynthesis, that promotes the release of CO from CORM-3 (McLean *et al.* 2012). This may also be applied to the situation seen after treatment of the mutant with iCORM-3. The inactive compound releases only residual amounts of CO and so produces a similar response as the wild type, in which haem traps the CO liberated from CORM-3, i.e. in both cases less CO is available to promote iron-starvation. The reason the *isc* system is more affected than the *suf* system after treatment of the mutant with the inactive compound (Figure 5.7) may be due to the lesser effect on iron transport and acquisition (Figure 5.6). For the most part, *cys* genes are up-regulated in the mutant treated with iCORM-3 (Figure 5.9), which could be a result of a limitation of cysteine/sulfur due to binding of sulfite to the CORM-3 backbone. This reaction is considered possible in light of the demonstration of sulfite-stimulated CO release from ruthenium-based carbonyls (McLean *et al.* 2012).

The transcriptomic data presented herein is suggestive of a different situation than demonstrated in a recent report where a group measured increased intracellular iron levels following treatment of *E. coli* with CORM-2 (Tavares *et al.* 2011). Accumulation of iron was attributed to the denaturation of Fe-S clusters caused by CORM-2-induced increases in ROS. The free iron may then go on to further increase radical formation via

the Fenton reaction. Electron paramagnetic resonance (EPR) studies carried out by the same group were suggested to show that CORM-2 promotes generation of $OH^{\bullet}$ radicals in the absence of cells. However, on closer inspection of the EPR spectra, although the signal is clearly that of a free radical, the spacing of the resonance obtained from the spin-trapped species is not consistent with that of an $OH^{\bullet}$ radical (B. E. Mann, personal communication). Additionally, although the generation of hydrogen peroxide has been observed following exposure of intact cell suspensions of *C. jejuni* to CORM-3 (Smith *et al.* 2011), the production of ROS by CORM-3-treated *E. coli* and *P. aeruginosa* has not been detected (Davidge *et al.* 2009b; Desmard *et al.* 2009; Desmard *et al.* 2012). It therefore seems there is no strong precedence to suggest that CORM-3 induces ROS generation (also refer to section 5.3.3).

5.3.2 CORM-3 perturbs the cell envelope

Targeting of the cell membrane by CO-RMs is supported by the number of genes involved in membrane transport that exhibit altered transcription in this study and others (Davidge *et al.* 2009b; Nobre *et al.* 2009). Furthermore, as mentioned in section 3.3, recent data has shown that CORM-3 promotes the transport of potassium and sodium across the membrane, albeit by a currently unidentified mechanism (Wilson *et al.* submitted). The effect of CO/CO-RM on membrane channels in mammalian cells has also been reported, for example inhibition of L-type calcium channels (Scragg *et al.* 2008), voltage-gated potassium channels (Jara-Oseguera *et al.* 2011) and modulation of ATP-gated human P2X receptors (Wilkinson *et al.* 2009; Wilkinson & Kemp 2011).

Mathematical modelling of the current transcriptomic data implicates OmpR, the outer membrane protein regulator, in the response of the mutant and the wild type to CORM-3. In addition, the up-regulation of *spy*, which can occur due to envelope stress (Raffa & Raivio 2002) and *cpxP*, which encodes the inhibitor of the Cpx response that is activated by misfolded envelope proteins (Figure 5.8), suggests the cell envelope in general may be a target. The expression of *spy* is controlled by CpxR and BaeR. CpxR also regulates *cpxP* and BaeR regulates the expression of *mdtABC* (Figures 5.8 and 5.15). This suggests that both of these transcription factors may have roles in the maintenance of envelope protein integrity and general response to envelope stress following exposure of both the mutant and the wild type to CORM-3. Such a role was

also attributed to the Cpx response by Davidge *et al*. (2009b). The effect of iCORM-3 was more modest (Figure 5.8) and an involvement of OmpR in the response was not predicted, suggesting these effects are CO-dependent. The lesser effect of iCORM-3 on the expression of the multidrug efflux system was also surprising, as this may have been a candidate for the means by which the backbone is extruded from the cell.

5.3.3 CORM-3 activity is not mediated by oxidative stress reactions

The Saraiva group clearly demonstrated the induction of oxidative stress responses by CORM-2 via transcriptomic studies under both aerobic and anaerobic conditions (Nobre *et al.* 2009) and via biochemical experiments (Nobre *et al.* 2009; Tavares *et al.* 2011). In addition they concluded that CO-RM-mediated bactericidal activity is largely a result of the generation of ROS (Tavares *et al.* 2011). However, this was not the conclusion of another group that demonstrated CORM-2-induced ROS production in *P. aeruginosa* (Murray *et al.* 2012). This group excluded the possibility of ROS-mediated toxicity as cysteine alleviated the action of CORM-2 without quenching ROS production. Furthermore, Desmard and co-workers showed that CORM-2, CORM-3, CORM-371 (manganese-based) and CORM-A1 (boron-based) did not increase ROS generation in *P. aeruginosa* (Desmard *et al.* 2012), which was consistent with previous data for CORM-3 alone (Desmard *et al.* 2009). Transcriptomic responses of *E. coli* stressed with CORM-3 did not highlight genes in this class either, although the regulatory protein SoxS was implicated in additional preliminary modelling (Davidge *et al.* 2009b).

In agreement with the latter reports, oxidative stress response pathways were barely notable in the current study, which would be expected under anaerobic conditions. Neither *soxS* nor *oxyR*, which were implicated in the response seen by Nobre *et al*. (2009), were altered in the mutant treated with either the active or inactive compound. The same was observed for the wild type exposed to CORM-3. However, the sRNA gene, *oxyS*, was up-regulated in the mutant and particularly the wild type after CORM-3 addition, whereas the effect of iCORM-3 was insignificant (Figure 5.8, section 5.2.4). Even though expression of *soxS* and *oyxR* are not affected here, predicted activities of SoxS and OxyR were identified by the modelling (Table 5.1). An alternative explanation for the theoretical activity of SoxS may include a response to zinc levels (Graham *et al.* 2012), hence its positive regulation of *yodA*. OxyR, on the other hand,

regulates the expression of the sRNA OxyS and is also involved in the up-regulation of the *suf* system for Fe-S cluster assembly under oxidative stress conditions, alongside IHF (Lee *et al.* 2004).

5.3.4 Enhanced expression of the gene encoding the NO-detoxification protein, Hmp, in the haem-deficient mutant

Interestingly, *hmp* is highly up-regulated in the mutant treated with CORM-3 (maximum of 94.2-fold, Figure 5.8), but is unaltered in the wild type and was up-regulated to a maximum of 23.9-fold in response to iCORM-3. This suggests that the effect may be abrogated in the presence of haem proteins and may be CO-dependent. Previous studies have shown that CO binds to the haem moiety of Hmp (Ioannidis *et al.* 1992), in which case it may act as a 'CO sink'. However, CO does not usually alter *hmp* expression (Stevanin *et al.* 2007), which is consistent with what was observed for the wild type in the current work and other studies (Davidge *et al.* 2009b; Nobre *et al.* 2009). An alternative explanation for the up-regulation of *hmp* in the mutant may relate to the release of iron from siderophores. Ferrisiderophore reductase activity of Hmp has been reported previously (Andrews *et al.* 1992; Eschenbrenner *et al.* 1994; Poole *et al.* 1997) and fits with the iron-starvation response observed in this study. The majority of genes involved in siderophore utilisation exhibit greater increases in fold-changes in the mutant treated with CORM-3 than the wild type, which may explain the differential regulation of *hmp* in the two strains. However, although Hmp can reduce iron(III) and cytochrome *c in vitro*, these reactions are not thought to to have any physiological significance.

An additional possibility is the endogenous production of NO by *E. coli*, a situation that is supported by recent data (Jia & Poole, unpublished) that show accumulation of high levels of the gas (c. 10 μM) in anaerobic, chemostat-grown cultures supplemented with glucose, in the absence of nitrate and nitrite. However, the mechanism behind this finding has not been elucidated. Neverthelss, this may explain why NsrR, the primary regulator of *hmp* transcription, is predicted to be active under all conditions tested in the present work (Table 5.1). What cannot be readily explained is why the activity of NsrR may be enhanced by CORM-3 or iCORM-3. There is no evidence in the literature that NsrR is affected by CO; on the other hand, another ligand-sensing protein in *E. coli*,

EcDos (section 1.5, Figure 1.4), is known to bind NO and CO (Delgado-Nixon *et al.* 2000) and is inhibited by both gases (Sasakura *et al.* 2002). It is also interesting to note that nitrate and nitrite increase expression of *hmp* (Poole *et al.* 1996) and regulators involved in the response to nitrate/nitrite (NarP and NarL) were implicated in the response of the mutant to CORM-3 (Table 5.2). An explanation for why the *hmp* gene is up-regulated in the mutant, but not the wild type, may be due to the inability of the former to synthesise haem and subsequently produce active Hmp. The wild type, however, can synthesise haem and thus make functional Hmp, therefore NO detoxification would occur as normal.

5.3.5 Mathematical modelling of the transcriptomic data highlighted a number of other transcription factors with predicted activity

Some of the regulatory proteins presented in Table 5.1 were also selected in the modelling by Davidge *et al*. (2009b) (see section 5.1). However, CRP, Fis and FNR were not predicted to be active under anaerobic conditions in the study by Davidge and co-workers. This inconsistency may not be surprising when taking into account the size of the data-sets obtained in the current study, which were collected from a time-series after compound addition, as opposed to a single time-point. CRP, Fis, IHF and also H-NS (Table 5.1), are implicated in the regulation of a number of gene classes. This is demonstrated herein: CRP and H-NS have been assigned as regulatory proteins for genes involved in iron acquisition (Figure 5.6), response to stress (Figure 5.8) and in the case of H-NS, genes involved in cysteine biosynthesis and sulfate assimilation (Figure 5.9), Fis is involved in the regulation of *hns* (Figure 5.8) and IHF regulates the *suf* system (Figure 5.7), expression of the heat shock proteins *ibpA* and *ibpB* (Figure 5.8) and is also involved in regulation of *cysH* (PAPS reductase) and *cysJI* (sulfite reductase) (Figure 5.9). These proteins therefore seem to be involved in a complex network of responses to CORM-3.

Interestingly, a number of transcription factors with predicted activity in the wild type, but not the mutant, are the same as those that were exclusively implicated in the mutant's response to iCORM-3 (Table 5.2). Such regulators are involved in carbon utilisation (AgaR, DpiA and MalT), carbohydrate metabolism (DgsA) and utilisation of ribonucleosides and deoxyribonucleosides (CytR). Due to the hypothesis that haem may

act as a 'sink' for CO liberated from CORM-3, a role of the compound's backbone in these processes may be an explanation for the observed similarity. If CO is trapped by haem in the wild type then an equilibrium between CO release and re-binding from/to the compound will be reduced, in effect mimicking the situation when iCORM-3 is present in the cell. This may be supported by recent data showing that a higher concentration of MbCO is formed when haem-deficient mutant cells are incubated with CORM-3 in the presence of ferrous myoglobin, in comparison with the wild type (McLean & Poole, unpublished). As might be expected, CO may not bind to other targets with as high affinity as haem, thus displacement of CO from the compound may be transient, whereby it can reattach to the backbone, or diffuse across the membrane, after interaction with intracellular proteins. Other transcription factors were predicted to be active only in the mutant treated with CORM-3, suggesting that some aspects of amino acid metabolism, metal homeostasis, responses to nitrogen levels and nitrate/nitrite may be more so, or solely, affected by CO in the absence of haem targets.

5.3.6 Conclusions

There are a number of similarities between the transcriptomic response to CORM-2 (Nobre *et al*. 2009) and CORM-3 (this work). Such parallels may be attributed to the ruthenium centre of these compounds and perhaps also that CORM-2 is the precursor of CORM-3 (Johnson *et al.* 2007). However, as to be expected, there are differences, for example the extent of the oxidative stress response, which may arise due to the differing stability of the compounds in solution and the ability of CORM-2 to generate radicals even in the absence of cells (Tavares *et al.* 2011). The parallels between the three studies discussed in this chapter (Davidge *et al*. 2009b; Nobre *et al*. 2009; this work) unequivocally identify certain responses to be due to CO-RM administration, including cellular metabolic adaptation, metal biochemistry, membrane transport, envelope integrity and stress response.

The most prominent finding presented herein is the effect of CORM-3 on metal homeostasis, with a particular emphasis on a response to iron-starvation in the mutant treated with the active compound. Moreover, this response appears to be CO-dependent as iCORM-3 did not elicit such a pronounced effect. Interestingly, neither did the wild type. This supports the hypothesis put forth in Chapter 4 (section 4.3) that haem

proteins may act as a 'CO-sink', thus reducing the tendency of CO to bind additional intracellular targets that may lead to increased CO-induced lethality. Other aspects of the data also indicate that the wild type and the mutant respond differently to CORM-3 exposure, which may be due to the prioritising of different mechanisms in order to better maintain their survival in the presence or absence of haem proteins.

Additionally, at least in part, iCORM-3 elicits a transcriptomic response in the mutant. Exactly what remains of the compound once the labile CO has dissociated, and the species that may then be formed in the cell, are unknown. Nor is it known whether either, or perhaps both, of the remaining carbonyls can be liberated in the presence of suitable ligands. Residual CO release may be responsible for some of the effects elicited by iCORM-3, as alterations in the transcriptome are generally not to the same degree as seen after CORM-3 addition. Nevertheless, an effect of the backbone cannot be ruled out. That said, the data presented in Chapter 4 demonstrate that even though these transcriptional changes are observed, iCORM-3 is not bactericidal against the haem-deficient mutant or the wild type.

To date, there are a number of questions that remain unanswered, in particular the effect of CO-RMs on genes such as *spy*, which was enormously up-regulated in this study (section 5.2.4) and highly up-regulated in others (Davidge *et al.* 2009b; Nobre *et al.* 2009). The biological/biochemical effects of CO-RMs on bacteria in light of the data from transcriptomic analyses have barely been investigated. However, the current study suggests that the first line of enquiry should be the determination of the specific effects of CO liberated from CO-RM.

Chapter 6. Effects of CORM-3 on *Neisseria meningitidis* and Macrophage Functionality

6.1 Introduction

The aim of the work in this chapter was to initially test the anti-bacterial effects of CO released from CORM-3 on meningococcus and then to elucidate its influence, if any, on the activity of the innate immune response *in vitro*. As introduced in section 1.5.3, current research on the anti-bacterial capacity of CO released from CO-RMs has mainly focused on the model laboratory organism, *E. coli* (Davidge *et al.* 2009b; Nobre *et al.* 2009; Nobre *et al.* 2007). The effect of such compounds on the growth and viability of pathogenic bacteria has been limited to mainly *P. aeruginosa* (Desmard *et al.* 2009; Desmard *et al.* 2012; Murray *et al.* 2012), with a small study on *S. aureus* (Nobre *et al.* 2007) and a more recent report on *C. jejuni* (Smith *et al.* 2011). Although the bacterial species tested to date exhibit differential sensitivity to CO-RMs, the studies unequivocally demonstrate the potent bactericidal effect of these novel CO donors and highlight their potential use as anti-bacterials in the future. However, for such a goal to be realised, it is important to test the effects of these compounds on the growth and viability of a broader range of bacteria in order to determine whether they have a more global effect. This may be possible if CO has multiple intracellular targets as suggested by analysis of changes in the *E. coli* transcriptome in response to CO-RM (Davidge *et al*. 2009b; Nobre *et al*. 2009; Chapter 5 of this work).

Neisseria meningitidis is a medically relevant pathogen of global concern that is ideal for studying the anti-bacterial effects of CO and is also a model organism for investigating host-pathogen interactions. It is a Gram-negative, β-Proteobacterium (Tettelin *et al.* 2000) that is the main cause of meningitis and septicaemia, particularly in infants and adolescents. It is a commensal in the human nasopharynx where the initial interaction between host and bacterium is established by aid of bacterial pili and adhesins. However, intimate contact between *N. meningitidis* and the epithelial cells of the nasopharynx is prevented by the bacterial capsule, which enables transmission from host-to-host during close contact via airborne salivary droplets (Taha *et al.* 2002). The pathogen requires the host for survival and therefore resultant harmful infection is likely to be an accident in its life-cycle (Tinsley & Nassif, 2001). The interaction usually stops

at the carriage stage; however, invasive infection may occur as a result of the host's susceptibility to the particular strains involved, the environment, and/or the individual's immune status. Infection occurs when bacteria enter the bloodstream, resulting in meningococcemia, and/or crossing the blood-brain barrier and accessing the cerebrospinal fluid leading to meningitis. The onset of infection can be extremely rapid and death can occur within 4 h. Successful treatment with antibiotics, particularly benzylpenicillin (Wilks & Lever 1996), is possible but the drug must be administered quickly (Taha *et al*., 2002). Five pathogenic serogroups have been determined by capsular polysaccharide typing; A, B, C, Y and W135 (Gotschlich *et al.* 1969a; Gotschlich *et al.* 1969b). *N. meningitidis* MC58 (serogroup B) was used for the work detailed in this chapter. Strains in this group are a major cause of meningococcal disease in developed countries, with no effective vaccine currently available.

In addition to investigating anti-bacterial activity, it is vital to establish the effect of CO-RMs on macrophage functionality during insult. As mentioned in Chapter 1, anti-inflammatory activity of CO is well documented, but studies on the subsequent effects on clearance of bacterial infections are sparse (Chin & Otterbein 2009; Chung *et al.* 2009; Sun & Chen 2009) and the current literature gives quite conflicting stories. Exposure to CO gas (250 ppm) has been shown to augment phagocytosis of *E. coli* by RAW264.7 murine macrophages *in vitro* via p38-mediated surface expression of toll-like receptor 4 (TLR-4), which binds Gram-negative bacteria via LPS. This was confirmed *in vivo* by enhanced uptake of *E. coli* by alveolar macrophages isolated from infected wild type C57BL/6 mice previously exposed to CO. It was suggested that CO may enable rapid presentation of antigens by macrophages via the TLR-4-p38 pathway of the innate immune response, which in turn could elicit the adaptive immune response in T cells to localise and neutralise the infection (Otterbein *et al.* 2005). CO derived from over-expression of HO-1, or by administration of CORM-2, also increased phagocytosis of *Enterococcus faecalis* by peritoneal polymorphonuclear neutrophils in wild type C57BL/6 mice. In conjunction with an improved phagocytic response elicited by CO, increased nucleotide-binding oligomerisation domain 2 (NOD2) protein expression appeared to be critical for the improved outcome of the animals. TLR-4 expression was not affected in response to *E. faecalis*, but NOD2 is able to recognise peptidoglycan from Gram-positive bacteria and plays a significant role in the intestinal immune response; therefore it is not unexpected that NOD2 expression is increased in

this case. Additionally, CORM-2 resulted in a decrease in circulating bacterial counts in wild type C57BL/6 mice and rescued HO-$1^{-/-}$ BALB/c mice from the exaggerated mortality of polymicrobial sepsis. Improved survival of wild type BALB/c mice was also observed when CORM-2 was administered 6 h after the onset of sepsis. However, in contrast to the results reported by Otterbein *et al*. (2005), over-expression of HO-1 in mice infected with *E. coli* did not result in increased phagocytosis. Inflammatory cells in the peritoneum appeared to exhibit a more selective response for Gram-positive *E. faecalis*. Furthermore, CO appeared to be capable of controlling the bacterial infection without producing an immunosuppressive environment, as the increase in HO-1 expression did not suppress circulating inflammatory cells or their accumulation at the site of injury (Chung *et al.* 2008). In contradiction with the ability of CO to increase phagocytosis, CORM-3 was seen to be effective in significantly reducing bacterial counts in the spleen of immunosuppressed BALB/c mice suffering from *P. aeruginosa* PAO1-induced bacteremia. As observed for immunocompetent BALB/c mice, the bacterial counts were reduced by the compound 1 h and 3 h after infection. Prolonged survival, as well as the bactericidal effect, was also seen in C57BL/6 mice that have a different immunological profile. These data suggest that *in vivo* bactericidal activity of CORM-3 occurs in the absence of an enhanced innate immune response elicited by the CO donor (Desmard *et al*. 2009).

CO administered by CO-RMs, or by super-induction of HO-1 in LPS-stimulated RAW264.7 murine macrophages, reduced NO production (Sawle *et al.* 2005; Srisook & Cha 2005; Srisook *et al.* 2006; Tsoyi *et al.* 2009). The mechanisms behind this activity are yet to be elucidated. Srisook & Cha (2005) suggest that super-induction of HO-1 in macrophages, as a result of redox stress or depletion of glutathione in association with endogenously generated NO, can reduce iNOS expression by mopping up free haem and subsequently preventing protein synthesis. This conclusion was suggested previously for HO-1-mediated inhibition of iNOS in LPS-activated BALB/c bone-marrow-derived macrophages (Turcanu *et al.* 1998). Additionally, existing iNOS protein may be targeted by CO, a by-product of HO-1 activity, which could bind to the haem moiety and inactivate NO production by inhibiting electron transfer (White & Marletta 1992). Administration of CO gas (250 ppm) mimicked the effect of increasing HO-1 expression. Decreased nitrite/nitrate levels were detected *in vitro* in rat lung macrophages and *in vivo* in the serum of LPS-treated rats, which correlated with a

decrease in iNOS expression in the lung and alveolar macrophages (Sarady *et al.* 2004). Likewise, CORM-2 at 10, 50 and 100 μM reduced expression of iNOS and subsequently decreased NO production *in vitro* and *in vivo*. The inhibitory activity of the compound was reported to be tightly associated with up-regulated expression of PPAR-γ, which plays a critical role in regulating the expression of genes involved in inflammatory signalling and can dampen the macrophage inflammatory response (Tsoyi *et al.* 2009).

CORM-2 (50 μM) was also seen to block the initial oxidative burst in macrophages, which acts as one of the first lines of defence against invading pathogens, by inhibiting NADPH oxidase activity. It was hypothesised that CO liberated from CORM-2 may target the haem centre of the oxidase and subsequently suppress the overproduction of superoxide. The redox-sensitive transcription factor, NF-kB, promotes upregulation of iNOS expression, therefore it was suggested that CORM-2 may indirectly inhibit expression of iNOS and NO production by decreasing superoxide generation, and subsequent ROS accumulation in macrophages (Srisook *et al.* 2006). However, in disagreement with the previously discussed reports, CORM-3, at equimolar concentrations to CORM-2, was without effect on basal or LPS-stimulated expression of iNOS (Sawle *et al.* 2005). This difference was suggested to be due to different periods of incubation before measurement of iNOS protein levels (Tsoyi *et al.* 2009).

Increased bacterial invagination by CO-treated macrophages suggests that their efficiency is improved. However, CO-elicited inhibition of iNOS expression/activity and subsequent decreased NO production, in parallel with a reduction in levels of ROS, suggests that once bacteria are internalised the bactericidal activity of the macrophages may be significantly impaired. Interestingly, infection with *E. coli* K1, a leading cause of neonatal meningitis in humans, resulted in expression of iNOS in the brains of newborn mice. Resistance to infection was noted in $iNOS^{-/-}$ mice and in wild type mice pre-treated with an iNOS specific inhibitor, aminoguanidine. Enhanced uptake of bacteria was seen by peritoneal macrophages and polymorphonuclear leukocytes isolated from these mice. Furthermore, bacterial counts in the blood were decreased, with more than 50 % survival of bacteria in wild type animals, whereas only 11 % and 14 % survived in $iNOS^{-/-}$ or aminoguanidine pre-treated mice, respectively, after a 60 min incubation. This suggests that NO plays a role in *E. coli* K1 infection (Mittal *et al.*

2010) and although CO is not used in this case, inhibition of iNOS results in increased phagocytosis and improved bacterial clearance; therefore application of CO may be beneficial. It also raises the question as to whether the ability of CO to increase phagocytosis may be due to its inhibition of iNOS/NO production.

Research on the effect of CO on the innate immune response is clearly inconclusive. Before CO can be considered as an anti-bacterial agent, it is vital to clarify the effects of this molecule on the ability of macrophages to eradicate infection. Although the previously discussed work highlights a beneficial aspect of CO in terms of reducing inflammation and increasing phagocytosis, it fails to directly elucidate whether the bactericidal activity of macrophages is affected. The ultimate aim of the work in this chapter is to establish whether CORM-3 affects the ability of human macrophages isolated from donated whole blood to phagocytose and, most importantly, kill *N. meningitidis*.

6.2 Results

6.2.1 *Neisseria meningitidis* grows sufficiently in defined medium

Rich broths significantly deplete the concentration of available CO liberated from CO-RMs; therefore it is necessary to use a defined medium to grow bacteria of interest (Davidge, personal communication). Baart *et al.* (2007) described a defined medium (section 2.1.2.9) in which *Neisseria* species were reported to grow sufficiently. Bacteria were initially grown in 10 ml MHB in 25 ml Universals followed by incubation for 3 h in a humidified atmosphere (37 °C and 5 % CO_2) to achieve cells in mid-log phase of growth. A 5 % inoculum was added to 10 ml defined medium and incubated overnight. An OD_{600} of c. 1.2 was recorded. The method was optimised to prevent carry-over of MHB, which may aid growth, by inoculating defined medium directly with 8 - 10 colonies of *N. meningitidis* grown on a CBA plate overnight. Good growth was observed after c. 7 h in defined medium (OD_{600} of 0.685) in comparison with bacteria grown in parallel in MHB (OD_{600} of 0.873). Growth of *N. meningitidis* was confirmed using a gram stain test. In all of the viability studies detailed in subsequent sections, no viable colonies were seen on plates prepared from CORM-3-treated or control culture samples taken at 24 h and viability of control cultures was maintained at a steady level

over the course of the experiments. This is similar to what is seen for *C. jejuni*, for which a rapid decline in viability is observed upon entry into stationary phase (Jackson *et al.* 2007; Kelly *et al.* 2001).

6.2.2 *Neisseria meningitidis* defined medium and RPMI-1640 do not affect CO release from CORM-3

It is good practice to assess the release of CO to ferrous myoglobin in each medium used in CO-RM experiments. The two main media are *N. meningitidis* defined medium, which will be used to determine the effects of CORM-3 on the growth and viability of bacteria, and RPMI, which will be used in macrophage experiments. CO plus reduced *minus* reduced spectra of 10 μM myoglobin solubilised in defined medium and RPMI treated with 2 - 20 μM CORM-3 were compared with equivalent spectra recorded for myoglobin solubilised in 0.1 M KPi buffer (pH 7). At physiological pH this buffer does not interfere with the formation of MbCO and thus is a suitable control for measuring the effects of media (Mann, Poole & Davidge, personal communication). Typical CO reduced *minus* reduced spectra are shown in Figure 6.1 A. The media were deemed suitable for testing the effect of CORM-3 on *N. meningitidis* and macrophages as the degree and rates of MbCO formation were similar to that seen in buffer (Figure 6.1 B).

6.2.3 CORM-3 is bactericidal against microaerobic *Neisseria meningitidis* cultures

CORM-3 at 75 μM resulted in growth inhibition after a maximum of 1 h (Figure 6.2 A), with an initial drop in viable counts seen within 30 min and complete loss of viability seen 1.5 h after addition (Figure 6.2 B). At 50 μM CORM-3 growth was inhibited and an initial 1-log reduction in viability were seen after a maximum of 1.5 h and 2.5 h, respectively, with loss in viability extending to a 2.5-log drop by the end of the day (maximum of 3.5 h after addition of compound, Figure 6.2). Variable rates of growth inhibition and effect on viability were elicited by low concentrations of CORM-3 (25 μM); therefore firm conclusions cannot be drawn from this data-set. Bacterial growth and viability followed the same pattern as the control in one experiment (Figure 6.2). While growth followed a likewise pattern initially in the second experiment, the OD_{600} at 8 h was 0.352 lower than the control, in comparison with 0.106 as shown in Figure 6.2 A, and a 1-log reduction in viability was noted. Although the exact extent of growth

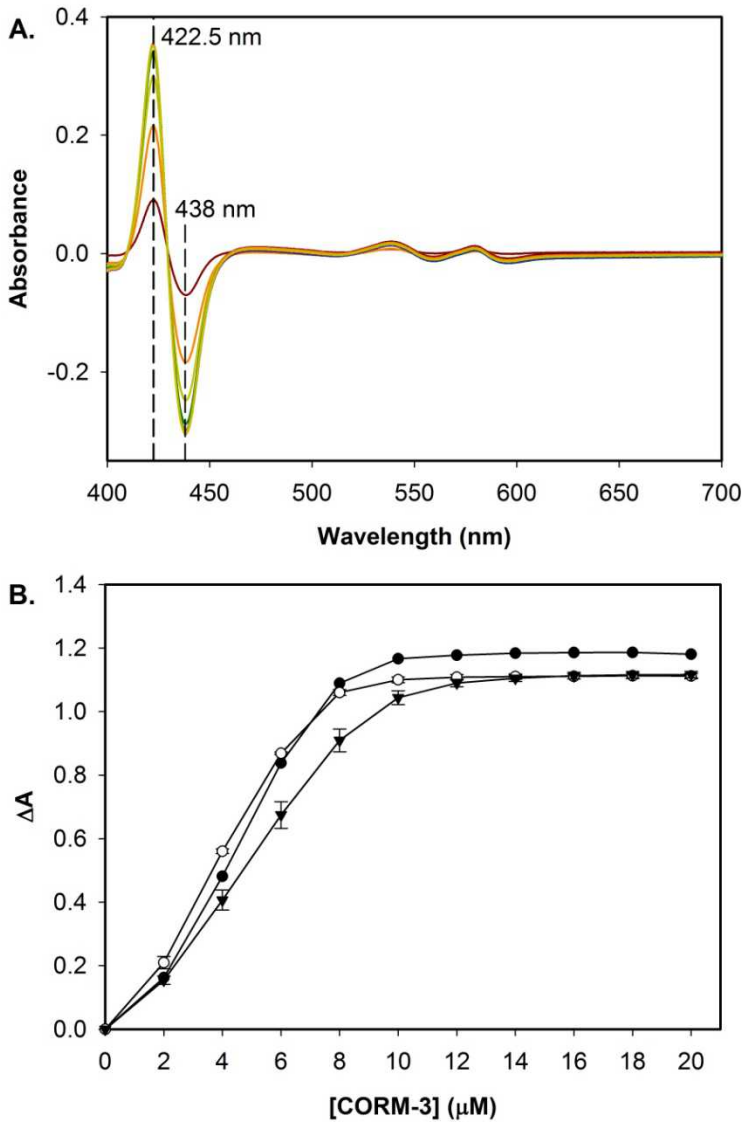

Figure 6.1. CO is released from CORM-3 to ferrous myoglobin in *Neisseria meningitidis* defined medium and RPMI-1640 compared with buffer. Fresh myoglobin was made up in the appropriate solution for each assay. CORM-3 (2 - 20 μM) was titrated into a 10 μM solution of ferrous myoglobin in 2 μM increments. **A.** CO reduced *minus* reduced spectra for CO release from CORM-3 to ferrous myoglobin in 0.1 M KPi (pH 7), recorded using a dual wavelength spectrophotometer. The average ΔA was calculated from such spectra recorded in duplicate for buffer and triplicate for media. **B.** CO release from CORM-3 in RPMI (closed triangles, ΔA = 1.12), defined medium (open circles, ΔA = 1.11) and 0.1 M KPi buffer (pH 7) (closed circles, ΔA = 1.19). The extinction coefficient for MbCO versus deoxymyoglobin is 177 mM^{-1} cm^{-1} (Wood 1984); therefore the ΔA of 10 μM MbCO is 1.77. Data for media were plotted as means ± SEM.

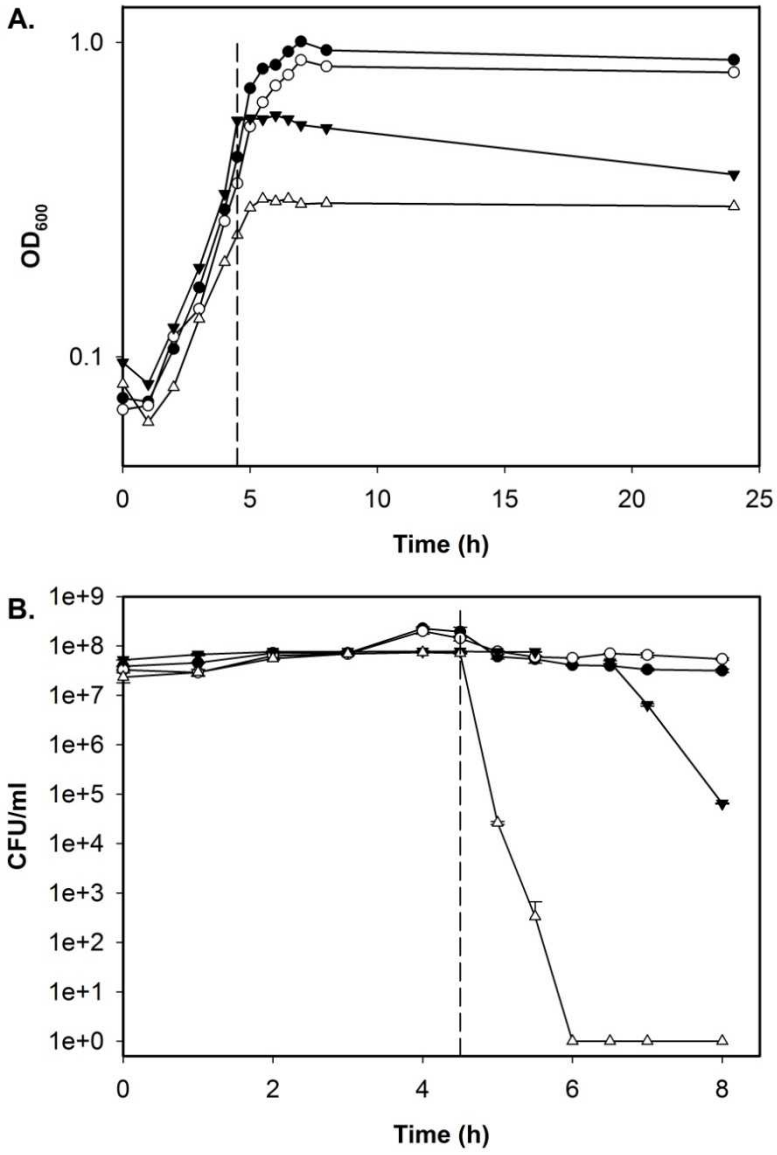

Figure 6.2. Micromolar concentrations of CORM-3 are bactericidal against *Neisseria meningitidis* in a concentration-dependent manner. Cell density was measured at 600 nm, using 1:1 dilutions of culture samples, every 60 min until CORM-3 addition and then every 30 min for 120 min. Sixty minute time-points were resumed until growth had commenced for 8 h. A 24 h reading was taken to complete the experiment. CORM-3 was added at an OD_{600} of c. 0.3 (dashed line). Cell viabilities were measured at time-points equal to those of cell density measurements. Effect of 25 μM (open circles), 50 μM (closed triangles) and 75 μM (open triangles) CORM-3 compared with control (nothing added, closed circles) on **A.** growth and **B.** viability. Data are representative of 2 biological replicates. Viability data are plotted as means ± SEM from 3 individual spots.

inhibition and decrease in viability were variable between biological experiments, the pattern was the same, with the CO donor appearing to elicit a dose-dependent effect; inhibition of bacterial growth and loss of viability were augmented as the concentration of CORM-3 was increased.

6.2.4 Control compounds are ineffective against microaerobically grown *Neisseria meningitidis*

To determine whether CO is the effecter molecule, sub-optimal (25 μM) and optimal (75 μM) concentrations of CORM-3 were compared with that of equimolar concentrations of $RuCl_2(DMSO)_4$ (Figure 6.3). $RuCl_2(DMSO)_4$ was not effective at either concentration and CORM-3 was ineffective at a concentration of 25 μM. Consistent with the results in Figure 6.2, 75 μM CORM-3 completely inhibited growth at a maximum of 1 h after addition. Additionally, the effect of miCORM-3 was tested, but due to the generation of a low stock concentration, aliquots of CORM-3, miCORM-3 and the relevant controls (dH_2O and KPi, respectively) were added to the defined medium in equal volumes prior to inoculation (section 2.1.5.4). Cultures treated with 30 and 50 μM miCORM-3 followed the same pattern of growth and viability as control-treated cultures (Figure 6.4). CORM-3 at 30 and 50 μM elicited a dose-dependent and sustained decreased rate of meningococcal growth (Figure 6.4 A). Reduction in viability was observed after 1 h of growth in the presence of the compound, with subsequent increasing rates of decline. Complete loss of viability was noted 4 h after addition of 50 μM CORM-3 and 5 h following treatment with 30 μM CORM-3 (Figure 6.4 B).

6.2.5 CO gas has no effect on the growth and viability of microaerobic cultures of *Neisseria meningitidis*

The concentration of CO in CO-saturated 50 mM Tris-base buffer pH 7.5 was found to be c. 1.15 mM; determined by assaying CO binding to an excess of ferrous myoglobin using a dual wavelength spectrophotometer. This is in-line with published values for the concentration of CO in solution at room temperature (Cargill 1990), and was the value used when calculating the volumes of CO saturated solution to be used in growth and viability assays. Cultures treated with CO gas at concentrations equimolar with that of an effective CORM-3 concentration (75 μM), and higher (150 μM), followed the same

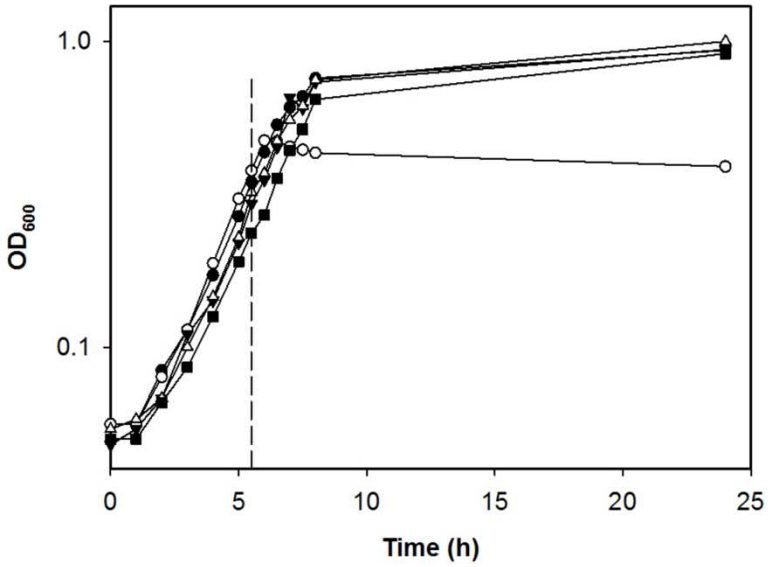

Figure 6.3. $RuCl_2(DMSO)_4$ does not affect the growth of *Neisseria meningitidis*. CORM-3 at 25 μM (closed circles) and 75 μM (open circles) was compared with 25 μM (closed triangles) and 75 μM (open triangles) $RuCl_2(DMSO)_4$ and control (nothing added, closed squares). Cultures were stressed at an OD_{600} of c. 0.3 (dashed line). Cell densities were measured at 600 nm, using 1:1 dilutions of culture samples, every 60 min until CORM-3 addition and then every 30 min for 150 min. A 24 h reading was taken to complete the experiment. Data represent the pattern seen in 2 biological replicates.

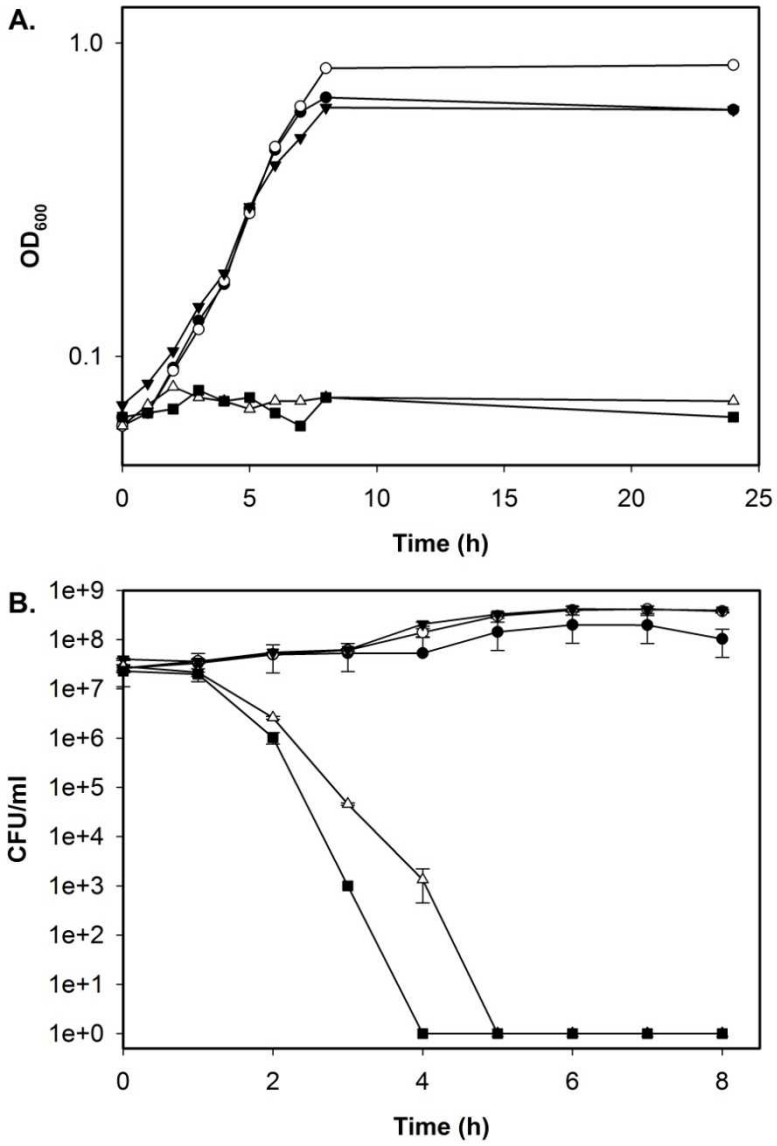

Figure 6.4. Myoglobin-inactivated (mi)CORM-3 is not bactericidal against *Neisseria meningitidis*. CORM-3 and miCORM-3 were added to the medium before inoculation to prevent dilution of the cultures. Cell densities were measured at 600 nm, taken every 60 min for 8 h. Cell viabilities were measured at time-points equal to those of cell density measurements. The effect of 30 µM (open circles) and 50 µM (closed triangles) miCORM-3 are presented in comparison with control (0.1 M KPi (pH 7), closed circles), 30 µM (open triangles) and 50 µM (closed squares) CORM-3 on **A.** growth and **B.** viability. Data are plotted as means ± SEM from 3 individual spots.

pattern of growth as the control cultures (Figure 6.5 A). CORM-3 at 75 μM was used as a positive control for growth inhibition and was in agreement with the results observed in previous experiments. To determine whether CO elicited a loss in viability, the effect of 75 μM CO saturated solution was compared with a control to which nothing was added. Cell density measurements are shown in parallel (Figure 6.5 B and C). As for growth, the viability of CO gas-treated cultures follows the same pattern as control cultures, with no significant drop in viable counts.

6.2.6 Effect of CORM-3 on the innate immune response

Preparation of human macrophages and details of experimental designs are described in section 2.2. To determine whether CORM-3 effects phagocytosis, the interaction between *N. meningitidis* and human macrophages was visualised by fluorescence microscopy. Gentamicin exclusion assays were utilised to elucidate whether CORM-3 affects the ability of macrophages to kill internalised bacteria.

6.2.6.1 Bactericidal activity of CORM-3 is disrupted in macrophage media

Figure 6.1 B shows that CO is released from CORM-3 to ferrous myoglobin in RPMI. To assess the extent of the bactericidal effect of the compound in macrophage media, the viability of *N. meningitidis* was measured after exposure to CORM-3. Briefly, cultures were grown to an OD_{600} of c. 0.3 in defined medium then harvested and resuspended in respective media. A 2.5 % inoculum was added to Dulbecco's Modified Eagle Medium (DMEM), Eagle's Minimum Essential Medium (EMEM), Roswell Park Memorial Institute medium (RPMI-1640) and *N. meningitidis* defined medium (a positive control for the bactericidal activity of CORM-3). Cultures were stressed with 75 μM CORM-3 immediately. Viability of *N. meningitidis* grown in each of the macrophage media maintained levels similar to that observed consistently for control cultures (nothing added, data not shown). As expected, bacteria grown in defined medium and treated with the compound showed a reduction in viable colonies after 30 min of exposure, with complete loss in viability seen at a maximum of 2 h (Figure 6.6). The drop in viability observed in this case was more gradual than seen in previous experiments, which may be a consequence of the different experimental design. To ensure that CORM-3 was not killing bacteria during the internalisation period under the specific conditions used in internalisation assays, samples of bacterial cultures

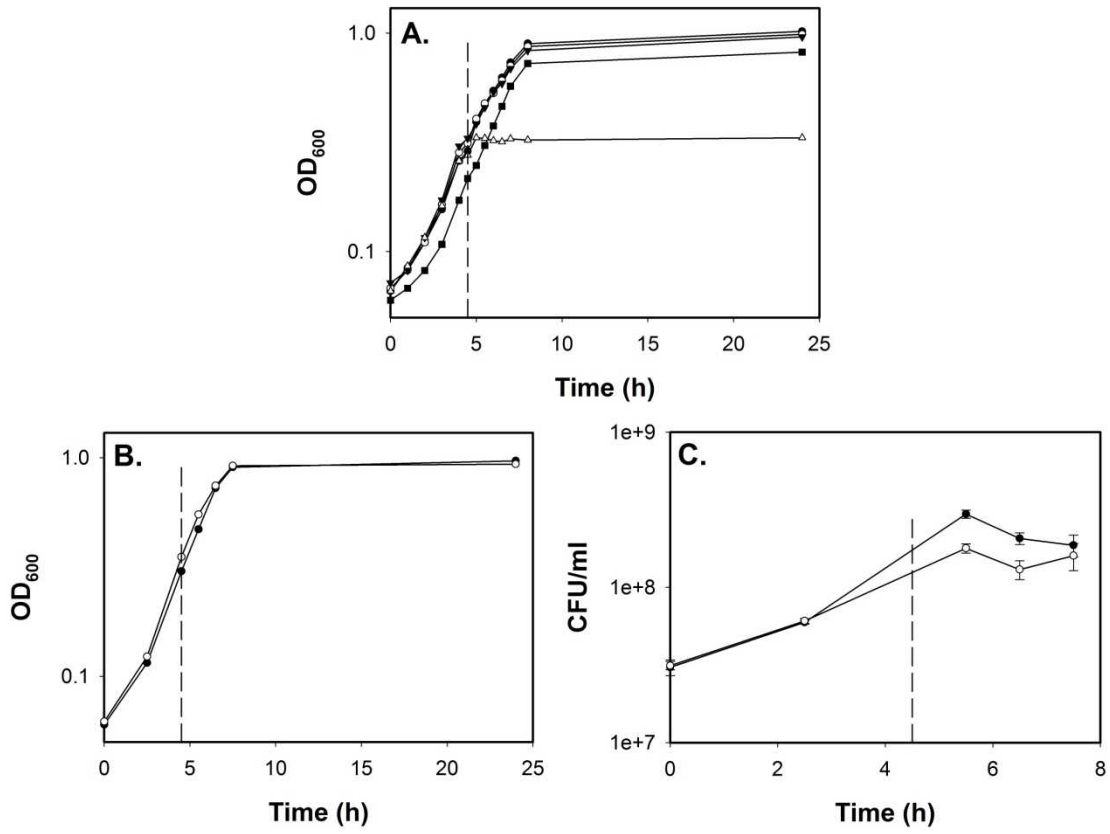

Figure 6.5. CO saturated solution does not affect the growth or viability of *Neisseria meningitidis*. CO saturated solution was added to cultures at an OD_{600} of c. 0.3 (dashed line). Cell densities were measured at 600 nm, using 1:1 dilutions of culture samples. **A.** Effect of 25 µM (closed circles), 75 µM (open circles) and 150 µM (closed triangles) CO compared with 75 µM CORM-3 (open triangles) and control (nothing added, closed squares) on growth. Data are a representation of the pattern seen in 2 biological replicates. Effect of 75 µM CO (closed circles) in comparison with control (nothing added, open circles) on **B.** growth and **C.** viability. Cell densities/viabilities were recorded at intervals of 150 min and 120 min (not viability) until CO exposure, then every 60 min thereafter. Data are an average of 2 technical repeats and represent data obtained in 2 biological replicates. Viability data are plotted as means ± SEM from 6 individual spots. Student's *t*-test, two-tailed; non-significant.

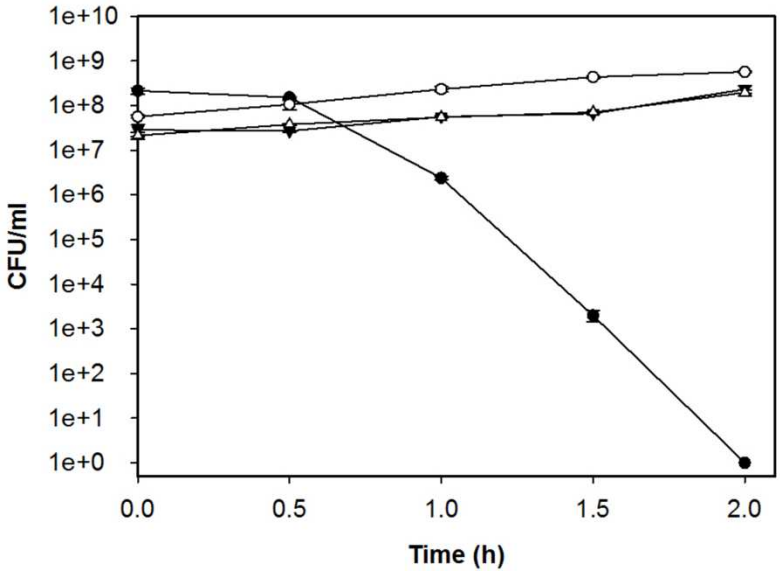

Figure 6.6. CORM-3 does not kill *Neisseria meningitidis* in macrophage media. Effect of 75 μM CORM-3 on the viability of bacteria grown in DMEM (open circles), EMEM (closed triangles), RPMI (open triangles) and *N. meningitidis* defined medium (closed circles). Cell viabilities were taken at $t = 0$ (immediately prior to stress) and every 30 min for 120 min thereafter. Data are plotted as means ± SEM from 3 individual spots and are representative of the pattern seen in 2 biological replicates.

suspended in RPMI were taken from control wells (no macrophages) every 30 min for the duration of the 90 min incubation. Consistent with previous results, no loss in bacterial viability was seen (data not shown).

6.2.6.2 CORM-3 does not alter macrophage activity

Firstly, the effect of 50 and 100 μM CORM-3 on bacterial invagination was quanitified by calculating: 1) the number of macrophages associated with bacteria in proportion to the number of macrophages in the field, i.e. the number of macrophages that are picking up bacteria (Figure 6.7 A), 2) the average number of bacteria associated with each macrophage (Figure 6.7 B) and 3) the number of internalised bacteria as a proportion of the total number of bacteria associated with macrophages, i.e. to determine the extent of internalisation (Figure 6.7 C). At both concentrations, CORM-3 was seen to be without a significant effect on the ability of macrophages to associate with, and phagocytose, *N. meningitidis* when compared with the control. Secondly, macrophages were treated with 50 and 100 μM CORM-3 after internalisation of bacteria (and removal of external bacteria using a cocktail of gentamicin and penicillin). The viability of *N. meningitidis* was assayed over 90 min post addition of the compound. Data are shown as CFU/ml (Figure 6.8). CORM-3 did not affect the ability of macrophages to kill internalised bacteria under these experimental conditions when compared with control.

6.3 Discussion

6.3.1 The bactericidal effect of CORM-3

Consistent with previous reports on the anti-bacterial effect of CO-RMs (Davidge *et al.* 2009b; Desmard *et al.* 2009; Nobre *et al.* 2007), CORM-3 at 50 and 75 μM elicited a concentration-dependent inhibition of meningococcal growth and reduction in viability (Figure 6.2). Results for lower concentrations (25 μM) were variable but consistent with a concentration-dependent effect of the compound. However, Figure 6.3 supports the lesser effect of 25 μM CORM-3. The differential sensitivity of *N. meningitidis* in this case may be a result of addition of the compound at slightly different cell densities between experiments. Furthermore, *N. meningitidis* was unaffected by CO gas applied as a CO-saturated solution at equimolar concentrations to CORM-3 (Figure 6.5), as reported for *E. coli* (Davidge *et al*. 2009b; Chapter 3 of this work).

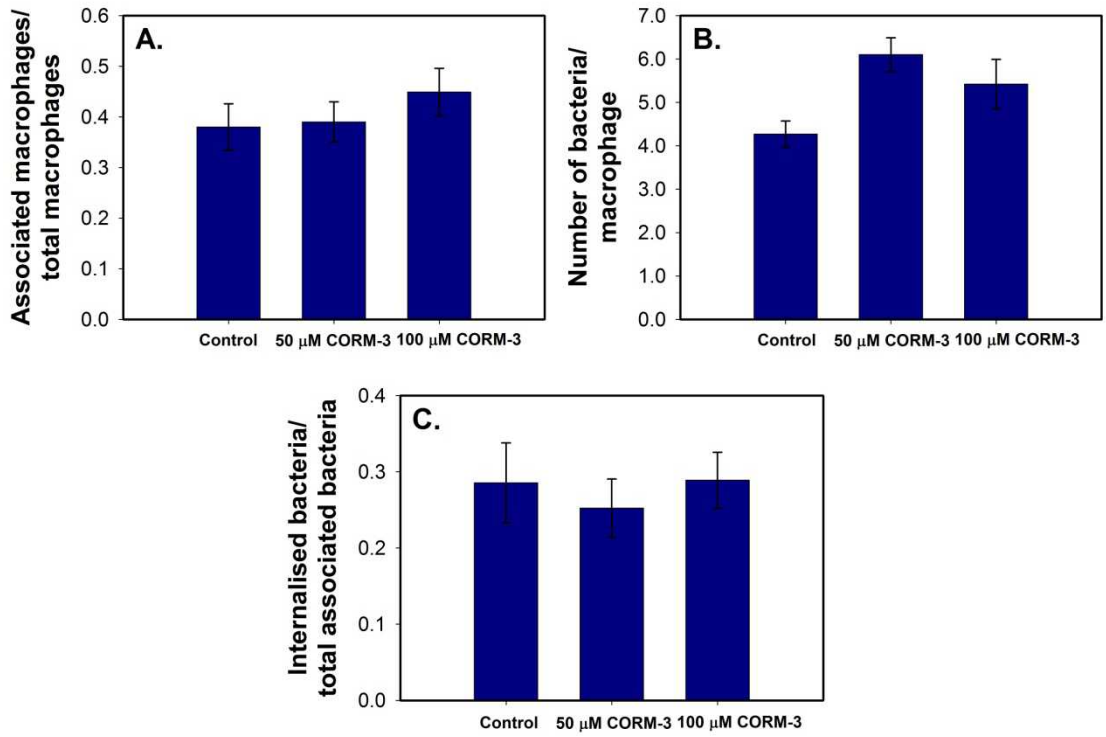

Figure 6.7. CORM-3 does not affect phagocytosis of *Neisseria meningitidis* by human macrophages *in vitro*. CORM-3 (50 and 100 μM) was added immediately following infection and cells were incubated for 90 min to allow for internalisation. The interaction between bacteria and macrophages was visualised by indirect immunofluorescence; initial treatment with a primary anti-meningococcal antibody followed by a secondary antibody labelled with the fluorescent dye fluorescein isothiocyanate (FITC). Further treatment with 4',6-diamidino-2-phenylindole (DAPI) allowed staining of macrophage nuclei. The following measurements for CORM-3-treated macrophages were compared with control (nothing added): **A.** the number of macrophages associated with bacteria, **B.** the number of bacteria associated with macrophages and **C.** the degree of internalisation of bacteria. Data are plotted as means ± SEM from 5 biological replicates, each with 2 technical repeats. Students t-test, two-tailed; non-significant after Bonferroni correction ($n = 2$).

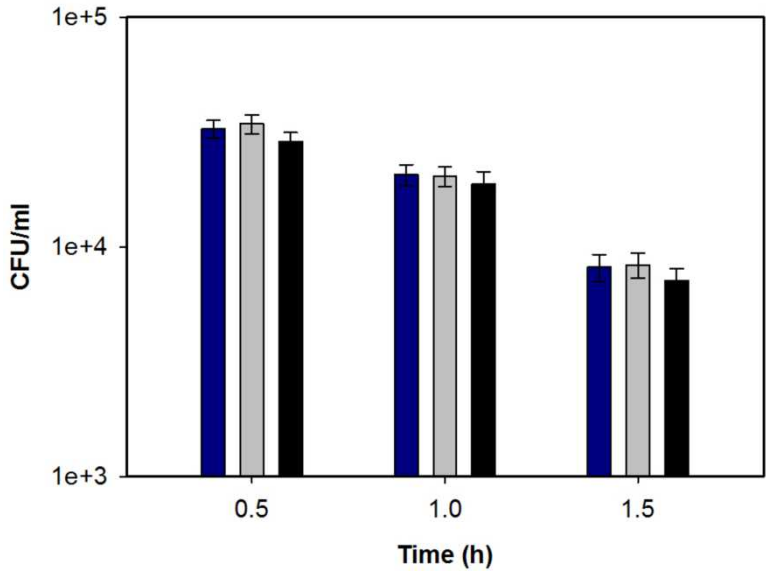

Figure 6.8. CORM-3 does not affect *Neisseria meningitidis* killing by human macrophages *in vitro*. Bacteria were incubated with macrophages for 90 min to allow for internalisation. External bacteria were killed using a cocktail of 100 µg/ml gentamicin and 10 µg/ml penicillin. CORM-3 at 50 µM (light grey) and 100 µM (dark grey) was added directly to the wells and macrophages were lysed using 2 % saponin at time-points of 30, 60 and 90 min. Viable counts allowed determination of the extent of killing in the presence of CORM-3 in comparison with the control (nothing added, black). Data are plotted as means ± SEM of 42 spots from 7 biological replicates.

Compared with the bacterial species previously tested, microaerobic cultures of *N. meningitidis* generally appear to be more sensitive to CORM-3 stress (Figure 6.2). Growth of anaerobic *E. coli* was slowed, but viability was not affected, within 2 h post-treatment with 100 μM of the compound and 200 μM was required for complete growth inhibition. Aerobic growth was inhibited at a concentration of 30 μM with a 1-log reduction in viable counts after 2 h. Further growth was prevented by 100 μM CORM-3 and 125 μM decreased viability by 4-log within 30 min (Davidge *et al.* 2009b). A much higher concentration (400 μM) was necessary to achieve complete loss in viability of aerobically and anaerobically grown *E. coli* at a maximum of 2 h post-stress, with an initial 70 - 75 % drop in survival after 30 min. Aerobic and microaerobic cultures of *S. aureus* were less sensitive to 500 and 400 μM CORM-3, respectively, with a decline in viable counts escalating with time, but not reaching complete loss, over 4 h (Nobre *et al.* 2007). Furthermore, 500 μM was ineffective at inhibiting growth of microaerobic cultures of *C. jejuni* (Smith *et al.* 2011). However, *N. meningitidis* was more resistant than *P. aeruginosa* PAO1 and three antibiotic-resistant clinical isolates of the bacterium. Concentrations as low as 0.1 - 10 μM were effective at inhibiting growth of PAO1, with a significant difference in cell density observed even at 18 h after addition of 0.5 μM CORM-3. Inhibition of growth as a result of exposure to the CO donor at a concentration of 10 μM was accompanied by a 4-log decrease in viability after 180 min. Growth of the clinical isolates was completely inhibited 18 h after addition of 10 μM of the compound (Desmard *et al.* 2009).

As seen in the aforementioned studies using different bacterial species (Desmard *et al.* 2009; Davidge *et al.* 2009b; Nobre *et al.* 2007), control compounds were ineffective against *N. meningitidis*. Neither $RuCl_2(DMSO)_4$ at 25 and 75 μM (Figure 6.3), nor miCORM-3 at 30 and 50 μM (Figure 6.4), inhibited growth and the latter was without effect on viability. Taken together, the results suggest that the bactericidal activity of CORM-3 is due to CO and not a consequence of the ruthenium moiety or any other part of the backbone. Interestingly, 30 μM CORM-3 inhibited growth and significantly reduced viability of *N. meningitidis* in the miCORM-3 experiment (Figure 6.4), whereas 25 μM was without effect in previous experiments. CORM-3 at 50 μM was also seen to be more potent. This could be due to a difference in cell density at the time of stress. Cultures were generally treated during mid-log phase of growth, but in this case the CO donor was added to the medium before inoculation. This is not an unexpected result as

there is a higher CO:cell ratio, but it does highlight the heightened sensitivity of *N. meningitidis* in comparison with *E. coli*; Davidge *et al*. (2009b) showed that 250 μM CORM-3 was required to prevent growth and kill a significant proportion of bacteria within 2 h when cells were inoculated into medium containing the compound.

The reasoning behind the differential sensitivity of individual bacterial species to CORM-3, and for the same species grown at different O_2 tensions, is yet to be explained. It is unlikely to be due to an effect of the backbone, in particular ruthenium, as multiple controls have ruled out this possibility: $RuCl_2(DMSO)_4$ (Davidge *et al.* 2009b; Desmard *et al.* 2009), addition of haemoglobin (Nobre *et al.* 2007) and miCORM-3 (this work). The work published to date suggests that the difference in the degree of sensitivity is not due to: 1) the skeleton of the compound, 2) pathogenicity, as both pathogenic and non-pathogenic strains are vulnerable, or 3) cell wall composition, as CORM-3 is effective against both Gram-negative and Gram-positive species.

As mentioned previously, the activity of CO-RMs appears to be dependent on medium composition. Components in rich media may either prevent release of the carbonyl, or trap liberated CO, subsequently preventing its binding to intracellular targets. The variation in species-specific response may therefore be due to the use of different media. This issue has been highlighted here as CORM-3 does not kill bacteria in macrophage media (Figure 6.6), but CO release to ferrous myoglobin was still detected (Figure 6.1 B). This supports the idea that components in rich media may prevent CO from reaching its targets; release of the carbonyl may be induced prior to cell entry. Alternatively, diminished CO-RM function could be due to better bacterial metabolism in rich media (Murray *et al.* 2012). Similar defined media were used to test the effects of CORM-3 on *E. coli* grown aerobically; however, Davidge *et al*. (2009b) and Nobre *et al*. (2007) used different carbon sources and the latter supplemented the medium with casamino acids. For anaerobic growth of *E. coli*, Davidge *et al*. (2009b) enriched the defined medium used for aerobic growth in order to achieve comparable growth rates between the two conditions. This may be the reason why anaerobic cultures were seen to be more resistant than aerobic cultures in this study, but the opposite was observed by Nobre *et al*. (2009), who used the same medium for bacteria grown under different O_2 tensions. To observe the effects of CO-RM on bacteria growing at the same rate one needs to risk the required supplements affecting the activity of the compound. Furthermore, *S. aureus*

was grown in LB (Nobre *et al.* 2007), which makes it difficult to compare its sensitivity with that of bacteria grown in defined media. Equally, the defined medium used for growth of *C. jejuni* (Smith *et al.* 2011) was considerably more complex than that used for *E. coli*, *N. meningitidis* and *P. aeruginosa*. However, *C. jejuni* is a microaerobic pathogen thus its tolerance in comparison with aerobic bacteria might not be surprising as its survival does not rely heavily on O_2-binding proteins, which are well-known targets of CO. *P. aeruginosa* was grown aerobically in M9 medium supplemented with glucose (Desmard *et al.* 2009), which is similar to the defined medium used for *E. coli*. Comparisons between aerobically grown cultures of these bacteria may therefore be more reliable. Although a difficult task, to obtain a more reliable comparison between different bacterial species, it would be necessary to standardise all of the conditions.

6.3.2 Effect of CORM-3 on macrophage activity

Although macrophage media prevent the bactericidal activity of CORM-3 (Figure 6.6), CO is still released (Figure 6.1 B). Furthermore, the concentrations used in the work detailed in this chapter (50 and 100 μM) are typical of those used in previous studies on the effect of CO-RMs on macrophage activity, as introduced in section 6.1. CO release to ferrous myoglobin in RPMI was slower than in defined medium and buffer, which may lower the compound's effectiveness initially. Ultimately, the formation of MbCO reached the same level in RPMI and defined medium; therefore CORM-3 should still be active in the time-course of the experiments. The lack of bactericidal activity may be advantageous as any changes observed for counts of internalised bacteria, or viability after macrophage lysis, should be solely due to an effect on macrophage efficiency.

The results presented in this chapter suggest that CORM-3 does not affect macrophage activity (Figure 6.7 and 6.8). As introduced in section 6.1, there are reports showing increased phagocytosis of bacteria by macrophages *in vitro* and *in vivo* in response to CO. But different results were obtained between research groups and for different bacterial species, for example Otterbein *et al*. (2005) showed that uptake of *E. coli* was increased, whereas Chung *et al*. (2008) saw augmented invagination of *E. faecalis* but not *E. coli*. However, the methods used in the two studies were different. Otterbein *et al*. (2005) exposed murine or primary alveolar macrophages to *E. coli* in the presence of CO gas (250 ppm) for up to 24 h and 5 h, respectively. Whereas, Chung *et al.* (2008)

inoculated the peritoneum of mice over-expressing HO-1 with *E. coli* and *E. faecalis*, or injected CORM-2 into the peritoneum of wild type mice 12 h and 2 h prior to injection of *E. faecalis*. Phagocytosis was measured 24 h post-inoculation. The macrophages and the source of CO were therefore different in each of the studies. It cannot be assumed that the mode of action of endogenously generated CO produced by HO-1 will have similar effects as CO administered in the gaseous form, or via CO-RMs. Furthermore, the macrophages in the lung and the peritoneum may differentially express surface receptors and consequently be more apt at responding to specific bacterial species.

Otterbein *et al*. (2005) expressed the uptake of *E. coli* as an increase in mean fluorescent intensity (MFI), rather than by direct counts of internalised bacteria, and Chung *et al*. (2008) used flow cytometry to determine phagocytic rates. It is unclear whether they measure association of bacteria with macrophages, or the levels of internalisation, as the bacteria were stained with FITC (green fluorescence) and this cannot penetrate macrophage cells. Otterbein *et al*. (2005) also suggest that the increase in phagocytosis was emphasised by the observed decrease in macrophage proliferation in the presence of *E. coli* and CO. If there are less macrophages present, but the same number of bacteria, then it might be expected that there is an increase phagocytosis. A higher number of bacteria would be available per macrophage and so the limiting factor in this situation would be the saturation point of macrophage activity. If there are more macrophages present, then uptake of bacteria would be more spread out and fewer bacteria might be phagocytosed per macrophage.

In a more indirect study, clearance of *P. aeruginosa*-induced bacteremia by CORM-3 in a mouse model of infection was seen to occur in the absence of an enhanced innate immune response. However, this report did not include direct measurements of bacterial uptake by macrophages. Taken together, the results suggest that the effect of CO on macrophage efficiency may be dependent on the species of bacteria in question. In addition, Otterbein *et al*. (2005) and Chung *et al*. (2008) used heat-killed bacteria, whereas Desmard *et al*. (2009) and the work described in this chapter used viable cultures. The response of macrophages may be dependent on the behaviour of live bacteria, in which case it might be plausible that heat-killed bacteria are easier targets for association/phagocytosis. In contrast to the work discussed above, human macrophages were utilised to assess the effect of CORM-3 on the uptake of *N.*

meningitidis, which may respond differently to CO when compared with murine macrophages.

There could be a number of reasons as to why CORM-3 might not be effective under the current conditions. For example, macrophages, as eukaryotes, possess a more complex cell structure than bacteria, which could influence the ability of CORM-3 to access intracellular targets. Also, the compound may not be able to enter macrophages with as much ease as bacterial cells, which could result in a reduction in intracellular levels of CO. However, metal carbonyl complexes have been detected inside human cancer cells at similar concentrations to those used in the present study (5, 10 and 50 μM) (Policar *et al.* 2010), and higher (2 mM) (Meister *et al.* 2010), by subcellular infrared imaging and raman microspectroscopy, respectively. Entry into the cells was observed after incubation with the compounds for 1 h and 3 h. Neither of the complexes were ruthenium-based; therefore it would be useful to determine whether CORM-3 gains entry into macrophages under the experimental conditions used in the current work. Other than Desmard *et al*. (2009), who also suggest that CO does not affect the innate immune response, none of the other previously discussed studies have used CORM-3. This supports the aforementioned suggestion that contrasting results may therefore be due to the method by which CO is delivered, and perhaps even the particular CO-RM used, which may also apply to cell entry. In addition, macrophages were exposed to CORM-3 for a maximum of 90 min in the experiments presented in this chapter. The compound was added either at the same time as *N. meningitidis*, or after a period of incubation to allow for internalisation. The shorter time-scales of CO treatment may be a reason why macrophage activity was not altered.

Direct, *in vitro* measurements of bacterial killing by macrophages exposed to CO have not been reported in previous studies, but the results in Figure 6.8 suggest that CO liberated from CORM-3 does not affect their bactericidal activity. This is surprising when taking into account CO-elicited inhibition of NO production (section 6.1); however, in most cases, CO alters the behaviour of a cell to most effectively establish homeostasis. CO may therefore fine tune the levels of NO produced by macrophages in response to bacteria. So perhaps NO production is reduced when comparing CO-treated and untreated macrophages as previously reported, but only to a level required to effectively eradicate bacteria, rather than being produced to a harmful extent that is

lethal in cases of sepsis. If bacteria are more effectively removed as a result of CO/CO-RM treatment, then a lesser immune response would be required. This may also explain why levels of inflammatory cytokines were not adjusted (Chung *et al.* 2008). On the other hand, studies reporting the effect of CO on iNOS/NO production generally use endotoxin, which is only a fragment of the bacterial cell wall. CO might influence macrophage function in a different manner in the presence of intact bacteria (Otterbein *et al.* 2005).

It seems that there are a number of variables in the experiments reported to date, for example: 1) the macrophages used in each study were isolated from different organs, 2) murine macrophages and human macrophages have been utilised, 3) macrophages have been exposed to different bacterial species and 4) different methods of CO delivery have been tested. In order to fairly establish the effect of CO on macrophage activity, it would be necessary to use the same conditions for each experiment and perhaps trial each of the different macrophages, bacterial species and modes of CO application to determine whether the effect is dependent on any of the above.

6.3.3 Conclusions

Micromolar concentrations of CORM-3 appear to elicit potent anti-bacterial effects against *N. meningitidis* in a concentration-dependent manner, a role which appears to be achieved by direct delivery of CO to its intracellular targets, as CO gas and the inactive compounds were ineffective. Although efficient at killing bacteria directly, the compound does not affect the ability of human macrophages to phagocytose and kill *N. meningitidis*. However, more work is required to validate this result, which is in disagreement with previously published data (see section 7.7).

Chapter 7. General Discussion

7.1 Summary

The work presented in this thesis highlights the complexity of CO/CO-RM function within cells, which has implications not only for elucidating the activity of CO against bacteria, but also on a larger scale in more complex systems. Although the bacterial respiratory chain is undoubtedly a major target of CO released from CORM-3 (Davidge *et al*. 2009b; Desmard *et al*. 2009; Desmard *et al*. 2012; Chapter 3 of this work), it is becoming increasingly apparent that this is unlikely to be the mode via which CO elicits bactericidal effects (Davidge *et al*. 2009b; Desmard *et al*. 2012; Nobre *et al*. 2009; Wilson *et al*. submitted; Chapter 3 of this work). This was confirmed here by the potent cytotoxicity of CO against haem-deficient bacteria, namely a well-defined *hemA* mutant of *E. coli* and naturally haem-deficient *L. lactis*. Surprisingly, the mutant was more susceptible to the deleterious effects of CORM-3 than the wild type, a finding that was corroborated by testing the effects of the compound on the mutant after reconstitution of the cellular haem-content with δ-ALA. This prompted the proposal that haem proteins may act as a 'CO-sink' and thus help protect additional targets from the deleterious effects of the gas. It is also important to note that inactive control compounds were generally ineffective against all of the strains tested, suggesting that liberated CO is responsible for the bactericidal activity of the metal carbonyl compound (Chapter 4). Transcriptomic profiling of the haem-deficient mutant following exposure to CORM-3 revealed a multifaceted network of responses, with between 6 - 20 % of the genome being altered over 120 min and changes in gene expression observed across several different functional categories. The most striking finding was the unprecedented effect of CORM-3 on intracellular iron homeostasis. Furthermore, treatment of the mutant with iCORM-3 elicited a transcriptomic response, albeit dampened, that may be attributed to residual CO release from the compound, but also raises the concern that the backbone of CORM-3 may impart effects of its own (Chapter 5). A final avenue of research presented here demonstrates that CORM-3 does not affect the capacity of the innate immune response during a model of meningococcal infection (Chapter 6). Although an important finding, further lines of investigation are required to strengthen these data (section 7.7).

Overall, it is apparent that a number of questions remain unanswered and further investigation is required to elucidate some of the queries and findings that have arisen during this project (see section 7.7). For now, one can but speculate on the full extent of the modes of action of CO/CO-RMs.

7.2 Hypothetical interactions of CORM-3 with thiols and subsequent consequences on iron homeostasis

The effect of CORM-3 on genes involved in the response to iron-limited conditions in the mutant is intriguing, but at present is difficult to explain. NO has been shown to reduce iron uptake by mammalian cells and reduce incorporation of iron into the storage protein ferritin. Furthermore, several reports demonstrate the involvement of NO in the extrusion of iron from the cell via a glutathione- and energy-dependent mechanism that may involve a multidrug resistance transporter, MRP1 (reviewed in (Richardson & Lok 2008)). Cells transfected with HO-1 exhibited decreased iron uptake and iron efflux (Ferris *et al.* 1999), suggesting that CO may mimic this activity of NO. Additionally, carbonyl-thiol-iron complexes can form *in vitro* (Cremer 1929; Schubert 1933; Szakacs-Schmidt *et al.* 1992). However, although CO gas was shown to decrease iron uptake and subsequent incorporation into ferritin, it did not mobilise iron out of the cell (Watts & Richardson 2004), but iron release was observed when both CO and OxyHb were present in the medium. This was attributed to a 'CO-sink' activity of the globin, which would prevent loss of CO from the medium, and subsequent dissociation of CO from OxyHb may lead to increased availability of the gas to the cells (Watts & Richardson 2004). Therefore, the minimal effects previously observed by this group may have been due to a low intracellular concentration of CO. In the current study, CORM-3 is likely to enable the delivery of CO into cells, where it will be released only in the presence of suitable ligands (e.g. sulfite (McLean *et al.* 2012)), and the ruthenium backbone acts as sink for CO re-binding should it detach from its targets. In the wild type, both the backbone and haem may compete for this role, which would reduce the ability of the gas to interact with other proteins. If CO does form a complex with glutathione and iron, and is then transported out of the cell, it may explain the modest up-regulation of the glutathione transport system in the mutant (section 5.2.5) and/or the multidrug efflux system (*mdtABC*) (Figure 5.8). An involvement of the latter could explain the lesser effect of iCORM-3 on the expression of genes encoding this efflux system.

However, as mentioned previously, thiols have been shown to affect CO-RM activity in a bacterial context. Glutathione, cysteine and NAC added externally abolish the anti-bacterial effects of CO-RMs (Desmard *et al.* 2009; Desmard *et al.* 2012; Murray *et al.* 2012; Tavares *et al.* 2011), but in the absence of changes in the intracellular glutathione pool (Desmard *et al.* 2009). This may explain why the expression of genes involved in glutathione biosynthesis was generally unaffected in the present study (section 5.2.5). The mechanism by which thiols inhibit CO-RM activity is currently unknown, but a recent report suggests that the effect is specific for metal-containing compounds and in particular those that are ruthenium-based. The activity of both CORM-2 and CORM-3 was completely inhibited, whereas the inhibitory effect of the manganese-based CORM-371 was only partially reversed and at lower concentrations. Furthermore, activity of the boron-based CORM-A1 was unaffected (Desmard *et al.* 2012). This group hypothesised that high concentrations of thiols, achieved by external administration, may induce the rapid release of CO from the compounds. Liberation of CO in the extracellular medium would prevent the gas from reaching its intracellular targets as efficiently as when transported into the cell by CO-RMs (Desmard *et al.* 2012). However, another recent study has shown that thiols do not promote release of CO from CORM-3 (McLean *et al.* 2012). Also, an interaction of thiols with the backbone and subsequent prevention of CO release has previously been ruled out due to the unaltered rate of MbCO formation after reacting deoxymyoglobin with CORM-3 in the presence of NAC (Desmard *et al.* 2009). However, this observation may be void as a result of the demonstration by McLean *et al*. (2012) that dithionite, the reducing agent commonly used in the standard myoglobin assay, promotes release of CO from CORM-2 and CORM-3.

The idea that thiols may interact with the backbone and 1) stabilise the compound, thus preventing CO release, or 2) render the compound unable to enter the cell and consequently preventing intracellular CO delivery, can therefore no longer be discarded. This is further supported by the demonstration that thiol activity is compound-specific (Desmard *et al.* 2012), and also by recent data from the Poole laboratory showing that the uptake of CORM-3 by *E. coli* cells is reduced c. 10-fold by the presence of NAC, as assayed by ICP-AES analysis of intracellular ruthenium levels (Jesse & Poole, unpublished). Additionally, colourimetric assays of free thiol levels in solution, by measuring the conversion of 5,5'-dithiobis-(2-nitrobenzoic acid) (Ellman's reagent) to thionitrobenzoic acid, revealed that CORM-3 is able to react with reduced glutathione,

cysteine and sodium hydrosulphide. Although to a lesser extent, the reaction was also seen with iCORM-3, but not with CO gas (Jesse & Poole, unpublished), suggesting a possible interaction between thiols and the ruthenium centre of the compound.

7.3 Does expression of microbial HO confer greater resistance or sensitivity to CO-RMs?

It is evident from the work published to date (Chapter 1, section 1.5.3) and that presented in the current study (Chapters 3 and 6), that different microbial species exhibit differing degrees of sensitivity to CO-RMs. The reasons behind this finding remain to be elucidated. In addition to the suggestions made in section 6.3.1, it may be hypothesised that microbes expressing HO could be more resistant to CO/CO-RM as they might naturally possess mechanisms for CO detoxification. On the other hand, such microbes could be more sensitive, as CO has been seen to increase HO-1 expression and activity in murine macrophages (Sawle *et al.* 2005). *N. meningitidis*, *P. aeruginosa*, *S. aureus*, *C. jejuni* and *C. albicans* all express at least one HO, but their sensitivity to CO varies, as demonstrated in previous studies (section 1.5.3) and in Chapters 3 and 6 of this work. Perhaps detoxification mechanisms cannot cope with large accumulations of the gas, or maybe the level of sensitivity is related to the microbe's efficiency at acquiring and subsequently breaking down haem. For example, *S. aureus* preferentially utilises haem as an iron source during the initial stages of infection and expresses two HOs (Skaar *et al.* 2004). If CO released from CO-RM up-regulates HO expression, then the bacterium may be better able to cope with the stress initially. Continuous accumulation of CO, as a result of enhanced HO activity in parallel with CO liberated from CO-RM, may explain the reduction in *S. aureus* viability that is observed over time (Nobre *et al.* 2007). *N. meningitidis* and *P. aeruginosa* only express one HO implicated in haem utilisation (Ratliff *et al.* 2001; Zhu *et al.* 2000b); therefore their ability to obtain iron may be less efficient, leading to increased sensitivity. *C. jejuni* only contains one HO, but it has been hypothesised to express additional inner membrane ATP-binding cassette transport system(s) for haem (Ridley *et al.* 2006), thereby enabling effective haem acquisition.

Furthermore, it has been suggested that the HO from *C. albicans* (*CaHMX1*) may not be involved only in iron utilisation, but may also play a role in protecting the pathogen

from the host immune response during invasive infection. This ability was attributed to the generation of by-products as a result of HO activity, i.e. including CO (Pendrak *et al.* 2004b). Thus, *C. albicans* may have unknown mechanisms in place to cope with accumulations of the gas. In addition to the more complex cell structure of this microbe in comparison with bacteria, the expression of CaHMX1 may contribute to the greater resistance of *C. albicans* respiration to CORM-3 stress (Chapter 3 of this work).

An understanding of why different compounds elicit differing degrees of toxicity, and why some species are more susceptible than others to CO-RM treatment, would enable the production of more efficient anti-microbial metal carbonyls. Investigations into the effect of CO-RMs on HO-deficient bacteria may be a good starting point.

7.4 CO-RMs: efficient CO donors, or toxic compounds?

CO-RMs have been consistently shown to elicit greater toxicity against bacteria than CO gas directly bubbled into growing cultures (Desmard *et al.* 2009; Nobre *et al.* 2007), or applied as a saturated solution (Davidge *et al*. 2009b; Chapter 3 and 6 of this work). However, these studies, and the current work, have shown that CO-depleted control compounds were generally ineffective at reducing bacterial growth and viability, thereby suggesting that the toxicity of CO-RMs is unlikely to be due to an effect of the metal complex that lacks CO. An alternative hypothesis is that the chemistry of the CO-RM is responsible for the effectiveness. For example, ruthenium-based compounds (CORM-2 and CORM-3) have been shown to be more effective than other CO-RMs containing either a different metal (CORM-371), or a non-metal (CORM-A1) (Desmard *et al.* 2012). This may be due to the high level of stability of the ruthenium complexes unless in the presence of specific ligands, as shown by Mclean *et al*. (2012). This compound chemistry could be responsible for the proposed accumulation of CO at specific intracellular sites, which may be at a level far greater than can be achieved via diffusion of the gas across the cell membrane, or by delivery of CO using other CO-RMs with different chemical properties. In support of this, analysis of intracellular ruthenium content carried out by Davidge and co-workers showed that the level of the metal was > 200 μM after adding only 30 μM of CORM-3 to growing cultures (Davidge *et al.* 2009b). Taken together, these observations may explain the different

intensity of action exhibited by different CO-RMs, and thus highlights the importance of developing compounds specific for particular applications.

7.5 Problems and challenges regarding CO-RM utilisation

The extensive library of CO-RMs that is now available (Mann 2010), and the continual advances in compound design (section 1.4.3.5), provide great promise from a therapeutic viewpoint. However, in the race to find the ideal compound, important aspects of CO-RM characterisation have been neglected. For example, although it is has been demonstrated that the compounds are taken up by cells, both eukaryotic (Meister *et al.* 2010; Policar *et al.* 2010) and prokaryotic (Davidge *et al.* 2009b; Nobre *et al.* 2007), the kinetics of uptake remain unknown. Also, the decomposition products of the compounds after CO release have not been identified, and more importantly, the ability of iCORM-3 to enter cells has never been established. The latter is critical if these inactive compounds are to be classed as proper controls. It is also imperative to delve more into the fundamental aspects of CO-RM function, for example, the mechanism and kinetics of CO release. Only recently has this been investigated for CORM-2, CORM-3 and CORM-401 (McLean *et al.* 2012), yet it comprises a vital avenue of study that is necessary if these CO-RMs are ever to be considered for clinical use.

Although inactive, i.e. CO-depleted, compounds have been shown to be non-toxic against bacteria, the data presented in Chapter 5 of the present study showed that iCORM-3 elicits a transcriptomic response. This may be attributable to the residual CO release from the compound, but direct interactions of the backbone of CORM-3 with intracellular targets cannot be ruled out at present. Examples of interactions between ruthenium and proteins have been reported in the literature. For example, a recent study demonstrated the ability of CORM-3 to interact with myoglobin, haemoglobin, human serum albumin, human transferrin and hen egg white lysozyme. In the case of the latter, the ruthenium moiety of the compound was shown to bind to the protein at three sites: His15, Asp18 and Asp52. The reaction between CORM-3 and the proteins resulted in the liberation of the chloride and glycinate ligands, in addition to one CO, which was released in the form of CO_2 (Santos-Silva *et al.* 2011). Studies by members of this group confirmed the binding of ruthenium to hen egg white lysozyme using different ruthenium compounds of the same family as CORM-3, namely $[Ru(CO)_3Cl_2$(1,3-

thiazole)] (Santos *et al.* 2012) and ALF 492 (section 1.4.3.5) (Pena *et al.* 2012). This prompted a proposal to explain the *in vivo* effectiveness of CO-RMs within this family. Briefly, after entering the blood, the compounds react rapidly with plasma proteins, lose one equivalent of CO as CO_2 and form protein-$Ru(CO)_2$ adducts, which are then transported throughout the body, decaying slowly to release the remaining carbonyls in a stepwise manner (Santos *et al.* 2012).

It is also important to note that a recent report revealed broad-spectrum anti-microbial activity of metal(II) amino acid complexes, i.e. devoid of carbonyl groups. These compounds contained cadmium, nickel, cobalt or manganese coordinated to glycine (a ligand coordinated to ruthenium in CORM-3) or phenylalanine. This study is one of many that has shown the anti-microbial activity of certain metals and amino acids, whether tested as separate entities, or in complexes (Aiyelabola *et al.* 2012). Of particular relevance is a study showing the anti-bacterial activity of non-carbonylated ruthenium(II) compounds against four human pathogens: *Proteus vulgaris*, *Proteus mirabilis*, *P. aeruginosa* and *E. coli* (Anthonysamy *et al.* 2008). Additionally, ruthenium compounds have also been reported to elicit inhibitory effects in *E. coli* K-12. For example, ATPase activity was shown to be sensitive to micromolar concentrations of ruthenium red, a polymeric compound obtained by acidification of $Ru(NH_3)_3Cl_3$ (Scott *et al.* 1980). Also, micromolar concentrations of a dimeric, mixed valence complex of ruthenium ($Ru_2(NH_3)_6Br_5(H_2O)$) inhibited succinate-driven calcium uptake by membrane vesicles of *E. coli*, but was without effect on respiration (Gibson *et al.* 1982).

Taken together, these reports demonstrate the importance of understanding the chemical interactions of CO-RMs, whether they are carrying CO or not, and the care that must be taken when selecting metal centres and coordinated ligands. Such knowledge is necessary in order to better assess the potential consequences of the pharmacological application of CO-RMs.

7.6 Conclusions

In light of the data reported in this thesis, the model previously shown in section 1.6 can be updated. A ‘Trojan Horse’ mechanism is now proposed for the activity of CO-RMs

in bacterial cells in comparison with CO gas (Figure 7.1). Here, it is envisaged that a CO-RM carries its toxic cargo of CO into the cell where the gas is delivered to sensitive sites. Unlike the Trojan Horse analogy, however, it is clear from the present work that the fate of the 'Horse' also needs to be considered.

In conclusion, the potential application of CO-RMs in the treatment of microbial infections is rapidly becoming apparent. The modes of CO-RM action are probably dissimilar to currently used antibiotics; therefore these compounds may have the potential for topical or targeted treatment of antibiotic-resistant bacteria. However, rational design and exploitation of CO-RMs requires a fundamental understanding of their activity and their intrinsic chemical properties. This thesis reports that CORM-3 has complex, time-dependent and multifaceted effects on bacteria in the presence, or absence, of traditional haem targets. This highlights the requirement for additional investigations into the mechanisms behind CO/CO-RM functionality, and the vast potential of CO-RMs for broad-spectrum utilisation in clinical microbiology. However, it is important to combine improved knowledge of CO-RM chemistry with continued CO-RM development, having the aim of tailoring the compounds for use in specific diseases states.

7.7 Further investigation

In addition to the unpublished data cited throughout this thesis, further work is currently ongoing in the Poole laboratory with the aim of understanding more fully the action of CO liberated from CO-RMs, or applied as the gas, on bacteria. For example, an interesting study on the treatment of *E. coli* with anti-microbial agents, including antibiotics such as novobiocin, oxacillin and doxycycline, in CO atmospheres clearly demonstrated the ability of CO to potentiate the activity of these drugs (Davidge & Poole unpublished). Interestingly, this effect is the opposite of that attributed to NO (Gusarov *et al.* 2009) and H_2S (Shatalin *et al.* 2011), which are synthesised by bacteria by the action of, respectively, bacterial NO synthases and several biosynthetic enzymes in diverse bacteria. Both studies suggest that the endogenous production of NO and H_2S is a mechanism of protection from the actions of antibiotics, and other anti-microbial compounds, that are encountered by bacteria in their natural environments.

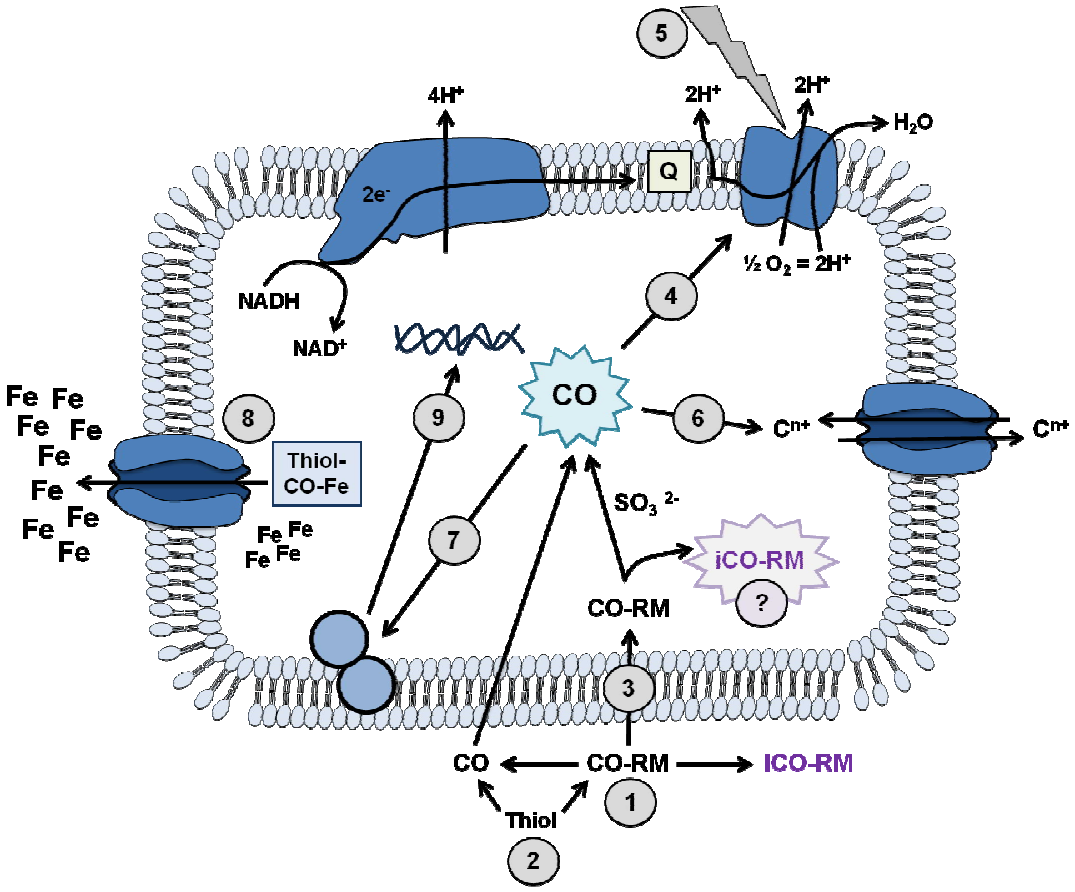

Figure 7.1. Up-dated model of CO-RM activity in bacterial cells. A CO-RM may lose its CO permanently in the extracellular milieu through, for example, the presence of a species to capture the CO, or a change in the compound after CO loss (1). Additionally, externally administered thiols interact with the CO-RM, and/or perhaps CO, outside of the cell thus abolishing CO-RM-mediated effects (2). Alternatively, the CO-RM is transported into the cell and concentrated several fold (Davidge *et al.* 2009b) carrying its CO cargo (Trojan Horse effect) and CO dissociation is promoted by reaction with intracellular ligands that include, but will not be restricted to, sulfite (McLean *et al.* 2012) (3). CO is therefore immediately accessible at relatively high concentrations to membrane-bound haem targets, to which it binds. Respiration is perturbed (4) in a light-reversible manner (5) and ion movement is modulated (6) (Wilson *et al*. submitted; section 3.3 of this work). Furthermore, CO, and perhaps iCO-RM, affects transcription factor activity, either by direct interaction with transcription factors (7), or indirectly by interfering with cellular homeostasis. In the case of CORM-3, an example of the latter may be the diminution of intracellular iron pools via a hypothetical thiol-CO-iron extrusion mechanism (8). These effects are then reflected in the transcriptome (9).

It should be noted, however, that an earlier study clearly showed that H_2S potentiated the toxicity of hydrogen peroxide in *E. coli* (Berglin & Carlsson 1985). This last result is more in line with the unpublished findings of Davidge & Poole on CO gas, as mentioned above. It is evident that the effects of all three gases, CO, NO and H_2S, require far greater study.

Additionally, uptake of the new water-soluble manganese-based CORM-401 (section 1.4.3.4, Table 1.2) by *E. coli* cells has been demonstrated, resulting in a concentrated intracellular level of the compound (Wareham & Poole, unpublished), as observed previously for CORM-3 (Davidge *et al.* 2009b). However, interestingly, CORM-401 did not inhibit growth of *E. coli* to the same extent as CORM-3, even though it releases two more molecules of CO. Likewise, preliminary data revealed that respiration in *E. coli* membrane particles and intact cells was not inhibited to the same extent following exposure to CORM-401, when compared with CORM-3, and respiratory stimulation was not observed (Wareham & Poole, unpublished). These findings further support the hypothesis that CO-RM activity is compound-dependent. More controlled microarray studies have also been performed recently by growing wild type *E. coli* in continuous culture in a chemostat (McLean & Poole, unpublished). The effect of CORM-3 and iCORM-3 under both aerobic and anaerobic conditions was tested. Again, differential regulation of genes across numerous functional classes was observed, similar to those reported by Davidge *et al*. (2009b) and Nobre *et al*. (2009), as well as in Chapter 5 of this work. Once again, *spy* was the most highly up-regulated gene in the study and, in support of CO-induced alterations in the transcriptome, iCORM-3 elicited only a minimal response (McLean & Poole, unpublished).

With regard to the work presented in this thesis, the avenues of study that require immediate attention stem from the transcriptomic analysis of the haem-deficient mutant of *E. coli*, and the effect of CORM-3 on the ability of macrophages to clear a bacterial infection. Previous transcriptomic studies that have utilised NO donors in comparison with NO gas revealed that the former can elicit their own responses, making it difficult to determine the changes that are solely a result of the gas (Spiro 2007). The situation appears to be the same in the present work and, although to a lesser extent, in the unpublished work by Mclean & Poole using stringent growth conditions. Thus, testing the effects of CO gas on the growth and viability of the mutant in comparison with the

wild type, followed by transcriptomic profiling after exposure of the bacterial strains to the gas alone, is the next logical step in this study. In addition to showing compound-dependent responses, the data may also clarify whether the use of a CO donor enhances CO-elicited alterations in the transcriptome. Such an outcome would test the hypothesis suggested by several groups that CO-RMs facilitate the accumulation of CO at specific intracellular sites. In parallel, it would be useful to employ ICP-AES metal analyses to determine intracellular levels of iron and other metals e.g. zinc. Furthermore, although *spy* has been identified as a highly up-regulated gene in each of the transcriptomic studies to date (Davidge *et al*. 2009b; Nobre *et al*. 2009; Chapter 5 of this work), no biological experiments have been performed to determine its contribution in the CO-RM-elicited response. Testing the effects of CO-RMs on a mutant deficient in this gene is therefore also of interest. However, to enable a more focused investigation into the effect of CO, the complete set of results including CO gas growth, viability and transcriptomic data are required before additional experiments can be identified. This may take us further towards pinpointing the targets/mechanisms by which CO elicits such pronounced toxicity in a haem-deficient mutant, and bacteria in general.

Although the results in Chapter 6 reveal that CORM-3 does not alter macrophage functionality during infection, it is of interest to continue this investigation to understand the different, and contradictory, results obtained to date. Pre-treatment of macrophages with CO-RM would allow a period of time for CO to be able to act exclusively on macrophages and exert transcriptional effects, which may lead to changes that could alter macrophage efficiency. Longer incubation times after infection may also be useful. For example, two parallel experiments could be performed; one allowing a normal mode of bacterial invagination and the other preventing bacterial uptake by macrophages as a result of treatment with cytochalasin D. In addition, it would be desirable to determine whether CORM-3 affects the regulation/activity of iNOS and/or the production of NO/ROS under the experimental conditions used in the present study (refer to Chapter 6). The latter may initially involve the use of macrophages in which the production of NO/ROS is inhibited, either specifically by the use of inhibitors, or by using cell-lines deficient in production of the relevant enzymes. These deficient macrophages could be tested against their controls in the presence and absence of CORM-3 to determine whether bacterial killing is adjusted. This may shed light on the effect of CORM-3 on the generation of these important species by human

macrophages exposed to live bacteria. If an effect was seen under such conditions then it would be interesting to assess transcriptional changes during host-pathogen interaction in the presence of CO.

Bibliography

Abraham, N. G. & Kappas, A. (2008). Pharmacological and clinical aspects of heme oxygenase. *Pharmacol Rev* **60**: 79-127.

Abu-Soud, H. M., Wu, C., Ghosh, D. K. & Stuehr, D. J. (1998). Stopped-flow analysis of CO and NO binding to inducible nitric oxide synthase. *Biochemistry* **37**: 3777-3786.

Aiyelabola, T. O., Ojo, I. A., Adebajo, A. C., Ogunlusi, G. O., Oyetunji, O., Akinkunmi, E. O. & Adeoye, A. O. (2012). Synthesis, characterization and antimicrobial activities of some metal(II) amino acids' complexes. *Advances in Biological Chemistry* **2**: 268-273.

Allanson, M. & Reeve, V. E. (2005). Ultraviolet A (320-400 nm) modulation of ultraviolet B (290-320 nm)-induced immune suppression is mediated by carbon monoxide. *J Invest Dermatol* **124**: 644-650.

Allanson, M. & Reeve, V. E. (2007). Carbon monoxide signalling reduces photocarcinogenesis in the hairless mouse. *Cancer Immunol Immunother* **56**: 1807-1815.

Almeida, A. S., Queiroga, C. S., Sousa, M. F., Alves, P. M. & Vieira, H. L. (2012). Carbon Monoxide Modulates Apoptosis by Reinforcing Oxidative Metabolism in Astrocytes: ROLE OF Bcl-2. *J Biol Chem* **287**: 10761-10770.

Alonso, J. R., Cardellach, F., Lopez, S., Casademont, J. & Miro, O. (2003). Carbon monoxide specifically inhibits cytochrome *c* oxidase of human mitochondrial respiratory chain. *Pharmacol Toxicol* **93**: 142-146.

Althaus, E. W., Outten, C. E., Olson, K. E., Cao, H. & O'Halloran, T. V. (1999). The ferric uptake regulation (Fur) repressor is a zinc metalloprotein. *Biochemistry* **38**: 6559-6569.

Andrews, S. C. (1998). Iron storage in bacteria. *Adv Microb Physiol* **40**: 281-351.

Andrews, S. C., Shipley, D., Keen, J. N., Findlay, J. B., Harrison, P. M. & Guest, J. R. (1992). The haemoglobin-like protein (HMP) of *Escherichia coli* has ferrisiderophore reductase activity and its C-terminal domain shares homology with ferredoxin NADP+ reductases. *FEBS Lett* **302**: 247-252.

Anthonysamy, A., Balasubramanian, S., Shanmugaiah, V. & Mathivanan, N. (2008). Synthesis, characterization and electrochemistry of 4'-functionalized 2,2':6',2''-terpyridine ruthenium(II) complexes and their biological activity. *Dalton Trans*: 2136-2143.

Aono, S. (2003). Biochemical and biophysical properties of the CO-sensing transcriptional activator CooA. *Acc Chem Res* **36**: 825-831.

Armstrong, F. A. (2004). Hydrogenases: active site puzzles and progress. *Curr Opin Chem Biol* **8**: 133-140.

Arregui, B., Lopez, B., Garcia Salom, M., Valero, F., Navarro, C. & Fenoy, F. J. (2004). Acute renal hemodynamic effects of dimanganese decacarbonyl and cobalt protoporphyrin. *Kidney Int* **65**: 564-574.

Asif, H. M., Rolfe, M. D., Green, J., Lawrence, N. D., Rattray, M. & Sanguinetti, G. (2010). TFInfer: a tool for probabilistic inference of transcription factor activities. *Bioinformatics* **26**: 2635-2636.

Avissar, Y. J. & Beale, S. I. (1989). Identification of the enzymatic basis for delta-aminolevulinic acid auxotrophy in a hemA mutant of *Escherichia coli*. *J Bacteriol* **171**: 2919-2924.

Baart, G. J., Zomer, B., de Haan, A., van der Pol, L. A., Beuvery, E. C., Tramper, J. & Martens, D. E. (2007). Modelling *Neisseria meningitidis* metabolism: from genome to metabolic fluxes. *Genome Biol* **8**: R136.

Bani-Hani, M. G., Greenstein, D., Mann, B. E., Green, C. J. & Motterlini, R. (2006). A carbon monoxide-releasing molecule (CORM-3) attenuates lipopolysaccharide- and interferon-gamma-induced inflammation in microglia. *Pharmacol Rep* **58 Suppl**: 132-144.

Bathoorn, E., Slebos, D. J., Postma, D. S., Koeter, G. H., van Oosterhout, A. J., van der Toorn, M., Boezen, H. M. & Kerstjens, H. A. (2007). Anti-inflammatory effects of inhaled carbon monoxide in patients with COPD: a pilot study. *Eur Respir J* **30**: 1131-1137.

Berglin, E. H. & Carlsson, J. (1985). Potentiation by sulfide of hydrogen peroxide-induced killing of *Escherichia coli*. *Infect Immun* **49**: 538-543.

Bernard, C. (1865). Introduction a l'etude de la medecine experimentale. Paris, J. B. Bailliere et Fils: 85-92, 101-104, 107-112, 265-301. A. S. Weber.

Berthold, D. A., Voevodskaya, N., Stenmark, P., Graslund, A. & Nordlund, P. (2002). EPR studies of the mitochondrial alternative oxidase. Evidence for a diiron carboxylate center. *J Biol Chem* **277**: 43608-43614.

Bibb, L. A., King, N. D., Kunkle, C. A. & Schmitt, M. P. (2005). Analysis of a heme-dependent signal transduction system in *Corynebacterium diphtheriae*: deletion of the *chrAS* genes results in heme sensitivity and diminished heme-dependent activation of the *hmuO* promoter. *Infect Immun* **73**: 7406-7412.

Bibb, L. A., Kunkle, C. A. & Schmitt, M. P. (2007). The ChrA-ChrS and HrrA-HrrS signal transduction systems are required for activation of the *hmuO* promoter and repression of the *hemA* promoter in *Corynebacterium diphtheriae*. *Infect Immun* **75**: 2421-2431.

Bloch, K. D., Ichinose, F., Roberts, J. D., Jr. & Zapol, W. M. (2007). Inhaled NO as a therapeutic agent. *Cardiovasc Res* **75**: 339-348.

Boczkowski, J., Poderoso, J. J. & Motterlini, R. (2006). CO-metal interaction: Vital signaling from a lethal gas. *Trends Biochem Sci* **31**: 614-621.

Boissiere, J., Lemaire, M. C., Antier, D., Courteix, D. & Bonnet, P. (2006). Exercise and vasorelaxing effects of CO-releasing molecules in hypertensive rats. *Med Sci Sports Exerc* **38**: 652-659.

Bonam, D., Lehman, L., Roberts, G. P. & Ludden, P. W. (1989). Regulation of carbon monoxide dehydrogenase and hydrogenase in *Rhodospirillum rubrum*: effects of CO and oxygen on synthesis and activity. *J Bacteriol* **171**: 3102-3107.

Borisov, V. B. (2008). Interaction of *bd*-type quinol oxidase from *Escherichia coli* and carbon monoxide: heme *d* binds CO with high affinity. *Biochemistry (Mosc)* **73**: 14-22.

Botros, F. T. & Navar, L. G. (2006). Interaction between endogenously produced carbon monoxide and nitric oxide in regulation of renal afferent arterioles. *Am J Physiol Heart Circ Physiol* **291**: H2772-2778.

Brooks, J. C., Brashears, M. M., Miller, M. F., Hoyle, A. R., Kellermeier, J. D. & Mehaffey, J. M. (2006). The spoilage characteristics of ground beef packaged in high-oxygen and low-oxygen modified atmosphere packages. Proceedings of the Reciprocal Meat Conference, University of Illinois at Urbana-Champaign, Urbana-Champaign.

Brouard, S., Berberat, P. O., Tobiasch, E., Seldon, M. P., Bach, F. H. & Soares, M. P. (2002). Heme oxygenase-1-derived carbon monoxide requires the activation of transcription factor NF-kappa B to protect endothelial cells from tumor necrosis factor-alpha-mediated apoptosis. *J Biol Chem* **277**: 17950-17961.

Bruggemann, H., Bauer, R., Raffestin, S. & Gottschalk, G. (2004). Characterization of a heme oxygenase of *Clostridium tetani* and its possible role in oxygen tolerance. *Arch Microbiol* **182**: 259-263.

Brune, B. & Ullrich, V. (1987). Inhibition of platelet aggregation by carbon monoxide is mediated by activation of guanylate cyclase. *Mol Pharmacol* **32**: 497-504.

Cairns, J. & Denhardt, D. T. (1968). Effect of cyanide and carbon monoxide on the replication of bacterial DNA *in vivo*. *J Mol Biol* **36**: 335-342.

Cargill, R. W., Ed. (1990). Carbon monoxide. IUPAC Solubility data series. Oxford, Pergamon Press.

Caumartin, Y., Stephen, J., Deng, J. P., Lian, D., Lan, Z., Liu, W., Garcia, B., Jevnikar, A. M., Wang, H., Cepinskas, G. & Luke, P. P. (2011). Carbon monoxide-releasing molecules protect against ischemia-reperfusion injury during kidney transplantation. *Kidney Int* **79**: 1080-1089.

Cepinskas, G., Katada, K., Bihari, A. & Potter, R. F. (2008). Carbon monoxide liberated from carbon monoxide-releasing molecule CORM-2 attenuates inflammation in the liver of septic mice. *Am J Physiol Gastrointest Liver Physiol* **294**: G184-191.

Chahal, H. K., Dai, Y., Saini, A., Ayala-Castro, C. & Outten, F. W. (2009). The SufBCD Fe-S scaffold complex interacts with SufA for Fe-S cluster transfer. *Biochemistry* **48**: 10644-10653.

Chance, B., Erecinska, M. & Wagner, M. (1970). Mitochondrial responses to carbon monoxide toxicity. *Ann N Y Acad Sci* **174**: 193-204.

Chance, B., Smith, L. & Castor, L. (1953). New methods for the study of the carbon monoxide compounds of respiratory enzymes. *Biochim Biophys Acta* **12**: 289-298.

Chin, B. Y. & Otterbein, L. E. (2009). Carbon monoxide is a poison... to microbes! CO as a bactericidal molecule. *Curr Opin Pharmacol* **9**: 490-500.

Chlopicki, S., Olszanecki, R., Marcinkiewicz, E., Lomnicka, M. & Motterlini, R. (2006). Carbon monoxide released by CORM-3 inhibits human platelets by a mechanism independent of soluble guanylate cyclase. *Cardiovasc Res* **71**: 393-401.

Chung, S. W., Hall, S. R. & Perrella, M. A. (2009). Role of haem oxygenase-1 in microbial host defence. *Cell Microbiol* **11**: 199-207.

Chung, S. W., Liu, X., Macias, A. A., Baron, R. M. & Perrella, M. A. (2008). Heme oxygenase-1-derived carbon monoxide enhances the host defense response to microbial sepsis in mice. *J Clin Invest* **118**: 239-247.

Clark, J. E., Naughton, P., Shurey, S., Green, C. J., Johnson, T. R., Mann, B. E., Foresti, R. & Motterlini, R. (2003). Cardioprotective actions by a water-soluble carbon monoxide-releasing molecule. *Circ Res* **93**: e2-8.

Coburn, R. F. (1979). Mechanisms of carbon monoxide toxicity. *Prev Med* **8**: 310-322.

Coburn, R. F., Williams, W. J. & Forster, R. E. (1964). Effect of Erythrocyte Destruction on Carbon Monoxide Production in Man. *J Clin Invest* **43**: 1098-1103.

Cooper, C. E. & Brown, G. C. (2008). The inhibition of mitochondrial cytochrome oxidase by the gases carbon monoxide, nitric oxide, hydrogen cyanide and hydrogen sulfide: chemical mechanism and physiological significance. *J Bioenerg Biomembr* **40**: 533-539.

Coves, J., Eschenbrenner, M. & Fontecave, M. (1993). Sulfite reductase of *Escherichia coli* is a ferrisiderophore reductase. *Biochem Biophys Res Commun* **192**: 1403-1408.

Cremer, W. (1929). Reactions of carbon oxide with metal compounds of cysteine. *Biochemische Zeitschrift* **206**: 228-239.

Crook, S. H., Mann, B. E., Meijer, A. J., Adams, H., Sawle, P., Scapens, D. & Motterlini, R. (2011). [Mn(CO)4{S2CNMe(CH2CO2H)}], a new water-soluble CO-releasing molecule. *Dalton Trans* **40**: 4230-4235.

Crosa, J. H. & Walsh, C. T. (2002). Genetics and assembly line enzymology of siderophore biosynthesis in bacteria. *Microbiol Mol Biol Rev* **66**: 223-249.

Cruz-Ramos, H., Crack, J., Wu, G., Hughes, M. N., Scott, C., Thomson, A. J., Green, J. & Poole, R. K. (2002). NO sensing by FNR: regulation of the *Escherichia coli* NO-detoxifying flavohaemoglobin, Hmp. *EMBO J* **21**: 3235-3244.

D'Amico, G., Lam, F., Hagen, T. & Moncada, S. (2006). Inhibition of cellular respiration by endogenously produced carbon monoxide. *J Cell Sci* **119**: 2291-2298.

D'Autreaux, B., Touati, D., Bersch, B., Latour, J. M. & Michaud-Soret, I. (2002). Direct inhibition by nitric oxide of the transcriptional ferric uptake regulation protein via nitrosylation of the iron. *Proc Natl Acad Sci U S A* **99**: 16619-16624.

Datsenko, K. A. & Wanner, B. L. (2000). One-step inactivation of chromosomal genes in *Escherichia coli* K-12 using PCR products. *Proc Natl Acad Sci U S A* **97**: 6640-6645.

David, G., Blondeau, K., Schiltz, M., Penel, S. & Lewit-Bentley, A. (2003). YodA from *Escherichia coli* is a metal-binding, lipocalin-like protein. *J Biol Chem* **278**: 43728-43735.

Davidge, K. S., Motterlini, R., Mann, B. E., Wilson, J. L. & Poole, R. K. (2009a). Carbon monoxide in biology and microbiology: surprising roles for the "Detroit perfume". *Adv Microb Physiol* **56**: 85-167.

Davidge, K. S., Sanguinetti, G., Yee, C. H., Cox, A. G., McLeod, C. W., Monk, C. E., Mann, B. E., Motterlini, R. & Poole, R. K. (2009b). Carbon monoxide-releasing antibacterial molecules target respiration and global transcriptional regulators. *J Biol Chem* **284**: 4516-4524.

Davydova, M. N. & Tarasova, N. B. (2005). Carbon monoxide inhibits superoxide dismutase and stimulates reactive oxygen species production by *Desulfovibrio desulfuricans* 1388. *Anaerobe* **11**: 335-338.

Degn, H., Lilleor, M. & Iversen, J. J. (1973). The occurrence of a stepwise-decreasing respiration rate during oxidative assimilation of different substrates by resting *Klebsiella aerogenes* in a system open to oxygen. *Biochem J* **136**: 1097-1104.

Degn, H., Lundsgaard, J. S., Petersen, L. C. & Ormicki, A. (1980). Polarographic measurement of steady state kinetics of oxygen uptake by biochemical samples. *Methods Biochem Anal* **26**: 47-77.

Delgado-Nixon, V. M., Gonzalez, G. & Gilles-Gonzalez, M. A. (2000). Dos, a heme-binding PAS protein from *Escherichia coli*, is a direct oxygen sensor. *Biochemistry* **39**: 2685-2691.

Desmard, M., Davidge, K. S., Bouvet, O., Morin, D., Roux, D., Foresti, R., Ricard, J. D., Denamur, E., Poole, R. K., Montravers, P., Motterlini, R. & Boczkowski, J. (2009). A carbon monoxide-releasing molecule (CORM-3) exerts bactericidal activity against *Pseudomonas aeruginosa* and improves survival in an animal model of bacteraemia. *FASEB J* **23**: 1023-1031.

Desmard, M., Foresti, R., Morin, D., Dagoussat, M., Berdeaux, A., Denamur, E., Crook, S. H., Mann, B. E., Scapens, D., Montravers, P., Boczkowski, J. & Motterlini, R. (2012). Differential antibacterial activity against *Pseudomonas aeruginosa* by carbon monoxide-releasing molecules. *Antioxid Redox Signal* **16**: 153-163.

Ding, B., Smith, E. S. & Ding, H. (2005). Mobilization of the iron centre in IscA for the iron-sulphur cluster assembly in IscU. *Biochem J* **389**: 797-802.

Ding, H. & Clark, R. J. (2004). Characterization of iron binding in IscA, an ancient iron-sulphur cluster assembly protein. *Biochem J* **379**: 433-440.

Dunn, A. K., Karr, E. A., Wang, Y., Batton, A. R., Ruby, E. G. & Stabb, E. V. (2010). The alternative oxidase (AOX) gene in *Vibrio fischeri* is controlled by NsrR and upregulated in response to nitric oxide. *Mol Microbiol* **77**: 44-55.

Edwards, C. & Lloyd, D. (1973). Terminal oxidases and carbon monoxide-reacting haemoproteins in the trypanosomatid, *Crithidia fasciculata*. *J Gen Microbiol* **79**: 275-284.

Eisenstein, R. S., Garcia-Mayol, D., Pettingell, W. & Munro, H. N. (1991). Regulation of ferritin and heme oxygenase synthesis in rat fibroblasts by different forms of iron. *Proc Natl Acad Sci U S A* **88**: 688-692.

Engel, R. R., Matsen, J. M., Chapman, S. S. & Schwartz, S. (1972). Carbon monoxide production from heme compounds by bacteria. *J Bacteriol* **112**: 1310-1315.

Eschenbrenner, M., Coves, J. & Fontecave, M. (1994). Ferric reductases in *Escherichia coli*: the contribution of the haemoglobin-like protein. *Biochem Biophys Res Commun* **198**: 127-131.

Ferris, C. D., Jaffrey, S. R., Sawa, A., Takahashi, M., Brady, S. D., Barrow, R. K., Tysoe, S. A., Wolosker, H., Baranano, D. E., Dore, S., Poss, K. D. & Snyder, S. H. (1999). Haem oxygenase-1 prevents cell death by regulating cellular iron. *Nat Cell Biol* **1**: 152-157.

Finazzi-Agro, A., Zolla, L., Flamigni, L., Kuiper, H. A. & Brunori, M. (1982). Spectroscopy of (carbon monoxy)hemocyanins. Phosphorescence of the binuclear carbonylated copper centers. *Biochemistry* **21**: 415-418.

Flatley, J., Barrett, J., Pullan, S. T., Hughes, M. N., Green, J. & Poole, R. K. (2005). Transcriptional responses of *Escherichia coli* to *S*-nitrosoglutathione under defined chemostat conditions reveal major changes in methionine biosynthesis. *J Biol Chem* **280**: 10065-10072.

Flemming, H. C. & Wingender, J. (2010). The biofilm matrix. *Nat Rev Microbiol* **8**: 623-633.

Foresti, R., Bani-Hani, M. G. & Motterlini, R. (2008). Use of carbon monoxide as a therapeutic agent: promises and challenges. *Intensive Care Med* **34**: 649-658.

Foresti, R., Hammad, J., Clark, J. E., Johnson, T. R., Mann, B. E., Friebe, A., Green, C. J. & Motterlini, R. (2004). Vasoactive properties of CORM-3, a novel water-soluble carbon monoxide-releasing molecule. *Br J Pharmacol* **142**: 453-460.

Freitas, A., Alves-Filho, J. C., Secco, D. D., Neto, A. F., Ferreira, S. H., Barja-Fidalgo, C. & Cunha, F. Q. (2006). Heme oxygenase/carbon monoxide-biliverdin pathway down regulates neutrophil rolling, adhesion and migration in acute inflammation. *Br J Pharmacol* **149**: 345-354.

Friebe, A., Schultz, G. & Koesling, D. (1996). Sensitizing soluble guanylyl cyclase to become a highly CO-sensitive enzyme. *EMBO J* **15**: 6863-6868.

Fukuto, J. M., Carrington, S. J., Tantillo, D. J., Harrison, J. G., Ignarro, L. J., Freeman, B. A., Chen, A. & Wink, D. A. (2012). Small molecule signaling agents: the integrated chemistry and biochemistry of nitrogen oxides, oxides of carbon, dioxygen, hydrogen sulfide, and their derived species. *Chem Res Toxicol* **25**: 769-793.

Furchgott, R. F. & Jothianandan, D. (1991). Endothelium-dependent and -independent vasodilation involving cyclic GMP: relaxation induced by nitric oxide, carbon monoxide and light. *Blood Vessels* **28**: 52-61.

Furci, L. M., Lopes, P., Eakanunkul, S., Zhong, S., MacKerell, A. D., Jr. & Wilks, A. (2007). Inhibition of the bacterial heme oxygenases from *Pseudomonas aeruginosa* and *Neisseria meningitidis*: novel antimicrobial targets. *J Med Chem* **50**: 3804-3813.

Gardner, P. R., Gardner, A. M., Martin, L. A. & Salzman, A. L. (1998). Nitric oxide dioxygenase: an enzymic function for flavohemoglobin. *Proc Natl Acad Sci U S A* **95**: 10378-10383.

Gibson, J. F., Poole, R. K., Hughes, M. N. & Rees, J. F. (1982). A dimeric complex of ruthenium: a new inhibitor of respiration-driven calcium transport in Escherichia coli K12. *J Gen Microbiol* **128**: 2211-2214.

Gibson, Q. H., Greenwood, C., Wharton, D. C. & Palmer, G. (1965). The reaction of cytochrome oxidase with cytochrome *c*. *J Biol Chem* **240**: 888-894.

Gilberthorpe, N. J. & Poole, R. K. (2008). Nitric oxide homeostasis in *Salmonella typhimurium*: roles of respiratory nitrate reductase and flavohemoglobin. *J Biol Chem* **283**: 11146-11154.

Goebel, U., Siepe, M., Mecklenburg, A., Stein, P., Roesslein, M., Schwer, C. I., Schmidt, R., Doenst, T., Geiger, K. K., Pahl, H. L., Schlensak, C. & Loop, T. (2008). Carbon monoxide inhalation reduces pulmonary inflammatory response during cardiopulmonary bypass in pigs. *Anesthesiology* **108**: 1025-1036.

Goebel, U., Siepe, M., Schwer, C. I., Schibilsky, D., Brehm, K., Priebe, H. J., Schlensak, C. & Loop, T. (2011). Postconditioning of the lungs with inhaled carbon monoxide after cardiopulmonary bypass in pigs. *Anesth Analg* **112**: 282-291.

Goldbaum, L. R., Ramirez, R. G. & Absalon, K. B. (1975). What is the mechanism of carbon monoxide toxicity? *Aviat Space Environ Med* **46**: 1289-1291.

Gotschlich, E. C., Goldschneider, I. & Artenstein, M. S. (1969a). Human immunity to the meningococcus. IV. Immunogenicity of group A and group C meningococcal polysaccharides in human volunteers. *J Exp Med* **129**: 1367-1384.

Gotschlich, E. C., Liu, T. Y. & Artenstein, M. S. (1969b). Human immunity to the meningococcus. 3. Preparation and immunochemical properties of the group A, group B, and group C meningococcal polysaccharides. *J Exp Med* **129**: 1349-1365.

Graham, A. I., Sanguinetti, G., Bramall, N., McLeod, C. W. & Poole, R. K. (2012). Dynamics of a starvation-to-surfeit shift: a transcriptomic and modelling analysis of the bacterial response to zinc reveals transient behaviour of the Fur and SoxS regulators. *Microbiology* **158**: 284-292.

Gullotta, F., di Masi, A. & Ascenzi, P. (2012). Carbon monoxide: an unusual drug. *IUBMB Life* **64**: 378-386.

Guo, Y., Guo, G., Mao, X., Zhang, W., Xiao, J., Tong, W., Liu, T., Xiao, B., Liu, X., Feng, Y. & Zou, Q. (2008). Functional identification of HugZ, a heme oxygenase from *Helicobacter pylori*. *BMC Microbiol* **8**: 226.

Guo, Y., Stein, A. B., Wu, W. J., Tan, W., Zhu, X., Li, Q. H., Dawn, B., Motterlini, R. & Bolli, R. (2004). Administration of a CO-releasing molecule at the time of reperfusion reduces infarct size *in vivo*. *Am J Physiol Heart Circ Physiol* **286**: H1649-1653.

Gusarov, I., Shatalin, K., Starodubtseva, M. & Nudler, E. (2009). Endogenous nitric oxide protects bacteria against a wide spectrum of antibiotics. *Science* **325**: 1380-1384.

Haddock, B. A. & Downie, J. A. (1974). The reconstitution of functional respiratory chains in membranes from electron-transport-deficient mutants of *Escherichia coli* as demonstrated by quenching of atebrin fluorescence. *Biochem J* **142**: 703-706.

Haddock, B. A. & Schairer, H. U. (1973). Electron-transport chains of *Escherichia coli*. Reconstitution of respiration in a 5-aminolaevulinic acid-requiring mutant. *Eur J Biochem* **35**: 34-45.

Hantke, K. (1983). Identification of an iron uptake system specific for coprogen and rhodotorulic acid in *Escherichia coli* K12. *Mol Gen Genet* **191**: 301-306.

Hanto, D. W., Maki, T., Yoon, M. H., Csizmadia, E., Chin, B. Y., Gallo, D., Konduru, B., Kuramitsu, K., Smith, N. R., Berssenbrugge, A., Attanasio, C., Thomas, M., Wegiel, B. &

Otterbein, L. E. (2010). Intraoperative administration of inhaled carbon monoxide reduces delayed graft function in kidney allografts in Swine. *Am J Transplant* **10**: 2421-2430.

Hasegawa, U., van der Vlies, A. J., Simeoni, E., Wandrey, C. & Hubbell, J. A. (2010). Carbon monoxide-releasing micelles for immunotherapy. *J Am Chem Soc* **132**: 18273-18280.

Hayashi, S., Omata, Y., Sakamoto, H., Higashimoto, Y., Hara, T., Sagara, Y. & Noguchi, M. (2004). Characterization of rat heme oxygenase-3 gene. Implication of processed pseudogenes derived from heme oxygenase-2 gene. *Gene* **336**: 241-250.

Heinemann, I. U., Jahn, M. & Jahn, D. (2008). The biochemistry of heme biosynthesis. *Arch Biochem Biophys* **474**: 238-251.

Hendgen-Cotta, U. B., Merx, M. W., Shiva, S., Schmitz, J., Becher, S., Klare, J. P., Steinhoff, H. J., Goedecke, A., Schrader, J., Gladwin, M. T., Kelm, M. & Rassaf, T. (2008). Nitrite reductase activity of myoglobin regulates respiration and cellular viability in myocardial ischemia-reperfusion injury. *Proc Natl Acad Sci U S A* **105**: 10256-10261.

Hou, S., Heinemann, S. H. & Hoshi, T. (2009). Modulation of BKCa channel gating by endogenous signaling molecules. *Physiology (Bethesda)* **24**: 26-35.

Hou, S., Xu, R., Heinemann, S. H. & Hoshi, T. (2008). The RCK1 high-affinity Ca2+ sensor confers carbon monoxide sensitivity to Slo1 BK channels. *Proc Natl Acad Sci U S A* **105**: 4039-4043.

Ibrahim, M., Kuchinskas, M., Youn, H., Kerby, R. L., Roberts, G. P., Poulos, T. L. & Spiro, T. G. (2007). Mechanism of the CO-sensing heme protein CooA: new insights from the truncated heme domain and UVRR spectroscopy. *J Inorg Biochem* **101**: 1776-1785.

Ioannidis, N., Cooper, C. E. & Poole, R. K. (1992). Spectroscopic studies on an oxygen-binding haemoglobin-like flavohaemoprotein from *Escherichia coli*. *Biochem J* **288 (Pt 2)**: 649-655.

Jackson, R. J., Elvers, K. T., Lee, L. J., Gidley, M. D., Wainwright, L. M., Lightfoot, J., Park, S. F. & Poole, R. K. (2007). Oxygen reactivity of both respiratory oxidases in *Campylobacter jejuni*: the *cydAB* genes encode a cyanide-resistant, low-affinity oxidase that is not of the cytochrome *bd* type. *J Bacteriol* **189**: 1604-1615.

Jara-Oseguera, A., Ishida, I. G., Rangel-Yescas, G. E., Espinosa-Jalapa, N., Perez-Guzman, J. A., Elias-Vinas, D., Le Lagadec, R., Rosenbaum, T. & Islas, L. D. (2011). Uncoupling charge movement from channel opening in voltage-gated potassium channels by ruthenium complexes. *J Biol Chem* **286**: 16414-16425.

Johnson, T. R., Mann, B. E., Teasdale, I. P., Adams, H., Foresti, R., Green, C. J. & Motterlini, R. (2007). Metal carbonyls as pharmaceuticals? [Ru(CO)3Cl(glycinate)], a CO-releasing molecule with an extensive aqueous solution chemistry. *Dalton Trans*: 1500-1508.

Jones, C. W., Poole, R. K. (1985). The analysis of cytochromes. Methods in Microbiology. G. Gottschalk. London, Academic Press. **18:** 285-328.

Justino, M. C., Almeida, C. C., Goncalves, V. L., Teixeira, M. & Saraiva, L. M. (2006). *Escherichia coli* YtfE is a di-iron protein with an important function in assembly of iron-sulphur clusters. *FEMS Microbiol Lett* **257**: 278-284.

Justino, M. C., Almeida, C. C., Teixeira, M. & Saraiva, L. M. (2007). *Escherichia coli* di-iron YtfE protein is necessary for the repair of stress-damaged iron-sulfur clusters. *J Biol Chem* **282**: 10352-10359.

Kajimura, M., Fukuda, R., Bateman, R. M., Yamamoto, T. & Suematsu, M. (2010). Interactions of multiple gas-transducing systems: hallmarks and uncertainties of CO, NO, and H2S gas biology. *Antioxid Redox Signal* **13**: 157-192.

Kalnenieks, U., Galinina, N., Bringer-Meyer, S. & Poole, R. K. (1998). Membrane D-lactate oxidase in *Zymomonas mobilis*: evidence for a branched respiratory chain. *FEMS Microbiol Lett* **168**: 91-97.

Kanehisa, M. & Goto, S. (2000). KEGG: kyoto encyclopedia of genes and genomes. *Nucleic Acids Res* **28**: 27-30.

Kanehisa, M., Goto, S., Sato, Y., Furumichi, M. & Tanabe, M. (2012). KEGG for integration and interpretation of large-scale molecular data sets. *Nucleic Acids Res* **40**: D109-114.

Karch, H., Tarr, P. I. & Bielaszewska, M. (2005). Enterohaemorrhagic *Escherichia coli* in human medicine. *Int J Med Microbiol* **295**: 405-418.

Keilin (1966). The History of Cell Respiration and Cytochrome, Cambridge University Press.

Kelly, A. F., Park, S. F., Bovill, R. & Mackey, B. M. (2001). Survival of *Campylobacter jejuni* during stationary phase: evidence for the absence of a phenotypic stationary-phase response. *Appl Environ Microbiol* **67**: 2248-2254.

Kerby, R. L., Hong, S. S., Ensign, S. A., Coppoc, L. J., Ludden, P. W. & Roberts, G. P. (1992). Genetic and physiological characterization of the *Rhodospirillum rubrum* carbon monoxide dehydrogenase system. *J Bacteriol* **174**: 5284-5294.

Kerby, R. L., Ludden, P. W. & Roberts, G. P. (1995). Carbon monoxide-dependent growth of *Rhodospirillum rubrum*. *J Bacteriol* **177**: 2241-2244.

Kerby, R. L., Youn, H. & Roberts, G. P. (2008). RcoM: a new single-component transcriptional regulator of CO metabolism in bacteria. *J Bacteriol* **190**: 3336-3343.

Kershaw, C. J., Brown, N. L. & Hobman, J. L. (2007). Zinc dependence of zinT (yodA) mutants and binding of zinc, cadmium and mercury by ZinT. *Biochem Biophys Res Commun* **364**: 66-71.

Kharitonov, V. G., Sharma, V. S., Pilz, R. B., Magde, D. & Koesling, D. (1995). Basis of guanylate cyclase activation by carbon monoxide. *Proc Natl Acad Sci U S A* **92**: 2568-2571.

Kim, B. H. G., G. M. (2008). Bacterial Physiology and Metabolism, Cambridge University Press.

Kim, H. P., Ryter, S. W. & Choi, A. M. (2006). CO as a cellular signaling molecule. *Annu Rev Pharmacol Toxicol* **46**: 411-449.

Kim, Y. M. & Hegeman, G. D. (1981). Electron transport system of an aerobic carbon monoxide-oxidizing bacterium. *J Bacteriol* **148**: 991-994.

King, G. M. (2006). Nitrate-dependent anaerobic carbon monoxide oxidation by aerobic CO-oxidizing bacteria. *FEMS Microbiol Ecol* **56**: 1-7.

King, G. M. & Weber, C. F. (2007). Distribution, diversity and ecology of aerobic CO-oxidizing bacteria. *Nat Rev Microbiol* **5**: 107-118.

Koneru, P. & Leffler, C. W. (2004). Role of cGMP in carbon monoxide-induced cerebral vasodilation in piglets. *Am J Physiol Heart Circ Physiol* **286**: H304-309.

Krenzelok, E. P., Roth, R. & Full, R. (1996). Carbon monoxide ... the silent killer with an audible solution. *Am J Emerg Med* **14**: 484-486.

Kuiper, H. A., Lerch, K., Brunori, M. & Finazzi Agro, A. (1980). Luminescence of the copper--carbon monoxide complex of *Neurospora tyrosinase*. *FEBS Lett* **111**: 232-234.

Kumar, A., Deshane, J. S., Crossman, D. K., Bolisetty, S., Yan, B. S., Kramnik, I., Agarwal, A. & Steyn, A. J. (2008). Heme oxygenase-1-derived carbon monoxide induces the *Mycobacterium tuberculosis* dormancy regulon. *J Biol Chem* **283**: 18032-18039.

Kumar, A., Toledo, J. C., Patel, R. P., Lancaster, J. R., Jr. & Steyn, A. J. (2007). *Mycobacterium tuberculosis* DosS is a redox sensor and DosT is a hypoxia sensor. *Proc Natl Acad Sci U S A* **104**: 11568-11573.

Kuo, M. M., Saimi, Y. & Kung, C. (2003). Gain-of-function mutations indicate that *Escherichia coli* Kch forms a functional K^+ conduit *in vivo*. *EMBO J* **22**: 4049-4058.

Lancel, S., Hassoun, S. M., Favory, R., Decoster, B., Motterlini, R. & Neviere, R. (2009). Carbon monoxide rescues mice from lethal sepsis by supporting mitochondrial energetic metabolism and activating mitochondrial biogenesis. *J Pharmacol Exp Ther* **329**: 641-648.

Lavitrano, M., Smolenski, R. T., Musumeci, A., Maccherini, M., Slominska, E., Di Florio, E., Bracco, A., Mancini, A., Stassi, G., Patti, M., Giovannoni, R., Froio, A., Simeone, F., Forni, M., Bacci, M. L., D'Alise, G., Cozzi, E., Otterbein, L. E., Yacoub, M. H., Bach, F. H. & Calise, F. (2004). Carbon monoxide improves cardiac energetics and safeguards the heart during reperfusion after cardiopulmonary bypass in pigs. *FASEB J* **18**: 1093-1095.

Lawford, H. G. & Garland, P. B. (1972). Proton translocation coupled to quinone reduction by reduced nicotinamide--adenine dinucleotide in rat liver and ox heart mitochondria. *Biochem J* **130**: 1029-1044.

Lawford, H. G. & Haddock, B. A. (1973). Respiration-driven proton translocation in *Escherichia coli*. *Biochem J* **136**: 217-220.

Lee, J. H., Yeo, W. S. & Roe, J. H. (2004). Induction of the *sufA* operon encoding Fe-S assembly proteins by superoxide generators and hydrogen peroxide: involvement of OxyR, IHF and an unidentified oxidant-responsive factor. *Mol Microbiol* **51**: 1745-1755.

Lee, J. W. & Helmann, J. D. (2007). Functional specialization within the Fur family of metalloregulators. *Biometals* **20**: 485-499.

Lee, L. J., Barrett, J. A. & Poole, R. K. (2005). Genome-wide transcriptional response of chemostat-cultured *Escherichia coli* to zinc. *J Bacteriol* **187**: 1124-1134.

Lee, P. J. & Otterbein, L. E., Eds. (2004). Carbon monoxide and signal transduction pathways. Signal Transduction and the Gasotransmitters. Totowa, New Jersey, Humana Press.

Li, H. & Jogl, G. (2007). Crystal structure of the zinc-binding transport protein ZnuA from *Escherichia coli* reveals an unexpected variation in metal coordination. *J Mol Biol* **368**: 1358-1366.

Li, L., Hsu, A. & Moore, P. K. (2009). Actions and interactions of nitric oxide, carbon monoxide and hydrogen sulphide in the cardiovascular system and in inflammation--a tale of three gases! *Pharmacol Ther* **123**: 386-400.

Li, L. & Moore, P. K. (2007). An overview of the biological significance of endogenous gases: new roles for old molecules. *Biochem Soc Trans* **35**: 1138-1141.

Lloyd, D., Edwards, S. W. & Chance, B. (1981). Carbon monoxide- and oxygen-reacting haemoproteins in the mitochondrial fraction from the soil amoeba *Acanthamoeba castellanii*. Studies at subzero temperatures. *Biochem J* **200**: 337-342.

Lo Iacono, L., Boczkowski, J., Zini, R., Salouage, I., Berdeaux, A., Motterlini, R. & Morin, D. (2011). A carbon monoxide-releasing molecule (CORM-3) uncouples mitochondrial respiration and modulates the production of reactive oxygen species. *Free Radic Biol Med* **50**: 1556-1564.

Madigan, M. T., Martinko, J. M. & Parker, J., Eds. (2003). Brock Biology of Microorganisms. 10th edn, London, Pearson Education, Inc.

Maines, M. D., Trakshel, G. M. & Kutty, R. K. (1986). Characterization of two constitutive forms of rat liver microsomal heme oxygenase. Only one molecular species of the enzyme is inducible. *J Biol Chem* **261**: 411-419.

Mann, B. E. (2010). Carbon Monoxide - an essential signalling molecule. Topics in Organometallic Chemistry. **32:** 247-285.

Mann, B. E. & Motterlini, R. (2007). CO and NO in medicine. *Chem Commun (Camb)*: 4197-4208.

Markwell, M. A., Haas, S. M., Bieber, L. L. & Tolbert, N. E. (1978). A modification of the Lowry procedure to simplify protein determination in membrane and lipoprotein samples. *Anal Biochem* **87**: 206-210.

Martin, E., Berka, V., Bogatenkova, E., Murad, F. & Tsai, A. L. (2006). Ligand selectivity of soluble guanylyl cyclase: effect of the hydrogen-bonding tyrosine in the distal heme pocket on binding of oxygen, nitric oxide, and carbon monoxide. *J Biol Chem* **281**: 27836-27845.

Masse, E. & Gottesman, S. (2002). A small RNA regulates the expression of genes involved in iron metabolism in *Escherichia coli*. *Proc Natl Acad Sci U S A* **99**: 4620-4625.

Matsuda, N. M., Miller, S. M., Sha, L., Farrugia, G. & Szurszewski, J. H. (2004). Mediators of non-adrenergic non-cholinergic inhibitory neurotransmission in porcine jejunum. *Neurogastroenterol Motil* **16**: 605-612.

Matzanke, B. F., Anemuller, S., Schunemann, V., Trautwein, A. X. & Hantke, K. (2004). FhuF, part of a siderophore-reductase system. *Biochemistry* **43**: 1386-1392.

McCoubrey, W. K., Jr., Huang, T. J. & Maines, M. D. (1997). Isolation and characterization of a cDNA from the rat brain that encodes hemoprotein heme oxygenase-3. *Eur J Biochem* **247**: 725-732.

McLean, S., Bowman, L. A., Sanguinetti, G., Read, R. C. & Poole, R. K. (2010). Peroxynitrite toxicity in *Escherichia coli* K12 elicits expression of oxidative stress responses and protein nitration and nitrosylation. *J Biol Chem* **285**: 20724-20731.

McLean, S., Mann, B. E. & Poole, R. K. (2012). Sulfite species enhance carbon monoxide release from CO-releasing molecules: Implications for the deoxymyoglobin assay of activity. *Anal Biochem* **427**: 36-40.

Meister, K., Niesel, J., Schatzschneider, U., Metzler-Nolte, N., Schmidt, D. A. & Havenith, M. (2010). Label-free imaging of metal-carbonyl complexes in live cells by Raman microspectroscopy. *Angew Chem Int Ed Engl* **49**: 3310-3312.

Migita, C. T., Zhang, X. & Yoshida, T. (2003). Expression and characterization of cyanobacterium heme oxygenase, a key enzyme in the phycobilin synthesis. Properties of the heme complex of recombinant active enzyme. *Eur J Biochem* **270**: 687-698.

Mihara, H. & Esaki, N. (2002). Bacterial cysteine desulfurases: their function and mechanisms. *Appl Microbiol Biotechnol* **60**: 12-23.

Miller, J. H. (1972). Experiments in Molecular Genetics. N.Y., Cold Spring Harbor Laboratory Press

Miller, J. H. (1992). A Short Course in Bacterial Genetics, Cold Spring Harbor Laboratory Press.

Mims, M. P., Porras, A. G., Olson, J. S., Noble, R. W. & Peterson, J. A. (1983). Ligand binding to heme proteins. An evaluation of distal effects. *J Biol Chem* **258**: 14219-14232.

Miro, O., Casademont, J., Barrientos, A., Urbano-Marquez, A. & Cardellach, F. (1998). Mitochondrial cytochrome *c* oxidase inhibition during acute carbon monoxide poisoning. *Pharmacol Toxicol* **82**: 199-202.

Mitchell, L. A., Channell, M. M., Royer, C. M., Ryter, S. W., Choi, A. M. & McDonald, J. D. (2010). Evaluation of inhaled carbon monoxide as an anti-inflammatory therapy in a nonhuman primate model of lung inflammation. *Am J Physiol Lung Cell Mol Physiol* **299**: L891-897.

Mitchell, P. & Moyle, J. (1967). Respiration-driven proton translocation in rat liver mitochondria. *Biochem J* **105**: 1147-1162.

Mittal, R., Gonzalez-Gomez, I., Goth, K. A. & Prasadarao, N. V. (2010). Inhibition of inducible nitric oxide controls pathogen load and brain damage by enhancing phagocytosis of *Escherichia coli* K1 in neonatal meningitis. *Am J Pathol* **176**: 1292-1305.

Morse, D., Pischke, S. E., Zhou, Z., Davis, R. J., Flavell, R. A., Loop, T., Otterbein, S. L., Otterbein, L. E. & Choi, A. M. (2003). Suppression of inflammatory cytokine production by carbon monoxide involves the JNK pathway and AP-1. *J Biol Chem* **278**: 36993-36998.

Motterlini, R., Clark, J. E., Foresti, R., Sarathchandra, P., Mann, B. E. & Green, C. J. (2002). Carbon monoxide-releasing molecules: characterization of biochemical and vascular activities. *Circ Res* **90**: E17-24.

Motterlini, R., Mann, B. E. & Foresti, R. (2005a). Therapeutic applications of carbon monoxide-releasing molecules. *Expert Opin Investig Drugs* **14**: 1305-1318.

Motterlini, R., Mann, B. E., Johnson, T. R., Clark, J. E., Foresti, R. & Green, C. J. (2003). Bioactivity and pharmacological actions of carbon monoxide-releasing molecules. *Curr Pharm Des* **9**: 2525-2539.

Motterlini, R. & Otterbein, L. E. (2010). The therapeutic potential of carbon monoxide. *Nat Rev Drug Discov* **9**: 728-743.

Motterlini, R., Sawle, P., Hammad, J., Bains, S., Alberto, R., Foresti, R. & Green, C. J. (2005b). CORM-A1: a new pharmacologically active carbon monoxide-releasing molecule. *FASEB J* **19**: 284-286.

Murray, T. S., Okegbe, C., Gao, Y., Kazmierczak, B. I., Motterlini, R., Dietrich, L. E. & Bruscia, E. M. (2012). The carbon monoxide releasing molecule CORM-2 attenuates *Pseudomonas aeruginosa* biofilm formation. *PLoS One* **7**: e35499.

Nakao, A., Faleo, G., Shimizu, H., Nakahira, K., Kohmoto, J., Sugimoto, R., Choi, A. M., McCurry, K. R., Takahashi, T. & Murase, N. (2008). *Ex vivo* carbon monoxide prevents cytochrome P450 degradation and ischemia/reperfusion injury of kidney grafts. *Kidney Int* **74**: 1009-1016.

Nakao, A., Toyokawa, H., Tsung, A., Nalesnik, M. A., Stolz, D. B., Kohmoto, J., Ikeda, A., Tomiyama, K., Harada, T., Takahashi, T., Yang, R., Fink, M. P., Morita, K., Choi, A. M. & Murase, N. (2006). *Ex vivo* application of carbon monoxide in University of Wisconsin solution to prevent intestinal cold ischemia/reperfusion injury. *Am J Transplant* **6**: 2243-2255.

Neto, J. S., Nakao, A., Kimizuka, K., Romanosky, A. J., Stolz, D. B., Uchiyama, T., Nalesnik, M. A., Otterbein, L. E. & Murase, N. (2004). Protection of transplant-induced renal ischemia-reperfusion injury with carbon monoxide. *Am J Physiol Renal Physiol* **287**: F979-989.

Nicholls, D. G. & Ferguson, S. J. (2002). Bioenergetics 3. London, Academic Press.

Nobre, L. S., Al-Shahrour, F., Dopazo, J. & Saraiva, L. M. (2009). Exploring the antimicrobial action of a carbon monoxide-releasing compound through whole-genome transcription profiling of *Escherichia coli*. *Microbiology* **155**: 813-824.

Nobre, L. S., Seixas, J. D., Romao, C. C. & Saraiva, L. M. (2007). Antimicrobial action of carbon monoxide-releasing compounds. *Antimicrob Agents Chemother* **51**: 4303-4307.

O'Brian, M. R. & Thony-Meyer, L. (2002). Biochemistry, regulation and genomics of haem biosynthesis in prokaryotes. *Adv Microb Physiol* **46**: 257-318.

Oelgeschlager, E. & Rother, M. (2008). Carbon monoxide-dependent energy metabolism in anaerobic bacteria and archaea. *Arch Microbiol* **190**: 257-269.

Otterbein, L. E., Bach, F. H., Alam, J., Soares, M., Tao Lu, H., Wysk, M., Davis, R. J., Flavell, R. A. & Choi, A. M. (2000). Carbon monoxide has anti-inflammatory effects involving the mitogen-activated protein kinase pathway. *Nat Med* **6**: 422-428.

Otterbein, L. E., Mantell, L. L. & Choi, A. M. (1999). Carbon monoxide provides protection against hyperoxic lung injury. *Am J Physiol* **276**: L688-694.

Otterbein, L. E., May, A. & Chin, B. Y. (2005). Carbon monoxide increases macrophage bacterial clearance through Toll-like receptor (TLR)4 expression. *Cell Mol Biol (Noisy-le-grand)* **51**: 433-440.

Outten, F. W., Djaman, O. & Storz, G. (2004). A *suf* operon requirement for Fe-S cluster assembly during iron starvation in *Escherichia coli*. *Mol Microbiol* **52**: 861-872.

Overton, T. W., Justino, M. C., Li, Y., Baptista, J. M., Melo, A. M., Cole, J. A. & Saraiva, L. M. (2008). Widespread distribution in pathogenic bacteria of di-iron proteins that repair oxidative and nitrosative damage to iron-sulfur centers. *J Bacteriol* **190**: 2004-2013.

Pae, H. O., Oh, G. S., Choi, B. M., Chae, S. C., Kim, Y. M., Chung, K. R. & Chung, H. T. (2004). Carbon monoxide produced by heme oxygenase-1 suppresses T cell proliferation via inhibition of IL-2 production. *J Immunol* **172**: 4744-4751.

Park, S. W., Hwang, E. H., Park, H., Kim, J. A., Heo, J., Lee, K. H., Song, T., Kim, E., Ro, Y. T., Kim, S. W. & Kim, Y. M. (2003). Growth of mycobacteria on carbon monoxide and methanol. *J Bacteriol* **185**: 142-147.

Park, S. W., Song, T., Kim, S. Y., Kim, E., Oh, J. I., Eom, C. Y. & Kim, Y. M. (2007). Carbon monoxide dehydrogenase in mycobacteria possesses a nitric oxide dehydrogenase activity. *Biochem Biophys Res Commun* **362**: 449-453.

Parr, S. R., Wilson, M. T. & Greenwood, C. (1975). The reaction of *Pseudomonas aeruginosa* cytochrome *c* oxidase with carbon monoxide. *Biochem J* **151**: 51-59.

Parshina, S. N., Sipma, J., Nakashimada, Y., Henstra, A. M., Smidt, H., Lysenko, A. M., Lens, P. N., Lettinga, G. & Stams, A. J. (2005). *Desulfotomaculum carboxydivorans* sp. nov., a novel sulfate-reducing bacterium capable of growth at 100% CO. *Int J Syst Evol Microbiol* **55**: 2159-2165.

Patzer, S. I. & Hantke, K. (1998). The ZnuABC high-affinity zinc uptake system and its regulator Zur in *Escherichia coli*. *Mol Microbiol* **28**: 1199-1210.

Pena, A. C., Penacho, N., Mancio-Silva, L., Neres, R., Seixas, J. D., Fernandes, A. C., Romao, C. C., Mota, M. M., Bernardes, G. J. & Pamplona, A. (2012). A novel carbon monoxide-releasing molecule fully protects mice from severe malaria. *Antimicrob Agents Chemother* **56**: 1281-1290.

Pendrak, M. L., Chao, M. P., Yan, S. S. & Roberts, D. D. (2004a). Heme oxygenase in *Candida albicans* is regulated by hemoglobin and is necessary for metabolism of exogenous heme and hemoglobin to alpha-biliverdin. *J Biol Chem* **279**: 3426-3433.

Pendrak, M. L., Yan, S. S. & Roberts, D. D. (2004b). Sensing the host environment: recognition of hemoglobin by the pathogenic yeast *Candida albicans*. *Arch Biochem Biophys* **426**: 148-156.

Pitchumony, T. S., Spingler, B., Motterlini, R. & Alberto, R. (2010). Syntheses, structural characterization and CO releasing properties of boranocarbonate [H3BCO2H]- derivatives. *Org Biomol Chem* **8**: 4849-4854.

Policar, C., Waern, J. B., Plamont, M. A., Clede, S., Mayet, C., Prazeres, R., Ortega, J. M., Vessieres, A. & Dazzi, A. (2010). Subcellular IR Imaging of a Metal-Carbonyl Moiety Using Photothermally Induced Resonance. *Angew Chem Int Ed Engl*.

Poole, R. K., Anjum, M. F., Membrillo-Hernandez, J., Kim, S. O., Hughes, M. N. & Stewart, V. (1996). Nitric oxide, nitrite, and Fnr regulation of *hmp* (flavohemoglobin) gene expression in *Escherichia coli* K-12. *J Bacteriol* **178**: 5487-5492.

Poole, R. K. & Cook, G. M. (2000). Redundancy of aerobic respiratory chains in bacteria? Routes, reasons and regulation. *Adv Microb Physiol* **43**: 165-224.

Poole, R. K., Lloyd, D. & Kemp, R. B. (1973). Respiratory oscillations and heat evolution in synchronously dividing cultures of fission yeast *Schizosaccharomyces pombe* 972h. *Journal of General Microbiology* **77**: 209-220.

Poole, R. K., Rogers, N. J., D'Mello R, A., Hughes, M. N. & Orii, Y. (1997). *Escherichia coli* flavohaemoglobin (Hmp) reduces cytochrome *c* and Fe(III)-hydroxamate K by electron transfer from NADH via FAD: sensitivity of oxidoreductase activity to haem-bound dioxygen. *Microbiology* **143 (Pt 5)**: 1557-1565.

Poss, K. D. & Tonegawa, S. (1997). Reduced stress defense in heme oxygenase 1-deficient cells. *Proc Natl Acad Sci U S A* **94**: 10925-10930.

Protchenko, O. & Philpott, C. C. (2003). Regulation of intracellular heme levels by HMX1, a homologue of heme oxygenase, in *Saccharomyces cerevisiae*. *J Biol Chem* **278**: 36582-36587.

Puri, S. & O'Brian, M. R. (2006). The *hmuQ* and *hmuD* genes from *Bradyrhizobium japonicum* encode heme-degrading enzymes. *J Bacteriol* **188**: 6476-6482.

Puskarova, A., Ferianc, P., Kormanec, J., Homerova, D., Farewell, A. & Nystrom, T. (2002). Regulation of *yodA* encoding a novel cadmium-induced protein in *Escherichia coli*. *Microbiology* **148**: 3801-3811.

Queiroga, C. S., Almeida, A. S., Alves, P. M., Brenner, C. & Vieira, H. L. (2011). Carbon monoxide prevents hepatic mitochondrial membrane permeabilization. *BMC Cell Biol* **12**: 10.

Queiroga, C. S., Almeida, A. S. & Vieira, H. L. (2012). Carbon monoxide targeting mitochondria. *Biochem Res Int* **2012**: 749845.

Raffa, R. G. & Raivio, T. L. (2002). A third envelope stress signal transduction pathway in *Escherichia coli*. *Mol Microbiol* **45**: 1599-1611.

Ragsdale, S. W. (2004). Life with carbon monoxide. *Crit Rev Biochem Mol Biol* **39**: 165-195.

Ratliff, M., Zhu, W., Deshmukh, R., Wilks, A. & Stojiljkovic, I. (2001). Homologues of neisserial heme oxygenase in gram-negative bacteria: degradation of heme by the product of the *pigA* gene of *Pseudomonas aeruginosa*. *J Bacteriol* **183**: 6394-6403.

Rattan, S., Al Haj, R. & De Godoy, M. A. (2004). Mechanism of internal anal sphincter relaxation by CORM-1, authentic CO, and NANC nerve stimulation. *Am J Physiol Gastrointest Liver Physiol* **287**: G605-611.

Richardson, D. R. & Lok, H. C. (2008). The nitric oxide-iron interplay in mammalian cells: transport and storage of dinitrosyl iron complexes. *Biochim Biophys Acta* **1780**: 638-651.

Ridley, K. A., Rock, J. D., Li, Y. & Ketley, J. M. (2006). Heme utilization in *Campylobacter jejuni*. *J Bacteriol* **188**: 7862-7875.

Rodkey, F. L., O'Neal, J. D., Collison, H. A. & Uddin, D. E. (1974). Relative affinity of hemoglobin S and hemoglobin A for carbon monoxide and oxygen. *Clin Chem* **20**: 83-84.

Rodriguez, A. I., Gangopadhyay, A., Kelley, E. E., Pagano, P. J., Zuckerbraun, B. S. & Bauer, P. M. (2010). HO-1 and CO decrease platelet-derived growth factor-induced vascular smooth muscle cell migration via inhibition of Nox1. *Arterioscler Thromb Vasc Biol* **30**: 98-104.

Romanski, S., Kraus, B., Schatzschneider, U., Neudorfl, J. M., Amslinger, S. & Schmalz, H. G. (2011). Acyloxybutadiene iron tricarbonyl complexes as enzyme-triggered CO-releasing molecules (ET-CORMs). *Angew Chem Int Ed Engl* **50**: 2392-2396.

Roughton, F. J. W. & Darling, R. C. (1944). The effect of carbon monoxide on oxyhemoglobin dissociation curve. *The American Journal of Physiology* **141**: 17-31.

Russel, P. J., Ed. (2010). *i*Genetics, A Molecular Approach. San Francisco, Pearson Education Inc., Benjamin Cummings.

Salvail, H., Lanthier-Bourbonnais, P., Sobota, J. M., Caza, M., Benjamin, J. A., Mendieta, M. E., Lepine, F., Dozois, C. M., Imlay, J. & Masse, E. (2010). A small RNA promotes siderophore production through transcriptional and metabolic remodeling. *Proc Natl Acad Sci U S A* **107**: 15223-15228.

Sandouka, A., Balogun, E., Foresti, R., Mann, B. E., Johnson, T. R., Tayem, Y., Green, C. J., Fuller, B. & Motterlini, R. (2005). Carbon monoxide-releasing molecules (CO-RMs) modulate respiration in isolated mitochondria. *Cell Mol Biol (Noisy-le-grand)* **51**: 425-432.

Sandouka, A., Fuller, B. J., Mann, B. E., Green, C. J., Foresti, R. & Motterlini, R. (2006). Treatment with CO-RMs during cold storage improves renal function at reperfusion. *Kidney Int* **69**: 239-247.

Sanguinetti, G., Lawrence, N. D. & Rattray, M. (2006). Probabilistic inference of transcription factor concentrations and gene-specific regulatory activities. *Bioinformatics* **22**: 2775-2781.

Sansom, M. S. (1999). Membrane proteins: A tale of barrels and corks. *Curr Biol* **9**: R254-257.

Santiago, B., Schubel, U., Egelseer, C. & Meyer, O. (1999). Sequence analysis, characterization and CO-specific transcription of the cox gene cluster on the megaplasmid pHCG3 of *Oligotropha carboxidovorans*. *Gene* **236**: 115-124.

Santos-Silva, T., Mukhopadhyay, A., Seixas, J. D., Bernardes, G. J., Romao, C. C. & Romao, M. J. (2011). CORM-3 Reactivity toward Proteins: The Crystal Structure of a Ru(II) Dicarbonyl-Lysozyme Complex. *J Am Chem Soc* **133**: 1192-1195.

Santos, M. F., Seixas, J. D., Coelho, A. C., Mukhopadhyay, A., Reis, P. M., Romao, M. J., Romao, C. C. & Santos-Silva, T. (2012). New insights into the chemistry of fac-[Ru(CO)(3)](2+) fragments in biologically relevant conditions: The CO releasing activity of [Ru(CO)(3)Cl(2)(1,3-thiazole)], and the X-ray crystal structure of its adduct with lysozyme. *J Inorg Biochem*.

Santos, R., Buisson, N., Knight, S., Dancis, A., Camadro, J. M. & Lesuisse, E. (2003). Haemin uptake and use as an iron source by *Candida albicans*: role of CaHMX1-encoded haem oxygenase. *Microbiology* **149**: 579-588.

Sarady, J. K., Zuckerbraun, B. S., Bilban, M., Wagner, O., Usheva, A., Liu, F., Ifedigbo, E., Zamora, R., Choi, A. M. & Otterbein, L. E. (2004). Carbon monoxide protection against endotoxic shock involves reciprocal effects on iNOS in the lung and liver. *FASEB J* **18**: 854-856.

Sasakura, Y., Hirata, S., Sugiyama, S., Suzuki, S., Taguchi, S., Watanabe, M., Matsui, T., Sagami, I. & Shimizu, T. (2002). Characterization of a direct oxygen sensor heme protein from *Escherichia coli*. Effects of the heme redox states and mutations at the heme-binding site on catalysis and structure. *J Biol Chem* **277**: 23821-23827.

Sawle, P., Foresti, R., Mann, B. E., Johnson, T. R., Green, C. J. & Motterlini, R. (2005). Carbon monoxide-releasing molecules (CO-RMs) attenuate the inflammatory response elicited by lipopolysaccharide in RAW264.7 murine macrophages. *Br J Pharmacol* **145**: 800-810.

Schatzschneider, U. (2011). PhotoCORMs: Light-triggered release of carbon monoxide from the coordination sphere of transition metal complexes for biological applications. *Inorganica Chim Acta* **374**: 19-23.

Schmitt, M. P. (1997a). Transcription of the *Corynebacterium diphtheriae hmuO* gene is regulated by iron and heme. *Infect Immun* **65**: 4634-4641.

Schmitt, M. P. (1997b). Utilization of host iron sources by *Corynebacterium diphtheriae*: identification of a gene whose product is homologous to eukaryotic heme oxygenases and is required for acquisition of iron from heme and hemoglobin. *J Bacteriol* **179**: 838-845.

Schubert, M. P. (1933). The action of carbon monoxide on iron and cobalt complexes of cysteine. *J Am Chem Soc* **55**: 4563-4570.

Scott, J. R., Chin, B. Y., Bilban, M. H. & Otterbein, L. E. (2007). Restoring HOmeostasis: is heme oxygenase-1 ready for the clinic? *Trends Pharmacol Sci* **28**: 200-205.

Scott, R. I., Edwards, S. W., Chance, B. & Lloyd, D. (1983). Terminal oxidase of *Crithidia fasciculata*. Reactions with carbon monoxide and oxygen at subzero temperatures and photochemical action spectra. *J Gen Microbiol* **129**: 1983-1989.

Scott, R. I., Gibson, J. F. & Poole, R. K. (1980). Adenosine triphosphatase activity and its sensitivity to ruthenium red oscillate during the cell cycle of *Escherichia coli* K12. *J Gen Microbiol* **120**: 183-198.

Scragg, J. L., Dallas, M. L., Wilkinson, J. A., Varadi, G. & Peers, C. (2008). Carbon monoxide inhibits L-type Ca^{2+} channels via redox modulation of key cysteine residues by mitochondrial reactive oxygen species. *J Biol Chem* **283**: 24412-24419.

Shatalin, K., Shatalina, E., Mironov, A. & Nudler, E. (2011). H2S: a universal defense against antibiotics in bacteria. *Science* **334**: 986-990.

Shelver, D., Kerby, R. L., He, Y. & Roberts, G. P. (1995). Carbon monoxide-induced activation of gene expression in *Rhodospirillum rubrum* requires the product of cooA, a member of the cyclic AMP receptor protein family of transcriptional regulators. *J Bacteriol* **177**: 2157-2163.

Shelver, D., Kerby, R. L., He, Y. & Roberts, G. P. (1997). CooA, a CO-sensing transcription factor from *Rhodospirillum rubrum*, is a CO-binding heme protein. *Proc Natl Acad Sci U S A* **94**: 11216-11220.

Shiloh, M. U., Manzanillo, P. & Cox, J. S. (2008). *Mycobacterium tuberculosis* senses host-derived carbon monoxide during macrophage infection. *Cell Host Microbe* **3**: 323-330.

Sjostrand, T. (1949). Endogenous formation of carbon monoxide in man. *Nature* **164**: 580.

Sjostrand, T. (1952). The formation of carbon monoxide by the decomposition of haemoglobin in vivo. *Acta Physiol Scand* **26**: 338-344.

Skaar, E. P., Gaspar, A. H. & Schneewind, O. (2004). IsdG and IsdI, heme-degrading enzymes in the cytoplasm of *Staphylococcus aureus*. *J Biol Chem* **279**: 436-443.

Skaar, E. P., Gaspar, A. H. & Schneewind, O. (2006). *Bacillus anthracis* IsdG, a heme-degrading monooxygenase. *J Bacteriol* **188**: 1071-1080.

Smerdon, S. J., Krzywda, S., Brzozowski, A. M., Davies, G. J., Wilkinson, A. J., Brancaccio, A., Cutruzzola, F., Allocatelli, C. T., Brunori, M., Li, T. & et al. (1995). Interactions among residues CD3, E7, E10, and E11 in myoglobins: attempts to simulate the ligand-binding properties of Aplysia myoglobin. *Biochemistry* **34**: 8715-8725.

Smith, H., Mann, B. E., Motterlini, R. & Poole, R. K. (2011). The carbon monoxide-releasing molecule, CORM-3 ($Ru(CO)_3Cl(Glycinate)$), targets respiration and oxidases in *Campylobacter jejuni*, generating hydrogen peroxide. *IUBMB Life* **63**: 363-371.

Soni, H., Pandya, G., Patel, P., Acharya, A., Jain, M. & Mehta, A. A. (2011). Beneficial effects of carbon monoxide-releasing molecule-2 (CORM-2) on acute doxorubicin cardiotoxicity in mice: role of oxidative stress and apoptosis. *Toxicol Appl Pharmacol* **253**: 70-80.

Spiro, S. (2007). Regulators of bacterial responses to nitric oxide. *FEMS Microbiol Rev* **31**: 193-211.

Spiro, S. & Guest, J. R. (1991). Adaptive responses to oxygen limitation in *Escherichia coli*. *Trends Biochem Sci* **16**: 310-314.

Srisook, K. & Cha, Y. N. (2005). Super-induction of HO-1 in macrophages stimulated with lipopolysaccharide by prior depletion of glutathione decreases iNOS expression and NO production. *Nitric Oxide* **12**: 70-79.

Srisook, K., Han, S. S., Choi, H. S., Li, M. H., Ueda, H., Kim, C. & Cha, Y. N. (2006). CO from enhanced HO activity or from CORM-2 inhibits both O2- and NO production and downregulates HO-1 expression in LPS-stimulated macrophages. *Biochem Pharmacol* **71**: 307-318.

Stevanin, T. M., Poole, R. K., Demoncheaux, E. A. & Read, R. C. (2002). Flavohemoglobin Hmp protects *Salmonella enterica* serovar Typhimurium from nitric oxide-related killing by human macrophages. *Infect Immun* **70**: 4399-4405.

Stevanin, T. M., Read, R. C. & Poole, R. K. (2007). The *hmp* gene encoding the NO-inducible flavohaemoglobin in *Escherichia coli* confers a protective advantage in resisting killing within macrophages, but not *in vitro*: links with swarming motility. *Gene* **398**: 62-68.

Stewart, R. D. (1975). The effect of carbon monoxide on humans. *Annu Rev Pharmacol* **15**: 409-423.

Stocker, R., Yamamoto, Y., McDonagh, A. F., Glazer, A. N. & Ames, B. N. (1987). Bilirubin is an antioxidant of possible physiological importance. *Science* **235**: 1043-1046.

Stone, J. R. & Marletta, M. A. (1996). Spectral and kinetic studies on the activation of soluble guanylate cyclase by nitric oxide. *Biochemistry* **35**: 1093-1099.

Stripp, S. T., Goldet, G., Brandmayr, C., Sanganas, O., Vincent, K. A., Haumann, M., Armstrong, F. A. & Happe, T. (2009). How oxygen attacks [FeFe] hydrogenases from photosynthetic organisms. *Proc Natl Acad Sci U S A* **106**: 17331-17336.

Suits, M. D., Pal, G. P., Nakatsu, K., Matte, A., Cygler, M. & Jia, Z. (2005). Identification of an *Escherichia coli* O157:H7 heme oxygenase with tandem functional repeats. *Proc Natl Acad Sci U S A* **102**: 16955-16960.

Suliman, H. B., Carraway, M. S., Tatro, L. G. & Piantadosi, C. A. (2007). A new activating role for CO in cardiac mitochondrial biogenesis. *J Cell Sci* **120**: 299-308.

Sun, B. W. & Chen, X. (2009). Carbon monoxide releasing molecules: new insights for anticoagulation strategy in sepsis. *Cell Mol Life Sci* **66**: 365-369.

Suzuki, H., Koyanagi, T., Izuka, S., Onishi, A. & Kumagai, H. (2005). The *yliA*, *-B*, *-C*, and *-D* genes of *Escherichia coli* K-12 encode a novel glutathione importer with an ATP-binding cassette. *J Bacteriol* **187**: 5861-5867.

Szabo, C. (2007). Hydrogen sulphide and its therapeutic potential. *Nat Rev Drug Discov* **6**: 917-935.

Szakacs-Schmidt, A., Kreisz, J., Marko, L., Nagy-Magos, Z. & Takacs, J. (1992). Iron(II) thiolates as reversible carbon monoxide carriers. *Inorganica Chim Acta* **198-200**: 401-405.

Taha, M. K., Deghmane, A. E., Antignac, A., Zarantonelli, M. L., Larribe, M. & Alonso, J. M. (2002). The duality of virulence and transmissibility in *Neisseria meningitidis*. *Trends Microbiol* **10**: 376-382.

Taille, C., El-Benna, J., Lanone, S., Boczkowski, J. & Motterlini, R. (2005). Mitochondrial respiratory chain and NAD(P)H oxidase are targets for the antiproliferative effect of carbon monoxide in human airway smooth muscle. *J Biol Chem* **280**: 25350-25360.

Takayama, Y., Kobayashi, Y., Yahata, N., Saitoh, T., Hori, H., Ikegami, T. & Akutsu, H. (2006). Specific binding of CO to tetraheme cytochrome c_3. *Biochemistry* **45**: 3163-3169.

Tavares, A. F., Teixeira, M., Romao, C. C., Seixas, J. D., Nobre, L. S. & Saraiva, L. M. (2011). Reactive oxygen species mediate bactericidal killing elicited by carbon monoxide-releasing molecules. *J Biol Chem* **286**: 26708-26717.

Techtmann, S. M., Colman, A. S., Murphy, M. B., Schackwitz, W. S., Goodwin, L. A. & Robb, F. T. (2011). Regulation of multiple carbon monoxide consumption pathways in anaerobic bacteria. *Front Microbiol* **2**: 147.

Tenhunen, R., Marver, H. S. & Schmid, R. (1969). Microsomal heme oxygenase. Characterization of the enzyme. *J Biol Chem* **244**: 6388-6394.

Tettelin, H., Saunders, N. J., Heidelberg, J., Jeffries, A. C., Nelson, K. E., Eisen, J. A., Ketchum, K. A., Hood, D. W., Peden, J. F., Dodson, R. J., Nelson, W. C., Gwinn, M. L., DeBoy, R., Peterson, J. D., Hickey, E. K., Haft, D. H., Salzberg, S. L., White, O., Fleischmann, R. D., Dougherty, B. A., Mason, T., Ciecko, A., Parksey, D. S., Blair, E., Cittone, H., Clark, E. B., Cotton, M. D., Utterback, T. R., Khouri, H., Qin, H., Vamathevan, J., Gill, J., Scarlato, V., Masignani, V., Pizza, M., Grandi, G., Sun, L., Smith, H. O., Fraser, C. M., Moxon, E. R., Rappuoli, R. & Venter, J. C. (2000). Complete genome sequence of *Neisseria meningitidis* serogroup B strain MC58. *Science* **287**: 1809-1815.

Tsoyi, K., Ha, Y. M., Kim, Y. M., Lee, Y. S., Kim, H. J., Seo, H. G., Lee, J. H. & Chang, K. C. (2009). Activation of PPAR-gamma by Carbon Monoxide from CORM-2 Leads to the Inhibition of iNOS but not COX-2 Expression in LPS-Stimulated Macrophages. *Inflammation* **32**: 364-371.

Turcanu, V., Dhouib, M. & Poindron, P. (1998). Nitric oxide synthase inhibition by haem oxygenase decreases macrophage nitric-oxide-dependent cytotoxicity: a negative feedback mechanism for the regulation of nitric oxide production. *Res Immunol* **149**: 741-744.

Uc, A., Husted, R. F., Giriyappa, R. L., Britigan, B. E. & Stokes, J. B. (2005). Hemin induces active chloride secretion in Caco-2 cells. *Am J Physiol Gastrointest Liver Physiol* **289**: G202-208.

van der Deen, H. & Hoving, H. (1979). An infrared study of carbon monoxide complexes of hemocyanins. Evidence for the structure of the co-binding site from vibrational analysis. *Biophys Chem* **9**: 169-179.

van der Ploeg, J. R., Eichhorn, E. & Leisinger, T. (2001). Sulfonate-sulfur metabolism and its regulation in *Escherichia coli*. *Arch Microbiol* **176**: 1-8.

Vasil, M. L. & Ochsner, U. A. (1999). The response of *Pseudomonas aeruginosa* to iron: genetics, biochemistry and virulence. *Mol Microbiol* **34**: 399-413.

Vasudevan, S. G., Armarego, W. L., Shaw, D. C., Lilley, P. E., Dixon, N. E. & Poole, R. K. (1991). Isolation and nucleotide sequence of the *hmp* gene that encodes a haemoglobin-like protein in *Escherichia coli* K-12. *Mol Gen Genet* **226**: 49-58.

Vera, T., Henegar, J. R., Drummond, H. A., Rimoldi, J. M. & Stec, D. E. (2005). Protective effect of carbon monoxide-releasing compounds in ischemia-induced acute renal failure. *J Am Soc Nephrol* **16**: 950-958.

Vinella, D., Brochier-Armanet, C., Loiseau, L., Talla, E. & Barras, F. (2009). Iron-sulfur (Fe/S) protein biogenesis: phylogenomic and genetic studies of A-type carriers. *PLoS Genet* **5**: e1000497.

Wang, R. (2002). Two's company, three's a crowd: can H2S be the third endogenous gaseous transmitter? *FASEB J* **16**: 1792-1798.

Wang, R. & Wu, L. (1997). The chemical modification of KCa channels by carbon monoxide in vascular smooth muscle cells. *J Biol Chem* **272**: 8222-8226.

Watts, R. N. & Richardson, D. R. (2004). Differential effects on cellular iron metabolism of the physiologically relevant diatomic effector molecules, NO and CO, that bind iron. *Biochim Biophys Acta* **1692**: 1-15.

Wegele, R., Tasler, R., Zeng, Y., Rivera, M. & Frankenberg-Dinkel, N. (2004). The heme oxygenase(s)-phytochrome system of *Pseudomonas aeruginosa*. *J Biol Chem* **279**: 45791-45802.

Weigel, P. H. & Englund, P. T. (1975). Inhibition of DNA replication in Escherichia coli by cyanide and carbon monoxide. *J Biol Chem* **250**: 8536-8542.

White, K. A. & Marletta, M. A. (1992). Nitric oxide synthase is a cytochrome P-450 type hemoprotein. *Biochemistry* **31**: 6627-6631.

Wilkinson, W. J., Gadeberg, H. C., Harrison, A. W., Allen, N. D., Riccardi, D. & Kemp, P. J. (2009). Carbon monoxide is a rapid modulator of recombinant and native P2X(2) ligand-gated ion channels. *Br J Pharmacol* **158**: 862-871.

Wilkinson, W. J. & Kemp, P. J. (2011). The carbon monoxide donor, CORM-2, is an antagonist of ATP-gated, human P2X4 receptors. *Purinergic Signal* **7**: 57-64.

Wilks, D. & Lever, A. M. (1996). Reasons for delay in administration of antibiotics to patients with meningitis and meningococcaemia. *J Infect* **32**: 49-51.

Wilson, J. L., Jesse, H. E., Hughes, B., Lund, V., Naylor, K., Davidge, K. S., Mann, B. E. & Poole, R. K. (submitted). $Ru(CO)_3Cl(glycinate)$ (CORM-3): a CO-releasing molecule with broad-spectrum antimicrobial and photosensitive activities against respiration and cation transport in *Escherichia coli*. *Submitted Antioxid Redox Signal*.

Wilson, J. L., Jesse, H. E., Poole, R. K. & Davidge, K. S. (2012). Antibacterial effects of carbon monoxide. *Curr Pharm Biotechnol* **13**: 760-768.

Wood, P. M. (1984). Bacterial proteins with CO-binding *b*- or *c*-type haem. Functions and absorption spectroscopy. *Biochim Biophys Acta* **768**: 293-317.

Wu, L. & Wang, R. (2005). Carbon monoxide: endogenous production, physiological functions, and pharmacological applications. *Pharmacol Rev* **57**: 585-630.

Wu, M., Ren, Q., Durkin, A. S., Daugherty, S. C., Brinkac, L. M., Dodson, R. J., Madupu, R., Sullivan, S. A., Kolonay, J. F., Haft, D. H., Nelson, W. C., Tallon, L. J., Jones, K. M., Ulrich, L. E., Gonzalez, J. M., Zhulin, I. B., Robb, F. T. & Eisen, J. A. (2005). Life in hot carbon monoxide: the complete genome sequence of *Carboxydothermus hydrogenoformans* Z-2901. *PLoS Genet* **1**: e65.

Xi, Q., Tcheranova, D., Parfenova, H., Horowitz, B., Leffler, C. W. & Jaggar, J. H. (2004). Carbon monoxide activates K_{Ca} channels in newborn arteriole smooth muscle cells by increasing apparent Ca^{2+} sensitivity of alpha-subunits. *Am J Physiol Heart Circ Physiol* **286**: H610-618.

Yabluchanskiy, A., Sawle, P., Homer-Vanniasinkam, S., Green, C. J., Foresti, R. & Motterlini, R. (2012). CORM-3, a carbon monoxide-releasing molecule, alters the inflammatory response and reduces brain damage in a rat model of hemorrhagic stroke. *Crit Care Med* **40**: 544-552.

Yachie, A., Niida, Y., Wada, T., Igarashi, N., Kaneda, H., Toma, T., Ohta, K., Kasahara, Y. & Koizumi, S. (1999). Oxidative stress causes enhanced endothelial cell injury in human heme oxygenase-1 deficiency. *J Clin Invest* **103**: 129-135.

Yamamoto, K., Ishikawa, H., Takahashi, S., Ishimori, K., Morishima, I., Nakajima, H. & Aono, S. (2001). Binding of CO at the Pro2 side is crucial for the activation of CO-sensing transcriptional activator CooA. (1)H NMR spectroscopic studies. *J Biol Chem* **276**: 11473-11476.

Yamamoto, K., Ogasawara, H. & Ishihama, A. (2008). Involvement of multiple transcription factors for metal-induced spy gene expression in Escherichia coli. *J Biotechnol* **133**: 196-200.

Yang, H., Wolff, E., Kim, M., Diep, A. & Miller, J. H. (2004). Identification of mutator genes and mutational pathways in *Escherichia coli* using a multicopy cloning approach. *Mol Microbiol* **53**: 283-295.

Yatsunyk, L. A., Easton, J. A., Kim, L. R., Sugarbaker, S. A., Bennett, B., Breece, R. M., Vorontsov, II, Tierney, D. L., Crowder, M. W. & Rosenzweig, A. C. (2008). Structure and metal binding properties of ZnuA, a periplasmic zinc transporter from *Escherichia coli*. *J Biol Inorg Chem* **13**: 271-288.

Yeo, W. S., Lee, J. H., Lee, K. C. & Roe, J. H. (2006). IscR acts as an activator in response to oxidative stress for the suf operon encoding Fe-S assembly proteins. *Mol Microbiol* **61**: 206-218.

Yoshida, J., Ozaki, K. S., Nalesnik, M. A., Ueki, S., Castillo-Rama, M., Faleo, G., Ezzelarab, M., Nakao, A., Ekser, B., Echeverri, G. J., Ross, M. A., Stolz, D. B. & Murase, N. (2010). *Ex vivo* application of carbon monoxide in UW solution prevents transplant-induced renal ischemia/reperfusion injury in pigs. *Am J Transplant* **10**: 763-772.

Zhang, X., Shan, P., Otterbein, L. E., Alam, J., Flavell, R. A., Davis, R. J., Choi, A. M. & Lee, P. J. (2003). Carbon monoxide inhibition of apoptosis during ischemia-reperfusion lung injury is dependent on the p38 mitogen-activated protein kinase pathway and involves caspase 3. *J Biol Chem* **278**: 1248-1258.

Zhu, W., Hunt, D. J., Richardson, A. R. & Stojiljkovic, I. (2000a). Use of heme compounds as iron sources by pathogenic neisseriae requires the product of the *hemO* gene. *J Bacteriol* **182**: 439-447.

Zhu, W., Wilks, A. & Stojiljkovic, I. (2000b). Degradation of heme in gram-negative bacteria: the product of the *hemO* gene of Neisseriae is a heme oxygenase. *J Bacteriol* **182**: 6783-6790.

Zlosnik, J. E., Tavankar, G. R., Bundy, J. G., Mossialos, D., O'Toole, R. & Williams, H. D. (2006). Investigation of the physiological relationship between the cyanide-insensitive oxidase and cyanide production in *Pseudomonas aeruginosa*. *Microbiology* **152**: 1407-1415.

Zuckerbraun, B. S., Chin, B. Y., Bilban, M., d'Avila, J. C., Rao, J., Billiar, T. R. & Otterbein, L. E. (2007). Carbon monoxide signals via inhibition of cytochrome *c* oxidase and generation of mitochondrial reactive oxygen species. *FASEB J* **21**: 1099-1106.